# Recycled Concrete Aggregate – A Viable Aggregate Source For Concrete Pavements

by

James Trevor Smith

A thesis
presented to the University of Waterloo
in fulfillment of the
thesis requirement for the degree of
Doctor of Philosophy
in
Civil Engineering

Waterloo, Ontario, Canada, 2009

## Author's Declaration

I hereby declare that I am the sole author of this thesis. This is a true copy of the thesis, including any required final revisions, as accepted by my examiners.

I understand that my thesis may be made electronically available to the public.

# Abstract

Virgin aggregate is being used faster than it is being made available creating a foreseeable shortage in the future. Despite this trend, the availability of demolished concrete for use as recycled concrete aggregate (RCA) is increasing. Using this waste concrete as RCA conserves virgin aggregate, reduces the impact on landfills, decreases energy consumption and can provide cost savings. However, there are still many unanswered questions on the beneficial use of RCA in concrete pavements.

This research addresses the many technical and cost-effective concerns regarding the use of RCA in concrete pavements by identifying concrete mixture and proportioning designs suitable for jointed plain concrete pavements; constructing test sections using varying amounts of RCA; monitoring performance through testing, condition surveys and sensor data; modeling RCA pavement performance; and predicting life cycle costs.

The research was carried out as a partnership between the Centre for Pavement and Transportation Technology (CPATT) at the University of Waterloo, the Cement Association of Canada, Dufferin Construction, and the Natural Sciences and Engineering Research Council of Canada.

The literature review provides an overview of sustainability and key performance indicators, the material properties of RCA both as an aggregate and in concrete, concrete mixture and proportioning designs with RCA, performance of existing RCA pavements, and the implementation of RCA highlighting some examples where RCA has been used successfully.

Twelve preliminary mixes were developed using three total cementitious contents amounts of 315 kg/m$^3$, 330 kg/m$^3$, and 345 kg/m$^3$ to determine four suitable mixes with varying coarse RCA contents (0%, 15%, 30% and 50%) to place at the CPATT test track. At 28-days, all of the twelve mixes exceed the 30 MPa design strength.

Four test sections containing 0%, 15%, 30% and 50% coarse RCA were constructed in June 2007. The test sections had identical cross sections consisting of 250 mm portland cement concrete (PCC), 100 mm asphalt-stabilized OGDL and a 450 mm granular base. For each coarse RCA content, one slab was instrumented with six vibrating wire concrete embedment strain gages to measure long-term longitudinal and transverse strain due to environmental changes, two vibrating wire vertical extensometers to monitor slab curling and warping, two vibrating wire inter-panel extensometers to monitor joint movement, and two maturity meters to measure maturity and temperature.

Quality assurance and quality control (QA/QC) testing showed that the mixes containing RCA exhibited similar or improved performance when compared to the conventional concrete for compressive and flexural strength, freeze-thaw durability and coefficient of thermal expansion.

Pavement performance of the four test sections was evaluated using visual surveys following the Ontario Ministry of Transportation's Manual for Condition rating of Rigid Pavements. Nine pavement evaluations have been performed every two to four months since construction. All test sections are in excellent condition with pavement condition index (PCI) values greater than 85 after two years in-service and approximately three hundred thousand Equivalent Single Axle Loads.

Sensor data from the strain gauges, and vertical and inter-panel extensometers are providing consistent results between the test sections.

Long-term performance modeling using the Mechanistic-Empirical Pavement Design Guide (ME-PDG) showed improved performance with respect to cracked slabs, joint faulting, and pavement roughness as the RCA content increased. Multivariable sensitivity analysis showed that the performance results were sensitive to CTE, unit weight, joint spacing, edge support, surface absorption, and dowel bar diameter.

Life cycle cost analysis (LCCA) illustrated the savings that can be expected using RCA as a replacement aggregate source as the cost of virgin aggregate increase as the sources becomes depleted. Multivariable sensitivity analysis showed that the LCCA results were sensitive to construction costs, discount rate, and maintenance and rehabilitation quantities.

# Acknowledgements

I wish to express a sincere thank you to my supervisor Dr. Susan Tighe. Your support, guidance, and encouragement are greatly appreciated.

I would also like to acknowledge the Centre for Pavement and Transportation Technologies (CPATT) at the University of Waterloo, the Cement Association of Canada (CAC), Dufferin Construction, Steed and Evans, Smith Recycling, the Natural Sciences and Engineering Research Council of Canada (NSERC), the Regional Municipality of Waterloo, Environment Canada, and Stantec Consulting Ltd. for their financial support and contributions to this research.

Special thank you to my wife Jennifer, and our children Victoria, Benjamin, and Nathaniel for their support and encouragement during this process.

# Table of Contents

# Appendices

# List of Figures

# List of Tables

# Chapter 1
# Introduction

## 1.1 Background

### 1.1.1 Current Aggregate Shortage

There is a dramatic decline in good quality aggregate available for construction use. World wide aggregate use is estimated to be ten to eleven billion tonnes each year. Of this, approximately eight billion tonnes of aggregate (sand, gravel, and crushed rock) is being used in portland cement concrete (PCC) every year [Naik 2005, Mehta 2001]. In central Canada, fourteen tonnes of aggregate are consumed per person each year. However, for every three tonnes of aggregate that is produced only one tonne is replaced by opening new aggregate sources or through recycling [McMacNaughton 2004]. Ontario is currently using aggregate faster than it is being made available resulting in an aggregate shortage [APAO 2004].

The current state of aggregate resources in Ontario is not fully known since the last detailed study was done in 1992 by the Ministry of Natural Resources (MNR) in "State of the Resource Report" [Miller 2005]. From 1992 to 2003 Ontario's yearly consumption of aggregate was approximately 170 million tonnes. More than sixteen tonnes of aggregate are used per person in Ontario each year [APAO 2004]. To construct one kilometer of six-lane expressway, 51,800 tonnes of aggregate are used. Aggregate production in Ontario is currently produced by 2800 licensed pit and quarries and it exceeded 160 million tonnes in 2001 [Miller 2005]. Aggregate consumption in Ontario over the next 25 years is estimated at four billion tonnes [APAO 2004]. Ontario is facing an aggregate shortage. It is estimated that some urban areas will run out of aggregate by 2010 [Miller 2005].

### 1.1.2 Impacts of Waste Concrete

There is a critical shortage of natural aggregate and an increasing amount of demolished concrete [Hansen 1984]. It is estimated that 150 million ton of concrete waste is produced in the United States annually [Salem 2003]. Concrete structures that are designed to have service lives of at least 50 years have to be demolished after 20 or 30 years because of early deterioration. In 2005, the American Society of Civil Engineers reported US infrastructure in poor condition with an estimated repair cost of $1.6 trillion over five years [ASCE 2005]. The environmental impact of waste concrete is significant. Not only is there the environmental impact of transporting the waste concrete away from the site but the waste concrete also fills up valuable space in landfills. The United States produces 123 million tons of waste from building demolition, and most ends up in landfills [FHWA 2004]. Construction and demolition (C&D) waste makes up a large portion of all generated solid waste [Meyer 2008]. In 1980 the Environmental Resources Limited in the East European Communities (EEC) estimated 80 million tonnes of demolition waste, mostly concrete, are produced each year. This number is expected to double by 2000, and triple by 2020 [Bairagi 1990]. There is a huge

potential to reuse this material as source of new aggregate. Due to concerns with space and cost, traditional disposal of C&D in landfills is no longer an acceptable option [Meyer 2008].

### 1.1.3 Costs

The cost of quality aggregate has increased above the inflation rate and it is projected that this trend will continue as further restrictions are placed on this resource in the future [MacNaughton 2004]. Concrete C&D waste will be recycled if it is less expensive than disposing of it in a landfill and recycled concrete aggregate (RCA) will be used if it is less expensive than virgin aggregate of similar quality [Kamel 2008]. RCA use is based on economics, including the cost of transporting C&D waste and virgin aggregate, the cost of C&D disposal, and government intervention on tipping fees and mandatory usage through legislation [Meyer 2008]. Approximately 60% of aggregate cost is due to transportation [APAO 2004]. The economics are starting to make recycled materials more attractive [Turley 2003]. It is estimated that the Canadian ready mixed concrete industry could save approximately $300 million annually by using RCA [NRMCA 2007].

### 1.1.4 Achieving Sustainability with Recycled Aggregate Concrete

Sustainability is defined as "Meeting the needs of the present without compromising the ability of the future generations to meet their own needs" [Naik 2005]. The current usage of aggregate is not sustainable as demonstrated by the growing shortage of natural aggregates in urban area. Recycling concrete, from deteriorated concrete structures, would reduce the negative impact on the environment and increase sustainability of aggregate resources [Oikonomou 2005, Hansen 1985]. Using RCA conserves virgin aggregate, reduces the impact on landfills and decreases energy consumption [FHWA 2004]. Using RCA, creates cost savings in the transportation of aggregate and waste products, and in waste disposal [FHWA 2004, ACPA 1993]. It is estimated that using RCA can save up to $4.80 $m^2$ [ACPA 2009]. Finding ways to re use C&D waste and minimize things that are not suitable for reuse will increase sustainability [Turley 2003].

### 1.1.5 Barriers to Recycled Concrete Aggregate Use

There are several barriers to overcome in order for RCA to become widely accepted [Rashwan 1997]. Initially there is a high investment cost to purchase concrete crushers. In addition, maintenance costs of concrete crushers are significant.

In Ontario, non-virgin aggregate consumption is estimated at three percent [Miller 2005]. This may be due to the lack of financial incentive. The Ontario government currently places a levy of only six cents per tonne on virgin aggregate.

Another barrier relates to the quality of the RCA. Highways require quality material that meets engineering, economic and environmental considerations [Turley 2003]. However, where high-performance concrete is not required, RCA can be used and virgin aggregate conserved [Meyer 2008]. An excess amount of fine RCA is created during the crushing process. This excess fine aggregate requires disposal or an alternate use. Depending on the source and type of RCA, the absorption, strength, and impurities vary. This can mean that it is unusable or that it might adversely

impact the new pavement structure. "Durability performance of RCA is not well understood because of the limited and contradictory research results" [Salem 2003]. Concrete that contains RCA has decreased compressive strength and flexural strength, increased dry shrinkage, decreased sulfate resistance and decreased chloride resistance. There is also a lack of knowledge on how RCA affects durability since most studies focus only on the properties of RCA concrete [Olorunsogo 2002].

Government agencies have been slow to embrace the use of RCA due to concerns about quality and a reluctance to change what has worked in the past [Turley 2003]. The use of material specifications are a barrier to the use of RCA. A performance-based or end result specification would allow more RCA use [Turley 2003]. However, specific standards on how to use RCA in new concrete are not currently available.

## 1.2 Thesis Scope and Objectives

This research has the following objectives.

1. Highlight the current issues associated with using RCA.
2. Provide a detailed literature review which outlines sustainability, RCA issues, material testing, mix design issues, concrete pavement design methods, data sources, and typical pavement performance values.
3. Determine whether RCA can be used as a viable aggregate source for concrete pavements in the Canadian environment.
4. Quantify the physical properties of four sources of RCA and assess their influence on concrete pavement performance.
5. Compare the RCA properties and concrete performance to virgin aggregate using statistical analysis.
6. Compare volumetric, property, performance, and functionality of different types of mix designs using RCA.
7. Identify tests that correlate with initial and long term performance for quality control purposes. Based on these tests, end result specifications and performance based specifications will be developed.
8. Develop input values for RCA for the use in the new Mechanistic-Empirical Pavement Design Guide (ME-PDG).
9. Detect pavement problems related to RCA use and provide guidelines on innovative tools and technologies for corrective measures that can be taken.
10. Identify mix design properties for RCA and relate to long term pavement performance.
11. Demonstrate the use of RCA through the design and construction of test sections/slabs to monitor RCA performance in the Canadian environment.
12. Develop a realistic life cycle cost model for RCA use in the pavement structure.

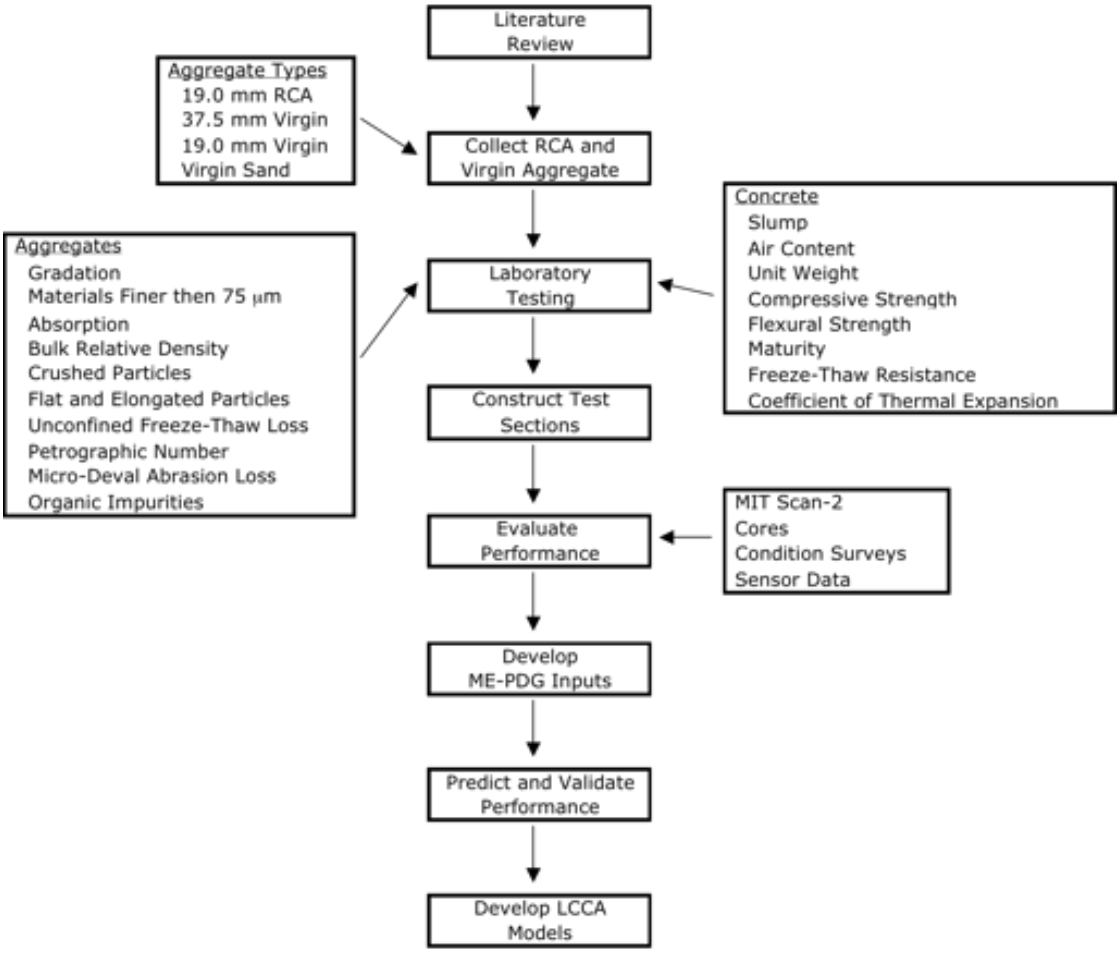


**Figure 1.1 Research Framework**

## 1.3 Project Significance

This research provides the provincial departments of transportation, state highway agencies, and the concrete pavement industry with information on using RCA as a source of aggregate for new concrete roadways and other applications in environments that have cold temperatures. Specifically, this research addresses the technical and cost-effective concerns regarding RCA use in the Canadian environment.

# Chapter 2

# Literature Review

## 2.1 Sustainability

Sustainability is defined by the World Commission on Environment and Development as "Meeting the needs of the present without compromising the ability of the future generations to meet their own needs" [Naik 2005]. One author describes achieving sustainability as the greatest challenge facing the concrete industry in the 21st century [Mehta 2001]. He claims that the industry has a short-term view point on the consumption of natural resources [Mehta 2001] and that "in a finite world the model of unlimited growth, unrestricted use of natural resources and uncontrolled pollution of the environment is a recipe for planetary self-destruction." The Factor of Ten Club states that "Within one generation, nations can achieve a ten-fold increase in the efficiency with which they use energy, natural resources and other materials" [Mehta 2001].

There are three keys to sustainable development in the concrete industry [Mehta 1999]. First, conserve concrete making material. This can be achieved by recycling aggregate by crushing demolished concrete. Also, using recycled water from mixing plants and wash water from trucks would decrease the need for fresh mixing water. Finally, using byproducts, such as fly ash, slag and silica fume, from other industries reduces the amount of cement needed in the concrete.

Second, to aid in sustainable development, concrete structures need improved durability. Sustainable concrete structures minimize the short and long-term societal impacts; however, to achieve this durable concrete is needed [Naik 2005]. The current thinking is that designing for high strength means durable concrete is achieved; however, designing concrete for durability and achieve the necessary strength could also potentially improve sustainability. Concrete designs are needed that minimize the greatest causes of deterioration such as corrosion, exposure to freeze/thaw, alkali-silica reaction and sulfate attack [Mehta 1999]. Decreasing the permeability of the concrete through the use of supplementary cementitious materials (SCMs) is an option.

Third, in order to achieve sustainable development training and education must be improved. A 1995 survey of Civil engineering departments showed that less than half of the responding schools have an optional full semester course on concrete technology. To properly educate tomorrow's engineers in schools today, North American students need more education on cement and concrete topics [Mehta 1999].

## 2.2 Recycled Concrete Aggregate

### 2.2.1 Producing Recycled Concrete Aggregate

Figure 2.1 shows a closed-loop concrete system [Kuroda 2005].

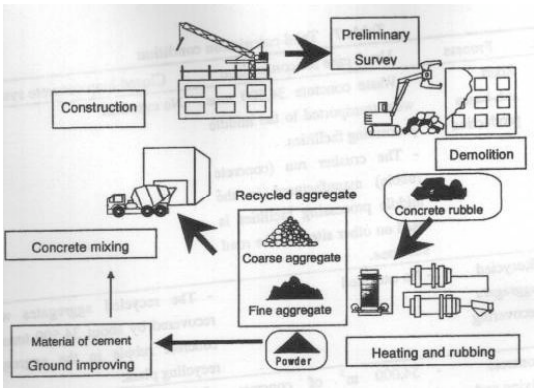


**Figure 2.1 Closed-Loop Concrete System**

Crushing concrete for use as RCA uses similar equipment and processes as when preparing virgin aggregate. There are two types of crushers: compression and impact. Figure 2.2 shows both a cone compression crusher and a jaw compression crusher [ACPA 2003]. Figure 2.3 shows a vertical and a horizontal impact crusher where repeated blows against break plates reduce the size of the concrete pieces [ACPA 2003].

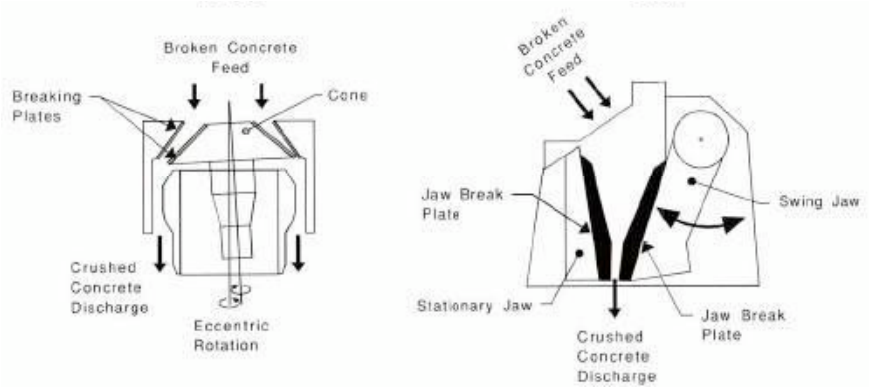


**Figure 2.2 Cone and Jaw Compression Crushers**

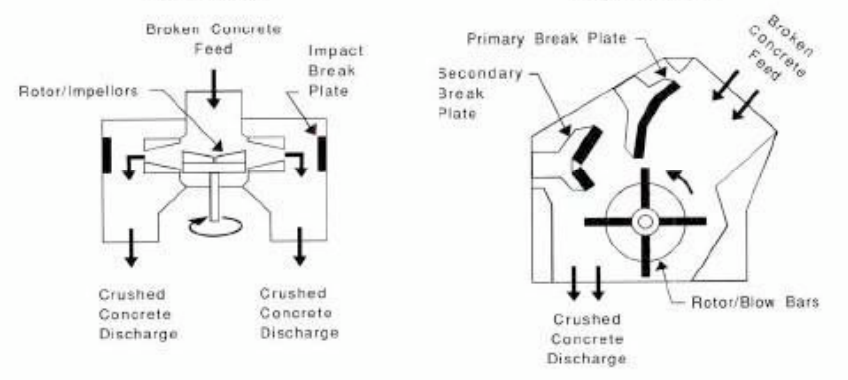


**Figure 2.3 Vertical and Horizontal Impact Crushers**

Defects and irregular voids can be reduced by over 50% by sending RCA through a jaw or impact crusher twice. Additional mechanical grinding will remove adherent mortar improving physical properties while only introducing a negligible amount of new cracking. Cracking of the interface transition zone was not affected significantly [Nagataki 2004].

### 2.2.2 Current Use of Recycled Concrete Aggregate

Many countries successfully use RCA including the United States, South Africa, Netherlands, United Kingdom, Germany, France, Russia, Canada, and Japan [Olorunsogo 2002]. Currently, RCA is used as an aggregate in granular subbases, lean-concrete subbases, soil-cement, and in new concrete as the only source of aggregate or as a partial replacement of new aggregate [CAC 2004] [Kuo 2002, Masood 01, ACPA 1993]. The Ministry of Land, Infrastructure, and Transportation has been instrumental in Japan recycling 96% of the nation's concrete waste through initiatives Recycling Plan 21 and Construction Recycling Promotion Plan '97 [Noguchi 2005]. Japan developed a special technique that removes the original mortar from the concrete. This technique produces only 20 – 35% coarse aggregate compared to the 60 – 70% coarse aggregate that is produced in the current system because of the large amount of adhered mortar [Dosho 2005].

In 2002, 28 states used RCA in pavement construction, 26 states use RCA as base or subbase material only and two states allow for subbase use only [Kuo 2002]. By 2004, 41 of the 50 states are recycling waste concrete into aggregate [FHWA 2004]. Figure 2.4 shows the 38 states where recycled material is used as aggregate in road construction base material. Figure 2.5 shows the eleven states where RCA is used in new concrete.

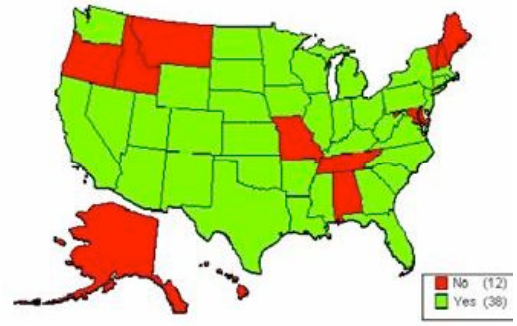


**Figure 2.4 United States Using RCA as Base Material**


**Figure 2.5 United States Using RCA as Concrete Aggregate**

The states leading the way in the use of RCA are Texas, Virginia, Michigan, Minnesota, and California [FHWA 2004]. In 1980 the Minnesota Department of Transportation saved approximately $600,000 by recycling sixteen miles of plain concrete pavement on US-59 [Salem 2003]. It is estimated that using RCA saves approximately $4.80 per $m^2$ ($4 $y^2$) [ACPA 1993]. A US geological survey conducted in 2000 showed that of the approximately 100 million tons of RCA produced annually, 68% is used as a broad base, six percent is used in new concrete, nine percent is used in asphalt, fourteen percent as riprap and other fill and seven percent in other uses [Li 2005].

In Canada there is very limited use of RCA. Ontario's non-virgin aggregate consumption is estimated at three percent [Miller 2005]. In general, the Ontario Ministry of Transportation (MTO) does not recycle old concrete into new concrete. Currently, the MTO is recycling old concrete by blending it with virgin granular material for use as base and subbase [Gilbert, 2004]. The MTO focuses on cost savings rather than on recycling. However, competitive bids in some areas of the province where virgin aggregate is very expensive usually include recycling the existing pavement [Gilbert, 2004].

### 2.2.3 Properties of RCA

Working with RCA can be challenging since often the specifics about the original concrete are unknown [Oikonomou 2005]. Recycled concrete aggregate is highly heterogeneous and porous, with a large amount of impurities. This makes it difficult to model and predict the resulting concrete properties [Zaharieva 2003]. Better characterization of the properties of RCA would increase the confidence needed to use RCA in new rigid pavements [Cuttell 2008].

#### 2.2.3.1 Shape, Texture, and Gradation

In general, RCA has 100% crushed faces [Salem 2003]. The age and strength at which concrete is crushed does not influence the amount of mortar attached to the aggregate or the gradation of the RCA [Katz 2003]. Coarse RCA material contains about 6.5% adherent original mortar and the fine material contains about 25% [Katz 2003].

#### 2.2.3.2 Specific Gravity

Specific gravity or relative density is defined by the ASTM as the ratio of the density of a material to the density of distilled water at a stated temperature. ASTM C 128 is the procedure for obtaining specific gravity. Virgin aggregate has a specific gravity of 2.7 and RCA is 2.4. This difference is due to the relative density of the old mortar attached to the RCA [Salem 2003] [Katz 2003]. Coarse RCA typically has a specific gravity between 2.2 and 2.6 for saturated surface dry conditions. This value decrease as the particle size decreases. Fine RCA has a specific gravity between 2.0 and 2.3 for saturated surface dry conditions [Katz 2003, ACPA 1993].

#### 2.2.3.3 Absorption

The ASTM defines absorption as the increase in mass of aggregate due to water penetration into the pores of the particles during a prescribed period of time, but not including water adhering to the outside surface of the particles, expressed as a percentage of the dry mass. Using the ASTM C 128 process virgin aggregate has a lower absorption of 0.3%. Coarse RCA has absorption of 2-6% and fine RCA has an even higher absorption of 4-12% [Katz 2003, Kerkhoff 2001, ACPA 1993]. This difference is due to the higher absorption of the old mortar contained in the RCA [Salem 2003] [ACPA 1993].

#### 2.2.3.4 Abrasion Resistance

Abrasion resistance is used as an index of aggregate quality and its ability to resist weathering and loading action [CAC 2002]. Abrasion resistance of RCA is twelve percent lower than virgin aggregate [Sagoe-Crentsil 2001]. The abrasion resistance results are not dependent on full or partial RCA use [Abou-Zeid 2005]. Abrasion resistance for RCA ranges between 20-45% with an upper range at 50% [ACPA 1993].

#### 2.2.3.5 RCA Fines

Creation of high quality RCA produces a large amount of fines that can be problematic to deal with [Naik 2005]. RCA fines can be mixed with a clay soil to improve the soil properties. Although the addition of RCA fines did not significantly impact the clay soils liquid limit initially or after 21 days, it almost doubled the plastic limit. The plasticity index at 21 days was 17.6 for clay soil containing RCA fines compared to 35.9 for the control. This improves the soil classification from clay to silty sand [Hansen 1986].

### 2.2.4 Properties of RCA Concrete

The cement mortar that is a part of the RCA significantly impacts the characteristics and performance of the RCA containing concrete [Sagoe-Crentsil 2001]. Removal of some of the adherent mortar helps to improve the properties of RCA containing concrete. The properties of the original concrete have a significant influence on the properties of the RCA containing concrete (compressive strength, tensile strength, bond stress at failure, F/T resistance) [Ajdukiewicz 2002].

There is a general lack of knowledge about how RCA use affects the durability of concrete. This is due to contradictory research results and studies focused only on the properties of RCA containing concrete not durability [Salem 2003]. RCA containing concrete performed in a comparable manner to virgin concrete in terms of strength and durability [Shayan 2003, Olorunsogo 2002]. In general, concrete durability is reduced as RCA content is increased [Olorunsogo 2002]. The increased absorption of the RCA leads to larger amounts of shrinkage and cracking in RCA containing concrete [Mesbah 1999]. However, durability properties can be improved with longer curing periods [Olorunsogo 2002].

#### 2.2.4.1 Workability

Concrete workability is defined as the effort required to manipulate a freshly mixed quantity of concrete with minimum loss of homogeneity [Mehta 2006]. After five to ten minutes, RCA mixes are stiffer and lose workability at a faster rate than mixes containing virgin aggregate [Salem 2003].

#### 2.2.4.2 Slump

Slump is defined as the "measure of the consistency of freshly mixed concrete, equal to the immediate subsidence of a specimen molded with a standard slump cone" [CAC 2002]. Admixtures in the RCA had no significant impact on the slump of the new RCA concrete [Hansen 1984]. The more RCA that is used in a cement mix, the higher the w/c ratio that is needed. This will result in a higher slump [Lin 2004]. However, assuming a constant w/c ratio, RCA concrete mixes have a decrease in slump compared to virgin concrete mixes. RCA has a higher absorption and an angular texture that increases the internal friction [Rashwan 1997]. As the amount of RCA increases at a constant w/c ratio, the workability decreases [Topcu 2003]. The moisture state of the RCA impacts the slump and slump loss of the concrete. Keeping a constant w/c ratio, slump and slump loss was the highest for concrete that contained oven-dried RCA as compared to air-dried or saturated surface dry RCA.

#### 2.2.4.3 Air Content

Air content of freshly mixed concrete is based on a change of volume for a change in pressure. RCA has a higher void content than virgin aggregate. This results in RCA containing concrete having a larger amount of entrapped air compared to virgin aggregate [Salem 2003]. The air content of RCA containing concrete is higher than the concrete from which the RCA was made since the new concrete contains both the air entrapped in the concrete and the air in the RCA [Katz 2003]. Admixtures in the original concrete that is made into RCA had no significant impact on the air content of the new RCA concrete [Hansen 1984].

#### 2.2.4.4 Initial Set Time

The time required for the cement paste to ceases being fluid and plastic is the initial set time [CAC 2002]. Admixtures in the original concrete had no significant impact on the initial set time of the new RCA concrete [Hansen 1984].

#### 2.2.4.5 Final Set Time

The final set time is the time required for the cement paste to develop a certain degree of strength [CAC 2002]. There was no significant difference in final set time for RCA containing concrete when the RCA was made from a concrete containing an admixture [Hansen 1984].

#### 2.2.4.6 Compressive Strength

Compressive strength is the ability to resist compression loads [CAC 2002]. In general, using RCA in the concrete mix decreases compressive strength compared to virgin aggregate. However, at 28 days, all mix designs usually exceed 50 MPa compressive strength [Shayan 2003]. One study showed the compressive strength of virgin concrete was 58.6 MPa, and the RCA concrete ranged from 50.9 to 62.1 MPa. There were higher values for concrete made with 50% RCA compared to 100% RCA [Poon 2002]. The loss of compressive strength is in the range of 30-40% for the concrete made with RCA at 28-days [Katz 2003]. There was a minor reduction in 28- and 56-day compressive strength when virgin aggregate was partially replaced with RCA and a much greater reduction when RCA was used in full [Abou-Zeid 2005].

The most influential parameter affecting compressive strength is the w/c ratio [Lin 2004]. Other influential parameters include fine RCA content, cleanness of aggregate, interaction between fine RCA content and crushed brick content, and interaction between w/c ratio and coarse RCA content [Lin 2004]. Keeping a constant w/c ratio, air-dried RCA containing concrete had the highest compressive strength compared to oven-dried and saturated surface dry RCA [Poon 2003]. Using unwashed RCA reduces compressive strength particularly at lower w/c ratios. Compressive strength is 60% of virgin concrete at 0.38 w/c and 75% at 0.6 w/c [Chen 2002].

There seems to be a strong interaction between maximum aggregate size and water-cement ratio when compared with compressive strength development [Tavakoli 1996a]. Compressive strength may increase for RCA due to a lower w/c ratio compared to virgin aggregate, 14% and 34% respectively. However, compressive strength may decrease for RCA since it has a higher air entrainment, 25%, compared to virgin aggregate 23% [Salem 2003].

The majority of strength loss for RCA concrete can be attributed to material smaller than 2 mm because natural sand has greater strength than RCA fines [ACPA 1993]. It is recommended to keep RCA fines less than 50% of the sand content [Shayan 2003]. Bonding between the RCA and the cement can be affected by loose particles created during the crushing process. Treating the RCA by impregnation of silica fume resulted in an increase in compressive strength of approximately at 30% at 7-days and 15% at 28-days. Exposing the RCA to ultrasound resulted in a uniform increase of 7% compressive strength over time [Katz 2004]. The age at which the RCA is crushed has a significant impact on the compressive strength of the final concrete. For example, crushing concrete into RCA after three days compared to one day resulted in a seven percent increase in compressive strength of the new RCA concrete at 7 days. The difference in compressive strength of the new RCA concrete increased to 13% when measured at 90 days [Katz 2003]. The compressive strength of the original crushed concrete influences the compressive strength of the RCA concrete [Tavakoli 1996a]. However, it has been reported that RCA concrete can produce higher compressive strengths than the original concrete [Ajdukiewicz 2002]. For example, an 80+ MPa concrete was created from an original 60MPa concrete [Ajdukiewicz 2002].

When comparing laboratory-made RCA and field demolished RCA, there was the same basic trend in all strength development [Tavakoli 1996a]. Admixtures in the original concrete had no significant impact on the compressive strength of the new RCA concrete [Hansen 1984]. When slag is added to the RCA concrete, it develops strength over a longer period of time compared to normal concrete

[Sagoe-Crentsil 2001]. Some research suggests that compressive strength is dependant on the amount of time the RCA spent in the stockpile after crushing [Rashwan 1997]. For example, concrete made with RCA that was in the stockpile one day had a 25% higher compressive strength than concrete made with RCA that was in the stockpile 28 days. Concrete made with RCA that was in the stockpile seven days had a seven percent lower compressive strength than concrete that was in the stockpile 28 days [Rashwan 1997]. RCA concrete showed good performance when exposed to temperatures up to 600$^{o}$C with a loss in compressive strength of 20-25% [Abou-Zeid 2005]. When RCA concrete fails it is usually because cracks passed through the RCA: however, when virgin concrete fails it is usually due to bond failure at the aggregate-paste interface [Salem 2003].

#### 2.2.4.7 Flexural Strength

Flexural strength or modulus of rupture is the ability to resist tension resulting from bending [CAC 2002]. There are conflicting results about how RCA use affects flexural strength. The results range from RCA decreasing flexural strength [Zaharieva 2004, Katz 2003, Salem 2003] to RCA increasing flexural strength [Poon 2002]. One study showed a decrease in flexural strength between 10-20% [Zaharieva 2004]. Other studies found comparable flexural strength results between RCA concrete and the control [Tavakoli 1996a, Abou-Zeid 2005]. And yet another study showed that flexural strength increased with the amount of RCA used. Virgin concrete had a flexural strength of 3.31 MPa, and RCA concrete ranged from 3.74 to 3.89 MPa with 100% RCA concrete having higher values than 50% RCA concrete [Poon 2002].

The parameters that influence flexural strength are not completely clear. However, minor decreases in strength can be attributed to material smaller than 2 mm resulting from natural sand having greater strength than RCA fines [ACPA 1993]. One study suggested that flexural strength was comparable to the w/c ratio [Tavakoli 1996a].

Flexural strength can be predicted by using ACI 363R equation.

$$f_r^{'} = 0.94\sqrt{f_c^{'}} \tag{2.1}$$

where $f_r^{'}$ = flexural strength (MPa)

$f_c^{'}$ = compressive strength (MPa)

However, the actual flexural strength is higher than what is predicted by ACI 363R equations [Katz 2003, Tavakoli 1996a] and the variation increases as the w/c ratio is increased [Tavakoli 1996a].

#### 2.2.4.8 Bond Strength

Bond strength is defined as the force required to break two materials apart [CAC 2002]. On average RCA concretes failed with a 20% lower force than virgin concretes [Ajdukiewicz 2002].

#### 2.2.4.9 Interfacial Transition Zone

The interfacial transition zone (ITZ) is a small region next to the particles of coarse aggregate. This is considered the strength-limiting phase in concrete [Mehta 2006]. The ITZ is an important factor in compressive strength development in RCA concrete [Poon 2004]. RCA cement has a higher ITZ due to higher porosity and absorption of the RCA resulting in a lower compressive strength [Poon 2004]. Normal RCA concrete had a loose and porous ITZ of 30-60 μm. Where as RCA concrete made from high-performance concrete had a dense ITZ of 10 μm [Poon 2004]. The ITZ strength, Vickers hardness, is related to the w/c ratio. RCA concrete with a high w/c ratio (0.55 and 0.7) produces a weaker ITZ than the original concrete from which the RCA is made; however, a low w/c ratio (0.25 and 0.4) produces an ITZ that is greater than the original concrete strength [Otuki 2003].

#### 2.2.4.10 Hardness

The hardness of concrete is tested by checking at the surface for concrete uniformity. This correlates to compressive strength and stiffness [CAC 2002]. The Schmidt hardness concrete values decreased from 21.3 MPa for virgin aggregate to 11.6 MPa for 100% RCA concrete [Topcu 1997]. This decline in hardness usually corresponds to a decrease in compressive strength [Topcu 1997].

#### 2.2.4.11 Modulus of Elasticity

The ratio of normal stress to corresponding strain is called the modulus of elasticity [CAC 2002]. Use of RCA causes a decrease in the modulus of elasticity [Katz 2003, Salem 2003, Salem 1998, Hansen 1985]. Research shows that a 20-30% decrease in modulus of elasticity is common when using RCA but up to a 40% decrease can be expected [Chen 2002, Hansen 1985]. Washing the aggregate did not cause any significant variation in modulus of elasticity values [Chen 2002]. Another study showed that even with the addition of fly ash and an increase in air content, the modulus of elasticity of the RCA concrete was lower compared to the virgin concrete [Salem 1998]. The actual modulus of elasticity results are approximately 25% lower than those calculated by the ACI Equation [Katz 2003].

$$E_c = 0.043 W_c^{1.5} \sqrt{f_c'} \tag{2.2}$$

where $E_c$ = modulus of elasticity

$W_c$ = correction factor for the lower density of RCA

$f_c'$ = compressive strength (MPa)

#### 2.2.4.12 Freeze-Thaw Resistance

Freeze-thaw resistance (F/T) is the ability of concrete to withstand cycles of freezing and thawing and is one of the measures of durability [CAC 2002]. Freeze-thaw resistance of RCA has produced mixed results [Gokce 2004, Salem 1998].

Increasing air content is the single most effective method of improving F/T resistance [Salem 1998] [Salem 2003]. It is difficult to produce a F/T resistant concrete from RCA containing no air-entrainment, therefore air-entrainment is recommended [Gokce 2004]. Air-entrained concretes have lower amounts of mass loss than non air-entrained concretes [Gokce 2004]. RCA made from air-entrained concrete performed better than the original concrete aggregate having a relative dynamic modulus of elasticity above 90% at 500 cycles. Where as RCA made from non air-entrained concrete performed poorly, the relative dynamic modulus of elasticity dropped below 60% at 90 F/T cycles [Gokce 2004]. Microscopic examination showed that the interfacial transition zone (ITZ) cracking ratio was significantly higher for all non air-entrained concretes [Gokce 2004]. Micro-crack development and propagation was due to the non air-entrained adherent mortar [Gokce 2004].

RCA concrete had a greater weight gain compared to virgin concrete. This is due to having a higher level of absorption and permeability [Salem 2003]. Use of SCMs can improve the F/T resistance of the RCA since it decreases permeability [Gokce 2004]. Increasing fly ash content significantly improved F/T resistance [Salem 1998]. Adding other SCM's, such as silica fume and 10% metakolin, to non air-entrained concrete improved the F/T resistance. Only the metakolin was able to improve the durability enough to exceed 300 cycles [Gokce 2004].

There are several other factors that have been identified as affecting F/T resistance. First, reducing the amount of adherent mortar on the RCA results in a limited benefit [Gokce 2004]. Second, RCA made from high performancy concrete resulted in improved F/T resistance for the RCA concrete [Ajdukiewicz 2002]. Third, decreasing the w/c ratio also improves F/T results [Salem 2003]. Finally, presoaking the RCA had a negative effect on F/T resistance of the RCA concrete. The best F/T resistance was in concrete made with only coarse RCA and virgin fines, followed by not presoaked, full RCA concrete and last full RCA concrete that was presoaked [Zaharieva 2004].

#### 2.2.4.13 Dry Shrinkage

The loss of moisture from the surface of hardened concrete leading to slab shrinkage may result in cracking [Mehta 2006]. RCA concrete has a greater amount of dry shrinkage compared to virgin concrete [Ajdukiewicz 2002, Tavakoli 1996b, Hansen 1985]. The increase in dry shrinkage for RCA concrete compared to virgin concrete ranges from 20-90% [Hansen 1985]. One study showed that RCA concrete had a dry shrinkage of 0.7 to 0.8 mm/m compared to virgin concrete with a dry shrinkage of 0.27 mm/m [Katz 2003]. The amount of dry shrinkage increases with the amount of RCA used in the concrete [Poon 2002]. The method of dry shrinkage is the same for RCA and virgin aggregate [Tavakoli 1996b].

Metallic fibres can be used to decrease strain at the interface between dry and moist concrete thereby reducing the number and severity of dry shrinkage cracks. At 600 days, RCA concrete containing metallic fibres had a 15% reduction in dry shrinkage compared to RCA concrete without metallic fibres [Mesbah 1999]. Polypropylene fibres actually increased dry shrinkage [Mesbah 1999]. When tested for restrained shrinkage, metallic fibres were most effective in minimizing the number of cracks and crack width compared to polypropylene fibres or no fibres. After 50 days, RCA concrete with 1% metallic fibres had a crack width of 0.14 mm, RCA concrete with 15%

polypropylene had a crack width of 0.24 mm and RCA concrete without metallic fibres had a crack width of 1.07 mm [Mesbah 1999].

There are several other factors that affect dry shrinkage. First, the amount of dry shrinkage was increased when 20% slag was added to the RCA concrete using the same w/c ratio [Sagoe-Crentsil 2001]. Second, increasing w/c ratio causes an increase in shrinkage [Tavakoli 1996b]. Third, the more mortar attached to the RCA the greater the amount of shrinkage. This is due to the increase in water absorption [Tavakoli 1996b]. Finally, increasing the maximum size of the RCA reduces the amount of shrinkage [Tavakoli 1996b]. The exact properties of the RCA are dependant on the original concrete and the RCA [Tavakoli 1996b].

#### 2.2.4.14 Alkali-Aggregate Reactivity

Aggregates that contain certain forms of silica or carbonates react with alkali hydroxides in the concrete producing an expansive gel [CAC 2002]. RCA concrete had increased AAR susceptibility. However, at one year the RCA mixes are considered non reactive [Shayan 2003]. Adding 25% fly ash to RCA concrete mitigated the alkali-silica reactivity to acceptable levels; however, fifteen percent fly ash was not significantly improve levels [Li 2006].

#### 2.2.4.15 Corrosion

The corrosion potential of steel is found using the half cell potential test which measures the voltage difference between the steel and a reference electron [Mehta 2006]. Corrosion usually results from exposure to sulfate, chloride and carbonates. Both virgin concrete and RCA concrete had a very low corrosion risk using the half cell potential test [Shayan 2003].

#### 2.2.4.16 Depth of Carbonation

Carbonation is the process by which carbon dioxide in the air penetrates the concrete and reacts with hydroxide to form carbonates. Once carbonates form, they decrease the pH of the concrete resulting in decreased corrosion protection for the reinforced steal [CAC 2002]. The depth of carbonation is 1.3-2.5 times greater for RCA concretes compared to virgin concretes [Katz 2003, Shayan 2003].

#### 2.2.4.17 Sulfate Resistance

The ability of concrete to resist penetration of sulfates from soil or water that reacts with the hardened cement paste resulting in strength loss [CAC 2002]. The standard for sulfate resistance, according to ASTM C 157, is expansion should be less than 0.1% at six months, or for high resistance expansion should be less than 0.05% at 6 months and 0.1% at one year [Shayan 2003]. RCA has better sulfate resistance than virgin aggregate. Generally expansion is below 0.025% at one year [Shayan 2003].

#### 2.2.4.18 Chloride Content

The ACI 201 recommends that cement for reinforced concrete in a moist environment and exposed to chloride have less than 0.1% soluble chloride ion, cement for reinforced concrete in a moist environment without exposure to chloride have a less than 0.15% soluble chloride ion, and concrete in a dry environment has no recommended limit [Hansen 1984]. Chlorides are usually introduced from concrete that was exposed to deicing chemicals. Coarse RCA had a chloride content of 0.07 to 0.09% and fine RCA had an approximate chloride content of 0.03% [ACPA 1993]. Both of these values are below the ACI recommended values. However, one study reported 0.69% soluble chloride ion by weight of cement for RCA concrete which is above the ACI recommended value [Hansen 1984].

#### 2.2.4.19 Chloride Penetration

Chloride penetration is the depth to which chloride penetrates when concrete is exposed to a chloride source such as deicing chemicals. This results in corrosion of the steel reinforcement. Penetration for RCA concrete was 2.3 mm and 2.2 mm deeper than virgin concrete for a fifteen percent NaCl solution for ten cycles and a five percent NaCl solution continuous for 112 days respectively [Shayan 2003].

#### 2.2.4.20 Chloride Conductivity

Chloride conductivity is the rate at which chloride ions diffuse into the concrete [Olorunsogo 2002]. Conductivity increases as RCA content increases [Olorunsogo 2002]. After curing for 56 days, virgin concrete and 50% RCA concrete had a very poor chloride conductivity rating and 100% RCA had a good rating [Olorunsogo 2002]. This is likely due to cracks and fissures in the attached mortar of RCA allowing fluid to pass easily through [Olorunsogo 2002]. In general, conductivity decreases as the length of curing increases [Olorunsogo 2002].

#### 2.2.4.21 Water Absorption

Water absorption measures how much water is absorbed into the concrete by capillary action [Olorunsogo 2002] [CAC 2002]. RCA concrete has higher water absorption. One study showed the water absorption of RCA concrete to be 7.2% compared to 3.8% in the virgin concrete [Katz 2003]. A second study states that the water absorption of RCA concrete was, on average, 25% greater than virgin concrete [Sagoe-Crentsil 2001]. As the amount of RCA in the concrete increases, so does the water absorption [Olorunsogo 2002]. The longer the concrete is allowed to cure, the lower the water absorption [Olorunsogo 2002].

#### 2.2.4.22 Permeability

The permeability of concrete is a measure of the passage of fluids or gases [CAC 2002]. The permeability of RCA concrete is highly variable and is approximately 10% to 45% higher than virgin

aggregate [Abou-Zeid 2005, Zaharieva 2003]. In general, RCA concrete has a higher w/c ratio due to water absorption by the aggregate. This water evaporates during curing resulting in greater porosity [Zaharieva 2003]. Increasing the length of curing creates a finer porosity reducing permeability by 50% [Zaharieva 2003].

#### 2.2.4.23 Skid Resistance

Skid resistance is a measure of the frictional characteristics of the pavements surface [TAC 1997]. Virgin concrete has a skid resistance of 98 British Pendulum Number (BPN) where as RCA concrete is higher, ranging from 108 BPN to 114 BPN. There was no significant difference in the skid resistance values when different amounts of RCA where used or when fly ash was added [Poon 2002].

#### 2.2.4.24 Ultra Sound Pulse Velocity

Ultrasound pulse velocity of virgin concrete is approximately 69-70 μs and increases to 92-93 μs for RCA concrete due to a widening of the air voids and a decrease in strength [Topcu 1997].

#### 2.2.4.25 Coefficient of Thermal Expansion

There is conflicting research on the impact of RCA on the coefficient of thermal expansion (CTE). One study showed that RCA containing concrete had higher CTE values of $8.9 \times 10^{-6}$ /$^{o}$C for a cylinder and $11.6 \times 10^{-6}$ /$^{o}$C for a prism compared to other types of coarse aggregate [Yang 2003]. Where as a Federal Highway Administration (FHWA) review of concrete containing RCA identified CTE as one of the characteristics that improved compared to concrete using virgin aggregate [FHWA 2004, Turley 2003].

#### 2.2.4.26 Pore Structure

The average pore radius increases as RCA content increases and is most significant at early age (7-days) and decreases over time (28- and 90-days). Reduction over time is due to the continued hydration of the cement. For example, the pore radius at 90 days for virgin concrete is 18.8 nm, for 30% RCA concrete is 19.6 nm, for 60% RCA is 21 nm, and for 100% RCA is 24.7 nm [Gomez-Soberon 2002].

### 2.2.5 RCA Properties Summary

A summary of RCA properties is provided in Table 2.1. Table 2.2 summarizes the properties of RCA concrete.

**Table 2.1 RCA Material Properties Summary**

| Aggregate Material Properties | Recycle Concrete Aggregate | Key Point |
|---|---|---|
| Shape and texture | 100% crushed faces | |
| | 6.5% adherent mortar (coarse) | Amount of adherent mortar will affect concrete properties |
| | 25% adherent mortar (fine) | |
| Specific gravity | Decreases up to 25% (coarse) | |
| | Decreases up to 35% (fine) | |
| Absorption | 2.0 – 6.0% (coarse) | |
| | 4.0 – 12.0% (fine) | |
| Abrasion resistance | Decreases up to 12% | |

**Table 2.2 RCA Concrete Properties Summary**

| Concrete Material Properties | Recycle Concrete Aggregate | Key Point |
|---|---|---|
| Workability | Decreases at a faster rate | |
| Slump | Decreases at same w/c ratio | Larger water demand for RCA |
| Air content | Increases total air content | Larger volume of entrapped air |
| Initial set time | Comparable results | |
| Final set time | Comparable results | |
| Compressive strength | Decreases up to 40% | Results based on maximum aggregate size and w/c ratio |
| Flexural strength | Comparable to decreases up to 20% | Influential parameter is not clear |
| Bond strength | Decreases up to 20% | |
| Interfacial transition zone | More porous and less dense | Higher porosity and absorption |
| Hardness | Decreases up to 45% | Corresponds to a decrease in compressive strength |
| Modulus of elasticity | Decreases up to 40% | |
| Freeze-thaw resistance | Variable results | Improvements by decreasing w/c ratio and adding a SCM |

| Concrete Material Properties | Recycle Concrete Aggregate | Key Point |
|---|---|---|
| Dry shrinkage | Increases up to 90% | Increases with the amount of RCA used |
| Alkali-aggregate reactivity | Increased susceptibility | |
| Corrosion | Comparable results | Based on half-cell potential reading |
| Depth of carbonation | Increased depth 1.3 – 2.0 times | Lower pH levels |
| Sulfate resistance | Improves resistance | |
| Chloride content | Comparable results | |
| Chloride penetration | Increases depth 2.2 – 2.3 mm | |
| Chloride conductivity | Increases | Increases with the amount of RCA used |
| Water absorption | Increases up to 25% | Increases with the amount of RCA used |
| Permeability | Increases up to 45% | Higher w/c ratio and absorption |
| Skid resistance | Comparable results | |

## 2.3 RCA Concrete Mix Designs

The main concern with using RCA in concrete mixes is the long-term properties of the finished product and the cost of using RCA [Abou-Zeid 2005].

### 2.3.1 Components of concrete mixes

#### 2.3.1.1 Aggregate

Many differences between RCA and virgin aggregate have been discussed in the previous section; however some studies show the differences to be minimal. One study showed no significant difference between the RCA concrete and the virgin concrete at 28-days [Sagoe-Crentsil 2001]. Another study showed that the addition of 20% coarse RCA had no significant difference in the properties and performance of the new concrete [Oikonomou 2005]. The main reason for differences in RCA is due to the attached mortar. There is a relationship between an increase in mortar resulting in a decrease in performance [Tavakoli 1996a]. Another reason for performance differences of RCA concrete is due to the size of the aggregate. Too many RCA fines results in an unworkable mix. The properties of RCA concrete are improved when natural sands are used [Ajdukiewicz 2002]. There are several recommendations in the literature regarding the amount of RCA that should be used in

concrete mixes. These recommendations include using a maximum of 30% coarse RCA to meet strength criteria [Topcu 2003] and a maximum of 50% coarse RCA [poon 2003]. Also, it is suggested that RCA fines be limited to 10 to 20% and natural sand be used for the rest [ACPA 1993]. The RCA fines do not qualify as hydraulic cement [Hansen 1983]. Reducing the maximum size of the aggregate to nineteen millimeter can decrease 'D' cracking [ACPA 1993].

#### 2.3.1.2 SCM

There is conflicting evidence as to how SCM's impact RCA concrete. One study reports that the addition of fly ash reduced compressive strength, flexural strengths and skid resistance while improving dry shrinkage [Poon 2002]. The ACPA suggests that the addition of 20% fly ash can enhance durability [ACPA 1993]. Silica fume greatly improves the concrete strength [Hansen 1983].

### 2.3.2 Mixing Methods

There are two mixing methods used in making concrete, conventional and double mixing method. The double mixing method divides the water into two equal proportions that are added at different stages of the mixing process. This creates areas of high and low w/c ratio paste thereby improving the characteristics of the concrete. The double mixing method increases compressive strength, tensile strength and ITZ strength and decreases ITZ thickness, depth of chloride penetration and depth of carbonation. [Otsuki 2003, Ryu 2002].

### 2.3.3 Testing

#### 2.3.3.1 Aggregate Testing

Table 2.3 presents two existing RCA specifications for use in concrete, the Greek Specification of Concrete Technology (GSCT) and the Japanese Industrial Standards (JIS), and one proposed specification limits for Egypt.

Since RCA is of similar standards to virgin aggregate, it should also be tested for: grain size, specific gravity, density, water absorption, and abrasion resistance [Topcu 1995]. The GSCT also draws attention to the importance of investigate the presence of chlorides, to reduce the potential for an alkali-silica reaction but does not give any specific limits.

**Table 2.3 Summary of RCA Specifications**

| | GSCT[1] | JIS[2,3] | | Egypt[4] |
|---|---|---|---|---|
| | | Coarse | Fine | |
| Specific gravity (kg/m$^3$) | > 2.2 | > 2.5 | > 2.5 | |
| Water absorption (%) | < 3.0 | < 3.0 | < 3.5 | < 7.0 |
| Foreign ingredients (%) | < 1.0 | < 1.0 | < 1.0 | |
| Foreign ingredients (kg/m$^3$) | | | | 2 – 10 |
| Organic ingredients (%) | < 0.5 | | | |
| Sulphate ingredients (%) | < 1.0 | | | |
| Amount of sand (%) | < 5.0 | | | |
| Amount of filler (%) | < 2.0 | | | |
| LA abrasion (%) | < 40.0 | < 35.0 | | 40 – 50 |
| Soft granulars | < 3.0 | | | |
| Soundness loss (%) | < 10.0 | | | |
| Sand equivalent (%) | > 80.0 | | | |
| Solid volume (%) | | < 55.0 | < 53.0 | |
| Material passing 75 μm (%) | | < 1.0 | < 7.0 | |
| 10% fineness value (kN) | | | | 50 – 150 |
| Chloride content | | < 0.04 | < 0.4 | |
| ASR | | Harmless | Harmless | |
| Flakiness index (%) | | | | 40 |

1. [Oikonomou 2005], 2. [Kuroda 2005], 3. [Noguchi 2005], 4. [Kamel 2008]

### 2.3.3.2 Concrete Testing

Table 2.4 shows the maximum amount of harmful substances that should be allowed in RCA concrete [Oikonomou 2005].

**Table 2.4 Maximum Limit of Harmful Substances Allowed in RCA Concrete**

| Element | As | Pb | Cd | Cr | Cu | Ni | I | Zn |
|---|---|---|---|---|---|---|---|---|
| Limit (mg/L) | 50 | 100 | 5 | 100 | 200 | 100 | 2 | 400 |

### 2.3.4 Mix Designs with RCA

Standard mix designs have been created as shown in Table 2.5 [Kuroda 2005]. Based on the type of RCA being used and the strength required, the w/c ratio and component amounts are given.

**Table 2.5 RCA Mix Designs**

| Aggregate Type | | Strength | w/c | Unit Weight (kg/m$^3$) | | | |
|---|---|---|---|---|---|---|---|
| Coarse | Fine | (MPa) | ratio | Cement | Water | Coarse | Fine |
| Recycled | Recycled | 27 | 0.517 | 323 | 167 | 1011 | 792 |
| | | 30 | 0.484 | 347 | 168 | 1011 | 769 |
| | | 33 | 0.455 | 374 | 170 | 1011 | 743 |
| Virgin | Recycled | 27 | 0.544 | 320 | 174 | 972 | 829 |
| | | 30 | 0.504 | 345 | 174 | 972 | 808 |
| | | 33 | 0.470 | 372 | 175 | 972 | 783 |
| Recycled | Virgin | 27 | 0.517 | 323 | 167 | 1080 | 722 |
| | | 30 | 0.484 | 347 | 168 | 1080 | 699 |
| | | 33 | 0.455 | 374 | 170 | 1080 | 673 |

Using the standard ACI mix design procedure with 100% RCA, the compressive strength at 28-days was reduced by ten percent. Other mix design methods generally have a 20% to 30% reduction in compressive strength [Bairagi 1990]. To compensate for the reduction in compressive strength when using RCA, an additional eight to thirteen percent of cement can be added [Bairagi 1990]. Traditionally the cement content of RCA concrete is increased using conventional volumetric mix proportioning ignoring the adherent mortar content of the RCA [Abbas 2008, Fathifaz 2008]. A new approach, equivalent mortar volume (EMV), looks at RCA as a two phase material of original aggregate and adherent mortar. This process accounts for a change in the mortar content, decreasing the amount of cement required [Abbas 2008]. Equation 2.3 is used to determine the EMV of RCA [Fathifazl 2008].

Using the EMV method, a conventional mix that requires 400kg/m3 of cement would be reduced to 337-354 kg/m$^3$ of cement [Abbas 2008]. At a constant w/c ratio, the EMV method provides improved fresh properties (slump and density), improved hardened properties (strength, elastic modulus, and creep) and better durability (F/T, chloride penetration) compared to the conventional method [Abbas 2008, Fathifazl 2008].

$$V_{RCA}^{RAC} = \frac{V_{NA}^{NAC} \times (1 - R)}{(1 - RMC)\left(\frac{SG_b^{RCA}}{SG_b^{VA}}\right)} \quad (2.3)$$

where: $V_{RCA}^{RAC}$ = volume fraction of the coarse RCA in recycled aggregate concrete

$V_{NA}^{NAC}$ = volume fraction of the natural aggregate in the normal concrete

$R$ =is the volumetric ratio of natural aggregate in RAC to normal concrete

$SG_b^{RCA}$ = bulk specific gravity of the RCA

$SG_b^{VA}$ =bulk specific gravity of the virgin aggregate

### 2.3.5 Pavement Performance

There are several studies showing the performance of RCA containing concrete. A study of 5 state highway agencies using RCA in paving applications showed comparable performance to conventional pavement; however, a difference in load transfer efficiency was observed due to the adherent mortar causing an increase in dry shrinkage and decrease in CTE [Cuttell 2008] . At the University of Central Florida's Circular Accelerated Test Track no distresses were observed for the RCA mixes (0%, 25%, 75%, and 100%) despite having lower compressive, flexural, and tensile strengths [Chini 2001]. The FHWA states that "when appropriately used recycled materials can effectively and safely reduce cost, save time, offer equal or, in some cases, significant improvements to performance qualities, and provide long-term environmental benefits" [FHWA 2007].

## 2.4 Implementation of RCA Use … Steps in the Right Direction … Going Green

"What started as a demand by a few environmentalists has now been adopted by the public at large and by governments on local, State, and national levels. Even owners and developers have discovered that "going green" is not only accepted now as politically correct or as a source of intangible benefits and good publicity, but it also is a way for them to improve their bottom line". [Meyer 2008]

### 2.4.1 FHWA Recycled Materials Policy

The FHWA has developed a Recycled Materials Policy as an initial step to increasing RCA use. The Recycled Materials Policy is made up of the following five points [FHWA 2007].

1. Recycling and reuse can offer engineering, economic and environmental benefits.
2. Recycled materials should get first consideration in materials selection.
3. Determination of the use of recycled materials should include an initial review of engineering and environmental suitability.
4. An assessment of economic benefits should follow in the selection process.

5. Restrictions that prohibit the use of recycled materials without technical basis should be removed from specifications.

### 2.4.2 LEED Program

The Leadership in Energy and Environmental Design (LEED) program is a point rating system (69 maximum) to evaluate the environmental performance of a structure and encourage market transformation towards sustainable design [USGBC 2005]. There are four levels of LEED certification. Achieving 26-32 points is classed as certified, 33-38 points achieves silver, 39-51 points achieves gold, and over 52 points achieves the platinum level. The LEED rating system has six categories: sustainable sites, water efficiency, energy and atmosphere, material and resources, indoor environmental quality, and innovation and design process. By using concrete as a building material it is possible to earn between 11-21 points. [PCA – An engineers guide to: building green with concrete]. Having RCA as an aggregate source contributes up to five points with the following credits:

1. MR Credit 4.1 Recycled Content, 10% - 1 point
2. MR Credit 4.2 Recycled Content, 20% - 1 point
3. MR Credit 5.1 Regional Materials, 10% Extracted, Processed & Manufactured – 1 point
4. MR Credit 5.2 Regional Materials, 20% Extracted, Processed & Manufactured – 1 point
5. MR Credit 6 Rapidly Renewable Materials – 1 point

If the RCA is obtained from an onsite source then an additional two points can be achieved due to diverting construction waste from landfill sites. These credits are:

1. MR Credit 2.1 Construction Waste Management, Divert 50% from Disposal, and
2. MR Credit 2.2 Construction Waste Management, Divert 75% from Disposal.

### 2.4.3 Success Stories

#### 2.4.3.1 Lester B. Pearson International Airport (LBPIA)

LBPIA is its own mini-ecosystem encompassing forests, grasslands, creeks, and streams, as well as runways, terminal buildings, and roadways. The GTAA recognizes the need to preserve and protect these natural resources while continuing to meet the demands of a growing air travel industry [GTAA 2007]. LBPIA was the first North American airport to achieve ISO 14001 certification in 1999. In order to obtain this prestigious certificate an Environmental Management System was established for all aspects of airport operations to monitor and improve environmental performance. To reach and maintain this standing the GTAA set goals to make continual improvement, prevent pollution, and comply with legislation. [Seow 2005] During demolition of Terminal 1 and more recently Terminal 2, targets called for a minimum of 80% and 85% respectively of C&D waste (concrete, rubble, metals, wood, and other material) to be reused and recycled. Demolition of Terminal 1 produced 253,000 tonnes of concrete that was 100% recycled. [GTAA 2007, Seow 2005] Recycling was

achieved by establishing an on-site mobile crushing plant to produce 2" minus RCA backfill material (similar to the gradation of a Granular B) for the new terminal's apron subbase [Seow 2005].

#### 2.4.3.2 Stapleton International Airport

In 1995, when Stapleton International Airport in Denver was decommissioned, enough concrete and asphalt recycled material was produced to construct approximately 10,000 miles of two lane roadway [Meyer 2008].

#### 2.4.3.3 Texas Department of Transportation (TxDOT)

The TxDOT has used RCA as an aggregate source for new concrete pavements and as a base material since the early 1990s. [Harrington 2004] The switch to using RCA was achieved through training and information sessions to dispel the perception that RCA is a substandard or waste material.

#### 2.4.3.4 Minnesota Department of transportation (MnDOT)

The MnDOT recycles close to 100% of the concrete from its pavements and uses it as a base material [Harrington 2004].

#### 2.4.3.5 Michigan Department of Transportation (MDOT)

The MDOT has successfully used RCA as a base and subbase material on I-75, I-94, and I-95, US 41 [Harrington 2004].

# Chapter 3
# Materials and Test Mixes

This chapter discusses the materials that are used in the research.

## 3.1 Aggregate Sources

### 3.1.1 Sources of Virgin Coarse Aggregate

In this research, two virgin coarse limestone aggregates were supplied by Dufferin Construction. The 37.5 mm minus aggregate came from Dufferin's Acton Quarry, Sand, and Gravel Pit, and the 19.0 mm minus aggregate came from Dufferin's Milton Quarry, Sand, and Gravel Pit.

### 3.1.2 Sources of Recycled Coarse Aggregate

The coarse recycled concrete aggregate (RCA) in this research was sourced from decommissioned concrete sidewalks, curbs and gutters from the Region of Waterloo. The original curb and gutter concrete had been cured properly with a maximum aggregate size of 19 mm, adequate air-entrainment, and a compressive strength in excess of 30 MPa at 28-days. The concrete sidewalks, curbs and gutters were chosen as the source or RCA since it did not contain foreign material and had a maximum aggregate size of 19 mm. Since the concrete that the RCA was crushed from contained a maximum aggregate size of 19 mm, this was the maximum size of the RCA that was used. Any RCA over 19 mm would contain excess interfacial transition zones that would negatively impact the strength of the concrete. Figure 3.1 shows the waste concrete prior to being crushed and the resulting coarse aggregate that was used in the study.

**Figure 3.1 Waste Concrete and Recycled Aggregate**

### 3.1.3 Source of Virgin Fine Aggregate

Natural sand was used as fine aggregate since it provides a greater strength than fine RCA [ACPA 1993]. The fine RCA contains many impurities and results in strength loss in the concrete. Virgin fine aggregate (natural sand) was supplied by Dufferin Construction from the Blair Quarry, Sand, and Gravel Pit.

## 3.2 Aggregate Testing

### 3.2.1 MTO Guidelines for Aggregate

In Ontario, the material specification for aggregates to be used in concrete is given in MTO Ontario Provincial Standards Specification (OPSS) 1002. The MTO gradation limits and properties for coarse aggregates used in concrete pavements are given in Table 3.1 and Table 3.2 respectively. Table 3.3 and Table 3.4 summarize the gradation limits and properties for fine aggregate.

**Table 3.1 Coarse Aggregate Gradation Limits**

| Sieve Size | Percent Passing | | |
|---|---|---|---|
| | 37.5 mm | 19.0 mm | Combined |
| 53.0 mm | 100 | - | 100 |
| 37.5 mm | 90-100 | - | 95-100 |
| 26.5 mm | 20-55 | 100 | - |
| 19.0 mm | 0-15 | 85-100 | 35-70 |
| 9.5 mm | 0-5 | 20-55 | 10-30 |
| 4.75 mm | - | 0-10 | 0-5 |

**Table 3.2 Limits of Coarse Aggregate Properties**

| Test | Limit |
|---|---|
| Material Finer than 75μm, by Washing (% maximum) | 2 |
| Absorption (% maximum) | 2 |
| Unconfined Freeze-Thaw Loss (% maximum) | 6 |
| Flat and Elongated Particles (% maximum) | 20 |
| Petrographic Number (maximum) | 125 |
| Micro-Deval Abrasion (% maximum loss) | 14 |
| Accelerated Mortar Bar (% maximum at 14 days) | 0.15 |

| Test | Limit |
|---|---|
| Potential Alkali-Carbonate Reactivity of Quarried Carbonate Rock | Non-Expansive |
| Concrete Prism Expansion (% maximum at 1 year) | 0.04 |

1. 1% for gravel

**Table 3.3 Fine Aggregate Gradation Limits**

| Sieve Size | Percent Passing |
|---|---|
| 9.5 mm | 100 |
| 4.75 mm | 95-100 |
| 2.36 mm | 80-100 |
| 1.18 mm | 50-85 |
| 600 μm | 25-60 |
| 300 μm | 25-60 |
| 150 μm | 0-10 |
| 75 μm[1] | 0-3 |

1. 0-6% for manufactured sand

**Table 3.4 Limits of Fine Aggregate Properties**

| Test | Limit |
|---|---|
| Organic Impurities (maximum organic plate number) | 2 |
| Micro-Deval Abrasion (% maximum loss) | 20 |
| Accelerated Mortar Bar (% maximum at 14 days) | 0.15 |
| Concrete Prism Expansion (% maximum at 1 year) | 0.04 |

### 3.2.2 Aggregate Test Results

Coarse and fine virgin aggregate testing was conducted at Dufferin Aggregates as part of their on going quality assurance (QA)/quality control (QC) process. Tests conducted in preparation for mixture proportioning included: absorption, bulk relative density, and gradation for all aggregates. Coarse RCA was also tested for crushed particles, flat and elongated particles, and micro-deval to better characterize the material properties. Figures 3.2 – 3.13 present the aggregate test results. The virgin aggregate is described by the results of the last 20 QA/QC periods as shown by the green

squares and blue diamonds. The MTO acceptance limit is shown as a solid line, and the RCA value is shown as the gray triangle at the right of the figure when available.

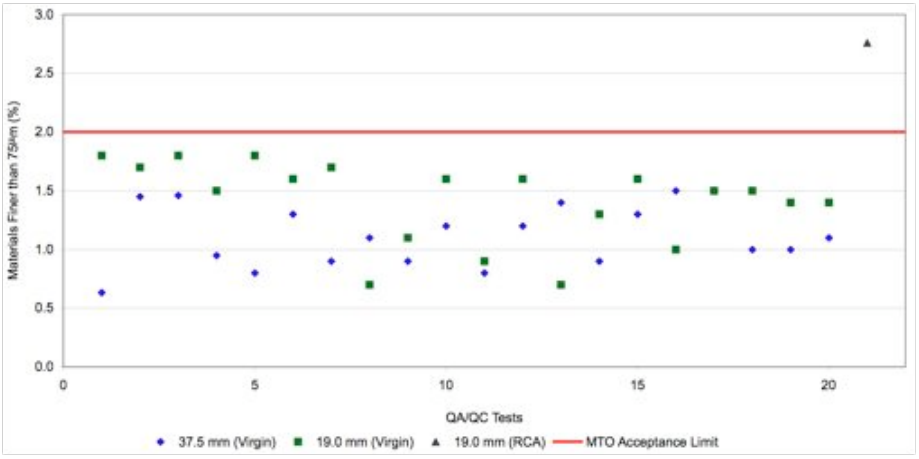


**Figure 3.2 Materials Finer than 75µm Test Results**

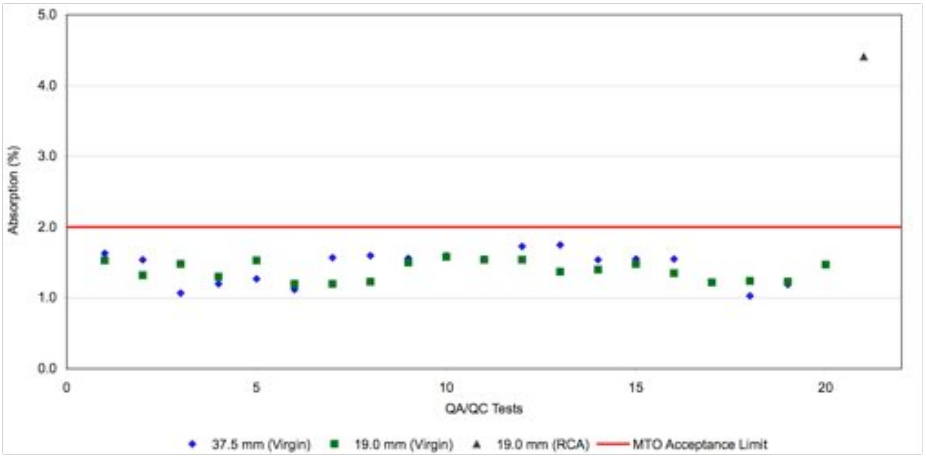


**Figure 3.3 Absorption Test Results**

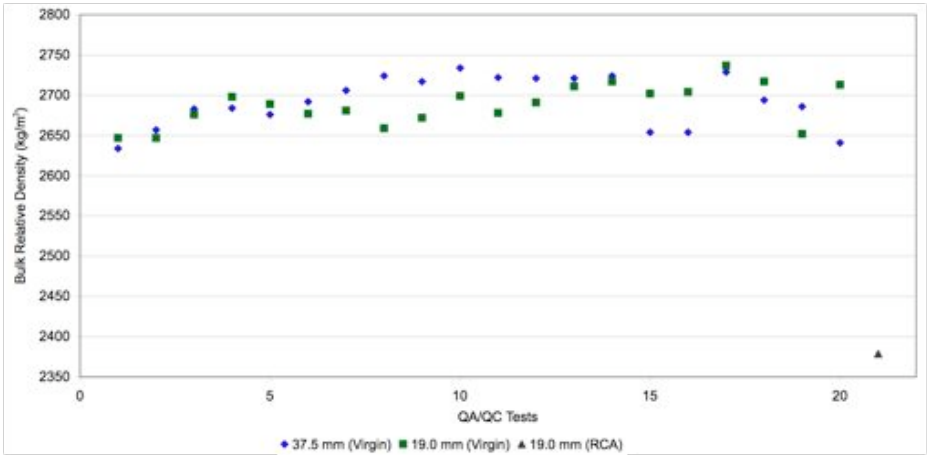


**Figure 3.4 Bulk Relative Density Test Results**

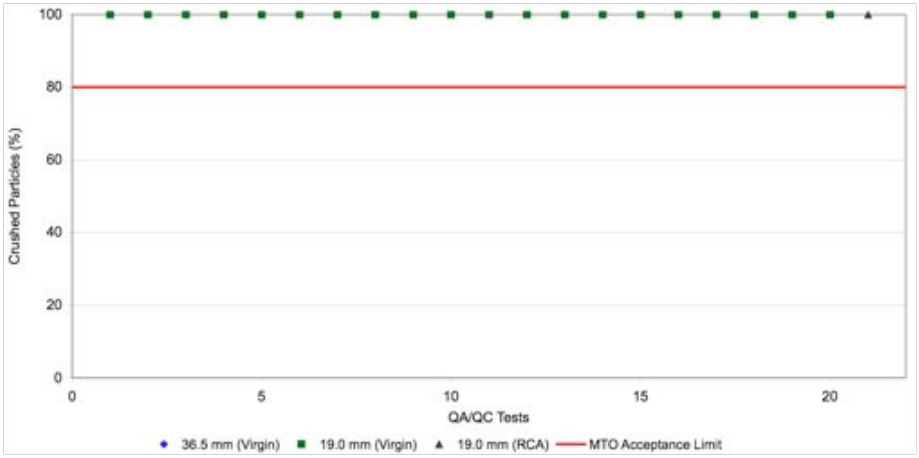


**Figure 3.5 Crushed Particles Test Results**

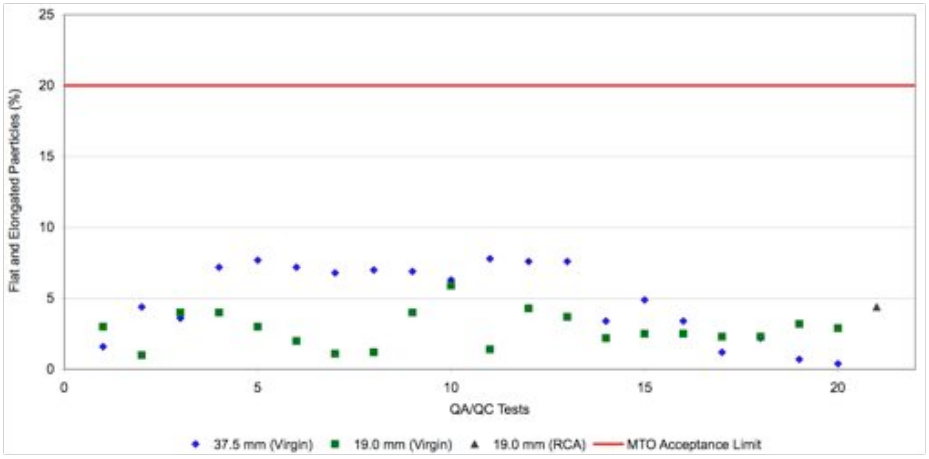


**Figure 3.6 Flat and Elongated Test Results**

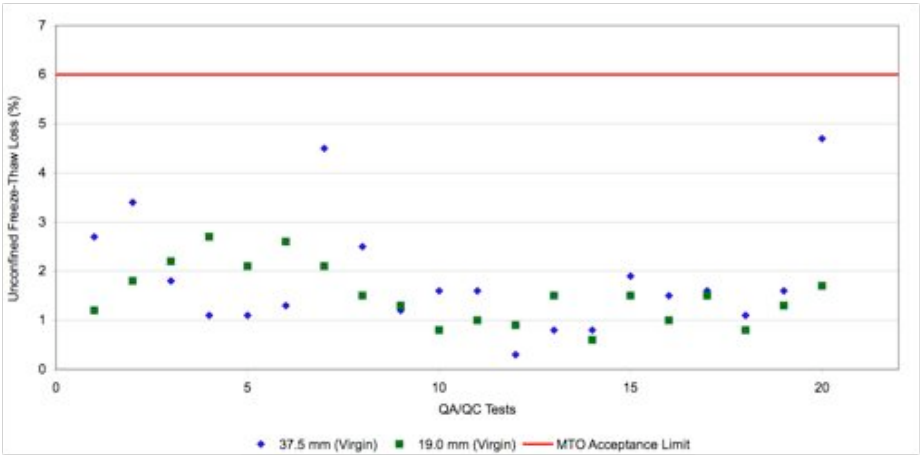


**Figure 3.7 Unconfined Freeze-Thaw Loss Test Results**

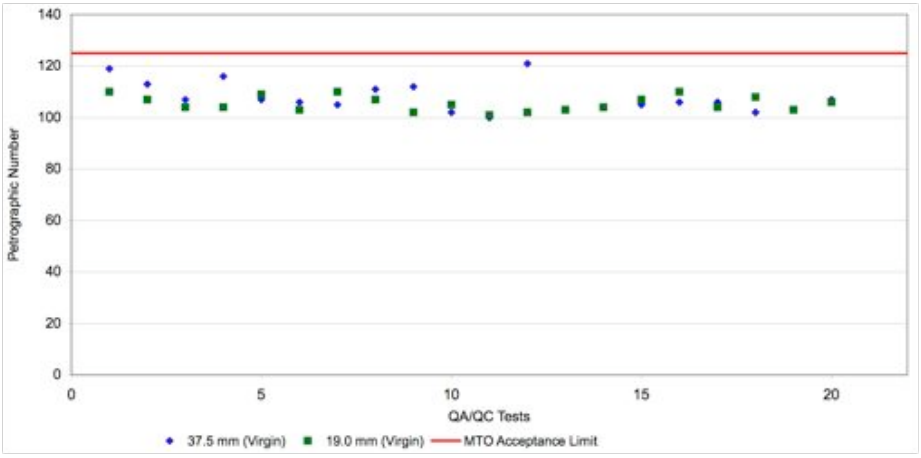


**Figure 3.8 Petrographic Number Test Results**

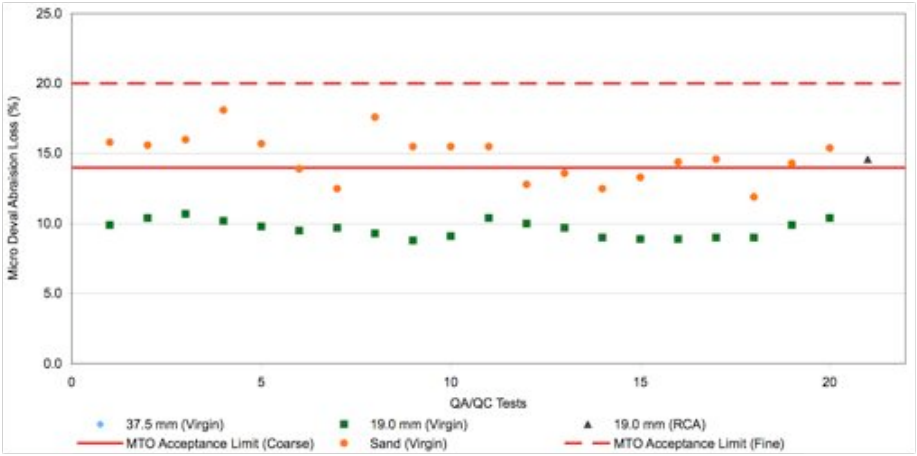


**Figure 3.9 Micro-Deval Abrasion Loss Test Results**

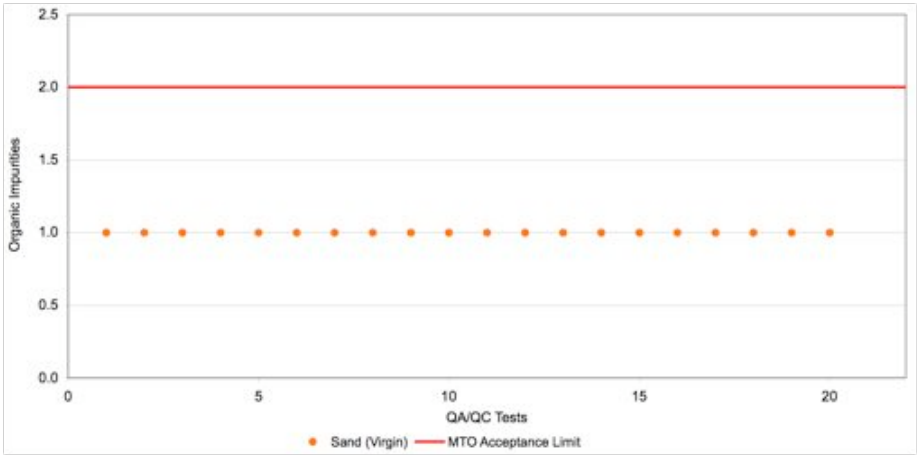


**Figure 3.10 Organic Impurities Test Results**

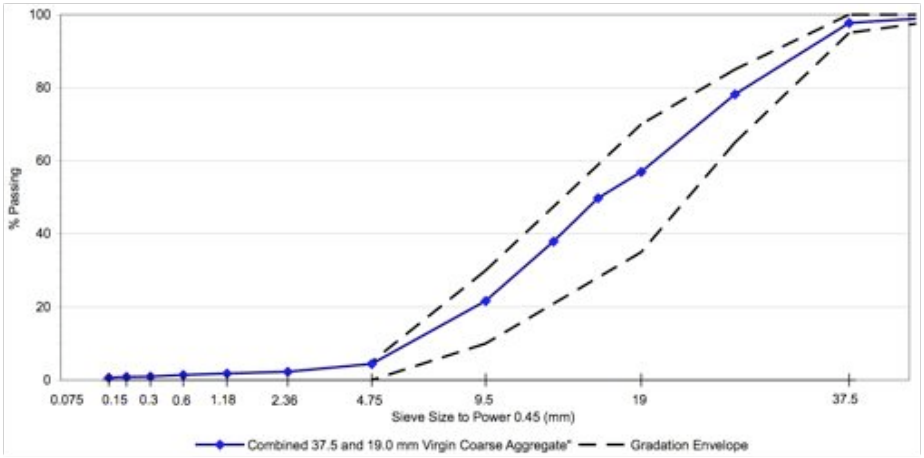


**Figure 3.11 Combined 37.5 mm and 19.0 mm Virgin Coarse Aggregate Gradation**

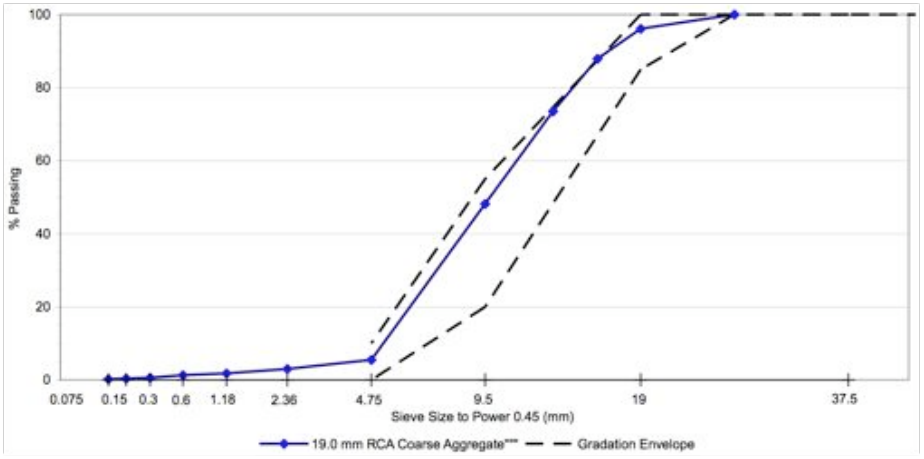


**Figure 3.12 19.0 mm minus RCA Coarse Aggregate Gradation**

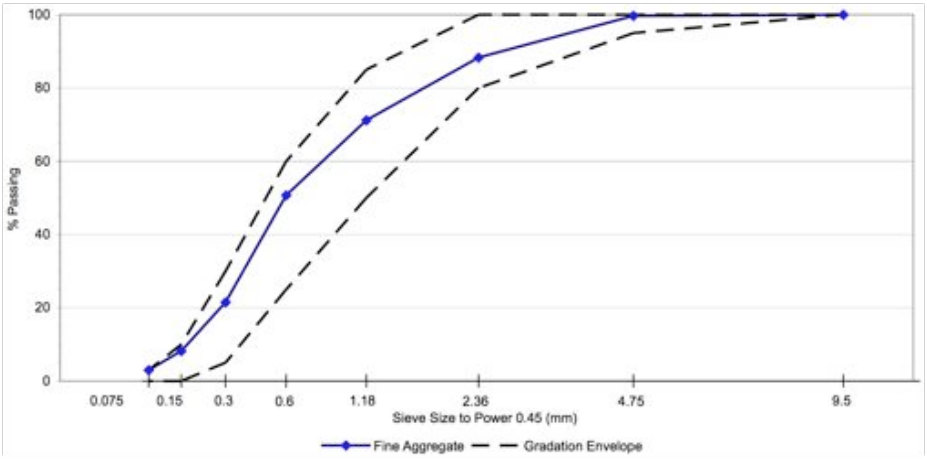


**Figure 3.13 Fine Aggregate Gradation**

Using the MTO OPSS virgin aggregate standards, the coarse RCA would have been rejected because it exceeded the allowable limits for absorption, material finer than 75 μm, and Micro-Deval.

## 3.3 Cement and Slag

The cement used for all concrete mixes in this research was St. Marys Cement General Use (GU) also known as Type 10. This cement is 53% tricalcium silicate ($C_3S$), 18% dicalcium silicate ($C_2S$), seven percent tricalcium aluminate ($C_3A$), and eight percent tetracalcium aluminoferrite ($CA_4F$) [St Marys Cement 2007]. As given by the manufacturer, the Blaine fineness is 410 $m^2$/kg and the compressive strength gain of neat paste is shown in Figure 3.14.

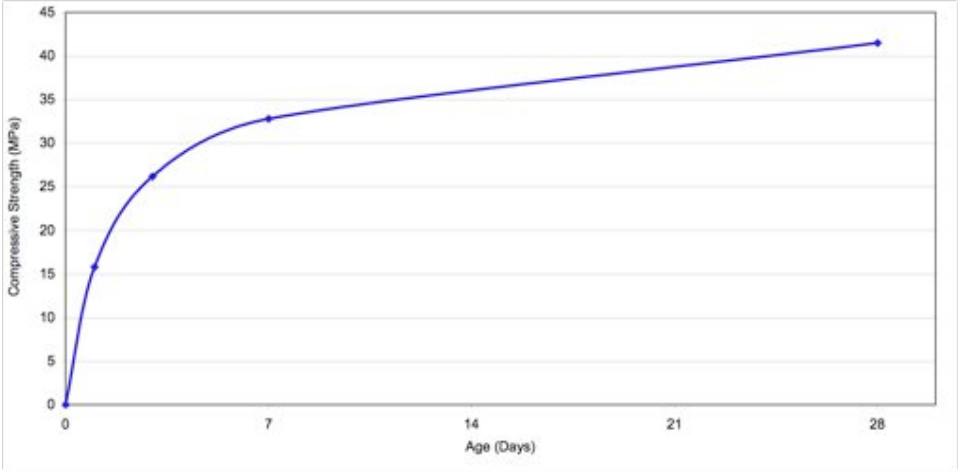


**Figure 3.14 Compressive Strength Development of Neat Paste**

St. Mary's Cement ground granulated blast furnace slag (GGBFS), with a Blain fineness of 532 $m^2/kg$, was used for all concrete mixes in this project. The benefits of GGBFS include that it has cementious properties, lowers the heat of hydration, increases durability and improves long-term strength.

## 3.4 Air Entrainment

Air entrainment provides freeze-thaw (F/T) resistance through the creation of a microscopic air void system distributed throughout the concrete. It also improves the fresh properties of the concrete mix by increasing workability, reducing segregation, and reducing bleeding. Euclid Airex-L was used in all mixes at a dose of 55 ml/100 kg of cement to achieve adequate air entrainment.

## 3.5 Water Reducer

Reducing the water in concrete using a water-reducing admixture is beneficial by providing more lubrication allowing for easier handling and finishing, increased strength and durability, and reduced shrinkage and permeability. Euclid Eucon WR was used in all mixes at a dose of 250 ml/100 kg.

## 3.6 Open Graded Drainage Layer

The field test sections had an asphalt stabilized open graded drainage layer (ODGL), design by Construction Testing Asphalt Lab Ltd. The asphalt contained PG 58-28 asphalt cement (AC) at 1.8%, Hot-Laid (HL) 8 stone with 1.07% absorption resulting in a bulk relative density of 2684 $kg/m^3$. The gradation of the asphalt stabilized open graded drainage layer are based on MTO Special Provision No. 313F07 and is shown in Figure 3.15. The primary purpose of the ODGL is to allow moisture that has infiltrated the pavement to drain away from the structure.

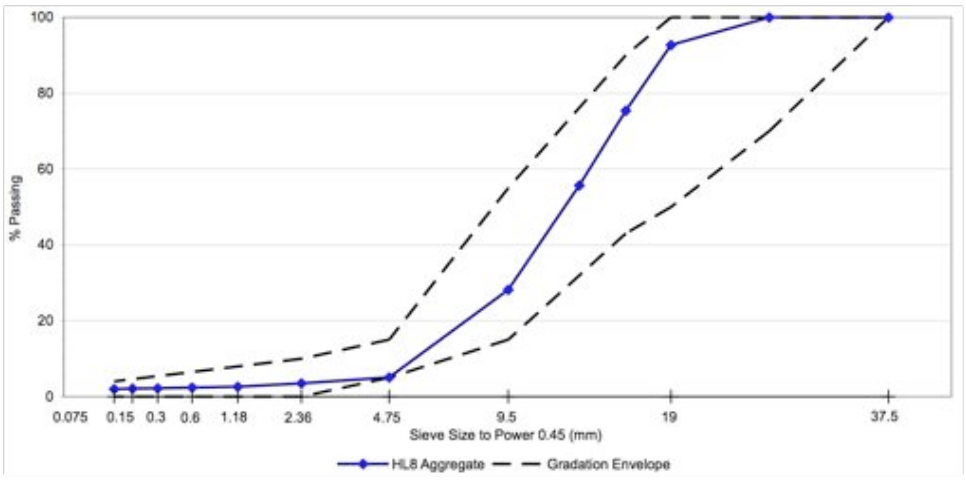


**Figure 3.15 HL8 Gradation for Asphalt Stabilized Open Graded Drainage layer**

## 3.7 Concrete Mixture Design

The CPATT test track is located at the Region of Waterloo Waste management Facility in Waterloo, Ontario, Canada. Waterloo is in the Southern part of Ontario, approximately three hours from the Windsor –Detroit border. It is located in a wet freeze zone with typical annual frost depths of 1.2 m. Figure 3.16 shows the average daily temperature and the average monthly precipitation from 1998 to 2006.

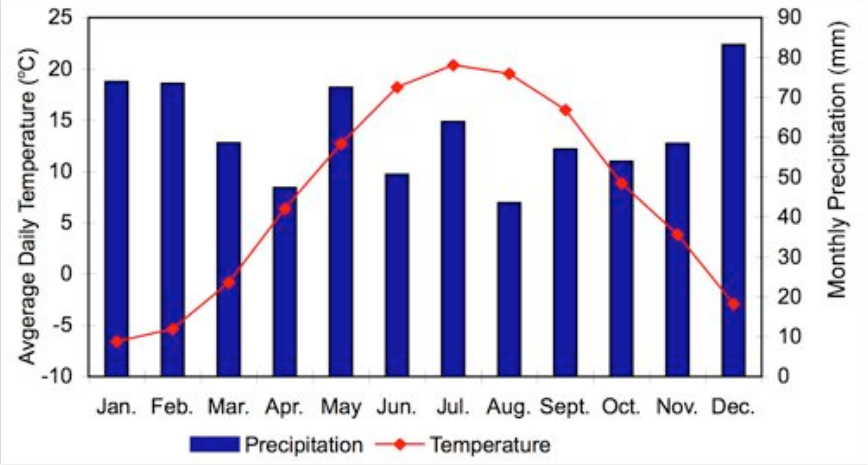


**Figure 3.16 Waterloo Climograph**

The weather conditions at the test track produce a freeze-thaw environment. The Canadian Standards Association (CSA) recommends that plain concrete in this type of freeze-thaw environment should meet the guidelines for an exposure level of C-2. The C-2 exposure level is defined as a plain concrete (no structural reinforcement) that is exposed to both chlorides and freezing/thawing [CSA 2000]. Based on the exposure level of C-2 the concrete must meet CSA A23.1 standard that includes the follow criteria [CSA 2000]:

- A water cement ratio less than 0.45,
- A 28-day compressive strength greater than 32 MPa,
- A maximum aggregate size of 14 to 20 mm, and
- An air content of 5% to 8%.

The American Concrete Pavement Association (ACPA) further recommends [ACPA 1993]:

- A cement content greater than 335 kg/m$^3$,
- A slump less than 100 mm,
- A well-graded aggregate, and
- Use of a curing compound.

Both the CSA and ACPA criteria were used as guidelines for optimzing the concrete mixture design. However, in order to increase the durability of concrete pavements for highway application, the MTO OPSS 1002 recommends increasing the aggregate to a maximum size of 37.5 mm. The MTO OPSS 1350 also recommends replacing 25% of the cement content by mass with GGBFS to increase durability and reduce costs.

As per the CSA standard, the final mix should achieve a compressive strength value of 32 MPa at 28 days. In order to reduce costs, the lowest cement content that reaches 32MPa at 28 days will be used even if it is less than the 335kg/$m^3$ recommended by ACPA. Three cement contents were chosen for initial testing 315 kg/$m^3$, 330 kg/$m^3$, and 345 kg/$m^3$.

## 3.8 Concrete Mixture Proportioning

The mixture components were calculated using the absolute volume proportioning method. The aggregate was proportioned as per MTO OPSS using 65% coarse and 35% fine aggregate. Table 3.5 presents the material characteristics used in the mixture proportioning.

**Table 3.5 Material Properties Used in Concrete Mixture Proportioning**

| Material | BRD[1] (kg/$m^3$) | Absorption (%) | Moisture Content (%) | Fineness Modulus |
|---|---|---|---|---|
| 37.5 mm Virgin Coarse Aggregate | 2641 | 1.47 | 1.2 | - |
| 19.0 mm Virgin Coarse Aggregate | 2713 | 1.47 | 2.7 | - |
| 19.0 mm RCA Coarse Aggregate | 2379 | 4.41 | 1.4 | - |
| Virgin Fine Aggregate | 2683 | 1.16 | 0.34 | 2.6 |
| Cement, General Use | 3140 | - | - | - |
| Slag, Type S | 2920 | - | - | - |
| Water | 1000 | - | - | - |
| Air Entrainment | | | | |
| Water Reducer | | | | |

1. BRD = Bulk Relative Density

### 3.8.1 Proportioning Example

The following is an example of the mix proportioning for the test mix with 15% RCA Coarse Aggregate and a 315 kg/$m^3$ total cement content. The same mixture proportioning procedure is followed for all test mixes.

Cement Content

- Total cement content 315 kg/m$^3$

  Cement $= (315 \times 0.75) = 236\ kg/m^3$

  Slag $= (315 - 236) = 79\ kg/m^3$

- Volume Required

  Cement $= \left(\frac{236}{3140}\right) = 0.075\ m^3$

  Slag $= \left(\frac{79}{2920}\right) = 0.027\ m^3$

Water Content

- 0.42 w/c

  Water $= (0.42 \times 315) = 132\ kg/m^3$

- Required Volume

  Water $= \left(\frac{132}{1000}\right) = 0.132\ m^3$

Air Content

- Required Volume

  Air $= \left(\frac{6}{100}\right) = 0.06\ m^3$

Aggregate Content

- Total Volume

  Aggregate $= \left(1 - (0.075 + 0.027 + 0.132 + 0.06)\right) = 0.706$

- Percent of Aggregate Requires

  37.5 mm Virgin $= (0.65 \times 0.4) \times 100\% = 26.0\%$

  19.0 mm Virgin $= (0.65 \times 0.45) \times 100\% = 29.25\%$

  19.0 mm RCA $= (0.65 \times 0.15) \times 100\% = 9.75\%$

  Sand $= \left(1 - (0.26 + 0.2925 + 0.0975)\right) \times 100\% = 35.0\%$

- Volume of Aggregate Required

| | |
|---|---|
| 37.5 mm Virgin | $= (0.706 \times 0.26) = 0.184\ m^3$ |
| 19.0 mm Virgin | $= (0.706 \times 0.2925) = 0.206\ m^3$ |
| 19.0 mm RCA | $= (0.706 \times 0.0975) = 0.069\ m^3$ |
| Sand | $= (0.706 \times 0.35) = 0.247\ m^3$ |

- Mass of Aggregate

| | |
|---|---|
| 37.5 mm Virgin | $= (0.184 \times 2641) = 485\ kg$ |
| 19.0 mm Virgin | $= (0.206 \times 2713) = 560\ kg$ |
| 19.0 mm RCA | $= (0.069 \times 2379) = 164\ kg$ |
| Sand | $= (0.247 \times 2683) = 663\ kg$ |
| Total | $= 1872\ kg$ |

Estimated Concrete Density

- Assuming SSD Condition of Aggregates

| | |
|---|---|
| Water | $= 132\ kg/m^3$ |
| Cement | $= 315\ kg/m^3$ |
| 37.5 mm Virgin | $= (485 \times 1.0147) = 492.13\ kg/m^3$ |
| 19.0 mm Virgin | $= (560 \times 1.0147) = 568.23\ kg/m^3$ |
| 19.0 mm RCA | $= (164 \times 1.0411) = 170.74\ kg/m^3$ |
| Sand | $= (663 \times 1.0116) = 670.69\ kg/m^3$ |
| Total | $= 2348.79\ kg/m^3$ |

Moisture Corrections

| | |
|---|---|
| 37.5 mm Virgin | $= (485 \times 1.012) = 490.82\ kg$ |
| 19.0 mm Virgin | $= (560 \times 1.027) = 575.12\ kg$ |
| 19.0 mm RCA | $= (164 \times 1.014) = 166.30\ kg$ |
| Sand | $= (663 \times 1.0034) = 665.25\ kg$ |
| Total | $= 1897.49\ kg$ |

Water To Be Added

| | |
|---|---|
| 37.5 mm Virgin | $= (0.0147 - 0.012) \times 485 = 1.31\ kg$ |
| 19.0 mm Virgin | $= (0.0147 - 0.027) \times 560 = -6.89\ kg$ |
| 19.0 mm RCA | $= (0.04411 - 0.014) \times 164 = 4.93\ kg$ |
| Sand | $= (0.0116 - 0.0034) \times 663 = 5.43\ kg$ |
| Water | $= 132 - (1.31 - 6.89 + 4.93 + 5.43)$ |
| | $= 137.08\ kg$ |

Batch Weights

| | |
|---|---|
| Water (to be added) | $= 137.08\ kg$ |
| Cement | $= 236.0\ kg$ |
| Slag | $= 79.0\ kg$ |
| 37.5 mm Virgin | $= 490.82\ kg$ |
| 19.0 mm Virgin | $= 575.12\ kg$ |
| 19.0 mm RCA | $= 166.30\ kg$ |
| Sand | $= 665.25\ kg$ |
| Total | $= 2349.57\ kg$ |

## 3.9 Testing Method

Laboratory testing was carried out on twelve test mixes in order to determine the best mixes to place on the CPATT test track. A four by three factorial design was used consisting of four coarse RCA amounts (0%, 15%, 30% and 50%) and three cement contents (315 kg/m$^3$, 330 kg/m$^3$, and 345 kg/m$^3$). The mixes were proportioned using an absolute volume design method. Table 3.6 summarizes the quantity of each material used in the test mixes based on an aggregate saturated surface dry condition. Values presented in the tables have been adjusted to reflect the moisture content of the aggregates.

Figure 3.17 shows the combined aggregate grading for the four RCA mixes. A ratio of 65% coarse aggregate to 35% fine aggregate was used.

**Table 3.6 Mixture Proportioning Values**

| | Mix | Cement (kg) | Slag (kg) | Water (kg) | 37.5mm Vir. (kg) | 19mm Vir. (kg) | 19mm RCA (kg) | Sand (kg) | Air (ml) | WR (ml) |
|---|---|---|---|---|---|---|---|---|---|---|
| 0% RCA | 1 | 236 | 79 | 130 | 491 | 767 | - | 665 | 173 | 788 |
| | 2 | 247 | 83 | 136 | 482 | 754 | - | 654 | 182 | 825 |
| | 3 | 259 | 86 | 143 | 475 | 742 | - | 644 | 190 | 863 |
| 15% RCA | 1 | 236 | 79 | 137 | 491 | 575 | 166 | 665 | 173 | 788 |
| | 2 | 247 | 83 | 143 | 482 | 566 | 163 | 654 | 182 | 825 |
| | 3 | 259 | 86 | 150 | 475 | 557 | 161 | 644 | 190 | 863 |
| 30% RCA | 1 | 236 | 79 | 144 | 491 | 383 | 332 | 665 | 173 | 788 |
| | 2 | 247 | 83 | 150 | 482 | 377 | 327 | 654 | 182 | 825 |
| | 3 | 259 | 86 | 157 | 475 | 371 | 321 | 644 | 190 | 863 |
| 50% RCA | 1 | 236 | 79 | 154 | 491 | 128 | 553 | 665 | 173 | 788 |
| | 2 | 247 | 83 | 160 | 482 | 126 | 544 | 654 | 182 | 825 |
| | 3 | 259 | 86 | 166 | 475 | 124 | 536 | 644 | 190 | 863 |

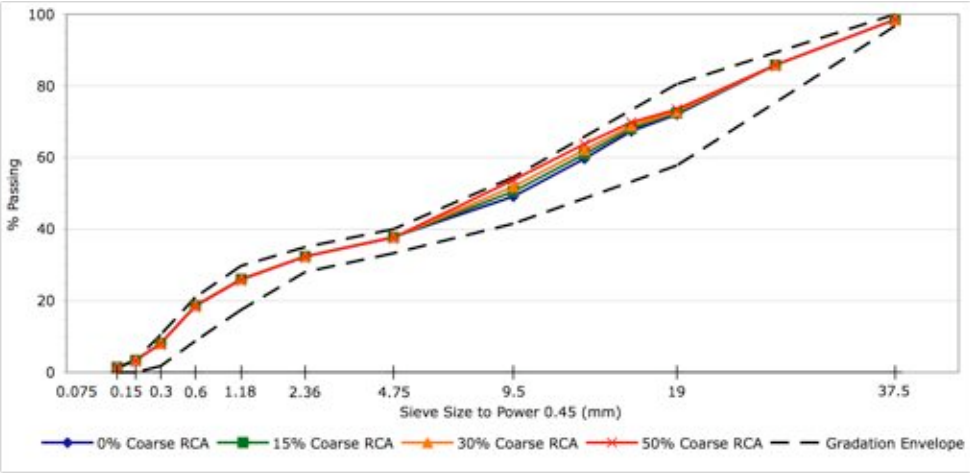


**Figure 3.17 Waste Concrete and Recycled Aggregate Combined Gradation**

The compressive strength development at 28 days will be used to select a cement content that is adequate for placement at the CPATT test track. For each of the twelve test mixes eight cylinders were prepared for compressive strength testing. Compressive strength testing was conducted at five, seven, fourteen, and 28 days. One of the two fourteen-day cylinders was used to conduct a hardened air void analysis. Fresh properties including unit weight, slump, and air content were measured to assess the mix for compliance with mix design.

### 3.9.1 Batching Method

The double mixing method is used to create areas of low w/c paste around the aggregates to improve the strength and durability properties of the concrete. The concrete was batched using a modification of the double mixing method. The double mixing method was modified to separate the addition of the coarse and fine aggregates, and ¼ of the total water was added at each stage. The mixing steps are outlined below:

1. Proportion all coarse aggregate and dry mix
2. Add water (1/4) and mix
3. Add proportioned fine aggregate and mix
4. Add water (1/4), AEA, WRA, and mix
5. Add cement and slag and mix
6. Add remaining water (1/2)
7. Mix and discharge,

A total of 0.06 $m^3$ (2.12 $ft^3$) of concrete was made for each of the twelve test mixes to perform fresh property and compressive strength testing. The concrete was mixed in a portable drum mixer. Each mix combination was batched in two 0.03 $m^3$ quantities. The first batch was mixed and the fresh properties of unit weight, air content, and slump were measured. Then, the first batch sat while the second batch was mixed. Based on the fresh properties of the first batch, adjustments were made to the amount of water in the second batch. The batches were then combined and mixed for approximately three minutes. The fresh properties of the combined mix were taken and cylinders were cast. For each of the twelve mixes, eight cylinders were cast in order to test for compressive strength and perform an air void analysis. The batching was performed on four separate days; 0% RCA mixes on May 31, 2007, 15% RCA mixes on June 1, 2007, 30% RCA mixes on June 4, 2007, and 50% RCA on June 5, 2007.

## 3.10 Results

### 3.10.1 Plastic Properties

Unit weight, air content, and slump were measured on the plastic concrete of each of the combined mixes. The unit weight was determined using CSA A23.2-6C (Density, Yield, and Cementing Factor of Plastic Concrete) and a vibrator for compaction. Air content was measured using CSA A23.2-4C (Air Content of Plastic Concrete by the Pressure Method). CSA A23.2-5C (Slump of Concrete) was the procedure used to measure slump. The results of the plastic concrete testing are presented in Table 3.7. All test mixes met the design criteria for an air content of 5%-8% and a slump of less than 100mm.

**Table 3.7 Plastic Properties**

| | Mix | Unit Weight ($kg/m^3$) | Air Content (%) | Slump (mm) |
|---|---|---|---|---|
| 0% RCA | 1 | 2350 | 5.9 | 40 |
| | 2 | 2367 | 5.6 | 40 |
| | 3 | 2338 | 6.1 | 40 |
| 15% RCA | 1 | 2325 | 6.8 | 60 |
| | 2 | 2340 | 5.8 | 40 |
| | 3 | 2338 | 5.8 | 40 |
| 30% RCA | 1 | 2323 | 6.1 | 40 |
| | 2 | 2315 | 6.0 | 40 |
| | 3 | 2321 | 6.1 | 40 |
| 50 %RCA | 1 | 2306 | 5.7 | 40 |
| | 2 | 2301 | 6.1 | 40 |
| | 3 | 2293 | 5.8 | 40 |

### 3.10.2 Hardened Properties

#### 3.10.2.1 Air Content and Spacing Factor

Air void analysis was used to confirm the air content and spacing factor for the test mixes containing 315 $kg/m^3$. Table 3.8 shows the results of the analysis and compares the air content of the plastic and hardened concrete. The air content and spacing factor (L) were determined using ASTM C 457 (Standard Test Method for Microscopical Determination of Parameters of the Air-Void Content and Parameters of the Air-Void System in Hardened Concrete).

**Table 3.8 Air Content and Spacing Factor**

| Mix | Air Content (%) | | Spacing Factor (mm) |
|---|---|---|---|
| | Plastic | Harden | |
| 0% RCA | 5.2 | 5.9 | 0.134 |
| 15% RCA | 6.6 | 6.8 | 0.180 |
| 30% RCA | 5.3 | 6.1 | 0.125 |
| 50% RCA | 5.6 | 5.7 | 0.143 |

The test mixes had an acceptable air content between 5-8%, and a spacing factor less than 0.23 mm. Since the mixes contain an acceptable air-void system they should provide sufficient freeze-thaw protection.

### 3.10.2.2 Compressive Strength

Tests for compressive strength followed CAS A 23.2-9C (Compressive Strength of Cylindrical Concrete Specimens). Compressive strength results are presented for each of the four coarse RCA contents in Figures 3.18 – 3.21. The results presented are based on the average results of two cylinders.

Due to equipment availability, the specified 5-day testing of the 0% RCA and 50% RCA was shifted to day six and the 15% RCA to day four. All test mixes except the 30% RCA 315 kg/m$^3$ reached 32 MPa compressive strength by fourteen days. All test mixes reached the design strength by 28-days. Compressive strength increased as cement content increased for all RCA mixes; however, the opposite was observed for the 0% RCA. Figure 3.22 shows the 28-day compressive strength for the varying RCA amount based on cement content.

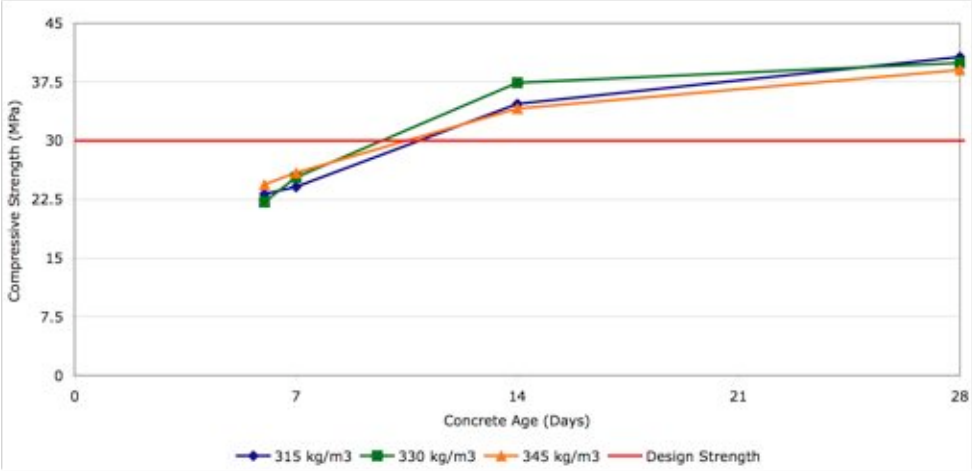


**Figure 3.18 Compressive Strength Development 0% Coarse RCA**

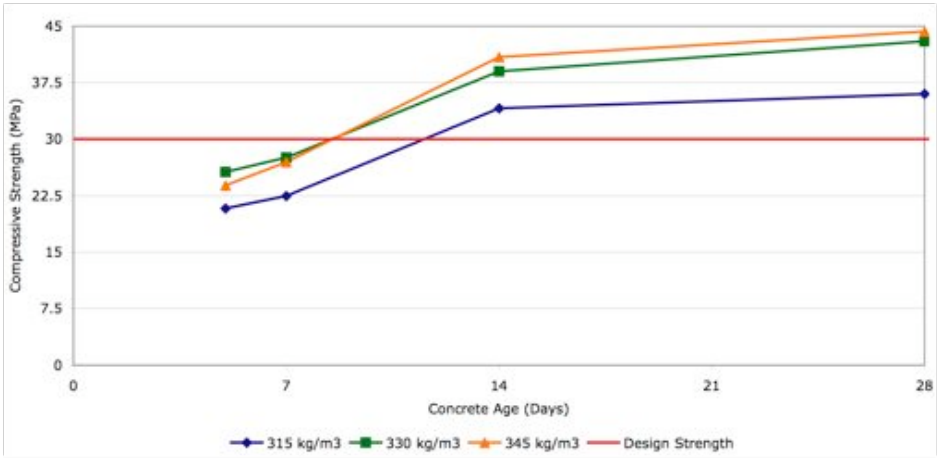


**Figure 3.19 Compressive Strength Development 15% Coarse RCA**

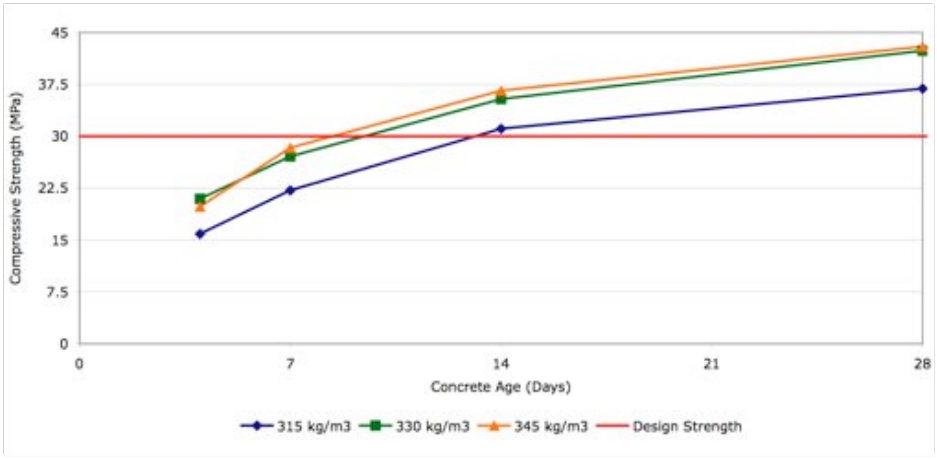


**Figure 3.20 Compressive Strength Development 30% Coarse RCA**

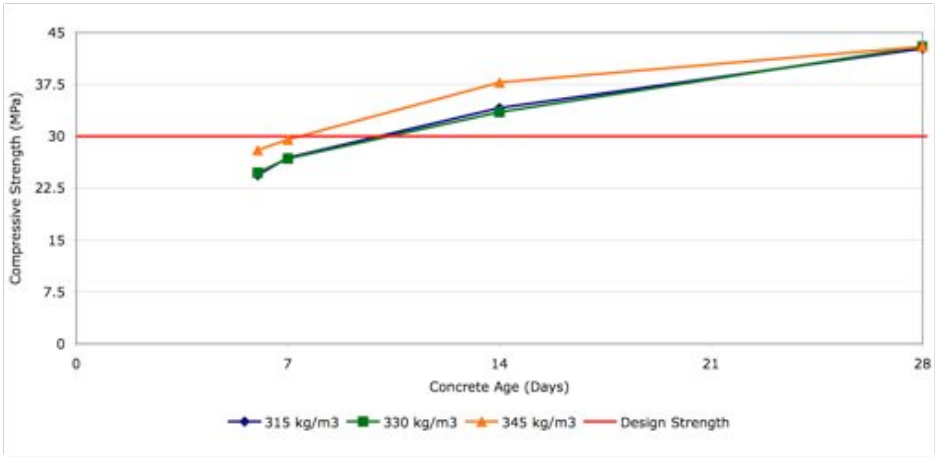


**Figure 3.21 Compressive Strength Development 50% Coarse RCA**

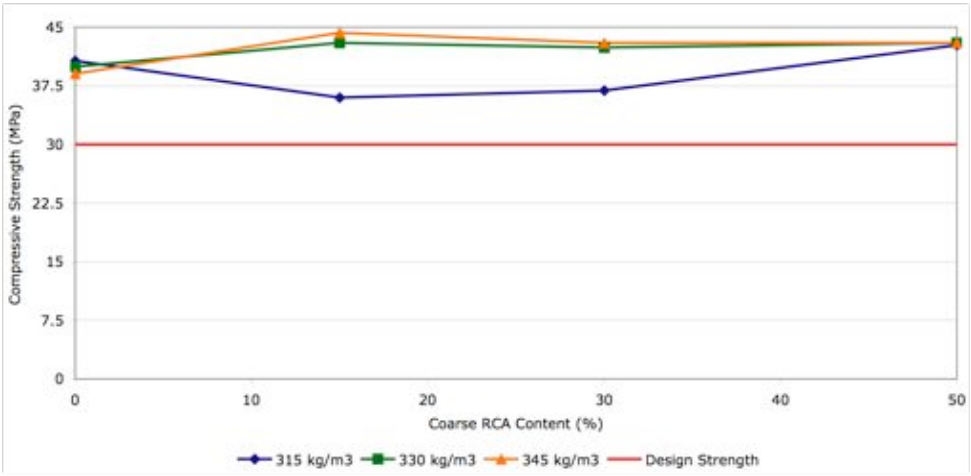


**Figure 3.22 Compressive Strength at 28 Days**

### 3.10.3 Selection of Mix

Since all mixes reached the specified 30 MPa at 28-days, the mixes with the smallest amount of cement content 315 kg/m$^3$ were selected for field placement at the CPATT test track. Although the cement content is lower than the ACPA recommended 335 kg/m$^3$, adequate strength was reached and it provides a more cost effective mix design.

## 3.11 Statistical Analysis

Two factor ANOVA analysis was performed to assess the significance of RCA content, cement content and any interaction on compressive strength. ANOVA was conducted at a 95% confidence interval with 2 replicates. The null hypothesis ($H_o$) for each of the three ANOVA replicates are as follows.

$H_o1$: There is no effect of RCA content on 28-day compressive strength.

$H_o2$: There is no effect of cement content on 28-day compressive strength.

$H_o3$: There is no interaction between RCA content and cement content on 28-day compressive strength.

The ANOVA results are summarized in Table 3.9.

Since F calculated is greater than F critical for each analysis, all three null hypothesis are rejected. Therefore the RCA content, cement content, and their interaction are statistically significant in explaining the observed variance in the resulting 28-day compressive strength.

**Table 3.9 Results of ANOVA**

| *Source* | *SS* | *df* | *MS* | *F* | *F critical* |
|---|---|---|---|---|---|
| RCA | 29.15 | 3 | 9.72 | 5.13 | 3.03 |
| Cement | 53.59 | 2 | 26.80 | 14.16 | 3.42 |
| Interaction | 73.89 | 6 | 12.32 | 6.51 | 2.53 |
| Error | 22.71 | 12 | 1.89 | | |
| Total | 179.34 | 23 | | | |

# Chapter 4

# Pavement Design

Prior to the design of the test track sections, information was gathered on the existing field conditions of the soil subgrade and granular base as well as traffic patterns and loads. Based on this information, the thickness and jointing strategy of the jointed plain concrete pavement surface (JPCP) was chosen.

In order to compare the long-term durability of JPCP containing RCA and conventional JPCP, sensors for strain, slab curling and warping, joint movement, maturity and temperature were included in the test track design.

## 4.1 Soil Investigation

MacLaren Engineering Ltd. conducted a soil investigation in the test track area on three occasions (February 1983, December 1993, and August 1995). Boreholes were drilled within the right-of-way of the future asphalt test sections. Results of the soil investigations are presented in Tables 4.1 to 4.3. The subgrade was classified as clayey silt sand and gravel with moist conditions. The standard penetration resistance 'N' values ranged from 18 to 50+ blows per 0.3 meters which is a medium to very dense soil classification [Craig 2007].

**Table 4.1 Borehole Log OW7-83**

| Depth (m) | Description |
|---|---|
| 0.0 - 1.7 | Grey brown clay, fine sandy silt |
| 1.7 - 3.2 | Grey brown fine sand silt |
| 3.2 - 4.7 | Grey brown silty clay till |
| 4.7 - 6.2 | Grey clay silt till |
| 6.2 - 12.2 | Grey silt clay till |
| 12.2 - 13.9 | Brown silt and fine to medium sand |
| 13.9 - 16.9 | Mottled brown and dark brown clay, fine cand and silt |
| 16.9 - 18.4 | Mottled brown and dark brown silty clay |
| 18.4 - 20.0 | Mottled brown and dark brown clayey silt |

**Table 4.2 Borehole Log OW8-93**

| Depth (m) | Description |
|---|---|
| 0.0 - 0.9 | Brown and grey fill |
| 0.9 -3.8 | Brown grey clay silt till |
| 3.8 - 11.4 | Grey clay silt till |
| 11.4 - 14.5 | Brown grey clay silt till |
| 14.5 - 20.6 | Brown grey fine san with medium sand and silt |

**Table 4.3 Borehole Log OW9-95**

| Depth (m) | Description |
|---|---|
| 0.0 - 3.7 | Brown clay silt with traces of sand |
| 3.7 - 5.2 | Brown silty sand till with traces of gravel |
| 5.2 - 6.7 | Brown sans silt till with traces of clay and gravel |
| 6.7 - 9.0 | Interceded layers of brown silt and silty sand tills |
| 9.0 - 12.7 | Brown silt and sand |

## 4.2 FWD Testing

Stantec Consulting Ltd conducted Falling Weight Deflectometer (FWD) testing of the granular base material on April 25, 2007 prior to paving. There were twelve tests conducted in total, the 15% and 50% RCA sections had two FWD test sites and the 0% and 30% RCA sections had one FWD test site. There were six test sites in each of the Northbound (NB) and Southbound (SB) lanes. FWD testing was conducted using a Dynatest Heavy Weight Deflectometer (HWD) as shown in Figure 4.1.

**Figure 4.1 Dynatest HWD**

Table 4.4 shows the Dynatest HWD spacing of the nine geophones from the applied load.

**Table 4.4 Geophone Sensor Configuration (mm)**

| D1 | D2 | D3 | D4 | D5 | D6 | D7 | D8 | D9 |
|---|---|---|---|---|---|---|---|---|
| 0 | 300 | 450 | 600 | 900 | 1,200 | 1,500 | 1,800 | -300 |

At each of the twelve test locations, four different loads were applied. A "seating" load ensured contact between the load plate and the pavement surface, then 40 kN (9,000 lb), 45 kN (10,115 lb), and 60 kN (13,500 lb) were applied. Table 4.5 presents the FWD results.

**Table 4.5 FWD Results**

| RCA | D1 (μm) | | $M_R$ (MPa) | | Ep | | SN | |
|---|---|---|---|---|---|---|---|---|
| Amount | NB | SB | NB | SB | NB | SB | NB | SB |
| 0 | 1,144 | 1,435 | 36.7 | 28.7 | 111,587 | 89,500 | 2.049 | 1.903 |
| 15 | 1,240 | 1,376 | 41.5 | 37.1 | 103,918 | 88,190 | 1.986 | 1.894 |
| 30 | 1,118 | 2,000 | 88.1 | 72.3 | 95,723 | 50,886 | 1.947 | 1.577 |
| 50 | 1,206 | 1,358 | 58.6 | 71.8 | 140,699 | 106,164 | 2.135 | 1.960 |

D1 sensor detected a larger deflection in the SB direction then in the NB direction. The largest deflection was the 30% RCA section in the SB direction indicating the weakest area of granular and subgrade. Other than the 30% RCA SB section all other sections gave consistent results.

Resilient modulus ($M_R$) is an indication of the subgrade elasticity under loading. An $M_R < 31$ MPa (4500 psi) is identified as a low or weak area. [AASHTO Design Guide Part 2, Chapters 1,2] There were variable results for both NB and SB directions. The 0% RCA section in the SB direction is classified as a weak section whereas the other sections were in the acceptable range. Using $M_R$, California Bearing Ratio (CBR) was calculated using the following equation [TAC 1997].

$$M_R(MPa) = 10.3\,CBR \tag{5.1}$$

CBR values range from 2.78 to 8.55 with an average of 5.27 and is representative of a clay material.

Ep measures the elasticity under loading of the aggregate base material. In general, the NB has a higher Ep demonstrating a faster return to its original shape after a load. The 30% RCA section had the lowest Ep.

The pavement structural number (SN) was consistent for both the NB and SB directions except for 30% RCA. This shows again that the 30% RCA SB section is the weakest. Using the following equation and the SN results from the FWD the layer coefficients can be calculated.

$$SN = a_1 D_1 + a_2 D_2 m_2 + a_3 D_3 m_3 \quad (5.2)$$

where: $a_1, a_2, and, a_3$= layer coefficients of the surface, base, and subbase layers

$D_1, D_2, and, D_3$ = thickness of the surface, base, and subbase layers (inches)

$m_2, and\ m_3$ = drainage coefficients of the base and subbase layers

Assuming a uniform granular layer of 450 mm (17.75 in) for each test sections, the layer coefficient is between 0.09 and 0.12. These values are representative of a crushed stone and are consistent with what is observed in the field.

## 4.3 Site Survey

CPATT conducted a site survey on April 17, 2007 to determine the centerline profile of the existing granular base. The length available to construct the four test sections is 172m. This was measured from the edge of existing asphalt to the start of the right-hand turn guardrail. The elevation decreased 5.15 m over the 172 m length of the test sections. Figure 4.2 shows the base profile along the proposed centerline.

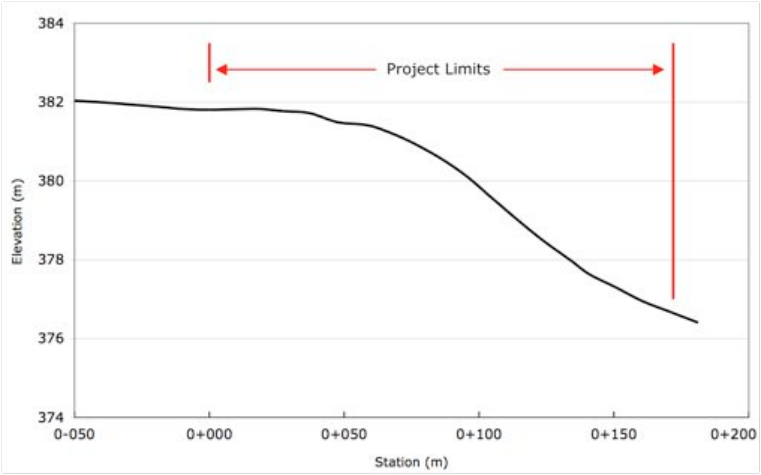


**Figure 4.2 Test Section Profile**

## 4.4 Estimated Traffic Load

Equivalent Single Axle Load (ESALs) on the test track sections was calculated using equation 4.3. This equation was developed for rigid pavement during the original AASHO road test [AASHTO 1993].

$$\frac{W_x}{W_{18}} = \left(\frac{L_{18} + L_{2s}}{L_x + L_{2s}}\right)^{4.62} \left(\frac{10^{\frac{G}{\beta_x}}}{10^{\frac{G}{\beta_{18}}}}\right) \left(L_{2x}\right)^{3.28} \tag{4.3}$$

where: $\frac{W_x}{W_{18}}$ = axle applications inverse of equivalency factors

$L_x$ = axle load being evaluated (kips)

$L_{18}$ = standard axle load based on 18,000 lb (80 kN) single axle load (kips)

$L_2$ = code for axle configuration

1 = single axle

2 = tandem axle

3 = triple axle

x = axle load equivalency factor being evaluated

s = standard single axle

$$G = \log\left(\frac{4.5 - p_t}{4.5 - 1.5}\right)$$

$p_t$ = terminal serviceability index

$$\beta = 1 + \left(\frac{3.63\left(L_x + L_{2x}\right)^{5.2}}{\left(D+1\right)^{8.46} L_{2x}^{\ 3.52}}\right)$$

$D$ = slab depth (in)

A Monte Carlo simulation, with 25,000 iterations, was used to estimate the ESAL value. The simulation was performed using two design vehicles, a Region of Waterloo standard garbage truck and an articulated dump truck. The traffic volume was simulated using 54,000 and 7,500 for the garbage and dump trucks respectively.

The loaded range of the garbage and articulated dump trucks are shown in Table 4.6 [Sterrling Acterra 2006, CAT 2006]. In the Monte Carlo simulation, a uniform distribution of axle loading was assumed. The loaded condition ranged from 75% to 110% of the manufacturers maximum load.

**Table 4.6 Manufacturer Stated Axle Loads**

| Axle | Garbage Truck | | Articulated Dump Truck | |
|---|---|---|---|---|
| | (tonnes) | (lbs) | (tonnes) | (lbs) |
| Sterring | 9.07 | 20,000 | 15.87 | 34,965 |
| Tandum | 20.87 | 46,000 | 35.10 | 77,404 |

Figure 4.3 shows the results of the Monte Carlo simulation run for the design year. Using a 95% confidence level the upper limit of the ESAL calculation is 1,510,000.

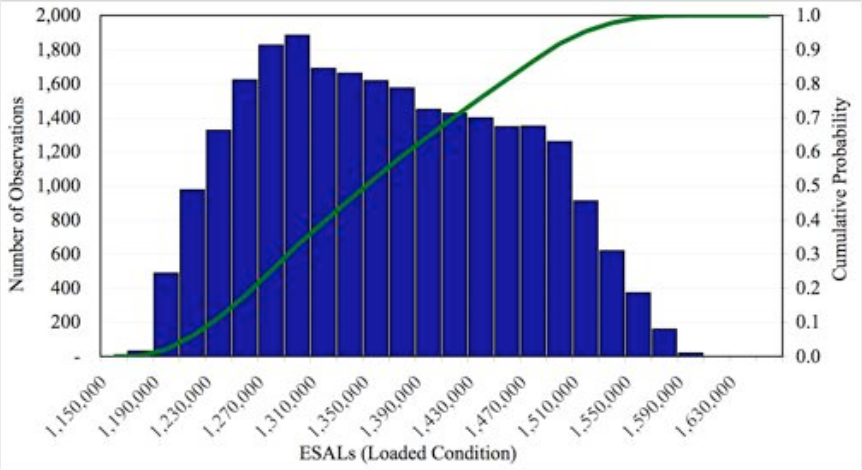


**Figure 4.3 Monte Carlo Simulation Results**

## 4.5 Sensors

Sensors were used to measure both static and dynamic conditions. Static measurements included longitudinal and transverse strain in the concrete, displacement of concrete (slab curl/warp, shrinkage, joint movement), concrete maturity, and temperature, moisture and humidity of the pavement layers. Sensors were needed to measure dynamic conditions of load, vertical displacement, and longitudinal and transverse strain in the concrete. Sensors needed to measure static conditions every one to two hours and dynamic conditions for each loading event.

Some key considerations in selecting sensors were taken from published literature [Farhey 2007].

- The measurement length of the sensor is proportional to the measurement range.

- If possible, embedment of sensors in the pavement should be avoided since it can potentially cause some micro-cracking ($stiffness_{sensor} > stiffness_{material}$) or the formation of voids ($stiffness_{sensor} < stiffness_{material}$) in the pavement causing a change in the systems behaviour.
- If embedment sensors are necessary, then choose sensors that have an unobtrusive shape and a distributed anchor system.
- Incorporate sensor redundancy as it is likely that the number of sensor failures will increase as the length of the test increases.
- Avoid sensors that require recalibration to correct measurement drift (i.e. fiber optic) for long-term monitoring.

Meetings were held with the distributor, Hoskins Scientific Limited, and the sensor manufacturer, RST Instruments Ltd, to select instrumentation for the test sections. Information was gathered on the type of sensor required for each type of measurement.

- Strain is measured using multiple vibrating wire embedment sensors.
- Moisture content is measured with time domain reflectometry (TDR) probes. There was concern about TDR probes being placed in concrete because of the alkaline pore solution reacting with the metal waveguides. A previous case in the literature showed that using a coated 20 cm waveguides TRD probes could accurately determine the actual moisture content of the cement without loss of refraction. The coating protected the TDR from the high alkaline content [Soilmoisture 1998].
- Curling and warping is measured with multiple vibrating wire embedment sensors and/or a tilt meter.
- Joint movement is measured using a vibrating wire embedement.

Displacement sensors for curling/warping and joint movement should have the stroke set in the middle to allow for both positive and negative movements. Separate systems are required to monitor static and dynamic measurements.

The first sensor design proposed included nine strain gages, three vertical extensometers to measure curling and warping, three inter-panel extensometers to measure joint movement and five TDR probes to measure moisture content. One JPCP slab was instrumented in each of the four test sections.

Each instrumented slab would have sensor cables running to the shoulder of the road connecting into a remote multiplexer, each multiplexer would need to contain three Flexi-Mux to accommodate the fifteen vibrating wire sensors. The desired sensor cable length is ten meters. The TDR cables are not compatible with the remote multiplexer so the cables would be stored in a small enclosure on the shoulder of the road for access at specific reading times. Each test sections remote multiplexer would be connected in series with the datalogger being located in the middle of the RCA sections. Prior to concrete placement, sensor cables would be placed inside PVC conduit that ran from the sensor

through the asphalt stabilized OGDL layer, into the granular material 0.3 m (1 feet) and out to the road shoulder. Figure 4.4 is a diagram of the sensor conduit.

Three conduits were required for each slab. One conduit contained the vertical extensometer cables along the south end of the instrumented slab. A second conduit, located mid-slab, housed the cable for the strain gages and maturity sensors. A third conduit ran along the north side of the instrumented slab and contained the cable from the inter-panel extensometers and strain gages.

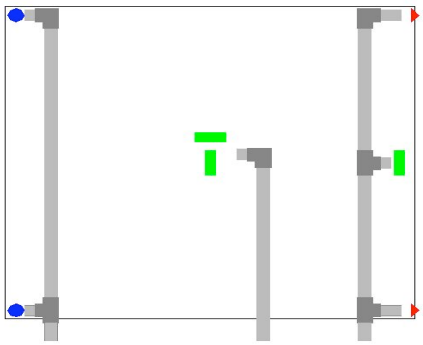

**Figure 4.4 Sensor Conduit**

Protecting the sensors from the slip form paver during placement of the concrete was of utmost importance. The strain gages were put on chairs with a solid base that could be anchored into the asphalt using dowel basket pins. The gages were mounded with concrete to protect them from the paver. The bottom of the vertical extensometer was attached to rebar anchored in the granular layer. It was mounded with concrete to protect them from the paver. The inter-panel extensometers were placed inside a blockout during paving for protection.

Due to cost restrictions, the first sensor design that was proposed was revised. The final layout of the sensors included twelve sensors in each test section. The sensors used in the revised design included six strain gauges, two vertical extensometers, two inter-panel extensometer and two maturity sensors. These twelve sensors were duplicated in each of the four sections (0%, 15%, 30%, and 50% RCA). The sensors removed from the first design are 3 strain gauges at slab mid-depth, and one each of the vertical and inter-panel extensometers along the mid-slab joint. Figure 4.5 shows the revised location of all the sensors.

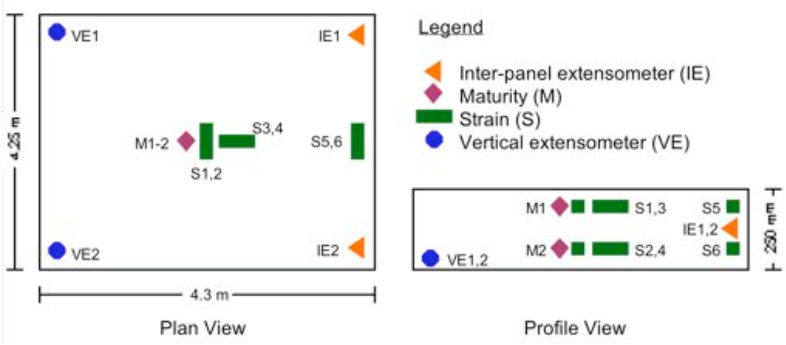


**Figure 4.5 Revised Sensor Locations**

## 4.6 Design Thickness

The American Concrete Pavement Association (ACPA) StreetPave design software was used to design the thickness of the JPCP. The entries for global settings and project level inputs were:

- climatic region mean annual air temperature (MAAT) of 7.2 $^{o}$C (45 $^{o}$F),
- terminal pavement serviceability index (PSI) of 2.25 to represent arterial and collector roads,
- 15% cracked concrete slabs at the end of the design life to represent arterial and collector roads,
- design life of 35 years with reliability set at 90%.

Since the actual traffic patterns may vary from the estimate, the StreetPave traffic settings were set to slightly over estimate the traffic. The traffic category was set as a major arterial road. The average annual daily truck traffic of 5000 was weighted evenly between the two lanes. A 4% traffic growth rate was used.

Pavement settings were chosen based on representative average values. A California Bearing Ratio (CBR) of five was used to represent the average field condition of clay. The compacted granular material was 450 mm with an MR of 200 MPa and the asphalt stabilized OGDL was 100 mm with an MR of 1200 MPa. The combined values give a composite modulus of subgrade reaction (k) equal to 148.2. The average 28-day flexural strength (MR) was set at five megapascals and the concrete modulus of elasticity (E) was set at 33,750 MPa.

StreetPave results indicated that the minimum thickness for the JPCP layer was 199.9 mm. The recommended thickness was 203.2 mm with a maximum transverse joint spacing of 4.27 m and a dowel bar diameter of 31.75 mm.

It was decided to use a pavement thickness of 250 mm to accommodate the cover requirements of the automatic dowel bar inserter, reduce the likelihood of vibrator trails from the slipform paver, allow for comparison of performance with MTO standard JPCPs, and to provide opportunity for multiple diamond grindings to restore the pavement's smoothness as required.

## 4.7 Preconstruction Meetings

In preparation for the placement of the test sections, six preconstruction meetings were held. Representatives from the University of Waterloo, the CAC and Dufferin attended. Summaries of the meetings are in Appendix B.

# Chapter 5
# Construction

## 5.1 Granular Base

The Region of Waterloo had previously constructed the granular base to use as the South access haul road for the proposed SE-1 and SE-3 landfill expansion cells. On June 5, 2007, prior to paving, Dufferin Construction preformed the final grading and compaction to bring the granular base structure to the desired profile.

## 5.2 Sensor Conduit

On June 9, 2007, conduits for the sensors were placed. The University of Waterloo laid out the test track sections by marking the location were paving is to start and the location of joints. The locations of the four slabs to be instrumented were identified and the location for the sensor conduits was marked as per Figure 4.4.

Each of the four slabs required 18.5 m of ABS pipe, 0.75 m of PVC pipe, three elbows, and three tees for the sensor conduits. Trenches for the sensor conduits were initially dug with pick-axes and shovels. Due to the compaction of the granular base, a jackhammer was obtained to help breakup the surface. Figure 5.1 pictures the excavation of the granular layer for sensor conduit placement.

**Figure 5.1 Digging Sensor Conduit Trenches**

The sensor conduit trenches were excavated to a depth of 305 mm (12 in). A 38 mm (1.5 in) ABS pipe burrier was used in the granular base and 38 mm PVC pipe was used to extend up through the base 100 mm to allow access to the conduit after the asphalt stabilized OGDL was placed. PVC pipe was used in the OGDL since it has a higher melting point, 212$^{o}$C, compared to ABS pipe, 105 $^{o}$C. The three sections of pipe were cut to the desired lengths allowing for the necessary couples, tees, and elbows to be added. Then a thin layer of bedding sand was spread on the excavated trench to protect

the conduit from protruding aggregate. After the conduit pipe was place in the trench the area around the conduit was backfilled with the excavated material in 50-76 mm (2-3 in) lifts and compacted with a Marshall hammer. A small amount of water was added to the backfill to aid compaction. Figure 5.2 shows the compaction with a Marshall hammer of the granular material around the sensor conduit.

**Figure 5.2 Marshall Hammer Compaction Around Sensor Conduit**

## 5.3 Asphalt Stabilized Open Graded Drainage layer

Dufferin Construction requested that the PVC sensor conduit extensions be cut flush with the granular base material so it would not interfere with paving. After the PVC conduit was cut approximately 10mm above the granular base, rags were stuffed into the conduit to prevent the asphalt stabilized ODGL from plugging the opening. Paving was cancelled the night of June 10, 2007 due to a breakdown at the plant that would not permit the manufacturing of the asphalt stabilized OGDL and was rescheduled for June 11, 2007. On June 11, 2007 UW and Dufferin construction were onsite by 6:00 pm. The first load of asphalt stabilized OGDL was placed at 6:24 pm. The outside temperature at the start of paving was 25 $^{o}$C, and by the end of paving the temperature had dropped by six degrees Celsius over four hours to nineteen degrees Celcius. There were clear skies with no precipitation.

A total of fourteen loads of asphalt stabilized OGDL, totaling 293.04 tonnes were used to pave both lanes (8.5 m wide) of the 180m test sections. Table 5.1 shows the details of each load of OGDL including the time the load was batched and placed, weight and location of placement. Figure 5.3 pictures the OGDL paving and compaction.

The test sections were paved one lane at a time. First the unloaded lane was paved then the loaded side in the northbound direction (i.e. station 0+280 to 0+100). Paving depth was consistently between 90 mm and 115 mm. A two percent cross slope towards the edge of the pavement was created. The OGDL was compacted using a vibratory asphalt compactor (CB-634D) over multiple passes and started 30 minutes (7:00 pm) after the start of paving (6:30 pm).

**Table 5.1 ODGL Load Details**

| Load | Time | | Tonnes | | Location | |
|---|---|---|---|---|---|---|
| | Batched | Placed | Current | Total | Start | Stop |
| 1 | 17:24 | 18:24 | 20.93 | 20.93 | NB 0+280 | NB 0+260 |
| 2 | 17:40 | 18:37 | 21.02 | 41.95 | NB 0+260 | NB 0+245 |
| 3 | 17:56 | 18:44 | 20.93 | 62.88 | NB 0+245 | NB 0+220 |
| 4 | 18:14 | 18:55 | 20.95 | 83.83 | NB 0+220 | NB 0+200 |
| 5 | 18:28 | 19:30 | 20.94 | 104.77 | NB 0+200 | NB 0+170 |
| 6 | 18:43 | 19:37 | 20.94 | 125.71 | NB 0+170 | NB 0+139 |
| 7 | 19:13 | 19:53 | 20.88 | 146.59 | NB 0+139 | NB 0+120 |
| 8 | 19:37 | 20:18 | 20.87 | 167.46 | NB 0+120 | NB 0+100 |
| 9 | 19:54 | 20:47 | 21.01 | 188.47 | SB 0+280 | SB 0+253 |
| 10 | 20:06 | 20:52 | 20.80 | 209.27 | SB 0+253 | SB 0+230 |
| 11 | 20:34 | 21:25 | 20.94 | 230.21 | SB 0+230 | SB 0+197 |
| 12 | 20:55 | 21:39 | 20.93 | 251.14 | SB 0+197 | SB 0+172 |
| 13 | 21:14 | 21:55 | 21.02 | 272.16 | SB 0+172 | SB 0+138 |
| 14 | 21:54 | 22:36 | 20.88 | 293.04 | SB 0+138 | SB 0+100 |

**Figure 5.3 Paving and Compaction of ODGL**

The temperature of each load was measured and recorded at the time of placement. The temperature was measured immediately after passing the screed of the paver and taken at mid-depth, 50 mm below the surface. The mid-depth temperatures ranged from 131.9 $^{o}$C to 171.8 $^{o}$C, with an average of 148.6 $^{o}$C, and a standard deviation of 8.8 $^{o}$C.

A plate sample was taken from each test section location for laboratory testing with the following details:

- 15%RCA sample from Load #3, temperature 158.0 $^{o}$C
- 50% RCA sample from Load #7, temperature 152.7 $^{o}$C
- 0% RCA sample from Truck #9, temperature 152.6 $^{o}$C
- 30% RCA sample from Truck # 12, temperature 148.2 $^{o}$C

The asphalt stabilized ODGL was allowed to cure 24 hours before concrete was placed.

On June 12, 2008, the openings to the buried conduit were located and clothesline was threaded through the conduit to allow for faster placement of sensors during concrete paving.

## 5.4 Jointed Plain Concrete Pavement

Paving of the PCC layer was carried out over two days on June 13 and 14, 2007. Construction of the JPCP started June 13, 2009. UW and Dufferin construction were onsite by 5:30 am and paving started at 6:59 am. Concrete was delivered to the test section site in ready-mix trucks from the Dufferin's Kitchener Plant on Forwell Road, sixteen kilometers away from the site or a 25-minute drive.

Paving was done using a slipform paver (Gunter and Zimmerman S850 Quadra) equipped with auto float and burlap drag. Wood and magnesium floats on long poles were used on either side of the road. Also, there was a hand finishing platform and a texture/cure machine. (Gomaco T/C 600) Figure 5.4 shows the view of the paving setup from on top of the slipform paver.

**Figure 5.4 Pavement Construction**

The slipform paver had multiple starts and stops to allow for discharging the concrete from ready mix trucks, sensor installation, and dowel basket installation. This produced localized low spots where the paver was stopped.

A set of two dowel baskets consisting of thirteen 38 mm diameter epoxy coated dowel bars were spaced every 300 mm with a height of 125 mm. The dowel baskets were placed using the variable

joint spacing sequence. Pins, 100 mm in length, were used to secure the load transfer devices to the asphalt stabilized OGDL. The pins were secured on both sides of the load transfer device and placed between every two to three dowel bars. The tie straps were cut and removed from the load transfer device except for the first set where they were cut but left attached.

Under the supervision of Jai Tiwari from Dufferin Construction, Eugene Kim, Xin Xu, and Jodi Norris from CPATT carried out concrete fresh property testing and specimen preparation. The fresh properties that were tested included air content, slump, temperature and unit weight and are shown in Table 5.2. Unit weight measurements were taken from the same load that was used to cast specimens for each RCA amount.

**Table 5.2 Concrete Fresh Properties**

| RCA Amount | Ticket Number | Time Tested | Air Content (%) | Slump (mm) | Unit Weight ($kg/m^3$) | Temperature ($^oC$) |
|---|---|---|---|---|---|---|
| 0% | 135147 | 6:21 | 5.6 | 20 | - | 22.5 |
| | 135151 | 6:45 | 6 | 30 | 2371 | 23.7 |
| | 135155 | 7:30 | 7.2 | 50 | - | 23.8 |
| 15% | 135162 | 8:38 | 6.8 | 40 | - | 22.3 |
| | 135165 | 9:05 | 6.1 | 50 | - | 22.9 |
| | 135168 | 9:55 | 5.9 | 50 | 2335 | 24.7 |
| | 135173 | 10:40 | 7 | 40 | - | 24.7 |
| | 135194 | 2:00 | 5.5 | 30 | - | 22.8 |
| 30% | 135198 | 2:30 | 5.3 | 50 | - | 23.6 |
| | 135201 | 3:25 | 6.2 | 40 | 2316 | 24.4 |
| | 135206 | 4:10 | 6 | 40 | - | 23.2 |
| | 135209 | 4:37 | 4.9 | 50 | - | 24 |
| 50% | 134213 | 5:15 | 5.5 | 40 | - | 22.9 |
| | 130217 | 6:05 | 5.8 | 30 | - | 24.8 |
| | 127220 | 6:25 | 6.2 | 40 | 2298 | 24.3 |
| | 121227 | 7:32 | 5.4 | 40 | - | 25.1 |
| | 114233 | 8:30 | 6.8 | 40 | - | 23.6 |

A number of specimens were cast for each RCA amount. There were nine cylinders for compressive strength testing, one cylinder for air void analysis, two cylinders for maturity testing, three beams for flexural strength testing, and two beams for freeze-thaw testing. Due to low slump values, a pencil vibrator was used to consolidate the concrete in the cylinders and beams as allowed by ASTM C 231. The cast specimens were cured in the field for 24 hours before being transferred to the CPATT lab at UW to be demolded and stored in the fog room until testing as per ASTM C31.

When paving started, the outside air temperature was 20.9$^{o}$C with sunny clear skies and no precipitation. The temperature increased 8.8 $^{o}$C over four hours to a temperature of 29.7 $^{o}$C at 11 am. At 11 am the temperature of the asphalt stabilized ODGL was 52$^{o}$C or higher. Due to the high air temperature and weak compressive and tensile strength of the asphalt stabilized ODGL it would deform when the trucks drove on it creating high and low spots and a non-uniform paving surface. Water was used to cool the asphalt stabilized ODGL to help prevent moisture loss of the concrete and reduce the deformations of the surface. However, the non-uniform surface of the asphalt stabilized ODGL caused vertical skewing of the dowel bars as seen in Figure 5.5.

**Figure 5.5 Skewing of the Dowel Bars**

CSA A23.1 states that for regular PCC evaporation rates greater than 1.0 kg/m$^2$, significantly increases the potential for shrinkage cracking. By adding in pozzolans (fly ash or silica fume) evaporation rates over 0.5 kg/m$^2$ increase shrinkage cracking potential. Although the RCA mixes did not contain any pozzolans, RCA is more susceptible to moisture loss, which also increases the risk of shrinkage cracking. The evaporation rate at 10:45 am was estimated at 0.6 kg/m$^2$ per hour. Using the Cement Association of Canada's Design and Control of Concrete Mixtures, the evaporation rate was calculated using an air temp of 29.3 $^{o}$C, a relative humidity of 41.1%, a concrete temperature of 28.3 $^{o}$C, and a wind velocity of 8.5 km/h. Dufferin construction decided to stop paving at 11 am since the concrete was becoming increasingly difficult to place and finish. Figure 5.6 illustrates the pavement condition including a loss of pavement edge and voids in the surface.

**Figure 5.6 Condition of JPCP**

The remaining mixed concrete already onsite was placed (station 0+223 to 0+210) and would be removed prior to paving the following day. As shown in Figure 5.7, plastic tarps were placed on top of the asphalt stabilized ODGL for easier removal of the waste concrete. Dowel bars in the basket were replaced with plastic tubes filled with sand to provide a reference of where the new bars would be placed.

**Figure 5.7 Placing Concrete for Removal**

The paving that was completed the first day is summarized in Table 5.3 and the texturing completed the first day is summarized in Table 5.4.

**Table 5.3 Day 1 Paving**

| RCA | NB (Unloaded) | | | SB (Loaded) | | |
|---|---|---|---|---|---|---|
| Amount | Starting Station | Finishing Station | Distance (m) | Starting Station | Finishing Station | Distance (m) |
| 0% | 0+280 | 0+253 | 27 | 0+280 | 0+258 | 22 |
| 15% | 0+253 | 0+223 | 30 | 0+258 | 0+223 | 35 |

**Table 5.4 Day 1 Texturization**

| Texturization | Starting Station | Finish Station | Distance (m) |
|---|---|---|---|
| Longitudinal burlap drag with 16 mm c/c longitudinal tining | 0+280 | 0+256 | 24 |
| Longitudinal burlap drag only | 0+256 | 0+223 | 33 |

UW and Dufferin construction were onsite by 11:00 pm on June 13. Prior to the start of paving, concrete from station 0+223 to 0+210 was cut into smaller pieces and removed as shown in Figure 5.8.

**Figure 5.8 Removal of Waste Concrete**

Removal of the JPCP disturbed the underlying asphalt stabilized OGDL. A sixteen-millimeter clear stone was used to replace the disturbed material without compaction. Dowel bar holes were drilled with a single hand-held drill. The dowel holes were cleaned before installing the grout and dowel bars. As shown in Figure 5.9, the reestablished joint prior to paving had some misalignment of the dowel bars, and some voids between the grout and the dowel.

**Figure 5.9 Reestablishing Joints Prior to Paving**

Paving began around 1:30 am and the last load was placed by 9:55 am. The 30% RCA and 50% RCA mixes were adjusted to include a Type R retarder to slow down the setting of the concrete, to counteract the effect of high temperature and allow time to properly finish the concrete. When paving started, the outside air temperature was 20.5 $^{o}$C with clear skies and no precipitation. The temperature increased 2.6 $^{o}$C over 8.5 hours for a final temperature of 23.1 $^{o}$C at 10 am. The highest temperature of the asphalt stabilized ODGL was 39 $^{o}$C.

Compared to the previous day, deformation of the asphalt stabilized ODGL layer continued but was less significant due to the lower ambient temperature. The amount that the slipform paver was stopped was reduced by running cable through the conduit ahead of time and creating a small trough in the asphalt stabilized OGDL for the cables so they would not be pinched and the sensor would not be run over. This allowed the ready-mix trucks greater access to the slipform paver.

The first application of curing compound was applied a maximum of one hour after the placement of the concrete. Paving that was completed on the second day is shown in Table 5.5 and the texturing completed is shown in Table 5.6.

**Table 5.5 Day 2 Paving**

| RCA | NB (Unloaded) | | | SB (Loaded) | | |
|---|---|---|---|---|---|---|
| Amount | Starting Station | Finishing Station | Distance (m) | Starting Station | Finish Station | Distance (m) |
| 15% | 0+223 | 0+205 | 18 | 0+223 | 0+210 | 13 |
| 30% | 0+205 | 0+165 | 45 | 0+210 | 0+160 | 50 |
| 50% | 0+165 | 0+100 | 65 | 0+160 | 0+100 | 60 |

**Table 5.6 Day 2 Texturization**

| Texturization | Starting Station | Finishing Station | Distance (m) |
|---|---|---|---|
| Longitudinal burlap drag with 16 mm c/c longitudinal tining | 0+223 | 0+180 | 43 |
| 16 mm c/c longitudinal tining | 0+180 | 0+149.5 | 30.5 |
| Transverse broom drag with 16 mm c/c transverse tining | 0+149.5 | 0+138 | 11.5 |
| Transverse broom drag with 16 mm c/c longitudinal tining | 0+138 | 0+110 | 28 |
| Longitudinal burlap drag with 16 mm c/c longitudinal tining | 0+110 | 0+100 | 10 |

The thickness of the JPCP was measured every fifteen meters over the length of the test sections for a total of eleven measurements. The thickness was measured to the nearest 5 mm. The thickness ranged from 250 mm to 310 mm and had an average of 272 mm and a standard deviation of 19.7. The thickness increased over the last two slabs approaching the asphalt to provide suitable depth for a proper transition.

Over the next 28-days at the test track the temperature ranged from 6.5 $^{o}$C to 32 $^{o}$C with an average temperature of 20.8 $^{o}$C, a standard deviation of 3.5 $^{o}$C and total precipitation of 37.8 mm.

## 5.5 Early Age Behaviour

During the first three days after placement, portland cement concrete pavements are particularly susceptible to shrinkage induced cracking. This cracking can have critical effects on the long-term performance of the pavement. Cracking occurs when the tensile stresses exceed the tensile strength of the concrete. Shrinkage induced cracking is caused by a number of factors including material type, mix design, pavement design, construction practices and climate conditions. The increased absorption rate of recycled concrete aggregate makes it particularly sensitive to weather conditions. Higher temperatures and wind will accelerate water loss from the concrete to the atmosphere or to the asphalt stabilized open graded drainage layer. This water loss can cause inadequate moisture in the concrete negatively impacting hydration, strength development and surface finishing.

Computer simulations were run using HIPERPAV II software [Transtec 2005]. HIPERPAV II uses data on pavement design, concrete mix design, the weather, and construction method to calculate stress development in the concrete and compares it to strength development over the first 72 hours. This allowed potential times of failure with uncontrolled cracking to be identified and avoided before the construction of test sections. The simulations identified the possible early age cracking of the RCA concrete when the ambient temperature exceeded 30 $^{o}$C during placement of the JPCP.

Inspection of the test sections after 72 hours showed no signs of uncontrolled cracking of the concrete pavement. Additional HIPERPAV II simulations were run using weather data from the onsite weather station to confirm the observations. Figures 5.10 to 5.14 shows the simulation results for all the test sections.

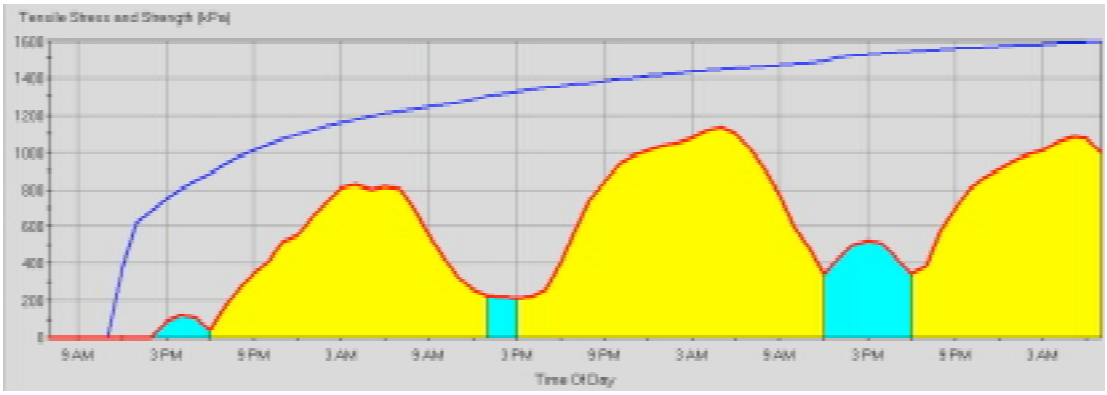


**Figure 5.10 HIPERPAV II Results 0% Coarse RCA, Day 1**

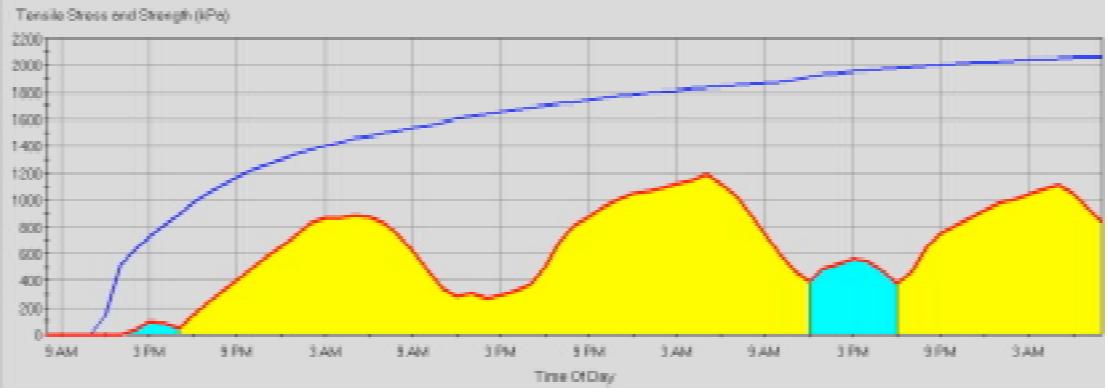


**Figure 5.11 HIPERPAV II Results 15% Coarse RCA, Day 1**

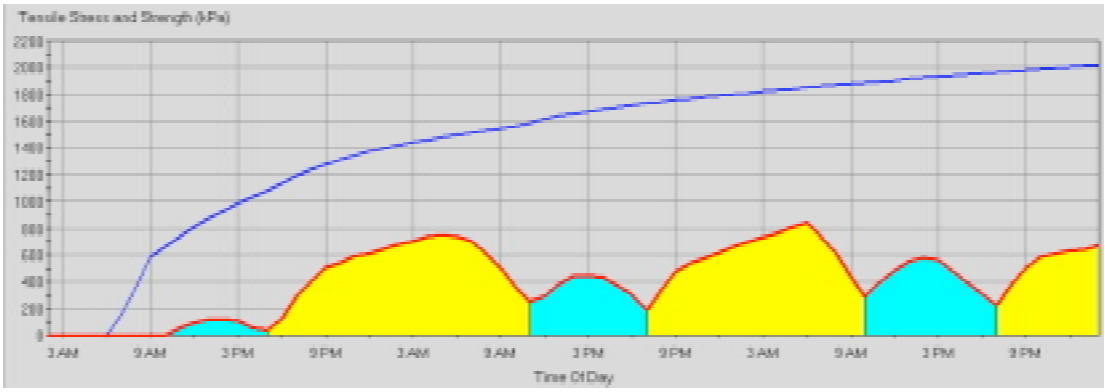


**Figure 5.12 HIPERPAV II Results 15% Coarse RCA, Day 2**

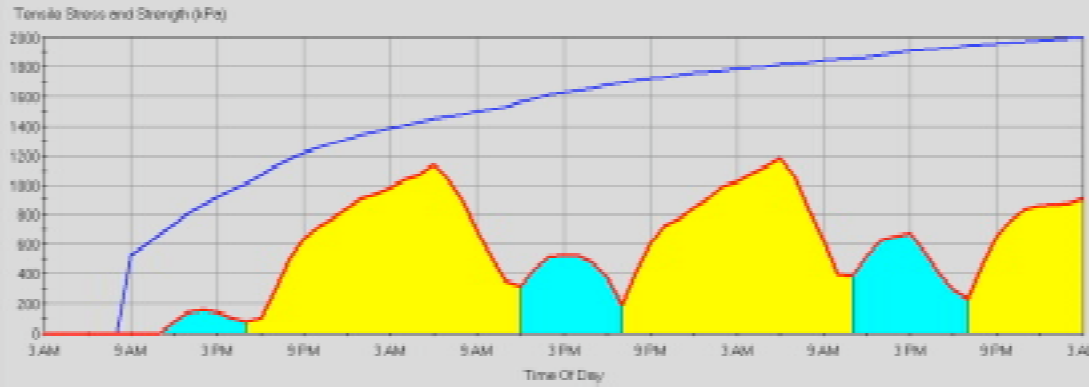


**Figure 5.13 HIPERPAV II Results 30% Coarse RCA, Day 3**

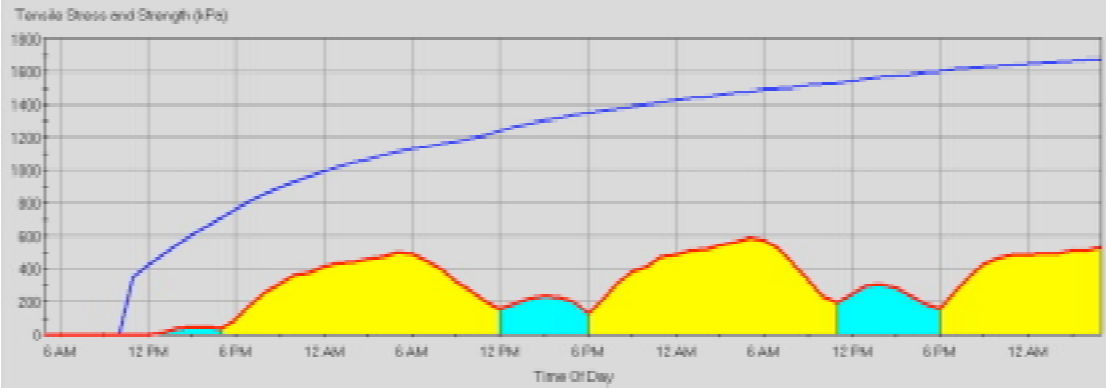


**Figure 5.14 HIPERPAV II Results 50% Coarse RCA, Day 4**

The simulation results confirmed the field observations that no uncontrolled cracking would develop. During the 72 hours the maximum tensile stresses to tensile strength ratio of the concrete reached 0.74 for the 30% Coarse RCA test section.

## 5.6 Joints

Dowel baskets were placed according to the variable joint spacing 3.7 m, 4.5 m, 4.0 m, and 4.3 m in a repeating pattern. The location of where the joints were to be cut was marked with spray paint using a string-line. Joints were marked with variable offsets from the centre of the dowel baskets at 0 mm, 25 mm, 50 mm, 75 mm and 100 mm as per Figure 5.15.

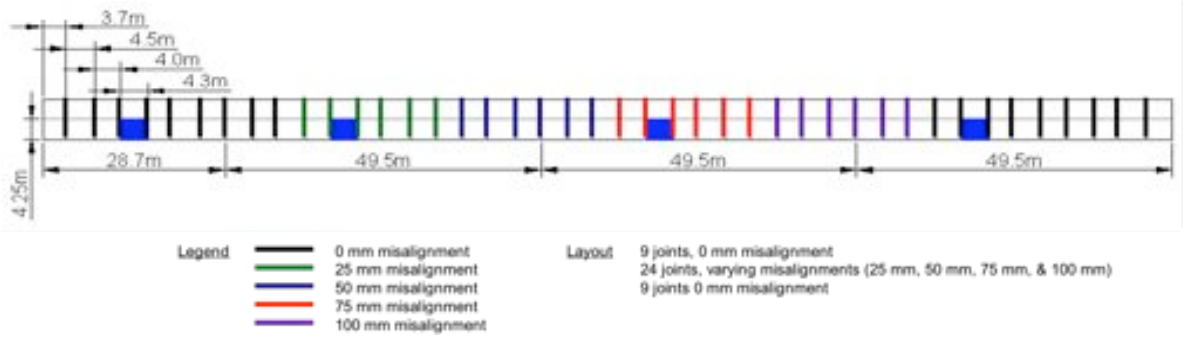


**Figure 5.15 Joint Offsets**

The initial sawing of the concrete joints was started 6.5 hours after paving started at 1:30 pm. Sawcutting was preformed by BASIC Concrete Cutting Inc. using a Husquvarna FS6600D concrete cutting saw. The saw was equipped with a 3.175 mm (1/8 inch) diamond saw blade and was set to cut a depth of a third of the thickness of the slab, 85 mm. The transverse joints were cut first followed by the longitudinal joints. Figure 5.16 shows the initial saw cut.

**Figure 5.16 Initial Saw Cuts**

On July 7, 2007, Road Master Construction widened the original transverse and longitudinal joints and sealed the joints. This joint sealing was a three-part process. First, the original cuts were widened to a width of fifteen millimeters and depth of 35 mm to create a reservoir for the joint sealant. The cuts were cleaned with dry sandblasting to clean away any cutting residue and add texture to the reservoir walls for extra adhesion. Joints were cleaned a second time using air to remove sand, dirt, and dust and a visual inspection of the joint was done to confirm it was clean. Second, the nineteen-millimeter backer rod was inserted into the joint using a steel roller. Inspection of the backer rod showed that it was cut or stretched by the roller during installation. Finally, asphalt rubber based joint sealant was poured into the reservoir. Figure 5.17 shows the widening and sealing of the transverse and longitudinal joints.

**Figure 5.17 Widening and Sealing the Initial Saw Cut**

During the widening of the joints, the edges of the pavement became damaged in several locations as pictured in Figure 5.18.

**Figure 5.18 Pavement Damage**

## 5.7 Sensors

The maturity sensors arrived on June 4, 2007 and the strain gauges, vertical extensometer, and inter-panel extensometer arrived on June 8, 2007. The datalogger, the four multiplexers and the solar panel were delivered approximately two to three weeks after the installation. On June 12, 2007, the strain gauges and maturity sensors were attached to the chair structure as shown in Figure 5.19.

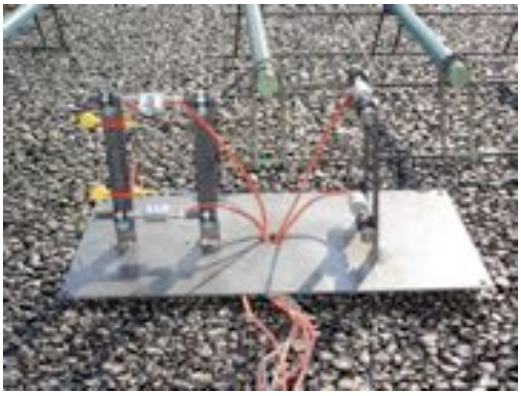

**Figure 5.19 Strain Gauge and Maturity Setup**

Chairs allowed the strain gauges to be securely fastened into the asphalt stabilized ODGL and held the strain gauges at 50 mm above the bottom of the JPCP and 50 mm below the top of the 250 mm thick pavement structure. As seen in Figure 5.20, rebar was added to the vertical and inter-panel extensometers to hold them in place.

**Figure 5.20 Vertical Extensometer**

To install the vertical extensometer, a pickaxe was used to create a small hole in the asphalt stabilized ODGL to insert the sensor. This allowed 50 mm of JPCP to cover above the rebar. Extracted asphalt material was placed around the sensor and gently compacted to hold it in place. Figure 5.21 shows how concrete was mounded over the sensor to protect it during paving.

The chair mounted strain gauges and maturity sensors were fastened to the asphalt stabilized OGDL using four dowel basket pins, one in each corner of the chair. As seen in Figure 5.22, concrete was mounded over the sensor to protect it during paving.

**Figure 5.21 Mounding the Vertical Extensometer with Concrete**

**Figure 5.22 Mounding the Stain Gauges and Maturity Sensors with Concrete**

The inter-panel extensometer sensor was wrapped in plastic and placed inside a blockout. The blockout was filled with dirt and anchored into the asphalt stabilized ODGL and the granular base. To accommodate the blockout two sections of the dowel basket were removed. Figure 5.23 shows the blockout and dowel basket prior to paving. Traffic cones were placed on top of the blockouts to make them more visible to the ready mix trucks backing up.

**Figure 5.23 Inter-panel Extensometer Blockout Before Paving**

The data logger and the four multiplexers were installed on July 5 and July 6, 2007. The multiplexers and datalogger boxes were installed on metal fence t-rails one to two meters from the edge of the pavement as shown in Figure 5.24.

**Figure 5.24 Location of Multiplexer and Dataloger Cabinets**

The landfill management requested that the multiplexers be moved away from the road so they would not be hit by a snowplow. On Nov 8, 2007 cable splicing was done in order to move the 0% RCA multiplexer. However, due to snow, splicing was completed but the multiplexer was not reinstalled and the other multiplexers were not moved at that time. The cables were spliced by removing five millimeters to ten millimeters of the protective coating to expose each individual wire. About 20 mm – 25mm of the first shrink tubing was placed on each individual wire, and 50 mm – 75mm of the second shrink tubing was placed over the cable. The exposed wires were twisted together and flux was applied. The individual wires were soldered and the shrink tubing heated to seal the cable. The splice was then wrapped with ducktape.

October 27 to 31, 2008, cable splicing for 30% and 50% sections was completed. All of the multiplexers and dataloggers (0%, 30%, and 50% sections) were moved along the fence line and the 15% section was moved inside the traffic control cabinet with the datalogger. The solar panel for the datalogger was also installed. All of the sensor cables joining the multiplexers to the datalogger were relocated as well.

Figure 5.25 shows the relocated multiplexer and dataloger cabinets and their wiring.

**Figure 5.25 Relocated Multiplexers and Datalogger, and Wiring**

# Chapter 6
# Test Results

## 6.1 Thickness

The design thickness of the JPCP was 250 mm. Three methods were used to measure the actual thickness of the JPCP test sections. First, the height of the JPCP surface above the asphalt stabilized OGDL was measured eleven times during paving. Second, the sixteen extracted cores were measured. Third, the MIT Scan-2 measures the distance to the centre of the dowel bar. This measurement is then added to the known height of the dowel bar, 125 mm above the OGDL. The MIT Scan-2 measure was performed 36 times. Figure 6.1 shows the thickness measurements made by the three methods.

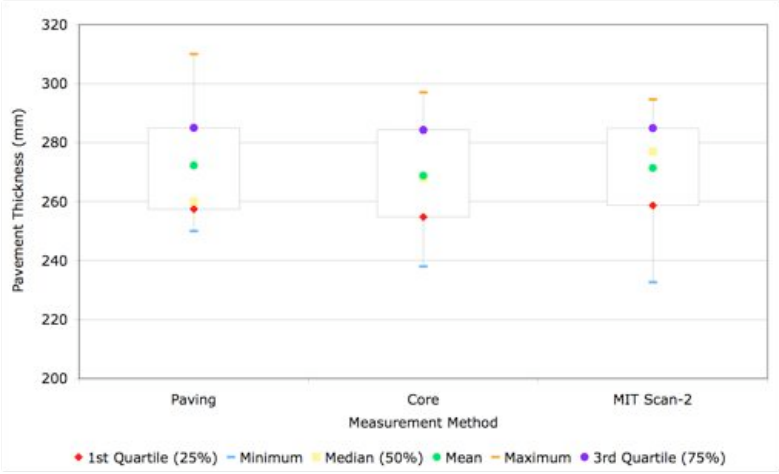


**Figure 6.1 Thickness of JPCP**

The results of the thickness testing showed that most of the pavement was thicker than designed. Only 7 measurements were below the 250 mm design thickness. All three test methods produced very similar averages and standard deviations, paving 272.3 mm + 19.7 mm, core 269.8 mm + 18.1 mm, and MIT Scan-2 271.4 mm + 18.1 mm.) The thickest parts of the test track occurred in the 15% and 30% RCA sections. Several reasons for the variation in thickness include many start and stop points, grade of the test sections and deformation of the asphalt stabilized OGDL.

## 6.2 MIT Scan-2

The MIT Scan-2 was designed for locating dowel bars inserted using a dowel bar inserter (DBI) but can also be used for dowels placed in baskets if the bars are epoxy coated insulating them from the basket and if the transport ties on the basket are cut [Yu 2005]. The MIT Scan-2 unit works by emitting an electromagnetic pulse creating a magnetic field in the dowel bars that is detected and

measured. Figure 6.2 shows how the MIT Scan-2 is centred over the joint and pulled across the pavement.

**Figure 6.2 MIT Scan-2**

An FHWA study shows the MIT Scan-2 is accurate to five millimeters for horizontal and vertical misalignment, eight millimeters side shift and four millimeters depth with a 95% confidence [Yu 2005]. The MTO tolerance for dowel bar alignment is set at fifteen millimeters for horizontal and vertical misalignment and 40 mm for side shift.

On June 18, 2007, Dufferin Construction performed an MIT Scan-2 to determine dowel bar orientation and depth in the concrete. The testing was set up to measure both lanes in the same pass. It took between 3.5 to 5 minutes to setup over the joint, scan, and move to the next joint. Figure 6.3 shows the distribution of dowel bar misalignment. Of the 928 dowel bars, 340 (37%) met MTO standard with less than fifteen millimeters vertical and horizontal displacement. There are several reasons for the large portion of dowel bars that did not meet MTO standard. During paving there was significant deformation of the asphalt stabilized OGDL and it is possible that dowel baskets were not fastened securely.

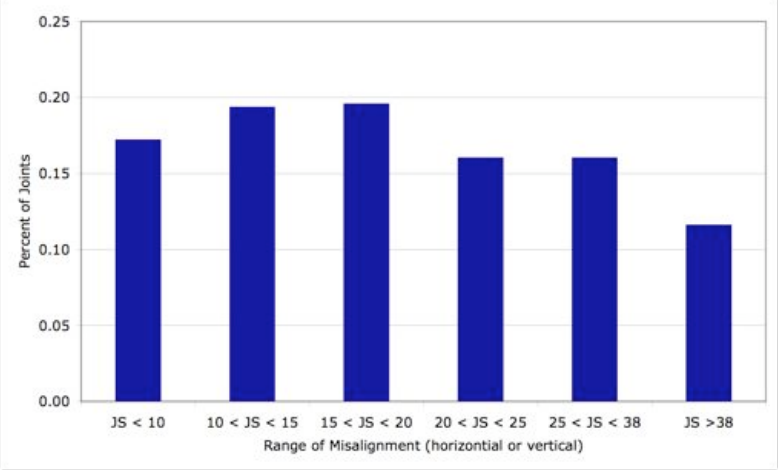


**Figure 6.3 Distribution of Dowel Bar Misalignment**

A rating system was developed by Yu [2005] to evaluate the quality of dowel bar alignment. This system uses a joint score for joint-by-joint evaluation and a rolling average joint score for a series of five joints. The joint score (JS) is calculated by multiplying the number of dowel bars in each misalignment category by its weighting factor, adding all of the categories together and one to the total. The calculation uses the greater of the horizontal or vertical misalignments. The weighting factors for the misalignment types are given in Table 6.1.

**Table 6.1 Joint Score Weighting Factors**

| Misalignment (mm) | Weighting Factor |
|---|---|
| d <= 15 | 0 |
| 15 < d <= 20 | 2 |
| 20 < d <= 25 | 4 |
| 25 < d <= 38 | 5 |
| d > 38 | 10 |

A joint score (JS) less than five has a very low risk of joint locking, between five and ten has a low risk of joint locking, between ten and fifteen has a moderate risk of joint locking, and greater than fifteen has a high risk of joint locking. Figure 6.4 shows the joint scores. The average joint score is 78 with a standard deviation of 52.2. Only one of the 36 joints would be classified as a low risk for joint locking. The other 35 joints had a JS greater than fifteen indicating a high risk for joint locking.

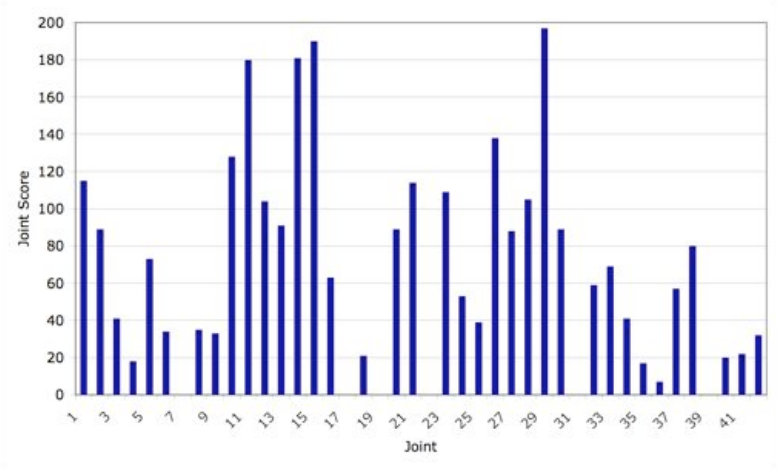


**Figure 6.4 Joint Scores**

In isolation, a locked joint should not influence pavement performance, however, a problem occurs if consecutive joints lock. The rolling average joint score is calculated by averaging five joint scores, the two before the joint, the evaluated joint, and the two joints after. Each individual joint score used in the calculation can have a maximum value of ten. A rolling average joint score of ten has a high

risk of developing distress because of two or more locked joints. Figure 6.5 presents the rolling average joint scores.

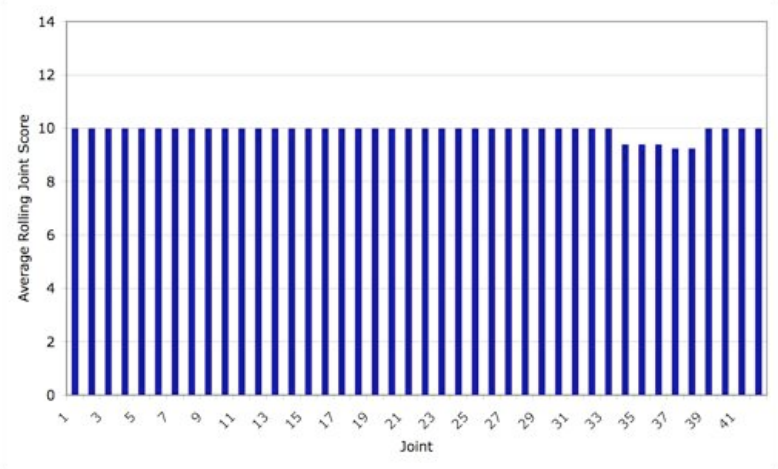


**Figure 6.5 Rolling Average Joint Scores**

Since an average rolling joint score of ten represent the possibility of two or more locked joints giving a high risk of developing distress.

## 6.3 Compressive Strength

Compressive strength testing was performed using 150 mm x 300 mm cylinders consolidated by vibration. Compressive strength testing was done according to ASTM C 39 - Standard Test Method for Compressive Strength of Cylindrical Concrete Specimens on days seven, fourteen, and twenty-eight [ASTM 2004]. Cylinders were demolded after 24 hours and cured in the moisture room before testing. A concrete specimen end grinder was used to prepare the samples prior to testing to ensure the ends of the cylinders were perpendicular. After end grinding the cylinders were placed back in the moisture room for half an hour to restore the moisture content of the cylinders lost during end grinding before testing. Load was applied at a constant rate without shock. Figure 6.6 shows the compressive strength development from the test track mixes.

A cone fracture occurred in 23 cylinders (63.9%), the remaining thirteen cylinders (36.1%) had both a cone and shear failure. Compressive strength increased from 0% RCA to 30% RCA. All of the RCA containing mixes reached the 28-day design strength, however, the control section containing no RCA did not. The control section is projected to reach the 28-day design strength at 36 days. The results show an RCA content of 30% can be used without negatively affecting the compressive strength.

A two-sample t analysis was performed to identify if a difference exists between the mean compressive strengths at 28-days for the preliminary and field mixes. A difference between the mixes would suggest a change to the mix had occurred. Testing was conducted at a 95% confidence interval. Results of the t procedure are summarized in Table 6.2.

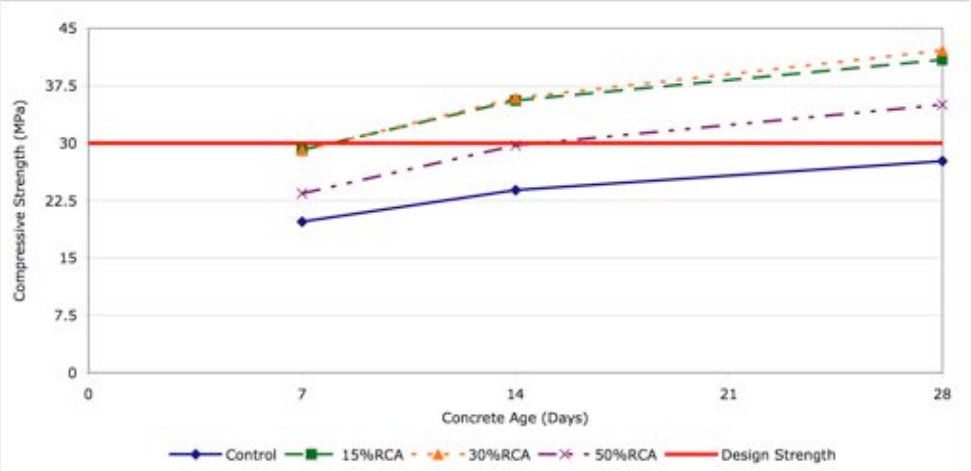


**Figure 6.6 Compressive Strength Results**

**Table 6.2 Results of t-Ttest**

| *Mix* | *df* | $t_{calculated}$ | $t_{critical}$ |
|---|---|---|---|
| 0% Coarse RCA | 2 | 22.45 | 4.303 |
| 15% Coarse RCA | 1 | 3.47 | 12.71 |
| 30% Coarse RCA | 1 | 4.88 | 12.71 |
| 50% Coarse RCA | 1 | 12.2 | 12.71 |

For 15%, 30%, and 50% Coarse RCA content $t_{critical}$ is greater the $t_{calculated}$ indicating that there is no evidence of a difference between the preliminary and field mixes. However, for 0% Coarse RCA there is a difference between the mixes based on the measured 28-day compressive strength values.

## 6.4 Flexural Strength

Flexural strength was tested with 150 mm X 150 mm X 600 mm beams consolidated by vibration. Beams were tested on day seven, and twenty-eight according to the three-point bending ASTM C 78 – Standard Test Method for Flexural Strength of Concrete using Simple Beam with Third-Point Loading [ASTM 2004]. The span length of the testing equipment was 450 mm and the load was applied at a constant rate without shock. Figure 6.7 shows the testing apparatus with a fractured flexural beam.

**Figure 6.7 Flexural Strength Testing**

The following equation was used to calculate the modulus of rupture in the middle third of the span length.

$$R = \frac{PL}{bd^2} \tag{6.1}$$

If a fracture was outside the middle third of the span length by a maximum of five percent, then the following equation was used.

$$R = \frac{3Pa}{bd^2} \tag{6.2}$$

where: $R$ = modulus of rupture, MPa

$P$ = maximum applied load indicated by the testing machine, N

$L$ = span length, mm

$b$ = average width of the specimen at the fracture, mm

$d$ = average depth of the specimen at the fracture, mm

$a$ = average distance between the line of fracture and beam nearest support, mm

All twelve flexural beams tested failed within the middle third of the span length. Figure 6.8 shows the results of the flexural strength testing.

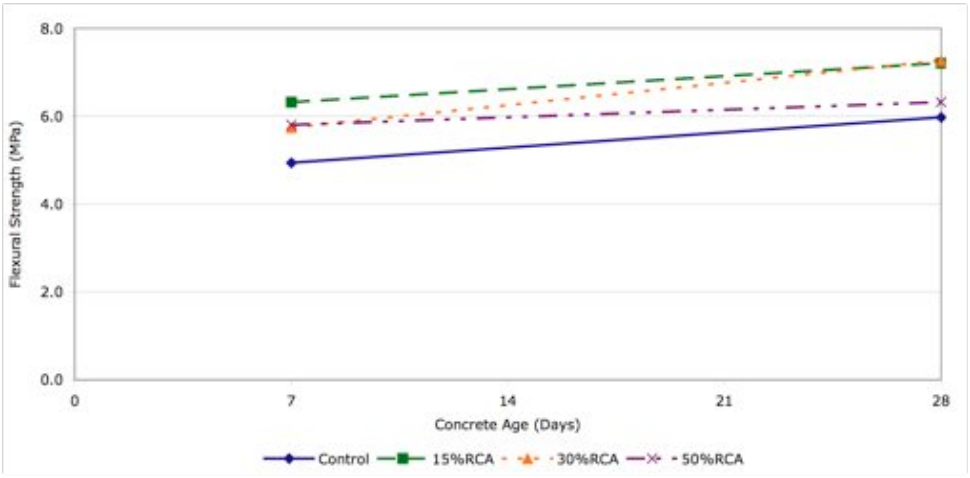


**Figure 6.8 Flexural Strength Testing Results**

Flexural strength development followed a similar trend as compressive strength. Flexural strength increased up to 30% RCA. The greatest increase in strength development from day seven to day 28, was the 30% RCA, while the 50% RCA had the smallest increase in strength. Flexural strength results are higher than the CAC recommended value of eight percent to twelve percent of the compressive strength or 0.6 to 0.8 square root of compressive strength [Kosmatka 2002]. Flexural strength values ranged from 17.3% of the compressive strength for the 30% RCA to 25.0% of the compressive strength for 0% RCA.

## 6.5 Maturity

Maturity testing was performed according to ASTMC 1074 – Standard Test Method for Estimating Concrete Strength by the Maturity Method [ASTM 2004]. COMMAND Center maturity system (sensors and software) by The Transtec Group was used to take time based temperature readings to calculate maturity.

In order to create the maturity curve, two concrete cylinders were installed with COMMAND Center sensors during the casting of the field specimens. The sensors were installed in the centre of the cylinder and at mid-depth. Once the cylinders were demolded after 24 hours they were moisture cured along with the other cylinders. Compressive strength testing was performed at seven, fourteen, and 28-days. At the end of 28-days, the maturity curves were created for each RCA amount by plotting a "best fit" line through the strength and maturity data.

To estimating in-place strength, two maturity sensors were attached to the strain gauge chair structure during the placement of the test sections. Maturity sensors took readings every 20 minutes for 28-days. This was used to estimate the concrete's strength based upon the created maturity curves. Maturity was calculated using the Nurse-Saul method (temperature-time factor). A semi-log maturity curve was created. The sigmodial relationship developed for the HIPERPAV program could not be used because of the upper predictive limit of 34.5 MPa (5,000 psi). The following equation was used to calculate the maturity curves for each percent RCA that are shown in Figure 6.9.

$$M(t) = \sum (T_a - T_o)\Delta t \tag{6.3}$$

where: $M(t)$ = temperature-time factor at age t, degree-day or degree-hour

$\Delta t$ = time interval, days or hours

$T_a$ = average concrete temperature during time $\Delta t$, °C

$T_o$ = datum temperature, °C

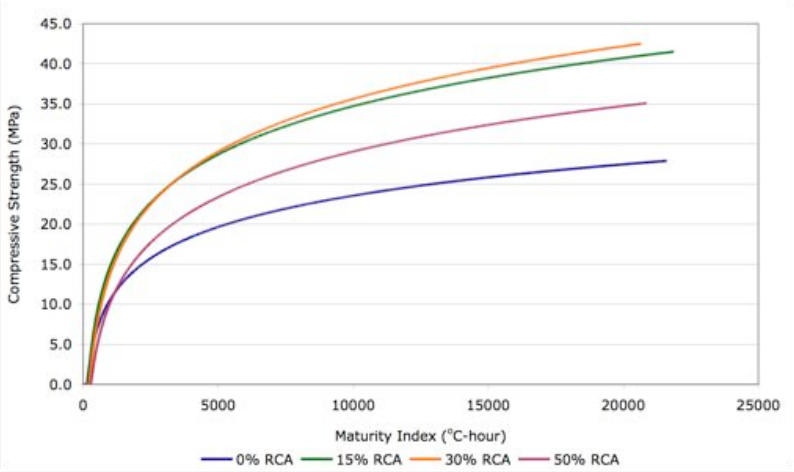


**Figure 6.9 RCA Maturity Curves**

Estimates of in-place strength were developed using the maturity curves and are shown in Table 6.3.

**Table 6.3 Strength Estimates of Placed Concrete**

| Time | In-Place Compressive Strength (MPa) | | | |
|---|---|---|---|---|
| | 0% RCA | 15% RCA | 30% RCA | 50% RCA |
| 1-day | 10.9 | 16.2 | 13.9 | 11.0 |
| 3-day | 16.5 | 24.7 | 24.0 | 19.5 |
| 7-day | 20.9 | 31.3 | 31.3 | 25.9 |
| 14-day | 24.3 | 36.6 | 37.4 | 31.0 |
| 28-day | 28.0 | 42.1 | 43.5 | 36.2 |

The estimated strength of the placed concrete was the same order as the cylinders, 30% RCA had the greatest strength and 0% RCA was the lowest. Strength developed faster in the field than the lab due to higher air temperatures accelerating curing and causing a loss of moisture for hydration in the concrete. Moisture was lost through evaporation, absorption into the coarse RCA, and being drawn into the asphalt-stabilized OGDL. At seven days, the strength development of the placed concrete was between 1.1 MPa (50% RCA) to 2.5 MPa (0% RCA) higher than the cylinders in the lab. At 28-days, the placed concrete was 0.3 MPa (0% RCA) to 1.4 MPa (30% RCA) higher than the lab.

## 6.6 Freeze-Thaw

Freeze-thaw testing was performed according to the ASTM C 666 Procedure A – Standard Test Method for Resistance of Concrete to Rapid Freezing and Thawing and ASTM C 215 – Standard Test Method for Fundamental Transverse, Longitudinal, and Torsional Resonate Frequencies of Concrete Specimens [ASTM 2004]. The optional length change test was not conducted. The samples were demolded after 24 hours and cured for eleven days before being placed in saturated lime water at room temperature for 48 before the start of the test. Figure 6.10 shows the beams placed in a freeze-thaw bed that cycled from -20 $^{o}$C to 4 $^{o}$C and back every 220 minutes (3.67 hours).

**Figure 6.10 Beams in the Freeze-Thaw Bed**

The beams were completely submerged in water and rotated in orientation and position within the freeze-thaw bed during testing to reduce effects from hotter of cooler areas.

The half of the freeze thaw bed not occupied by samples contained pervious concrete or dummy specimens. An oscilloscope and Erudite MkIV by CNS Farnell were used for the testing the relative dynamic modulus (RDM) of elasticity as shown in Figure 6.11. The frequency range used for all tests was 1,000 Hz to 2,000 Hz. For each beam, four fundamental transverse frequency sweeps, one sweep on each side, were conducted to calculate an average.

**Figure 6.11 Erudite MkIV Testing Equipment and Setup**

Testing was interrupted at cycle 214 for a period of two weeks to isolate and repair a loose connection causing a short in the wires connecting the contact vibrator and the electronics unit.

The relative dynamic modulus of elasticity was calculated using the following equation.

$$P_c = \left( \frac{n_1^2}{n^2} \right) \times 100 \tag{6.4}$$

where: $P_c$ = relative dynamic modulus of elasticity, after c cycles of freezing and thawing, %

$n$ = fundamental transverse frequency at 0 cycles of freezing and thawing

$n_1$ = fundamental transverse frequency at c cycles of freezing and thawing

The durability factor was calculated using the equation below.

$$DF = \frac{PN}{M} \tag{6.5}$$

where: $DF$ = durability factor of the test specimen

$P$ = relative dynamic modulus of elasticity at N cycles, %

$N$ = number of cycles at which P reaches the specified minimum value for discontinuing the test or the specified number of cycles at which the exposure is terminated, which ever is less

$M$ = specified number of cycles at which the exposure is to be terminated

Table 6.4 summarizes the properties of the beams before testing.

**Table 6.4 Properties of Beams Prior to Testing**

| Beam | Width | Depth | Length | Fundamental Transverse Frequency (kHz) | | | | | Mass |
|---|---|---|---|---|---|---|---|---|---|
| ID | (mm) | (mm) | (mm) | [1] | [2] | [3] | [4] | [Avg] | (kg) |
| 0% FT1 | 102 | 78 | 407 | 1.791 | 1.793 | 1.772 | 1.774 | 1.783 | 7.552 |
| 0% FT2 | 101 | 78 | 407 | 1.749 | 1.749 | 1.738 | 1.742 | 1.745 | 7.431 |
| 15% FT1 | 102 | 78 | 406 | 1.820 | 1.820 | 1.818 | 1.813 | 1.818 | 7.721 |
| 15% FT2 | 102 | 78 | 407 | 1.889 | 1.889 | 1.887 | 1.888 | 1.888 | 7.865 |
| 30% FT1 | 101 | 77 | 407 | 1.785 | 1.781 | 1.760 | 1.759 | 1.771 | 7.660 |
| 30% FT2 | 102 | 77 | 408 | 1.767 | 1.769 | 1.782 | 1.787 | 1.776 | 7.638 |
| 50% FT1 | 101 | 78 | 406 | 1.739 | 1.739 | 1.739 | 1.734 | 1.740 | 7.538 |
| 50% FT2 | 101 | 78 | 406 | 1.759 | 1.750 | 1.757 | 1.769 | 1.759 | 7.514 |

Table 6.5 shows the results at the end of the 300 freeze-thaw cycles for relative dynamic modulus (RDM) and weight change. The RDM is similar for all of the beams, approximately 90%.

**Table 6.5 Freeze-Thaw Testing Results**

| Beam ID | RDM (%) | Δ Mass (%) |
|---|---|---|
| 0% FT1 | 91.2 | -0.54 |
| 0% FT2 | 89.3 | -0.54 |
| 15% FT1 | 90.3 | -0.62 |
| 15% FT2 | 89.7 | -0.54 |
| 30% FT1 | 92.0 | -0.68 |
| 30% FT2 | 86.2 | -0.84 |
| 50% FT1 | 88.9 | -0.19 |
| 50% FT2 | 91.3 | -0.35 |

The amount of mass loss increases as the RCA content increases to 30% and decreases at 50%. Figure 6.12 shows the change in RDM of beams over the 300 cycles. There is a similar trend for all RCA contents with the majority of the change in RDM occurring during the first 117 cycles. There was not a continuous decrease in RDM values throughout the testing. Each RCA content had an increasing trend for a segment of the freeze-thaw cycles.

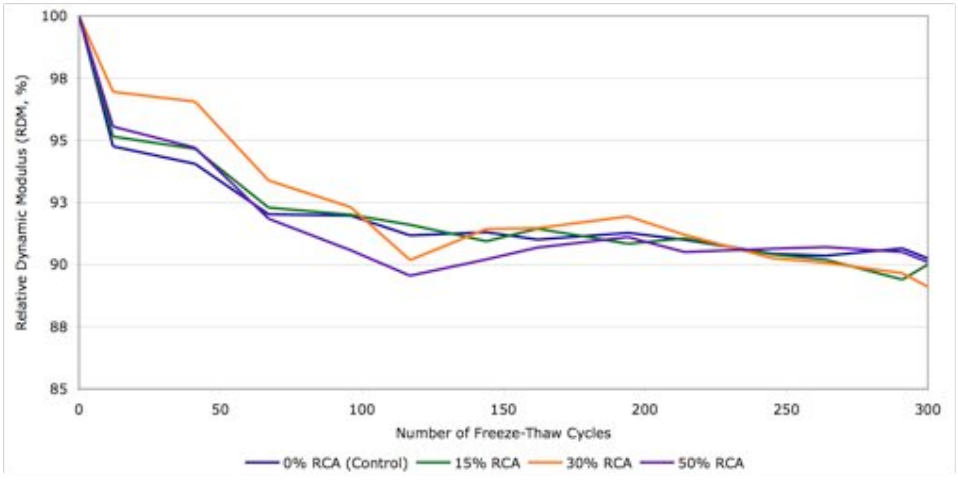


**Figure 6.12 Changes in Relative Dynamic Modulus**

## 6.7 Coefficient of Thermal Expansion

AASHTO TP60 is the provisional standard method for measuring CTE. It is also the method recommended for use in the MEPDG. Steps to measure CTE using AASHTO TP60 include [AASHTO 2004]:

1. Soaking a 100 mm (four inch) or 150 mm (six inch) core in water for a minimum of 48 hours before testing begins.
2. Measuring the length of the saturated core using calipers.
3. The core is placed in a support frame and submerged in a water bath.
4. The temperature of the water bath is changed from ten degrees Celsius (50 $^{o}$F) to 50 $^{o}$C (120 $^{o}$F) where it remains until three consecutive Linear Variable Differential Transformer (LVDT) readings, taken 10 minutes apart, change by less than 0.00025 mm (0.00001 in.). Then this step is repeated several times.

Since the AASHTO TP60 requires specialized equipment that is often not readily available, a simplified approach was used to calculate CTE. The method used to evaluate CTE is adapted from ASTM C 531, Standard Test Method for Linear Shrinkage and Coefficient of Thermal Expansion of Chemical-Resistant Mortars, Grouts, Monolithic Surfaces, and Polymer Concretes [West 2005, ASTM 2004]. The following are the steps to perform this simplified method for CTE testing.

1. Cores dry for a period of 28 days after being taken from the field.
2. Reference points are installed along the vertical axis of a cylinder 200 mm apart and allowed to cure for five hours.
3. The air temperature is cycled between 20 $^{o}$C (68 $^{o}$F) and -20 $^{o}$C (-4 $^{o}$F). It remains constant at each of these temperatures for a minimum of sixteen hours to ensure that the cores reach the ambient temperature. Mechanical strain readings where taken at each of the temperatures. In this study the temperature was held constant for 24 hours and two cycles were completed. The temperature was controlled using a large walk-in freezer.

Both the AASHTO TP60 and the modified method calculate strain using equation 7.6 [West 2005, AASHTO 2004].

$$\alpha_{PCC} = \frac{\Delta L}{(\Delta T \times L)} \tag{6.6}$$

where: $\alpha_{PCC}$ = coefficient of thermal expansion (CTE), strain per $^{o}$C

$\Delta L$ = change in unit length due to a temperature change $\Delta T$

$\Delta T$ = change in temperature ($T_2 - T_1$), $^{o}$C

$L$ = length of specimen, mm

Using the measured lengths, strain and the corresponding CTE values were calculated. These values are presented in Table 6.6. Strain was calculated by comparing the change of the measured length with the original length.

**Table 6.6 CTE Testing Results**

0% RCA

| Cycle | A1-1 | | A1-2 | | A1-3 | | A2 | | A3 | | A4 | |
|---|---|---|---|---|---|---|---|---|---|---|---|---|
| | $\Delta L$[1] | $\alpha$[2] | $\Delta L$ | $\alpha$ | $\Delta L$ | $\alpha$ | $\Delta L$ | $\alpha$ | $\Delta L$ | $\alpha$ | $\Delta L$ | $\alpha$ |
| 1 | -56 | 6.90 | -58 | 7.03 | -59 | 7.34 | -57 | 6.65 | -65 | 7.89 | -68 | 8.11 |
| | -10 | 5.88 | 2 | 7.49 | -4 | 6.94 | 1 | 7.03 | -5 | 7.66 | 3 | 8.97 |
| 2 | -68 | 7.22 | -54 | 6.96 | -57 | 6.69 | -64 | 8.04 | -58 | 6.66 | -46 | 6.29 |
| | -3 | 7.78 | 2 | 6.21 | 7 | 7.80 | 8 | 8.64 | 6 | 7.89 | 6 | 6.64 |
| Average | | 6.95 | | 6.29 | | 7.19 | | 7.59 | | 7.53 | | 7.50 |

15% RCA

| Cycle | B1 | | B2 | | B3 | | B4-1 | | B4-2 | | B4-3 | |
|---|---|---|---|---|---|---|---|---|---|---|---|---|
| 1 | -46 | 5.42 | -49 | 5.86 | -49 | 5.86 | -56 | 7.06 | -47 | 5.89 | -48 | 6.02 |
| | 1 | 5.92 | -4 | 5.70 | 4 | 6.68 | 6 | 7.88 | 3 | 6.45 | 6 | 6.86 |
| 2 | -58 | 7.7 | -53 | 6.30 | -54 | 7.46 | -51 | 7.17 | -55 | 7.34 | -43 | 6.22 |
| | 0 | 7.34 | -1 | 6.39 | 5 | 7.43 | 4 | 6.75 | 6 | 7.56 | -1 | 5.20 |
| Average | | 6.60 | | 6.06 | | 6.86 | | 7.22 | | 6.81 | | 6.08 |

30% RCA

| Cycle | C1 | | C2 | | C3-1 | | C3-2 | | C3-3 | | C4 | |
|---|---|---|---|---|---|---|---|---|---|---|---|---|
| 1 | -40 | 4.85 | -33 | 3.97 | -48 | 5.92 | -39 | 4.88 | -44 | 5.60 | -39 | 4.72 |
| | -5 | 4.41 | 5 | 4.78 | 6 | 6.80 | -1 | 4.88 | 1 | 5.80 | 6 | 5.61 |
| 2 | -47 | 5.32 | -36 | 5.10 | -39 | 5.63 | -47 | 5.84 | -37 | 4.82 | -40 | 5.76 |
| | -8 | 6.72 | 11 | 5.70 | 1 | 4.89 | -14 | 4.09 | 5 | 5.17 | 2 | 5.13 |
| Average | | 5.33 | | 4.89 | | 5.81 | | 4.92 | | 5.35 | | 5.31 |

50% RCA

| Cycle | D1 | | D2-1 | | D2-2 | | D2-3 | | D3 | | D4 | |
|---|---|---|---|---|---|---|---|---|---|---|---|---|
| 1 | -33 | 4.03 | -25 | 3.10 | -34 | 4.25 | -31 | 3.83 | -33 | 4.09 | -30 | 3.70 |
| | -5 | 3.50 | 5 | 3.71 | -6 | 3.50 | 1 | 5.1 | -3 | 3.76 | -2 | 3.52 |
| 2 | -35 | 4.74 | -33 | 4.74 | -32 | 3.26 | -28 | 4.72 | -36 | 4.07 | -35 | 4.11 |
| | 2 | 4.89 | 7 | 4.89 | -1 | 3.81 | 8 | 4.41 | 3 | 4.70 | 9 | 5.31 |
| Average | | 4.29 | | 4.11 | | 3.71 | | 4.52 | | 4.15 | | 4.16 |

1. ΔL (um), 2. $\alpha$ ($10^{-6}$ /°C)

The CTE values obtained for samples containing 15% RCA and 30% RCA are within the typical range of values for a concrete made with a limestone aggregate ($5.9x10^{-6}$ /°C to $9.2x10^{-6}$ /°C). Figure 6.13 shows that CTE decreased as the amount of coarse RCA increased. This relationship is strong as demonstrated by the high $R^2$ value. The decreasing CTE trends is due to replacing larger amount of virgin limestone aggregate with the coarse RCA concrete that has a lower CTE value.

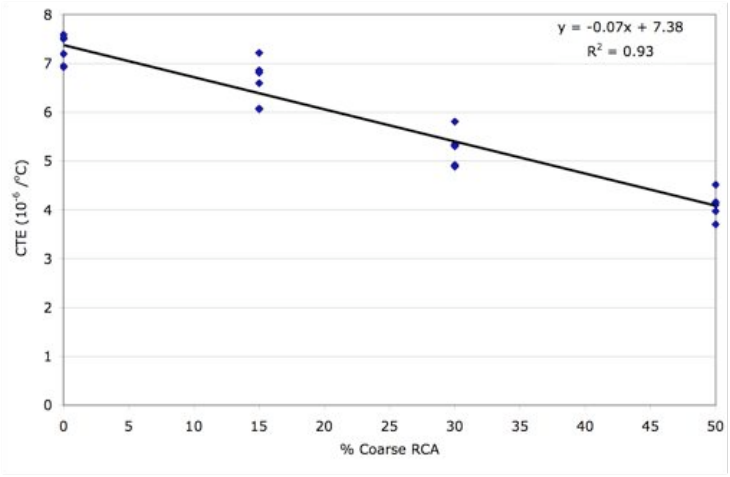


**Figure 6.13 CTE Values for RCA**

Higher CTE values are associated with increased joint deterioration, expand/shrink (slab curl), and cracking, a lower CTE is more desirable. This testing clearly shows that using a quality RCA gives a lower CTE than virgin aggregate. This is contradictory to previous research by Yang et al. [2003]. Since the research by Yang et al does not state any specific information about the quality of RCA used, it is likely that the RCA was a lower quality than in this study. A high quality RCA of a specific size was used in this study, and is likely the reason for the difference in results.

A recent CTE study by Tanesi et al using the AASHTO TP 60 method with automated equipment produced results with an average variability of $0.7x10^{-6}$ /°C [Tanesi 2007]. Variability in the study was defined as

$$\delta_{\alpha_{PCC}} = \alpha_{PCC(\max)} - \alpha_{PCC(\min)} \quad (6.7)$$

where: $\delta_{\alpha pcc}$ = coefficient of thermal expansion (CTE) variability, strain per $^{o}$C

$\alpha_{PCC(\max)}$ = maximum CTE test value, strain per $^{o}$C

$\alpha_{PCC(\min)}$ = minimum CTE test value, strain per $^{o}$C

Using this definition for variability, the simplified method used in this study had approximately double the variability at $1.53 \times 10^{-6}$ /$^{o}$C. Although the variability is increased with the simplified method, it is still a useful method for calculating CTE and had a very strong correlation with the amount of RCA in the concrete.

## 6.8 Testing Summary

Table 6.7 compares the characteristics of concrete containing coarse RCA with existing literature. The coarse RCA used in this research showed improvements in compressive strength, flexural strength, and CTE, while no difference in freeze-thaw durability was observed. These results contrary to the existing literature can be explained by the high quality RCA used in the study. The in-service concrete had sufficient strength and durability showing no visible signs of deterioration and when crushed all visible contaminates were removed.

**Table 6.7 CTE Testing Results**

| | Literature [ACPA 2009] | UW RCA |
|---|---|---|
| Compressive Strength | Up to 24% lower | Up to 50% greater |
| Flexural Strength | Up to 10% lower | Up to 25% greater |
| Freeze-Thaw | Depends on air void system | Similar results |
| Coefficient of Thermal Expansion | Up to 30% greater | Up to 45% lower |

# Chapter 7
# Field Performance

## 7.1 Method

The performance of the four pavement test sections was evaluated using visual surveys conducted following the MTO "Manual for Condition Rating of Rigid Pavements" [Chong 1995]. The MTO uses distress type, severity, and density with a measure of ride quality to calculate a pavement condition index (PCI) value. Equation 8.1 presents the MTO calculation for PCI.

$$PCI = \left(10 \times \sqrt{0.1 \times RCI} \times DMI \times 0.924\right) + 8.856 \tag{7.1}$$

where: $PCI$ = Pavement Condition Index

$RCI$ = Riding Comfort Index

$DMI$ = Distress Manifestation Index, from Equation 8.2.

The DMI is a weighted total of all the observed pavement distress and is calculated using Equation 8.2.

$$DMI = 10 \times \left( \frac{DMI_{Max} - \sum_{i=1}^{n} W_i \left(s_i + d_i\right)}{DMI_{Max}} \right) \tag{7.2}$$

where: $DMI$ = Distress Manifestation Index

$DMI_{Max}$ = Theoretical maximum value, 196 for concrete

$i$ = Distress type

$W_i$ = Pavement Distress Weight, values 0.5 to 3.0

$s_i$ = Distress severity, values 0 to 4.0

$d_i$ = Distress density, values 0 to 4.0

A summary of pavement distress types, weighting, and distress severity and density are presented in Tables 7.1 to 7.3.

**Table 7.1 Pavement Distress Weights**

| Pavement Distress | Weight ($W_i$) |
|---|---|
| Ravelling | 0.5 |
| Polishing | 1.5 |
| Scaling/Abrasion | 1.5 |
| Potholing | 1.0 |
| Joint Cracking/Spalling | 2.0 |
| Faulting | 2.5 |
| Distortion | 1.0 |
| Sealant Loss | 0.5 |
| Joint failure | 3.0 |
| Longitudinal Cracking | 2.0 |
| Transverse Cracking | 2.0 |
| Diagonal/Edge Cracking | 2.5 |

**Table 7.2 Distress Severity Levels and Weights**

| Severity Level | None | V. Slight | Slight | Moderate | Severe | V. Severe |
|---|---|---|---|---|---|---|
| Weight ($s_i$) | 0 | 0.5 | 1 | 2 | 3 | 4 |

**Table 7.3 Distress Density Levels and Weights**

| Density Level | None | Few | Intermittent | Frequent | Extensive | Throughout |
|---|---|---|---|---|---|---|
| Weight ($d_i$) | 0 | 0.5 | 1 | 2 | 3 | 4 |
| % Area | 0 | < 10 | < 20 | < 50 | < 80 | > 80 |

A description of the different pavement distress severities is presented in Appendix C. The PCI value is used for determining maintenance options, pavement deterioration rates, and maintenance priority scheduling; it is not a measure of structural capacity, surface roughness or skid resistance. The PCI scale ranges from 100 (perfect/excellent) to zero (fully deteriorated/failed). Table 7.4 illustrates the PCI rating scale.

**Table 7.4 PCI Rating Scale**

| Rating | Excellent | V. Good | Good | Fair | Poor | V. Poor | Failed |
|---|---|---|---|---|---|---|---|
| PCI Value | 85 - 100 | 70 - 85 | 55 - 70 | 40 - 55 | 25 - 40 | 10 - 25 | 0 - 10 |

## 7.2 Evaluations

Nine evaluations have been completed by the researcher and they were reviewed for consistency by the supervisor who has experience in evaluations. The initial evaluation was conducted on June 18, 2007 five days after paving was completed. Additional evaluations were performed on September 20, 2007, November 9, 2007, April 4, 2008, June 25, 2008, September 21, 2008, November 1, 2008, April 23, 2009, and June 6, 2009.

### 7.2.1 Evaluation #1 – June 18, 2007

For this first evaluation, no deterioration was observed, and all test sections received a PCI of 100. No shrinkage cracking was observed in any of the test sections. The pavement shoulders had not yet been constructed. There was cutting residue along all joints, approximately 0.3 m to each side. The entire pavement surface was covered in a fine dust. There was a rough pavement surface due to the tining experiment. There were noticeable transverse dips in the pavement caused by a stationary paver. Figure 7.1 show the general condition of the test section four days after construction. Figure 7.2 shows a close-up of some of the experimental tining

**Figure 7.1 0% Coarse RCA Northbound View and 50% Coarse RCA Southbound View**

**Figure 7.2 Pavement Surface Tining Close-up**

### 7.2.2 Evaluation #2 – September 20, 2007

No change in performance was seen on the second evaluation. All of the test sections still have a PCI of 100. The joints are widened and properly sealed. One joint in each of the four test sections NB direction have small patches from checking the accuracy of the MIT-2 scan data. Gravel shoulders are constructed.

### 7.2.3 Evaluation #3 – November 9, 2007

The third evaluation was carried out approximately five months after the test sections were placed. All of the test sections had some deterioration from the last evaluation but were all rated in excellent condition with a PCI greater than 85. Table 7.5 summarizes the test track conditions observed during the third evaluation.

**Table 7.5 Evaluation 3 – Test Track Conditions**

| Test Section | PCI | Pavement Distress | Severity | Density |
|---|---|---|---|---|
| 0% Coarse RCA | 97 | Abrasion | Very Slight | Intermittent |
| | | Joint Cracking/Spalling | Very Slight | Intermittent |
| 15% Coarse RCA | 98 | Joint Cracking/Spalling | Very Slight | Intermittent |
| 30% Coarse RCA | 98 | Joint Cracking/Spalling | Very Slight | Intermittent |
| 50% Coarse RCA | 98 | Joint Cracking/Spalling | Very Slight | Intermittent |

The 0% coarse RCA test section is showing some minor amounts of abrasion loss. The exposed interface at the South end of the control section experienced heavy loads from trucks turning onto the test section from an unpaved extension. These trucks tracked gravel and debris onto the test section that degraded the surface. Figure 7.3 shows the joint spalling that is common to all four test sections. No cracking or deterioration of patches was noted. Figure 7.4 shows intermittent spalling of the pavement edge and shoulder settlement of approximately 15% of all SB sections (loaded). Wide loads not always traveling on the pavement surface cause this. The damage to the pavement edge is not included in the PCI calculation because it does not directly affect the performance of the road.

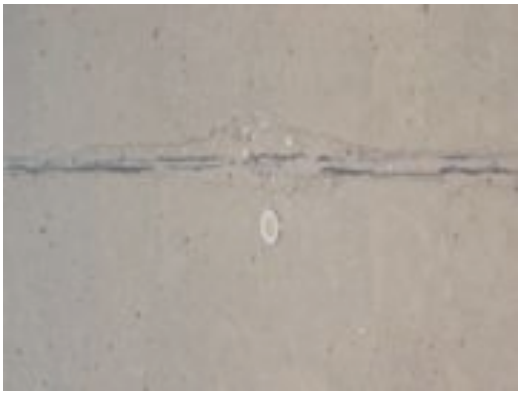

**Figure 7.3 Joint Spalling**

**Figure 7.4 Pavement Edge Spalling and Shoulder Settlement**

### 7.2.4 Evaluation #4 – April 4, 2008

Each test section had some additional deterioration compared to the last evaluation. All of test sections are still in excellent condition with a PCI greater than 85. Table 7.6 summarizes the conditions observed in the fourth evaluation. Figure 7.5 portrays some of the deterioration observed during this evaluation. The abrasion of the 0% coarse RCA test section has been accelerated because of some water pooling at the end of the end of the test section. Figure 7.6 shows a core hole with settlement surrounding the hole but no cracking. Figure 7.7 shows the transverse depressions due to a stationary slipform paver. The cracking of the asphalt adjoining the test sections is shown in Figure 7.8. Finally, Figure 7.9 shows the failure of the blockout containing inter-panel sensors spanning the joint in 0% and 15% Coarse RCA. These areas will need repair.

**Table 7.6 Evaluation 4 – Test Track Conditions**

| Test Section | PCI | Pavement Distress | Severity | Density |
|---|---|---|---|---|
| 0% Coarse RCA | 92 | Abrasion | Severe | Frequent |
| | | Joint Cracking/Spalling | Moderate | Frequent |
| 15% Coarse RCA | 96 | Joint Cracking/Spalling | Moderate | Frequent |
| 30% Coarse RCA | 95 | Joint Cracking/Spalling | Moderate | Frequent |
| | | Ravelling | Very Slight | Few |
| 50% Coarse RCA | 96 | Joint Cracking/Spalling | Moderate | Frequent |

**Abrasion**

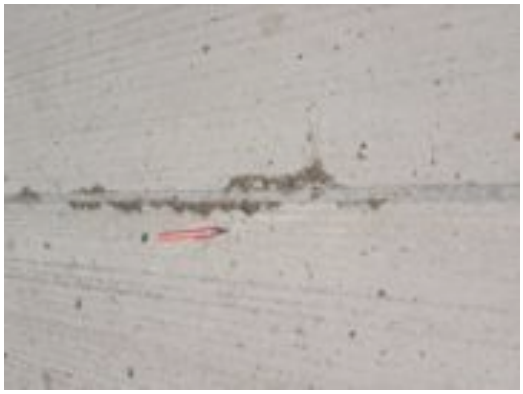

**Joint Craking/Spalling**

**Ravelling**

**Edge and Shoulder Settlement**

**Figure 7.5 Evaluation 4 - Pavement Distresses**

**Figure 7.6 Core Hole Settlement**

**Figure 7.7 Transverse Depression from Slipform Paver**

**Figure 7.8 Asphalt Adjoining Test Sections**

**Figure 7.9 Blockout Failure**

### 7.2.5 Evaluation #5 – June 25, 2008

The test sections remain unchanged from the last evaluation. Table 7.7 shows that all of the test sections are in excellent condition with a PCI greater than 85.

**Table 7.7 Evaluation 5 – Test Track Conditions**

| Test Section | PCI | Pavement Distress | Severity | Density |
|---|---|---|---|---|
| 0% Coarse RCA | 92 | Abrasion | Severe | Frequent |
| | | Joint Cracking/Spalling | Moderate | Frequent |
| 15% Coarse RCA | 96 | Joint Cracking/Spalling | Moderate | Frequent |
| 30% Coarse RCA | 95 | Joint Cracking/Spalling | Moderate | Frequent |
| | | Ravelling | Very Slight | Few |
| 50% Coarse RCA | 96 | Joint Cracking/Spalling | Moderate | Frequent |

Figure 7.10 shows the extensive spalling, approximately 80%, of the pavement edge and shoulder settlement in all sections of the SB (loaded) direction. Settlement of the shoulder has increased to over 25mm.

**Figure 7.10 Pavement Edge Spalling and Shoulder Settlement**

### 7.2.6 Evaluation #6 – September 21, 2008

Compared to evaluation five, evaluation six showed some minor deterioration with very slight raveling of three sections (0%, 15%, and 50%). All of the test sections are still in excellent condition with a PCI greater than 85. Table 7.8 summarizes the conditions observed during evaluation six.

Figure 7.11 to Figure 7.13 show some of the pavement distress. Joint spalls with loose or missing pieces are shown in Figure 7.11, new raveling is shown in Figure 7.12 and an increase in severity and density of asphalt cracking at the start of the test sections is shown in Figure 7.13.

**Table 7.8 Evaluation 6 – Test Track Conditions**

| Test Section | PCI | Pavement Distress | Severity | Density |
|---|---|---|---|---|
| 0% Coarse RCA | 92 | Abrasion | Severe | Frequent |
| | | Joint Cracking/Spalling | Moderate | Frequent |
| | | Ravelling | Very Slight | Few |
| 15% Coarse RCA | 95 | Joint Cracking/Spalling | Moderate | Frequent |
| | | Ravelling | Very Slight | Few |
| 30% Coarse RCA | 95 | Joint Cracking/Spalling | Moderate | Frequent |
| | | Ravelling | Very Slight | Few |
| 50% Coarse RCA | 95 | Joint Cracking/Spalling | Moderate | Frequent |
| | | Ravelling | Very Slight | Few |

**Figure 7.11 Joint Spalling**

**Figure 7.12 New Raveling**

**Figure 7.13 Asphalt Cracking**

An automated distress survey was conducted of the test sections during evaluation six; however, the results are currently unavailable.

### 7.2.7 Evaluation #7 – Nov 1, 2008

The test sections remain unchanged since the last evaluation. All of the test sections are in excellent condition with a PCI greater than 85. Table 7.9 summarizes the conditions of the test sections.

**Table 7.9 Evaluation 7 – Test Track Conditions**

| Test Section | PCI | Pavement Distress | Severity | Density |
|---|---|---|---|---|
| 0% Coarse RCA | 92 | Abrasion | Severe | Frequent |
| | | Joint Cracking/Spalling | Moderate | Frequent |
| | | Ravelling | Very Slight | Few |
| 15% Coarse RCA | 95 | Joint Cracking/Spalling | Moderate | Frequent |
| | | Ravelling | Very Slight | Few |
| 30% Coarse RCA | 95 | Joint Cracking/Spalling | Moderate | Frequent |
| | | Ravelling | Very Slight | Few |
| 50% Coarse RCA | 95 | Joint Cracking/Spalling | Moderate | Frequent |
| | | Ravelling | Very Slight | Few |

### 7.2.8 Evaluation #8 – April 23, 2009

Abrasion is now evident in all test sections and is the worst in the 0% and 30% coarse RCA sections. At these points large amounts of gravel, dirt, and garbage are being placed on the test sections and driven over causing the distress. All of the test sections are still in excellent condition with a PCI greater than 85. Table 7.10 outlines the observed condition of the test track.

**Table 7.10 Evaluation 8 – Test Track Conditions**

| Test Section | PCI | Pavement Distress | Severity | Density |
|---|---|---|---|---|
| 0% Coarse RCA | 91 | Abrasion | Severe | Extensive |
| | | Joint Cracking/Spalling | Moderate | Frequent |
| | | Ravelling | Very Slight | Few |
| 15% Coarse RCA | 95 | Joint Cracking/Spalling | Moderate | Frequent |
| | | Abrasion | Very Slight | Few |
| | | Ravelling | Very Slight | Few |
| 30% Coarse RCA | 95 | Joint Cracking/Spalling | Moderate | Frequent |
| | | Abrasion | Slight | Intermittent |
| | | Ravelling | Very Slight | Few |
| 50% Coarse RCA | 95 | Joint Cracking/Spalling | Moderate | Frequent |
| | | Abrasion | Very Slight | Few |
| | | Ravelling | Very Slight | Few |

Scaling in 0% coarse RCA test section has increased in density to almost 70% of the area. Figure 7.14 shows the spalling of the pavement edge and shoulder settlement in all sections. This spalling is almost 100% of the SB (loaded) direction. The settlement of the shoulder has also increased to over 50 mm in some areas. The asphalt adjoining the test sections had additional deterioration over the winter so some patching was attempted of the area as shown in Figure 7.15.

**Figure 7.14 Pavement Edge Spalling and Shoulder Setlement**

**Figure 7.15 Patching of Adjoining Asphalt**

### 7.2.9 Evaluation #9 – June 6, 2009

There was only one change, a new pothole, from the previous evaluation. All test sections continue to be in excellent condition with a PCI greater than 85. Table 7.11 and Figure 7.16 summarize the test section conditions. Figure 7.17 shows the new pothole in the 0% coarse RCA test sections looks to have been caused by machinery. The pavement shoulders are shown in Figure 7.18.

**Table 7.11 Evaluation 9 – Test Track Conditions**

| Test Section | PCI | Pavement Distress | Severity | Density |
|---|---|---|---|---|
| 0% Coarse RCA | 91 | Abrasion | Severe | Extensive |
| | | Joint Cracking/Spalling | Moderate | Frequent |
| | | Ravelling | Very Slight | Few |
| | | Pothole | Slight | Few |
| 15% Coarse RCA | 95 | Joint Cracking/Spalling | Moderate | Frequent |
| | | Abrasion | Very Slight | Few |
| | | Ravelling | Very Slight | Few |
| 30% Coarse RCA | 94 | Joint Cracking/Spalling | Moderate | Frequent |
| | | Abrasion | Slight | Intermittent |
| | | Ravelling | Very Slight | Few |
| 50% Coarse RCA | 95 | Joint Cracking/Spalling | Moderate | Frequent |
| | | Abrasion | Very Slight | Few |
| | | Ravelling | Very Slight | Few |

**0% Coarse RCA**

**15% Coarse RCA**

**30% Coarse RCA**

**50% Coarse RCA**

**Figure 7.16 Evaluation 9 – Test Section Conditions**

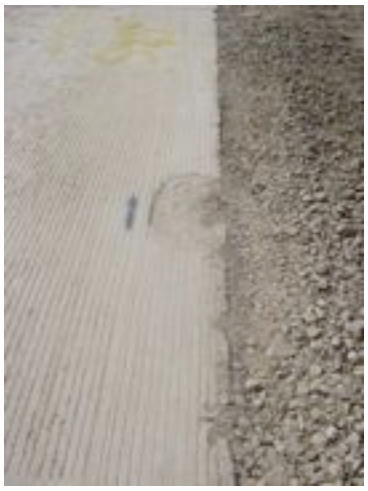

**Figure 7.17 New Pothole in 0% Coarse RCA**

**Figure 7.18 Regraded Southbound Shoulder**

## 7.3 Summary

The results of the nine evaluations over the previous 24 are shown in Figure 7.19. All of the test sections are in excellent conditions with a PCI value greater than 85 and are showing no significant difference in performance. The PCI decreased the most after each winter season.

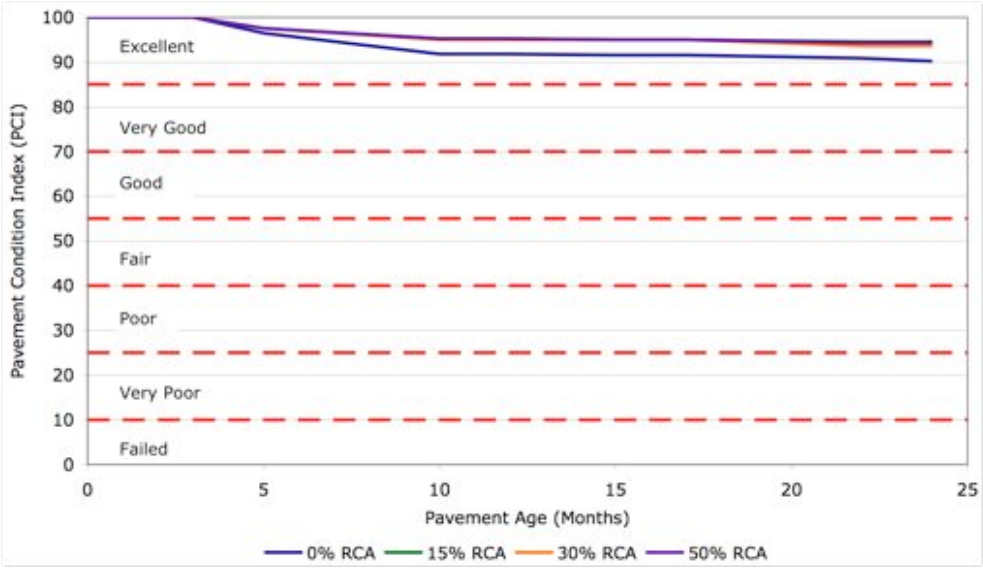


**Figure 7.19 PCI Progression**

# Chapter 8

# Sensor Evaluation

Each test section had one slab that was instrumented with twelve sensors. Each instrumented slab contained six vibrating wire concrete embedment strain gages to measure long term longitudinal and transverse strain due to environmental changes, two vibrating wire vertical extensometers to monitor slab curling and warping, two vibrating wire inter-panel extensometers to monitor joint movement, and two maturity meters to measure maturity and temperature.

On September 6, 2007 continuous readings started. On November 8, 2007 the 0% RCA multiplexer was disconnected to lengthen the sensor cables and to relocate the multiplexer cabinet. The waste management facility staff buried the cable before it was reconnected. A snowplow cut the cable connecting the 30% and 50% RCA mutiplexers to the datalogger in December 2007 and the 15% RCA multiplexer cable was cut in February 2008.

On October 31, 2008 cable splicing was done to add 10m-13m of cable for each sensor in the 30% and 50% RCA sections and relocation of the 4 remote multiplexer cabinets and datalogger were completed. Continuous monitoring was restarted November 8, 2008. When the data was downloaded on November 15, 2008, there was an error for every sensor at each time interval. The sensor errors at each interval for every sensor were NAN (not-a-number) for strain and displacement measurements and -104 for the temperature measurements. The NAN error can be due to the voltage exceeding the specified range or an open circuit. The temperature is calculated using Equation 8.1.

$$Temperature = -104.78 + 378.11\omega - 611.59\omega^2 + 544.27\omega^3 - 240.91\omega^4 + 43.089\omega^5 \quad (8.1)$$

where: $\omega$ = sensor reading

Many steps were taken to solve the error readings. The system was checked after each step and since error messages were still showing then further steps were carried out.

1. The connections were checked and adjusted to ensure there was not an open circuit from wires touching each other. The wiring was checked against the wiring diagram.
2. The order of wiring for the temperature side of the connection was switched.
3. The datalogger program was compared to the Interlocking Concrete Paver (ICP) Project datalogger program and a number of differences were noted. The delay value was 5 for RCA and 15 for ICP. The end frequency was 1,200 for RCA and 1,000 for ICP. Finally the time sweep was 250 in the RCA program and 200 in the ICP program.
4. Several modifications were made to the computer program. The order that the remote multiplexers were called was changed to one then two, instead of two then one. The voltage range was adjusted (2.5, 7.5, 25, and 250 mV) for the measurement of strain and

displacement. The start and ending frequency were modified (20 to 5000 Hz) for the measurement of strain and displacement. The voltage range (2.5, 7.5, 25, 250, 2500 mV, and autorange) for the measurement of temperature was adjusted. Finally, the "frequency range on the strain and displacement measurement was increased.

5. RST Instruments was contacted for assistance and suggested that an open circuit was causing the errors.
6. Again the wiring and connections were checked and adjusted. The protected line was connected correctly, however, the in/out of the lighting protection board had two wires connected incorrectly. Once these wires were fixed, the errors for multiplexers one and two were resolved, however, multiplexer three and four still had the same error.
7. RST Instruments was again contacted and recommended that the delay be increased.
8. A new cable was installed to run from the datalogger to multiplexers three and four. The length of the delay value was increased to account for the added wire length to each sensor. This resolved the errors for multiplexers three and four.

On March 6, 2009 the NAN and temperature errors were resolved and continuous monitoring was restarted.

## 8.1 Datalogger Program

RST Instruments developed the datalogger program used to collect the sensor data. This program records static sensor readings every two hours. The remote multiplexers are turned on and off in series, multiplexers one for 15% RCA and two for 0% RCA, then three for 30% RCA and four for 50% RCA. Each multiplexer takes the readings from six strain gauges first, followed by the two vertical extensometers, and two inter-panel extensometers. Sensor readings are converted into strains and displacement. James Smith and Terry Ridgeway made modifications to the program to match the sensor serial numbers for the vertical and inter-panel extensometers to their proper channel and to increase the amount of time between reading successive sensors to account for the longer cable lengths. The revised datalogger program is presented in Appendix D.

## 8.2 Sensor Readings

### 8.2.1 Strain Gauges

The impact of weather on JPCP performance can be monitored through strain data. Strain is the ratio of an object's change in length to it's original length due to an external action (load, temperature, etc.). Using strain information the onset of cracking can be identified and predicted. Crack formation in a 30 MPa concrete in compression (crushing) and tension (flexural) is approximately 3500 με and 130 με respectively [Neville 1995].

To calculate the strain caused by changes in climate, the raw strain data recorded by the datalogger, Figure 8.1, is zeroed and corrections made to account for temperature variations and coefficients of

thermal expansion based on Equation 8.2. A positive strain value denotes that the pavement is in tension, and a negative strain value shows compression.

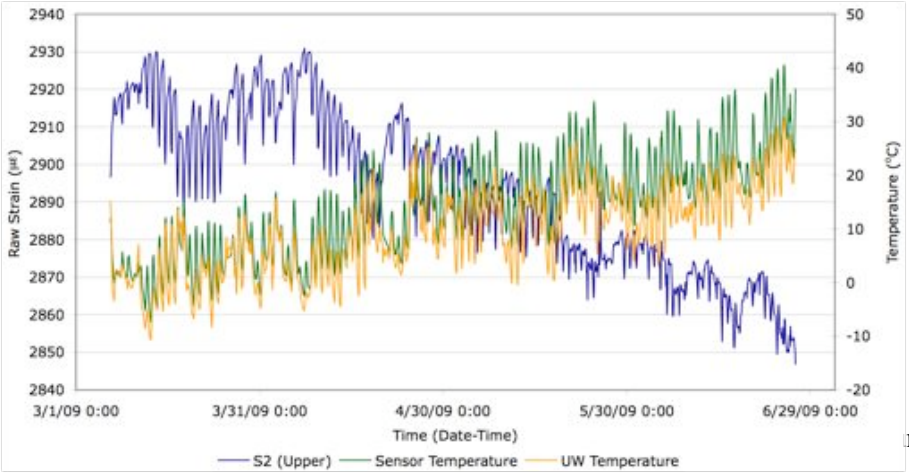


**Figure 8.1 Sample Raw Strain Data, 15% Coarse RCA**

$$\mu\varepsilon_{(Calculated)} = (R_1 - R_0)\left(\frac{F}{F_0}\right) + (T_1 - T_0)(C_1 - C_2) \tag{8.2}$$

where: $R_0$ = initial strain reading

$R_1$ = subsequent strain reading

$F$ = strain gauge calibration factor, 3.405

$F_0$ = default strain gauge factor, 4.062

$T_1$ = initial temperature reading ($^o$C)

$T_0$ = subsequent temperature reading ($^o$C)

$C_1$ = coefficient of expansion of gauge (12.2 $\mu\varepsilon$)

$C_2$ = coefficient of expansion of concrete ( $\mu\varepsilon$)

Figure 8.2 presents the calculated strain profiles for four sensors in the 15% coarse RCA test section over a four-month period from March to June 2009. The sensors include: S2 transverse orientation located centre slab in the upper part of the JPCP; S1 transverse orientation located centre slab in the lower part of the JPCP; S3 longitudinal orientation located centre slab in the lower part of the JPCP; and S6 transverse orientation located at the join in the upper part of the slab. Table 8.1 highlights the minimum and maximum strain values for the sensors.

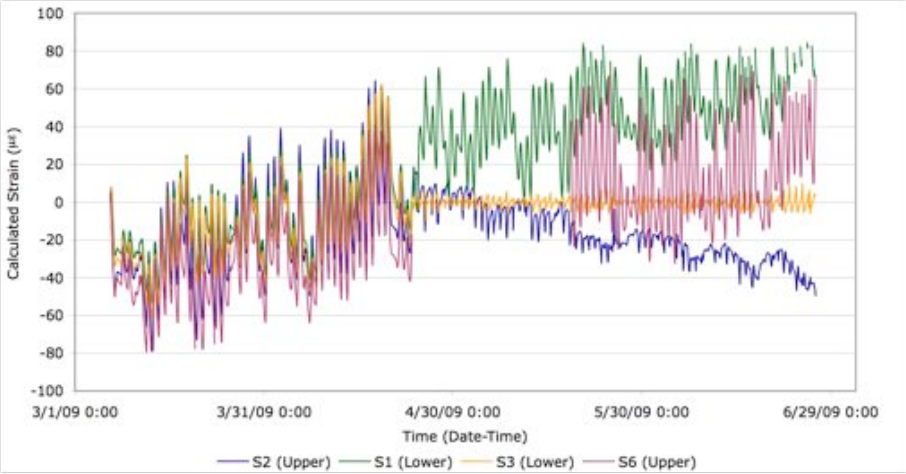


**Figure 8.2 Calculated Strain Profile, 15% Coarse RCA**

**Table 8.1 Maximum and Minimum Strain Values**

| | Transverse Upper (S2) | Transverse Lower (S1) | Longitudinal Lower (S3) | Joint Upper (S6) |
|---|---|---|---|---|
| Compression strain | | | | |
| Calculated strain value (με) | -79.1 | -53.7 | -61.9 | -79.7 |
| Date | Mar. 13 | Mar. 13 | Mar. 13 | Mar. 12 |
| Time | 08:00 | 08:00 | 08:00 | 08:00 |
| Concrete temperature ($^{o}$C) | -7.4 | -5.1 | -5.2 | -6.4 |
| Ambient temperature ($^{o}$C) | -8.4 | -8.4 | -8.4 | -8.3 |
| Tension strain | | | | |
| Calculated strain value (με) | 64.4 | 84.6 | 62.6 | 69.3 |
| Date | Apr. 17 | Jun. 25 | Apr. 18 | Jun. 16 |
| Time | 16:00 | 06:00 | 16:00 | 16:00 |
| Concrete temperature ($^{o}$C) | 23.3 | 28.5 | 19.3 | 29.2 |
| Ambient temperature ($^{o}$C) | 18.9 | 20.8 | 20.2 | 23.6 |
| Change in calculated strain (με) | 143.5 | 138.3 | 124.4 | 149.0 |
| Change in concrete temperature ($^{o}$C) | 30.7 | 33.6 | 24.5 | 35.6 |
| Change in ambient temperature ($^{o}$C) | 27.3 | 29.2 | 28.6 | 31.9 |

Several observations were made from the strain results.

- The maximum calculated strain values are between 1.5% and 2.5% required for crushing, and between 48% and 65% necessary for cracking.
- The change in strain is greater for the sensors located in the top portion of the slab compared to the bottom. This is due to relative changes in temperature of each senor. The upper portion of the slab has less cover and would be affected by constant changes in ambient temperature. The lower portion of the slab has more cover and is not influenced as much by the temperature changes. Therefore the greater the range of temperature the sensor experiences the greater the induced strain.
- The change in strain is greater for the sensors placed in the transverse direction compared to the longitudinal. The difference in the strain results is due to the difference in the number of restrained boundaries of each direction. Sensors in the transverse have only one restrained edge at the centre of the pavement allowing for greater slab movement for a given temperature. The sensors longitudinal are restrained by both joints at either end of the pavement reducing the slab movement in that direction.
- The change in strain is constant for the sensors located in the transverse direction located at the mid slab and at the joint. Strain at mid slab and at the joint should be equal when placed at the same depth. This is because the movement is restrained by only the pavement centreline and consistent temperature.

Additional strain results for 0%, 15%, 30%, and 50% Coarse RCA are presented in Appendix E.

### 8.2.2 Vertical Extensometers

Slab curling is caused by temperature gradients that develop when one side of the pavement slab is either warmer or cooler than the other. Figure 8.3 illustrates the curling of the pavement during the day and night [MDOT 2007].

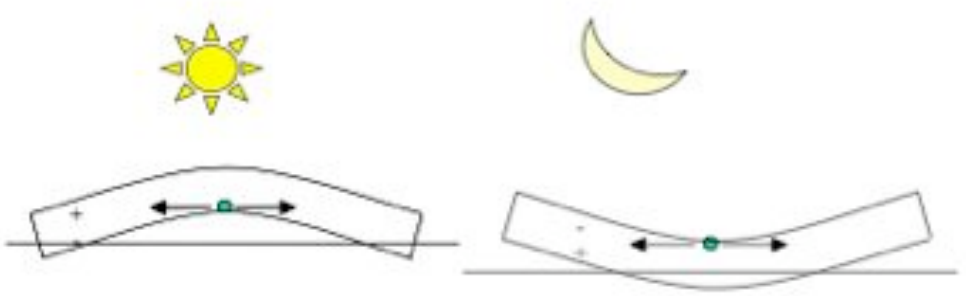

**Figure 8.3 Slab Curling**

During the day the surface of the slab is warmer than the bottom of the slab causing a positive temperature differential (warmer on top and cooler on the bottom) creating a convex shape where the

middle of the slab is higher than the edges. In this position the surface is in tension and the bottom is in compression. The opposite is observed during the night when a negative temp gradient is created resulting in a concave shape of the slab with the edges being higher than the middle of the slab. Figure 8.4 shows sample vertical displacement profiles at the edge of pavement over a four-month period from March to June 2009 for the 15% coarse RCA sensors. The normalized vertical displacements for the edge of pavement and centre slab presented in Figure 8.5.

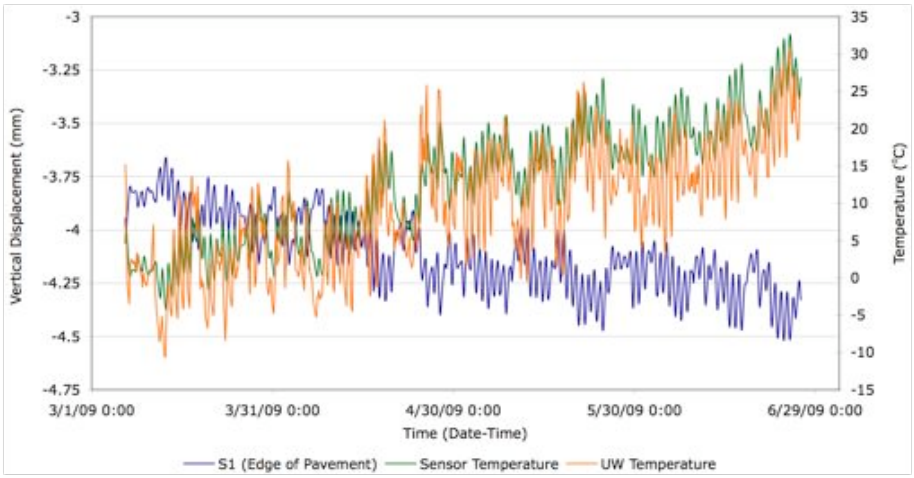


**Figure 8.4 Sample Vertical Displacement, 15% Coarse RCA**

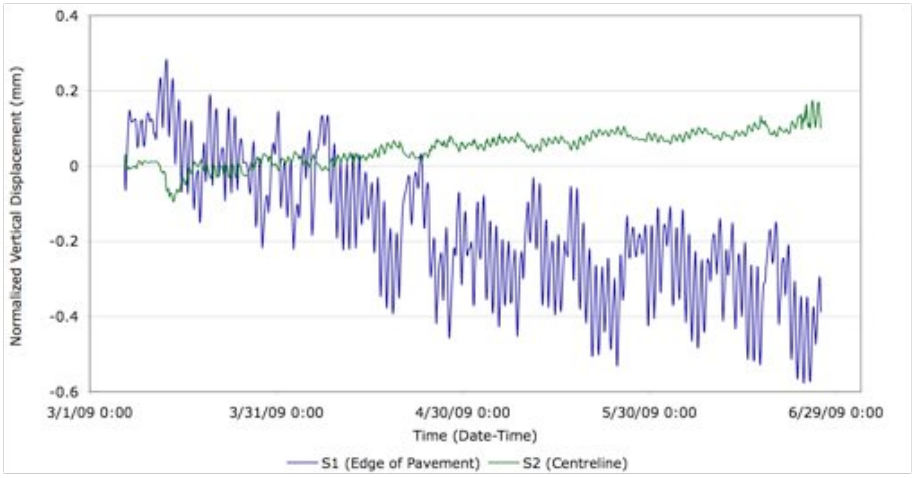


**Figure 8.5 Normalized Vertical Displacement, 15% Coarse RCA**

Several observations can be noted from the vertical displacement. The shape of the pavement slab becomes more convex as the ambient temperature increases at the edge of the pavement. The opposite trend is true for the vertical extensometer readings at the centreline. There is a greater

amount of displacement at the edge of the pavement. The temperature recorded by the sensor follows the same trend as the ambient temperature but with a time lag.

Table 8.2 shows the minimum and maximum vertical displacement values for sensors S1 and S2.

**Table 8.2 Maximum and Minimum Vertical Displacement Values**

| | Edge (S1) | Centreline (S2) |
|---|---|---|
| Maximum displacement | | |
| Vertical displacement (mm) | -4.52 | -6.25 |
| Date | Jun. 23 | Mar. 14 |
| Time | 20:00 | 10:00 |
| Concrete temperature ($^{o}$C) | 32.10 | -2.30 |
| Ambient temperature ($^{o}$C) | 24.79 | 1.42 |
| Minimum displacement | | |
| Vertical displacement (mm) | -3.66 | -5.88 |
| Date | Mar. 13 | Jun. 25 |
| Time | 08:00 | 06:00 |
| Concrete temperature ($^{o}$C) | -4.30 | 28.58 |
| Ambient temperature ($^{o}$C) | -8.43 | 20.83 |
| Change in displacement (mm) | 0.86 | 0.27 |
| Change in concrete temperature ($^{o}$C) | 36.4 | 30.88 |
| Change in ambient temperature ($^{o}$C) | 33.22 | 19.41 |

Several observations were made from the strain results.

- The change in vertical displacement is three times greater at the edge of pavement compared to the centreline.

Additional vertical displacement results for 0%, 30%, and 50% Coarse RCA are presented in Appendix E.

### 8.2.3 Inter-Panel Extensometers

The change in temperature throughout the day causes the pavement slab to expand and contract. During the daytime when the surface temperature is higher than the bottom of the slab, the slab expands, reducing the space between the joints. Figure 8.6 shows sample horizontal displacement

profiles at the edge of pavement over a four-month period from March to June 2009 for the 15% coarse RCA sensors. The normalized horizontal displacements for the edge of pavement and centre slab presented in Figure 8.7.

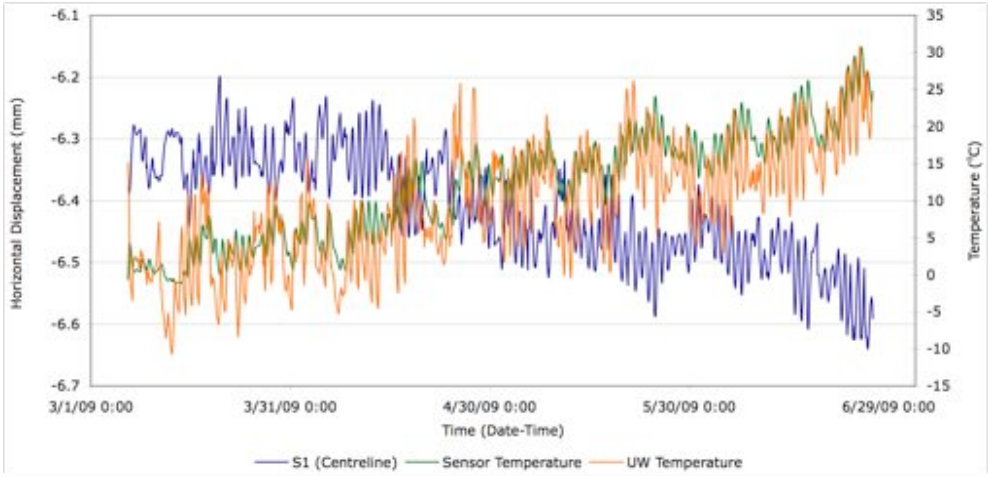


**Figure 8.6 Sample Horizontal Displacement, 15% Coarse RCA**

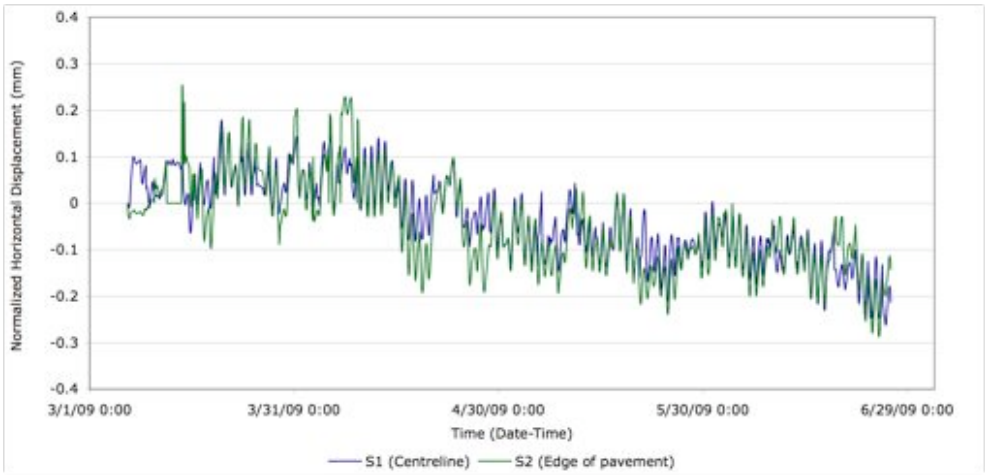


**Figure 8.7 Normalized Horizontal Displacement, 15% Coarse RCA**

The data shows that the space between adjoining slabs decreases as the ambient temperature increases. There is a greater amount of displacement at the edge of pavement. Joint movement follows the same trend as the ambient temperature, but with a time lag. Table 8.3 shows the minimum and maximum horizontal displacement values for sensors S5 and S6.

**Table 8.3 Maximum and Minimum Horizontal Displacement Values**

| | Centreline (S1) | Edge (S2) |
|---|---|---|
| Maximum displacement | | |
| Horizontal displacement (mm) | -6.20 | -4.42 |
| Date | Mar. 20 | Mar. 14 |
| Time | 10:00 | 14:00 |
| Concrete temperature ($^{o}$C) | -0.05 | -1.00 |
| Ambient temperature ($^{o}$C) | -2.18 | 5.36 |
| Minimum displacement | | |
| Horizontal displacement (mm) | -6.64 | -4.96 |
| Date | Jun. 25 | Jun. 24 |
| Time | 20:00 | 20:00 |
| Concrete temperature ($^{o}$C) | 27.47 | 30.67 |
| Ambient temperature ($^{o}$C) | 20.94 | 24.83 |
| Change in displacement (mm) | 0.44 | 0.54 |
| Change in concrete temperature ($^{o}$C) | 27.52 | 31.67 |
| Change in ambient temperature ($^{o}$C) | 23.12 | 19.47 |

Several observations were made from the strain results.

- The change in horizontal displacement is equal along the joint at the edge of pavement and centerline locations.

Additional horizontal displacement results for 0%, 15%, and 50% Coarse RCA are presented in Appendix E.

The movement of longitudinal joints in a JPCP is influenced by four key factors. Theses factor include: temperature change, slab length, CTE, and frictional forces created between the base and slab. Equation 8.3 presents the AASHTO 1986 "Guide for the Design of Pavement Structures" formula to estimate joint movement [FHWA 1990].

$$z = CL(e\Delta T) \tag{8.3}$$

where: $z$ = joint opening (in)

$C$ = base/slab frictional restraint factor (0.65 for stabilized bases, 0.8 for granular bases)

$L$ = slab length (in)

$e$ = PCC coefficient of thermal expansion ( /$^{o}$F)

$\Delta T$ = maximum temperature range ($^{o}$F)

To validate the inter-panel extensometer results, sensor readings were combined with the calculated CTE values of the RCA mixes. Values used in the calculation are shown in Table 8.4.

**Table 8.4 Joint Movement Calculation Values**

| RCA Content | 0% Coarse | | 15% Coarse | | 30% Coarse | | 50% Coarse | |
|---|---|---|---|---|---|---|---|---|
| Sensor ID | S3 | S4 | S1 | S2 | S5 | S6 | S7 | S8 |
| Slab length (m) | 4.3 | | 4.3 | | 4.3 | | 4.3 | |
| CTE – Maximum ($10^{-6}$/$^{o}$C) | 8.97 | | 6.86 | | 5.76 | | 5.31 | |
| CTE – Average ($10^{-6}$/$^{o}$C) | 7.28 | | 6.60 | | 5.27 | | 4.10 | |
| CTE – Minimum ($10^{-6}$/$^{o}$C) | 6.29 | | 5.20 | | 4.72 | | 3.52 | |
| Temperature change ($^{o}$C) | NA* | NA* | 27.52 | 29.94 | 39.03 | 30.25 | 28.32 | 24.51 |

* Inter-panel extensometers S3 and S4 are not working

The measured joint movement for the inter-panel extensometers falls within the calculated limited of Equation 9.3 for all of the sensors S6 as illustrated by Figure 8.8. This confirms that the sensors are working properly and the estimated CTE range of the RCA concretes.

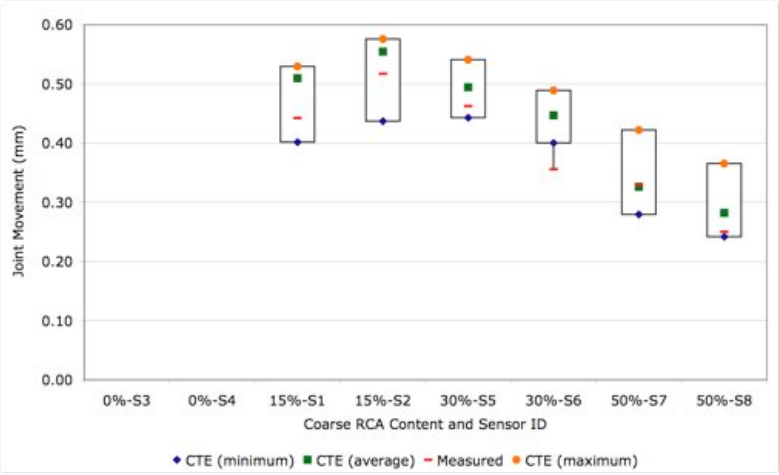


**Figure 8.8 Calculated and Measured Joint Movement**

## 8.3 Predictive Models

Predictive models were created to estimate the temperature and strain or displacement readings of the sensors. Predictive models for strain and displacement were created in a three-step process.

- Step 1: Estimate the temperature for the strain and displacement sensors.
- Step 2: Create predictive models for strain and displacement using the actual measured temperature sensor data.
- Step 3: Use the predictive models from Step Two with the temperature estimates from Step One to predict raw strain and displacement values.

### 8.3.1 Temperature

In order to estimate the sensor temperature reading an average of the current and preceding ambient temperatures was used. The same model was used for all RCA amounts.

Two temperature models were created for the strain sensors because they are located at different depths in the pavement. Strain sensors located in the upper part of the pavement used an average of the current and one preceding ambient temperature reading. Whereas strain sensors located in the lower part of the pavement used an average of the current and five preceding ambient temperature readings.

One temperature model was created for the vertical extensometers. The temperature was estimated using an average of the current and six preceding ambient temperature readings.

One temperature model was created for the inter-panel extensometers. The temperature was estimated using an average of the current and five preceding ambient temperature readings.

Figure 8.9 shows the correlation between the weighted ambient temperature and the measured concrete temperature for the 15% RCA strain sensor located in the lower part of the pavement. The $R^2$ value is 0.847 showing good correlation between the predictive model and the actual sensor measurements.

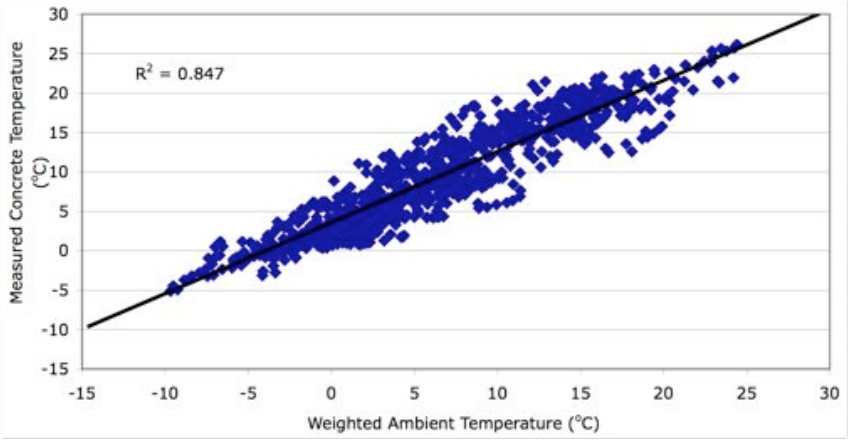


**Figure 8.9 Strain Temperature Prediction**

Table 8.5 shows the predictive ability of the temperature models based on the coefficient of determination ($R^2$) values.

**Table 8.5 Temperature Coefficient of Determination Values**

| | 0% RCA | 15% RCA | 30% RCA | 50% RCA |
|---|---|---|---|---|
| Strain | | | | |
| Transverse (Upper) | 0.854 | 0.852 | 0.588 | 0.837 |
| Transverse (Lower) | 0.837 | 0.847 | 0.842 | 0.822 |
| Longitudinal (Upper) | 0.855 | 0.853 | 0.636 | 0.838 |
| Longitudinal (Lower) | 0.836 | 0.846 | 0.803 | 0.818 |
| Joint (Upper) | - | 0.849 | 0.853 | 0.839 |
| Joint (Lower) | 0.780 | 0.847 | 0.830 | 0.819 |
| Vertical Extensometer | | | | |
| Edge of pavement | 0.764 | 0.881 | 0.878 | 0.850 |
| Centreline | - | 0.879 | 0.758 | 0.868 |
| Inter-panel Extensometer | | | | |
| Edge of pavement | - | 0.870 | 0.761 | 0.861 |
| Centreline | - | 0.865 | 0.879 | 0.864 |

The models are able to predict the correct temperature within plus minus five degree Celsius. The $R^2$ is greater than 0.8 for 32 of 40 sensors demonstrating a high correlation. Four of the 0% RCA sensors are yielding values that are more positive and negative than the corresponding ambient temperatures indicating a failure of the sensor.

### 8.3.2 Strain

A model for each of the 24 sensors was created to predict the raw strain values recorded by the datalogger. The strain for each of the coarse RCA contents and locations within the slab were best described using a second-degree polynomial equation. Figures 8.10 and 8.11 show a sample of the predictive ability of the strain equations for the 15% coarse RCA transverse orientation in the upper and lower part of the slab.

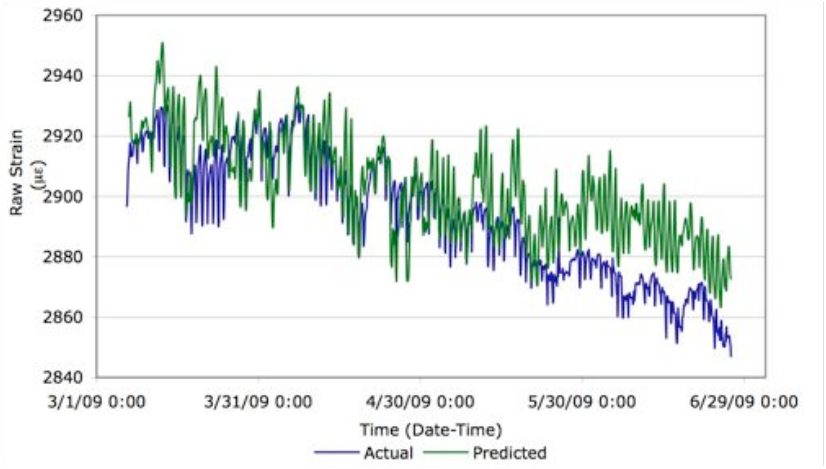


**Figure 8.10 Actual vs. Predicted Raw Transverse Strain, Centre Slab, Upper**

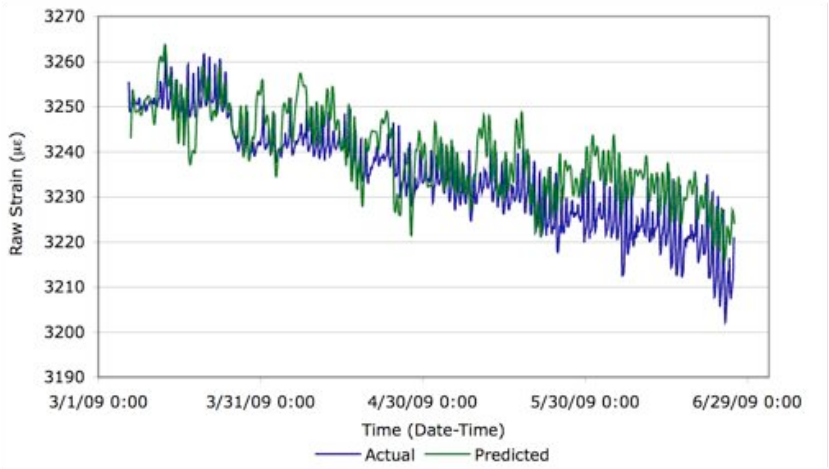


**Figure 8.11 Actual vs. Predicted Raw Transverse Strain, Centre Slab, Lower**

The models for sensors in the lower part of the slab had a better predictive ability than those in the upper part of the slab. The difference between the actual and predicted strain increase as the ambient temperature increases with a greater discrepancy for the upper sensors. Table 8.6 presents the predictive strain equations for each sensor.

**Table 8.6 Predictive Strain Equations**

| Sensor ID | Sensor Location | Predictive Raw Strain Equation | $R^2$ |
|---|---|---|---|
| 0% Coarse RCA | | | |
| S7 | Longitudinal | $\mu\varepsilon_{(Raw)} = -0.0254T^2 - 2.7993T + 2671.6$ | 0.78 |
| S8 | Longitudinal | $\mu\varepsilon_{(Raw)} = -0.026T^2 - 0.6455T + 2908.1$ | 0.73 |
| S9 | Transverse | $\mu\varepsilon_{(Raw)} = 0.0086T^2 - 3.3884T + 2851.5$ | 0.92 |
| S10 | Transverse | $\mu\varepsilon_{(Raw)} = -0.0615T^2 - 0.0098T + 2555$ | 0.91 |
| S11 | Joint | NA | |
| S12 | Joint | NA | |
| 15% Coarse RCA | | | |
| S1 | Transverse | $\mu\varepsilon_{(Raw)} = 0.0009T^2 - 1.2727T + 3251.5$ | 0.80 |
| S2 | Transverse | $\mu\varepsilon_{(Raw)} = 0.0149T^2 - 2.4403T + 2923.5$ | 0.79 |
| S3 | Longitudinal | $\mu\varepsilon_{(Raw)} = 0.0198T^2 - 1.2711T + 2910.6$ | 0.61 |
| S4 | Longitudinal | $\mu\varepsilon_{(Raw)} = -0.0521T^2 - 1.1931T + 3169.7$ | 0.90 |
| S5 | Joint | $\mu\varepsilon_{(Raw)} = -0.0656T^2 + 0.3693T + 2894$ | 0.86 |
| S6 | Joint | $\mu\varepsilon_{(Raw)} = 0.013T^2 - 2.3861T + 2142.4$ | 0.81 |
| 30% Coarse RCA | | | |
| S13 | Transverse | $\mu\varepsilon_{(Raw)} = -0.0029T^2 - 0.696T + 2062.6$ | 0.81 |
| S14 | Longitudinal | $\mu\varepsilon_{(Raw)} = 0.1321T^2 - 6.5697T + 15826$ | 0.80 |
| S15 | Transverse | NA | |
| S16 | Longitudinal | $\mu\varepsilon_{(Raw)} = 0.1361T^2 - 8.3703T + 15991$ | 0.62 |
| S17 | Joint | $\mu\varepsilon_{(Raw)} = 0.0268T^2 - 4.6955T + 14333$ | 0.93 |
| S18 | Joint | $\mu\varepsilon_{(Raw)} = 0.0347T^2 - 3.5693T + 2887.6$ | 0.84 |
| 50% Coarse RCA | | | |
| S19 | Longitudinal | $\mu\varepsilon_{(Raw)} = 0.0128T^2 - 2.1798T + 2990$ | 0.81 |
| S20 | Transverse | $\mu\varepsilon_{(Raw)} = -0.0201T^2 - 1.3888T + 2973.8$ | 0.89 |
| S21 | Transverse | $\mu\varepsilon_{(Raw)} = 0.0237T^2 - 2.5257T + 3096.1$ | 0.84 |
| S22 | Longitudinal | $\mu\varepsilon_{(Raw)} = -0.0043T^2 - 0.2215T + 2946.1$ | 0.51 |
| S23 | Joint | $\mu\varepsilon_{(Raw)} = -0.0424T^2 + 0.1077T + 2978.5$ | 0.76 |
| S24 | Joint | $\mu\varepsilon_{(Raw)} = -0.0212T^2 - 0.1235T + 2756.8$ | 0.70 |

### 8.3.3 Vertical Extensometer

A model for each sensor was created to predict the vertical displacement. The displacement for each of the coarse RCA contents and locations within the slab were best described using a second-degree polynomial equation. Figures 8.12 and 8.13 show a sample of the predictive ability of the displacement equations for 15% coarse RCA located at the edge of the pavement and at the centreline.

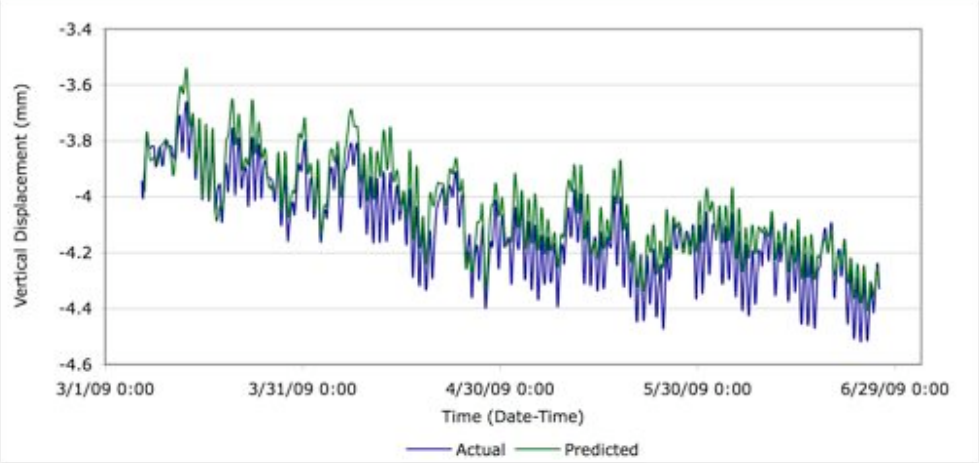


**Figure 8.12 Actual vs. Predicted Vertical Displacement at Edge of Pavement**

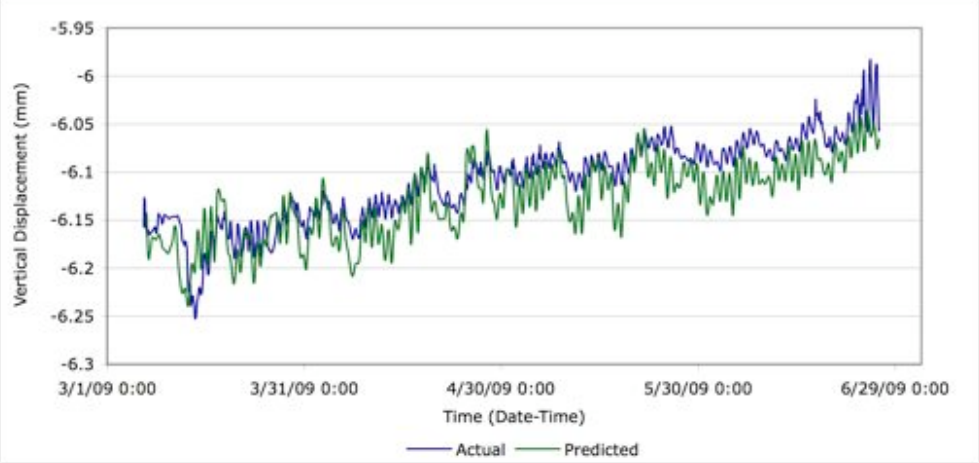


**Figure 8.13 Actual vs. Predicted Vertical Displacement at Centreline**

Several observations were made about the predictive equations. First, they tend to over predict vertical displacement at the edge of the pavement and under predict the vertical displacement.

Second, there was a consistent difference between the actual and predicted strain increase as the ambient temperature increased. Table 8.7 presents the predictive vertical displacement equations.

**Table 8.7 Predictive Vertical Displacement Equations**

| Sensor ID | Sensor Location | Predictive Vertical Displacement Equation | $R^2$ |
|---|---|---|---|
| 15% Coarse RCA | | | |
| S1 | Edge | $D_{(Vertical)} = 0.0002T^2 - 0.0264T - 3.8137$ | 0.95 |
| S2 | Centreline | $D_{(Vertical)} = 0.00003T^2 - 0.0059T - 6.18$ | 0.90 |
| 50% Coarse RCA | | | |
| S7 | Centreline | $D_{(Vertical)} = -0.00001T^2 - 0.002T - 5.4392$ | 0.96 |
| S8 | Edge | $D_{(Vertical)} = -0.0002T^2 + 0.0014T - 5.6976$ | 0.92 |

### 8.3.4 Inter-Panel Extensometer

A model was developed for each of the eight sensors to predict the horizontal displacement. The displacement for each of the coarse RCA contents and locations within the slab were best described using a linear equation. Figures 8.14 and 8.15 show a sample of the predictive ability of the displacement equations for 15% coarse RCA located at the edge of the pavement and at the centreline.

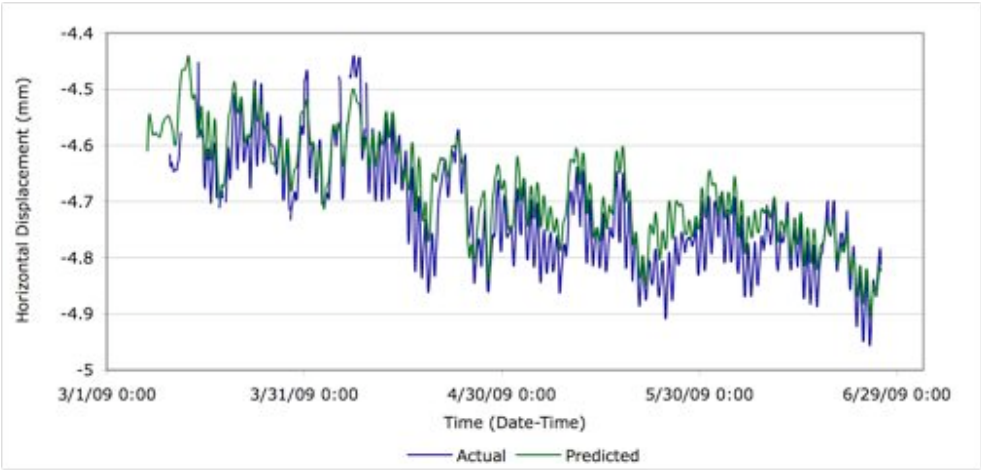


**Figure 8.14 Actual vs. Predicted Horizontal Displacement at Edge of Pavement**

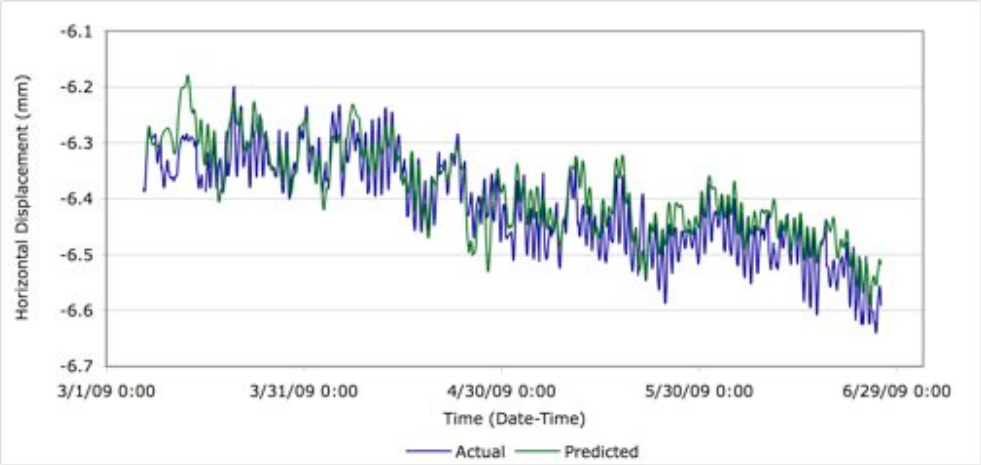


**Figure 8.15 Actual vs. Predicted Horizontal Displacement at Centreline**

Comparing the actual and the predicted displacement results shows that the predictive equations under estimate the horizontal displacement at both the edge of the pavement and at the centreline. There is a consistent difference between the actual and predicted strain increase as the ambient temperature increases. The predictive vertical displacement equations are shown in Table 8.8

**Table 8.8 Predictive Horizontal Displacement Equations**

| Sensor ID | Location | Predictive Horizontal Displacement Equation | $R^2$ |
|---|---|---|---|
| 15% Coarse RCA | | | |
| S1 | Centreline | $D_{(Horizontal)} = -0.0112T - 6.2798$ | 0.88 |
| S2 | Edge | $D_{(Horizontal)} = -0.0127T - 4.5546$ | 0.85 |
| 30% Coarse RCA | | | |
| S5 | Edge | $D_{(Horizontal)} = 0.0203T - 15.455$ | 0.91 |
| S6 | Centreline | $D_{(Horizontal)} = 0.0078T - 13.068$ | 0.82 |
| 50% Coarse RCA | | | |
| S7 | Edge | $D_{(Horizontal)} = 0.0047T - 0.587$ | 0.88 |
| S8 | Centreline | $D_{(Horizontal)} = 0.003T - 6.2021$ | 0.84 |

# Chapter 9

# Mechanistic-Empirical Pavement Design Guide Performance

## 9.1 ME-PDG Background and How It Works

The development of ME-PDG began in 1997 by the American Association of State and Transportation Officials (AASHTO) Joint Task Force on Pavements (JTFP) under National Cooperative Highway Research Program Projects 1-37 and 1-37a [ARA 2004]. The ability to develop the ME-PDG came through advancements in computers, modeling technologies, vast amounts of pavement performance data available though the SHRP and LTPP programs and more rigorous pavement design procedures [Dore 2005].

A new pavement design guide was needed to more accurately simulate climate, pavement design, changes in traffic and new materials. A design guide that could accurately model the conditions of a specific location was needed. The new guide should provide multiple design options with longer analysis periods. Truck volume and loading had increased significantly from the original American Association of State Highway Officials (AASHO) Road Test. Changes in the truck characteristics axle configurations and tire pressure also had to be accounted for. New asphalt and concrete materials had been developed since AASHO and the ability to better characterize all pavement properties was needed. The new pavement design guide would allow specific confidence levels as opposed to applying factors of safety multipliers based on traffic levels alone.

The ME-PDG goes beyond designing for pavement thickness as in previous design guides. It looks at the interaction of climate, materials, and traffic on the pavement structure using both mechanistic and empirical model to calculate damage over time leading to the distresses observed. Mechanistic results (stress and strains) are used to estimate pavement distress, where as empirical results are used when data is calibrated to observed performance [Hall 2005]. Figure 9.1 illustrates this concept.

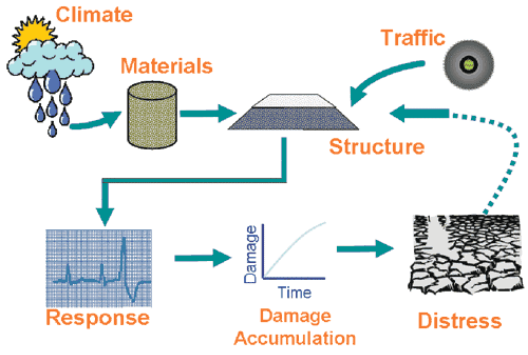


**Figure 9.1 ME-PDG Flow Chart**

The ME-PDG simulates both new and rehabilitation designs at three input levels. Level One obtains the highest degree of accuracy by using specific site and material information. Level Two

uses values similar to the AASHTO Design Guides. Level Three uses the national average default values based on data taken from LTPP in 2000. Regardless of the level used, the analysis procedure is the same.

The ME-PDG requires a large amount of inputs, these include:

- General site and project information (e.g., design type, design life, construction and opening dates);
- Analysis parameters (e.g., initial and terminal IRI, various forms of cracking, permanent deformation), critical values, and reliability (used to account for error in predictions of various distresses);
- Traffic assumptions (e.g., lane alignment, baseline volume and future growth and distribution of truck traffic);
- Pavement structure (e.g., specification of layer thicknesses and material properties); and
- Climate (e.g., station location and elevation, groundwater table level, hourly temperature data).

The JPCP module of the MEPDG predicts pavement performance based on three parameters: transverse cracking, joint faulting, and pavement roughness. The transverse cracking model, Equations 9.1 and 9.2, calculates the percentage of slabs that fall within the specified project limits. Both modes of transverse cracking top-down and bottom –up are included in the model.

$$CRK = \frac{1}{1 + FD^{-1.68}} \tag{9.1}$$

$$FD = \sum \frac{n_{i,j,k,l,m,n}}{N_{i,j,k,l,m,n}} \tag{9.2}$$

where: $CRK$ = predicted amount of top-down or bottom-up cracking (fraction)

$FD$ = total fatigue damage (top-down or bottom-up cracking)

$n_{i,j,k,...}$ = applied number of axle load applications at condition i, j, k, l, m, n

$N_{i,j,k,...}$ = allowable number of axle load applications at condition i, j, k, l, m, n

$i$ = age

$j$ = month

$k$ = axle type

$l$ = load level

$m$ = temperature difference

$n$ = traffic path

The faulting model, Equations 9.3 to 9.6, predicts the cumulative transverse joint faulting each month.

$$Fault_m = \sum_{i=1}^{m} \Delta Fault_i \tag{9.3}$$

$$\Delta Fault_i = \left(0.001725 + \left(0.0008(FR)^{0.25}\right)\right)\left(FAULTMAX_{i-1} - Fault_{i-1}\right)^2 DE_i \tag{9.4}$$

$$FAULTMAX_i = FAULTMAX_0 + 1.2\left(\sum_{j=1}^{m} DE_j\right)\left(\log\left(1 + 250(5.0)^{EROD}\right)^{0.4}\right) \tag{9.5}$$

$$FAULTMAX_0 = \left(1.29 + \left(1.1(FR)^{0.25}\right)\right)$$
$$\left(\delta_{curling}\right)\left(\log\left(1 + 250(5.0)^{EROD}\right) \times \log\left(\frac{P_{200}(WetDays)}{P_S}\right)\right)^{0.4} \tag{9.6}$$

where: $Fault_m$ = mean joint faulting at the end of month m (in)

$\Delta Fault_i$ = incremental monthly change in mean transverse joint faulting during month i (in)

$FAULTMAX_i$ = maximum mean transverse joint faulting for month i (in)

$FAULTMAX_0$ = initial maximum mean transverse joint faulting (in)

$EROD$ = base/subbase erodibility factor

$DE_i$ = differential deformation energy accumulated during month i

$\delta_{curling}$ = maximum mean monthly slab corner upward deflection PCC

$P_S$ = overburden on subgrade (lb)

$P_{200}$ = percent of subgrade material passing #200 sieve

$WetDays$ = average annual number of wet days greater than 0.1 in rainfall

$FR$ = base freezing index

The IRI model predicts the pavement roughness combining the results from the transverse cracking and faulting models with joint spalling and a site factor as per Equations 9.7 to 9.10.

$$IRI = IRI_1 + 0.8203(CRK) + 0.4417(SPALL) + 1.4929(TFAULT) + 25.24(SF) \tag{9.7}$$

$$SPALL = \frac{AGE}{AGE + 0.01}\left(\frac{100}{1 + 1.005^{(-12(AGE)+SCF)}}\right) \tag{9.8}$$

$$SCF = -1400 + 350(AIR\%)(0.5 + PREFORM) + 3.4(0.4f'c) - 0.2(FTCYC(AGE)) + 43h_{PCC} - 536WC\_Ratio \quad (9.9)$$

$$SF = AGE(1 + 0.5556FI)(1 + P_{200}) \times 10^{-6} \quad (9.10)$$

where: $IRI$ = predicted IRI (in/mi)

$IRI_1$ = initial pavement smoothness, measured as IRI (in/mi)

$CRK$ = percent slabs cracked with transverse cracks (all severities)

$SPALL$ = percentage of joints with spalling (medium and high severities)

$TFAULT$ = total joint faulting cumulated per mi (in)

$SF$ = site factor

$SPALL$ = percentage joints spalled (medium- and high-severities)

$AGE$ = pavement age since construction (years)

$SCF$ = spalling prediction scaling factor

$AIR\%$ = PCC air content (percent)

$PREFORM$ = 1 if perform sealant is present; 0 if not

$f'c$ = PCC compressive strength (psi)

$FTCYC$ = average annual number of freeze-thaw cycles

$h_{PCC}$ = PCC slab thickness (in)

$WC\_Ratio$ = PCC water/cement ratio

$FI$ = freezing index ($^{o}$F-days)

$P_{200}$ = percent subgrade material passing #200 sieve

## 9.2 ME-PDG Sensitivity

NCHRP 01-47 Sensitivity Evaluation of ME-PDG Performance Prediction call for proposals identified that the current sensitivity analysis being conducted do not consider the effect of varying two or more input parameters in a systematic fashion. The University of Arkansas conducted one of the most recognized sensitivity analysis in 2005 [Hall 2005]. In this study 29 variables within the JPCP module were analyzed individually for their influence on the three performance models

(cracking, faulting, and roughness) in the ME-PDG. The results of the sensitivity analysis are presented in Table 9.1.

**Table 9.1 MEPDG Sensitivity Analysis**

| Input Parameter | Performance Model | | |
|---|---|---|---|
| | Cracking | Faulting | Roughness |
| Curl/Warp Effective Temperature Difference | X | X | X |
| Joint Spacing | X | X | X |
| Sealant Type | | | |
| Dowel Diameter | | X | X |
| Dowel Spacing | | | |
| Edge Support | X | X | X |
| PCC-Base Interface | | | |
| Erodibility Index | | | |
| Surface Shortwave Absorptivity | X | | |
| Infiltration of Surface Water | | | |
| Drainage Path Length | | | |
| Pavement Cross Slope | | | |
| PCC Layer Thickness | X | X | X |
| Unit Weigh | X | X | X |
| Poisson's Ratio | X | | |
| Coefficient of Thermal Expansion | X | X | X |
| Thermal Conductivity | X | | |
| Heat Capacity | | | |
| Cement Type | | | |
| Cementitous Content | | | |
| Water-Cement Ratio | | | |
| Aggregate Type | | | |
| PCC Set Temperature | | | |
| Ultimate Shrinkage at 40% Relative Humidity | | | |
| Reversible Shrinkage | | | |
| Time to Develop 50% of Ultimate Shrinkage | | | |

| Input Parameter | Performance Model | | |
|---|---|---|---|
| | Cracking | Faulting | Roughness |
| Curing Method | | | |
| 28-day PCC Modulus of Rupture | X | | X |
| 28-day PCC Compressive Strength | X | | X |

The sensitivity analysis shows that the key input variables are curl/warp effective temperature difference, joint spacing, dowel diameter, edge support, surface shortwave absorption, PCC layer thickness, unit weight, Poisson's ratio, coefficient of thermal expansion, thermal conductivity, 28-day modulus of rupture, and 28-day compressive strength.

### 9.2.1 Experimental Design

To addresses the issues raised by NCHRP 01-07 a screening design was used to determine which input parameters are the most influential prior to modeling the RCA concrete. Sensitivity analysis was performed using ME-PDG Version 1.0 release May 24, 2007. A Plackett-Burman (PB) design was selected for the sensitivity analysis because it is able to screen a large amount of variables using a limited number of runs compared to a full- or partial-factorial design. The standard PB design is a resolution III design. This means that the effects of main variables can be confounded with second order interactions produce some inconclusive results by not being able to distinguish between the main and second order interaction effects. Applying a "foldover" technique to the PD design allows the resolution of the design to be increased to IV, confounding results between the main and third order interactions. The "foldover" creates a mirror image of the design with +'s becoming -'s and vice-versa and adds an extra factor to the design. Two separate seven factor PD designs with "foldover", eight factors total, were used to test the sensitivity of the input parameters in the JPCP layer module and the design features module of the ME-PDG. Adding an additional run using the midpoints (0) of the +'s and -'s was run for comparison of the results. If multiple runs of the midpoints were conducted an error estimate could be calculated to be included in ANOVA. This however, is not possible because the ME-PDG keeps returning the same value resulting in no error.

Tables 9.2 and 9.3 present the eight factors and values used to examine the sensitivity of the JPCP layer and design feature inputs. A broad range of values was analyzed for each factor to determine the sensitivity.

**Table 9.2 JPCP Layer Sensitivity Factors and Values**

| | JPCP Factors | - | + | 0 |
|---|---|---|---|---|
| A | Unit Weight (kg/m$^3$) | 2240 | 2560 | 2400 |
| B | Poisson's Ratio | 0.15 | 0.25 | 0.2 |
| C | Coefficient of Thermal Expansion (per $^o$C x10$^{-6}$) | 6.0 | 9.2 | 7.6 |
| D | Thermal Conductivity (J/m-s-$^o$C)[1] | 1.5 | 2.4 | 1.95 |
| E | Heat Capacity (J/kg-$^o$C) | 630 | 1890 | 1260 |
| F | Cementitous Content (kg/m$^3$) | 300 | 360 | 330 |
| G | Water-Cement Ratio | 0.33 | 0.53 | 0.43 |
| H | 28-day Compressive Strength (MPa)[2] | 25 | 45 | 35 |

1. A typical thermal conductivity values for a concrete made with limestone aggregate 3.2 J/m-s-$^o$C [Neville 1995], however this value was reduced because of an ICM satiability error associated with this input parameter.
2. Alternatively 28-day modulus of rupture values could have been used to quantify strength development.

**Table 9.3 Design Sensitivity Factors and Values**

| | Design Factors | - | + | 0 |
|---|---|---|---|---|
| A | Joint Spacing (m) | 3.7 | 4.5 | 4.1 |
| B | Sealant Type | Liquid | Preformed | Silicon |
| C | Dowel Diameter (mm) | 25.4 | 44.5 | 32 |
| D | Dowel Spacing (mm) | 254 | 356 | 305 |
| E | Edge Support[1] | None | Tied Shoulder | Widened Slab |
| F | PCC-Base Interface[2] (months) | 0 | 480 | 240 |
| G | Erodibility Index[3] | 5 | 1 | 3 |
| H | Surface Shortwave Absorpitivity | 0.7 | 1 | 0.85 |

1. Tied shoulder has a 40% load transfer efficiency, and widened slab has a width of 12 feet.
2. PCC-Base interface values represent the time of loss of friction.
3. Erodibility index values: 1 = extremely resistant, 3 = erosion resistant, and 5 = very erodeable.

To estimate the first and second order effects for each of the two sensitivity analyses seventeen ME-PDG runs are required. Table 9.4 shows the generated design for each PB screening analysis. Runs seven through sixteen represent the "foldover" that is used to create the extra variable H.

**Table 9.4 PB Design Run Variability Levels**

| Run | Variable | | | | | | | |
|---|---|---|---|---|---|---|---|---|
| | A | B | C | D | E | F | G | H |
| 1 | - | - | - | + | + | + | - | + |
| 2 | + | - | - | - | - | + | + | + |
| 3 | - | + | - | - | + | - | + | + |
| 4 | + | + | - | + | - | - | - | + |
| 5 | - | - | + | + | - | - | + | + |
| 6 | + | - | + | - | + | - | - | + |
| 7 | - | + | + | - | - | + | - | + |
| 8 | + | + | + | + | + | + | + | + |
| 9 | + | + | + | - | - | - | + | - |
| 10 | - | + | + | + | + | - | - | - |
| 11 | + | - | + | + | - | + | - | - |
| 12 | - | - | + | - | + | + | + | - |
| 13 | + | + | - | - | + | + | - | - |
| 14 | - | + | - | + | - | + | + | - |
| 15 | + | - | - | + | + | - | + | - |
| 16 | - | - | - | - | - | - | - | - |
| 17 | 0 | 0 | 0 | 0 | 0 | 0 | 0 | 0 |

#### 9.2.1.1 Calculations

The effect of each variable is calculated using Equation 9.11.

$$Effect = \left(Average\ response\ "+"\right) - \left(Average\ response\ "-"\right) \tag{9.11}$$

If two or more centre points (0) are used the experimental error can be calculated and used in an ANOVA (analysis of variance) test to determine the significance of the variables. To complete the ANOVA table a sum of squares (SS) and mean square (MS) values need to be calculated.

$$SS = R2^{k-2}\left(Effect\right)^2 \tag{9.12}$$

where: $R$ = the fraction or complete replication of the design

$k$ = number of variables

$$MS = \frac{SS(Effect)}{df} \tag{9.13}$$

where: $df$ = degrees of freedom

#### 9.2.1.2 Interpretation of the Results

To identify the influential parameters the calculated effects are plotted against their expected normal value. Significant variables do not fall along the straight line plotted thought the data. Also, the magnitude of the calculated effect is also important. Figure 9.2 presents the results of a simplified three factor PB design, to be used for illustration

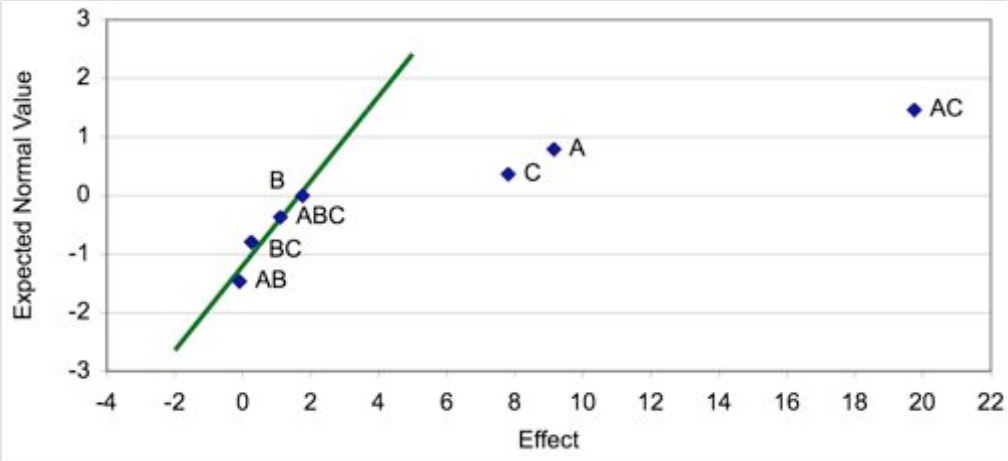


**Figure 9.2 Example Results**

Based on this example the variables "A", "C," and their interaction "AC" are influential over the range of limits tested. It is important to note that because the interaction "AC" was identified as a significant variable, the effects of "A" or "C" can not be talked about independently.

### 9.2.2 Results

The PB results of the 50-year ME-PDG simulations for percent slabs cracked, joint faulting and pavement roughness and time of failure (TOF) are given in Tables 9.5 and 9.6.

**Table 9.5 JPCP Factor Results**

| JPCP Factor | Cracking (% slabs) | | Faulting (mm) | | Roughness (m/km) | |
|---|---|---|---|---|---|---|
| Run | 50-year | TOF | 50-year | TOF | 50-year | TOF |
| 1 | 0.0 | NR | 1.17 | NR | 2.38 | NR |
| 2 | 1.0 | NR | 1.47 | NR | 2.60 | NR |
| 3 | 0.3 | NR | 2.16 | NR | 2.84 | 48 |
| 4 | 8.0 | NR | 1.60 | NR | 2.65 | NR |
| 5 | 47.7 | 13 | 4.67 | 22 | 4.37 | 20 |
| 6 | 30.8 | 36 | 2.46 | NR | 3.26 | 41 |
| 7 | 5.4 | NR | 4.39 | 25 | 3.62 | 30 |
| 8 | 48.9 | 28 | 2.92 | NR | 3.75 | 35 |
| 9 | 99.8 | 3 | 2.92 | NR | 4.62 | 16 |
| 10 | 65.7 | 25 | 3.53 | 38 | 4.35 | 29 |
| 11 | 98.7 | 5 | 2.49 | NR | 4.39 | 20 |
| 12 | 44.7 | 32 | 3.33 | 43 | 4.05 | 31 |
| 13 | 16.4 | 49 | 1.07 | NR | 2.81 | 49 |
| 14 | 94.2 | 4 | 2.36 | NR | 4.34 | 20 |
| 15 | 1.8 | NR | 0.81 | NR | 2.59 | NR |
| 16 | 30.5 | 37 | 1.42 | NR | 3.12 | 44 |
| 17 | 4.7 | NR | 2.84 | NR | 3.22 | 41 |

**Table 9.6 Design Factor Results**

| Design Factor | Cracking (% slabs) | | Faulting (mm) | | Roughness (m/km) | |
|---|---|---|---|---|---|---|
| Run | 50-year | TOF | 50-year | TOF | 50-year | TOF |
| 1 | 0.1 | NR | 4.67 | 25 | 4.04 | 27 |
| 2 | 26.4 | 42 | 6.58 | 15 | 4.61 | 25 |
| 3 | 0.2 | NR | 3.48 | 37 | 3.11 | 39 |
| 4 | 41.3 | 28 | 8.66 | 8 | 5.04 | 17 |
| 5 | 0.9 | NR | 1.68 | NR | 2.82 | 48 |
| 6 | 14.3 | NR | 2.90 | NR | 3.26 | 41 |
| 7 | 0.5 | NR | 2.41 | NR | 2.67 | NR |

| Design Factor | Cracking (% slabs) | | Faulting (mm) | | Roughness (m/km) | |
|---|---|---|---|---|---|---|
| Run | 50-year | TOF | 50-year | TOF | 50-year | TOF |
| 8 | 7.5 | NR | 2.01 | NR | 2.44 | NR |
| 9 | 3.3 | NR | 1.73 | NR | 2.29 | NR |
| 10 | 0.0 | NR | 1.45 | NR | 2.27 | NR |
| 11 | 1.2 | NR | 2.49 | NR | 2.95 | 46 |
| 12 | 0.0 | NR | 1.04 | NR | 2.55 | NR |
| 13 | 0.2 | NR | 6.76 | 14 | 3.89 | 26 |
| 14 | 0.0 | NR | 3.35 | 45 | 3.05 | 41 |
| 15 | 0.7 | NR | 5.13 | 25 | 3.37 | 35 |
| 16 | 0.1 | NR | 4.45 | 29 | 3.50 | 31 |
| 17 | 4.7 | NR | 2.84 | NR | 3.22 | 41 |

Using the results of Table 10.5 and 10.6, the effects of the eight JPCP and design inputs variables and second order interactions were calculated. Figures 9.3 to 9.8 show the effect values plotted against the expected normal values for the JPCP and Design variables. In each of the six plots only the significant variables are identified.

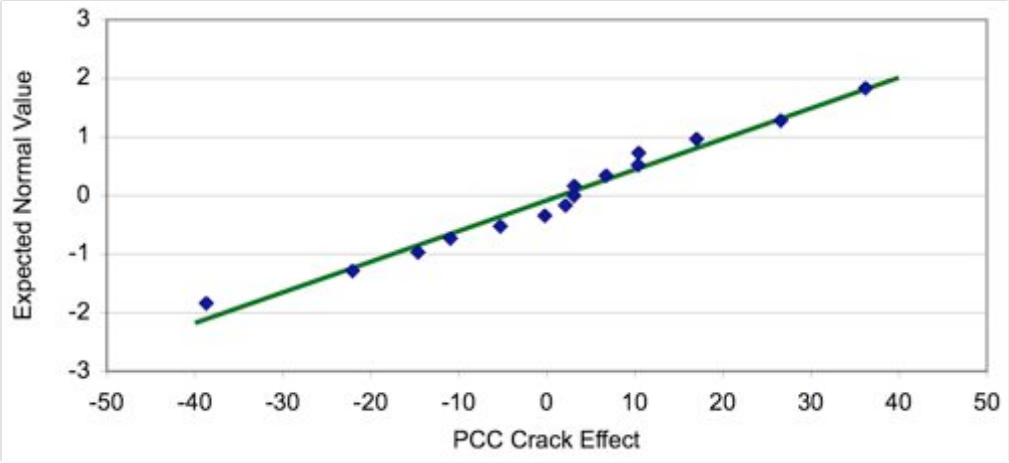


**Figure 9.3 JPCP Crack Effect Results**

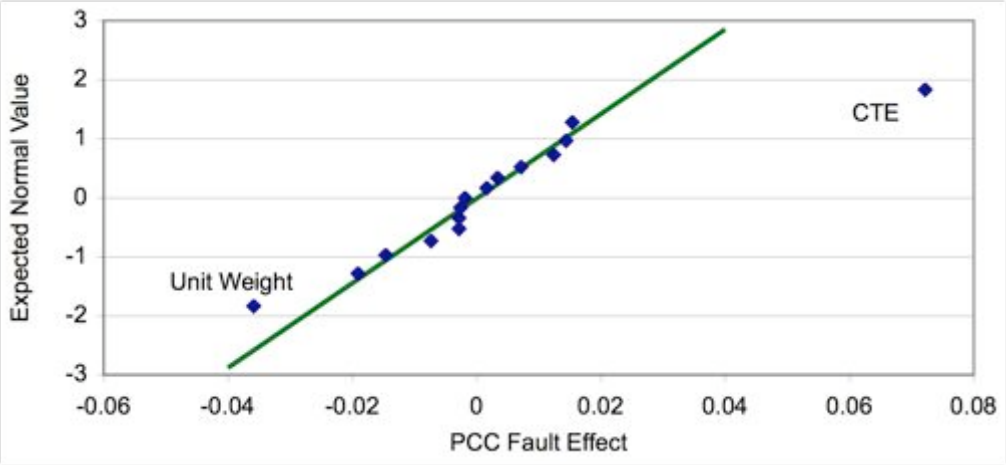


**Figure 9.4 JPCP Faulting Effect Results**

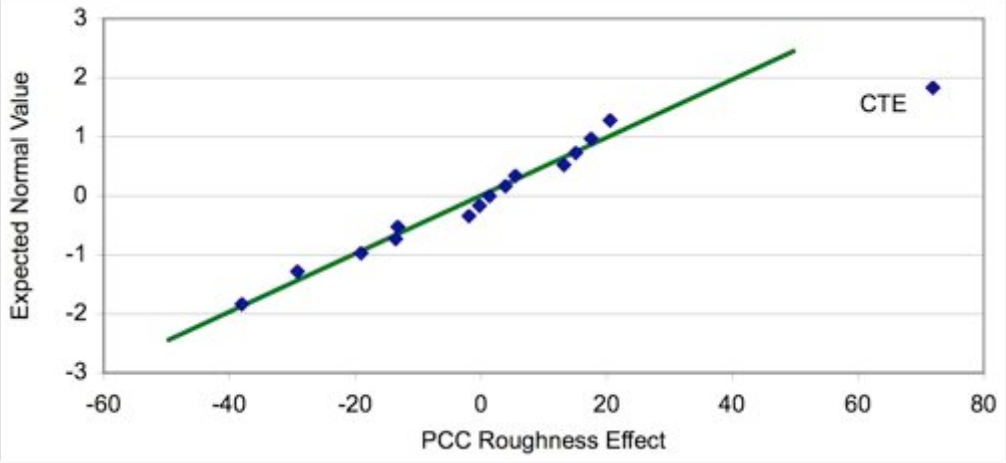


**Figure 9.5 JPCP Pavement Roughness Effect Results**

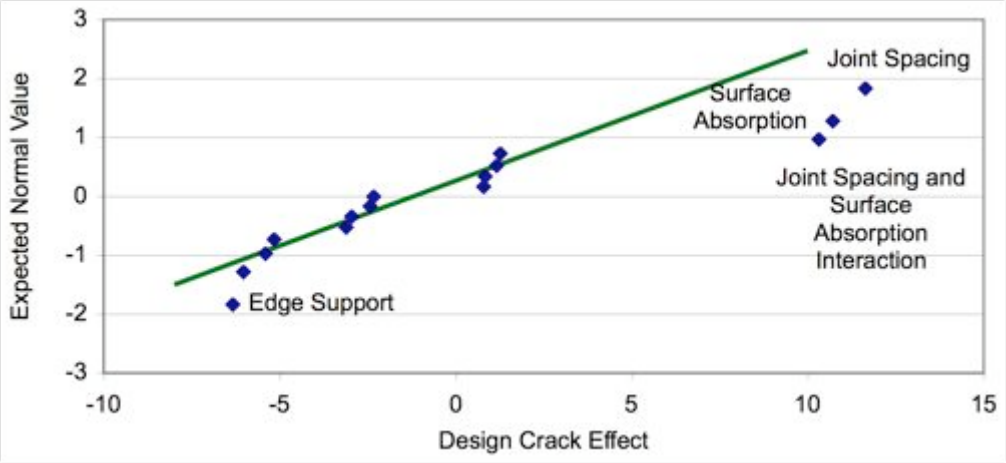


**Figure 9.6 Design Crack Effect Results**

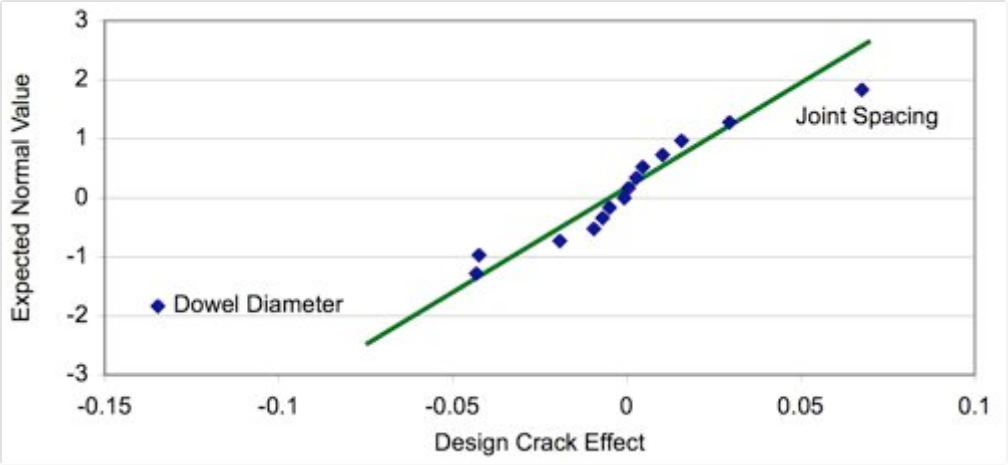


**Figure 9.7 Design Faulting Effect Results**

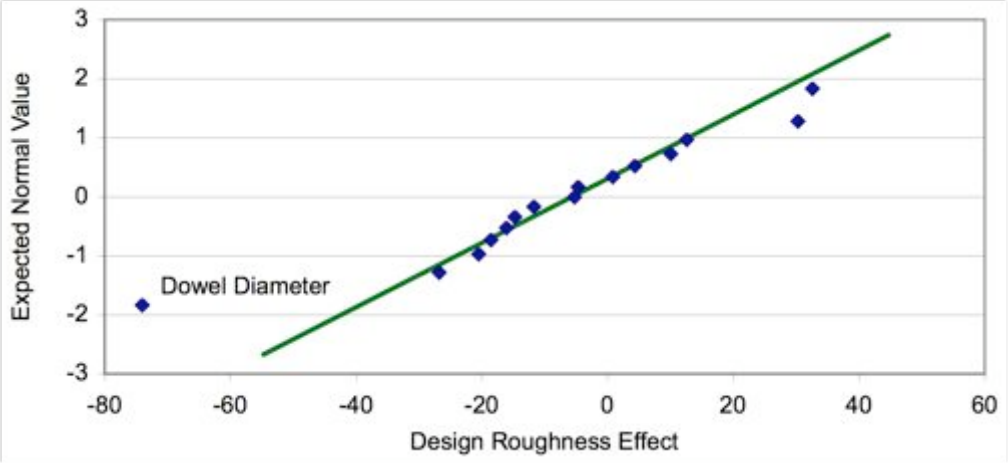


**Figure 9.8 Design Pavement Roughness Effect Results**

PB testing identified four independent variables and one interaction as having a significant influence on the results obtained from the ME-PDG simulations. These variables included:

- CTE,
- Unit weight,
- Edge support,
- Dowel diameter, and
- Interaction between joint spacing and surface shortwave absorption.

The majority of the significant variables are known quantities and fixed values for the design, however, special care needs to be taken in determining the CTE value.

## 9.3 Modeling Test Sections

Since CTE was identified as a sensitive variable impacting the results of the ME-PDG, three simulations were run using each of the four RCA amounts used in the test section (0%, 15%, 30%, and 50% coarse RCA) for a total of twelve ME-PDG simulations. The average CTE, minimum CTE, and maximum CTE values were simulated for each RCA amount. The pavement structure consisted of 250 mm JPCP of varying RCA amounts, 100 mm asphalt-stabilized ODGL, and 450 mm granular base material on a clay subgrade.

### 9.3.1 Materials

Table 9.7 summarizes the inputs for the JPCP and asphalt stabilized base layers. The values are based on the laboratory testing of the construction material and represent Level One and Level Two inputs.

**Table 9.7 ME-PDG Inputs for JPCP and Asphalt Layers**

| | 0% RCA | 15% RCA | 30% RCA | 50% RCA |
|---|---|---|---|---|
| Concrete | | | | |
| Cement Content (kg/m$^3$) | | 315 | | |
| w/c Ratio | | 0.43 | | |
| Unit Weight (kg/m$^3$) | 2350 | 2325 | 2323 | 2306 |
| Compressive Strength (MPa) | | | | |
| 7-day | 19.8 | 29.8 | 29.1 | 23.4 |
| 14-day | 23.9 | 35.6 | 35.9 | 29.7 |
| 28-day | 27.7 | 40.9 | 42.1 | 35.0 |
| 90-day | 35.2 | 45.4 | 46.8 | 38.9 |
| 20-year/28-day | | 1.32 | | |
| CTE ($10^{-6}$/$^o$C) | | | | |
| Average | 7.280 | 6.603 | 5.265 | 4.103 |
| Maximum | 8.973 | 6.857 | 5.761 | 5.314 |
| Minimum | 6.287 | 5.203 | 4.717 | 3.519 |
| Ultimate Shrinkage at 40% R.H. ($10^{-6}$) | 594 | 654 | 689 | 736 |

| | 0% RCA | 15% RCA | 30% RCA | 50% RCA |
|---|---|---|---|---|
| Asphalt Stabilized Base | | | | |
| Binder Grade | | PG 65-28 | | |
| AC Content (%) | | 2 | | |
| Air Voids (%) | | 20 | | |
| Unit Weight (kg/m$^3$) | | 2015 | | |
| Poisson's ratio | | 0.35 | | |
| Thermal Conductivity (J/m-s-$^o$C) | | 1.2 | | |
| Heat Capacity (J/kg-$^o$C) | | 966 | | |
| Gradation | | | | |
| % Retained 3/4" | | 7.4 | | |
| % Retained 3/8" | | 72.5 | | |
| % Retained #4 | | 95.9 | | |
| % Passing #200 | | 1 | | |

ME-PDG default inputs were used for the crushed granular and CL layers and reflect the values presented in Table 9.8, these values were also used in the sensitivity analysis

**Table 9.8 ME-PDG Inputs for Granular Base and CL Subgrade**

| | Granular Base | CL Subgrade |
|---|---|---|
| Strength Properties | | |
| Poison's ratio | 0.27 | 0.38 |
| Ko | 0.37 | 0.62 |
| Modulus (MPa) | 175 | 110 |
| ICM | | |
| Plasticity Index (PI) | 1 | 17 |
| Liquid Limit (LL) | 6 | 18 |
| D60 | 10.82 | 0.028 |
| % passing #200 sieve | 8.7 | 70.5 |
| Dry unit weight (kg/m$^3$) | 2035 | 1635 |
| Specific gravity | 2.7 | 2.7 |
| Hydraulic conductivity (mm/hr) | 1.55 | 0.0013 |

| | Granular Base | CL Subgrade |
|---|---|---|
| Gravimetric water content (%) | 7.4 | 20 |
| Degree of saturation (%) | 61.2 | 83 |

### 9.3.2 Climate

Since no ME-PDG Canadian climatic files exist, some had to be developed. Environment Canada provided fifteen years of historical climate data (1990-2005) to facilitate the development of a Southern Ontario (wet-freeze) climatic file. Data for temperature, wind speed, percent sunlight, precipitation, and relative humidity was gathered to produce the hourly climatic data (HCD) files. The data provided for temperature, wind speed, percent sunlight, and relative humidity was provided on an hourly basis. Environment Canada data provided precipitation on a six-hour basis (00:00-06:00, 06:00-12:00, 12:00-18:00, and 18:00-00:00). However, the ME-PDG requires precipitation data input on an hourly basis. So in order to modify the data appropriately, eight test climatic files were prepared to see if allocating the precipitation differently within the six–hour window would affect the performance results. Precipitation was allocated using:

1. A rectangular distribution,
2. A standard normal distribution N(0,1), and
3. All of the precipitation in one hour. (This was done six times, so each hour within the six-hour window could be evaluated.)

A graphical representation of the three distributions is presented in Figure 9.9 based on 5 mm of precipitation over a 6-hour period.

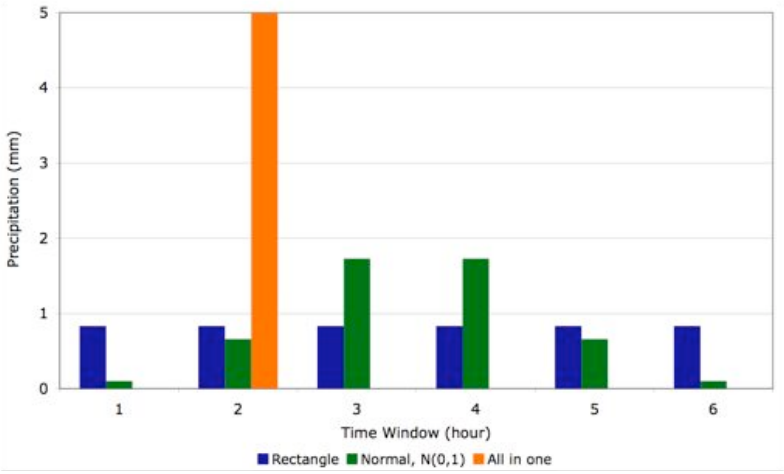


**Figure 9.9 Precipitation Distribution Scenarios**

The results using each of the eigth test climatic files gave exactly the same performance results for percent slabs cracked, joint faulting, and pavement roughness (IRI).

Since the precipitation distribution did not impact the results the remaining HCD files were developed for the remaining provinces in Canada using the standard normal N(0,1) distribution. A sample of the Ontario HCD format is presented below.

[Year][Month][Day][Hour],[Temp.],[Wind Speed],[% Sunlight],[Precip.],[Rel.Humidity]

1990010100,33.98,8.08,40,0,61

1990010101,28.94,3.73,50,0,75

1990010102,30.38,3.73,30,0,79

…

2005103123,33.08,6.84,0,0,92

The above HCD example summarizes that on January 1, 1990 the temperature at 12 pm was 33.98 $^{o}$F, wind was 8.08 MPH, 4 tenths cloud opacity, 0 inches of precipitation and the relative humidity was 60%. The developed climatic file for Southern Ontario on average would be exposed to 68 freeze-thaw cycles, a freezing index of 505.4$^{o}$C Day, mean temperature of 8.3 $^{o}$C and 801.1 mm of rainfall per year.

### 9.3.3 Test Section Results and Discussion

The performance results of the ME-PDG simulations at the end of the 50-year analysis period for the four concrete mixes using the average CTE values are presented in Figures 9.10 through 9.12.

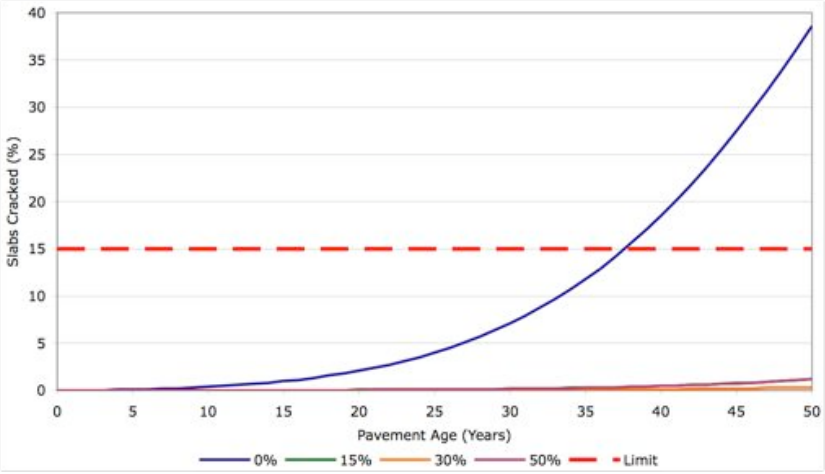


**Figure 9.10 Percent Slabs Cracked Performance Results**

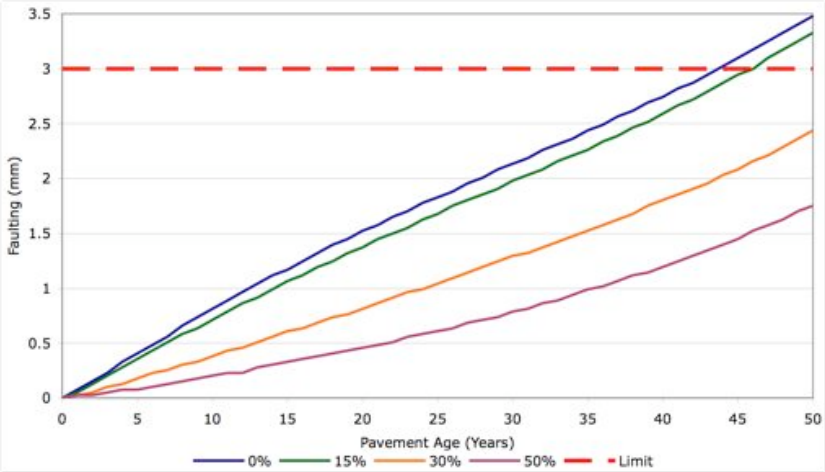


**Figure 9.11 Faulting Performance Results**

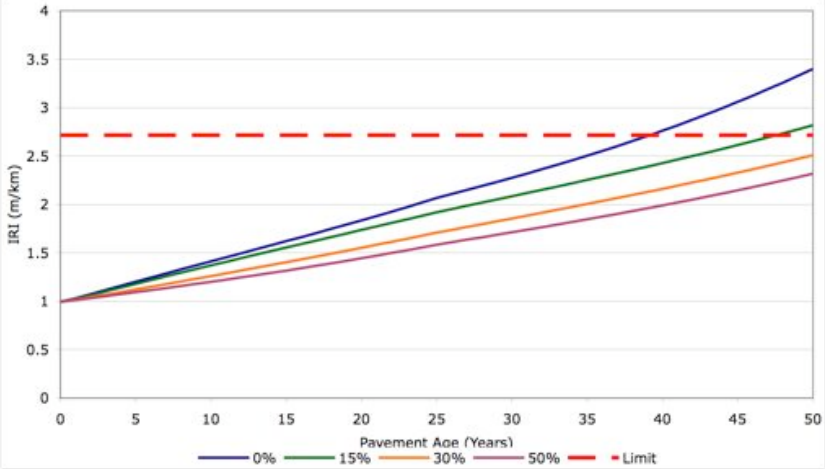


**Figure 9.12 Pavement Roughness Performance Results**

The following trends were observed from the ME-PDG simulations.

1. All three of the performance indicators (IRI, cracking, and faulting) improved as the amount of coarse RCA increased. The improvements in performance can be attributed to the decreasing CTE values as the coarse RCA content increases.
2. The threshold to trigger maintenance and rehabilitation (M&R) is exceeded by the 0% coarse RCA in percent slabs cracked, faulting, and roughness, and 15% coarse RCA in faulting and roughness. M&R limits are not reached for 30% and 50% coarse RCA for all the performance indicators.

3. The significant difference in performance for the percentage of slabs cracked between the 0% coarse RCA and the other sections can also be caused by the lower compressive strength of the test section increasing the rate of load related cracking.
4. Although RCA improved the performance of the pavement in the ME-PDG simulations, the improvements are not significant in a practical sense. For example an increase in faulting from 1.75 mm to 3.48 mm is not significant in the field.

To examine the effect of CTE variability on the slab cracking, faulting, and pavement roughness, twelve additional simulations were completed using the minimum CTE, average CTE or maximum CTE laboratory values for each coarse RCA amount. The CTE variability results are shown in Table 9.9.

**Table 9.9 CTE Variability Results**

Slabs Cracked (%)

| RCA Amount | CTE(Avg.) | CTE(Max.) | CTE(Min.) | Range |
|---|---|---|---|---|
| 0% | 38.6 | 93.6 | 22.8 | 70.8 |
| 15% | 1.2 | 1.4 | 0.5 | 0.9 |
| 30% | 0.3 | 0.5 | 0.2 | 0.2 |
| 50% | 1.2 | 2.3 | 0.9 | 1.4 |

Faulting (mm)

| RCA Amount | CTE(Avg.) | CTE(Max.) | CTE(Min.) | Range |
|---|---|---|---|---|
| 0% | 3.48 | 5.00 | 2.69 | 2.31 |
| 15% | 3.33 | 3.56 | 2.21 | 1.35 |
| 30% | 2.44 | 2.82 | 2.01 | 0.81 |
| 50% | 1.75 | 2.67 | 1.40 | 1.27 |

Roughness - IRI (mm)

| RCA Amount | CTE(Avg.) | CTE(Max.) | CTE(Min.) | Range |
|---|---|---|---|---|
| 0% | 3.40 | 4.60 | 2.94 | 1.66 |
| 15% | 2.82 | 2.89 | 2.44 | 0.45 |
| 30% | 2.51 | 2.64 | 2.37 | 0.27 |
| 50% | 2.32 | 2.63 | 2.20 | 0.43 |

The CTE Variability results show two important trends.

1. As the CTE value was increased from the minimum value to the average and then to the maximum value, IRI, cracking and faulting increased, demonstrating a decrease in performance. The range in values reinforces the importance of correctly characterizing the CTE of the concrete.
2. As the amount of RCA increased the range of the results decrease until the 30% RCA amount and increases again for the three performance indicators.

A summary of the performance results and time of failure for the coarse RCA JPCP test sections are presented in Table 9.10.

**Table 9.10 Summary Results**

| RCA Content | Cracking (% slabs) | | Faulting (mm) | | Roughness (m/km) | |
|---|---|---|---|---|---|---|
| | 50-year | TOF | 50-year | TOF | 50-year | TOF |
| 0% | 38.6 | 38 | 3.5 | 44 | 3.4 | 39 |
| 15% | 1.2 | NR* | 3.3 | 46 | 2.8 | 48 |
| 30% | 0.3 | NR | 2.4 | NR | 2.5 | NR |
| 50% | 1.2 | NR | 1.8 | NR | 2.3 | NR |

* NR = not reached

# Chapter 10
# Life Cycle Cost Analysis

There is increasing demand on transportation departments to provide longer lasting roads and better maintenance with decreasing funds and increasing product costs. An effective tool in selecting the most cost effective design alternatives is life cycle cost analysis (LCCA). LCCA is defined in the Transportation Equity Act for the 21st Century as "a process for evaluating the total economic worth of a usable project segment by analyzing initial costs and discounted future costs, such as maintenance, user, reconstruction, rehabilitation, resurfacing costs, over the project segment" [FHWA 2008]. LCCA is not a new concept; it was first proposed for use in transportation projects by Gillespie in 1847 and became more popular in the 1950's and 60's through the works of Winfrey and also the American Association of State Highway Officials (AASHO) Red Book [Ozbay 2004].

## 10.1 LCCA Steps

There are five general steps in conducting a LCCA [Smith 2008].

1. Establish alternative pavement design strategies for the analysis period.
2. Determine performance periods and activity timing.
3. Estimate agency and user costs.
4. Compute life cycle costs.
5. Analyze the results.

### 10.1.1 Step 1: Establish Alternative Designs

LCCA was used to examine the potential benefit of using three different amounts of coarse RCA (15%, 30%, and 50%) as a replacement for virgin aggregate using varying pricing scenarios to simulating the change in cost of virgin aggregate as the supply becomes depleted. Scenario One has increasing costs as the RCA amount increases, Scenario Two equal costs for all RCA mixes, and Scenario Three has decreasing costs as the RCA amount increases. The design of the test sections are based on the CPATT test sections described in Chapter Six and Seven. These include a 250 mm MTO/OPSS 30 MPa PCC Mix, 100 mm asphalt-stabilized OGDL and a 450 mm granular base.

### 10.1.2 Step 2: Determine Performance Periods and Activity Timings

A 50-year performance period was selected for the LCCA based on the current practices of the MTO [Lane 2008, ARA 2007]. Based on the limited empirical performance data for concrete containing RCA, the standard rigid LCC model used by the MTO was chosen as a starting point. Figure 10.1 presents this model

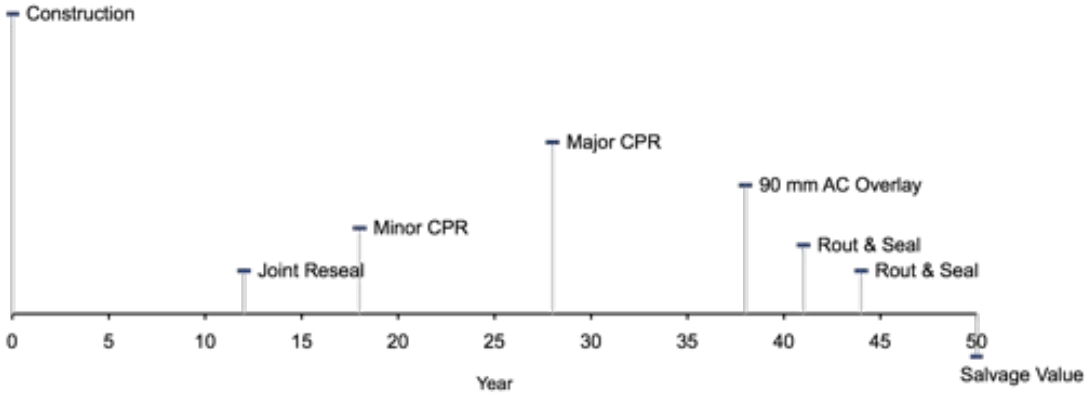


**Figure 10.1 Standard Rigid LCCA Model Used**

Minor concrete pavement restoration (CPR) at year 18 consists of diamond grinding, joint resealing, and limited partial- and full-depth patching. Major concrete pavement restoration (CPR) at year 28 consists of diamond grinding, joint resealing, and limited partial- and full-depth patching. A 90 mm AC overlay at year 38 consists of 40 mm SuperPave (SP) 12.5 mm Friction Course (FC) 2, and 50 mm SP 19 mm. The activity timings of the MTO rigid LCC model were modified to reflect concrete material testing results, pavement evaluations, and ME-PDG simulations. The timing of activities were modeled using a triangular distribution with minimum, most likely, and maximum values. The timing of the four proposed design alternatives is presented in Table 10.1.

**Table 10.1 Proposed Activity Timing Schedules**

| Activity | 0% RCA | 15% RCA | 30% RCA | 50% RCA |
|---|---|---|---|---|
| Joint Reseal | 9, 12, 14 | 10, 12, 15 | 11, 12, 16 | 10, 12, 15 |
| Minor CPR | 15, 18, 20 | 16, 18, 21 | 17, 18, 22 | 16, 18, 21 |
| Major CPR | 25, 28, 30 | 26, 28, 31 | 27, 28, 32 | 26, 28, 31 |
| 90 mm AC Overlay | 35, 38, 40 | 36, 39, 41 | 37, 40, 42 | 36, 39, 41 |
| Rout & Seal #1 | 39, 41, 43 | 39, 42, 43 | 39, 43, 45 | 39, 42, 43 |
| Rout & Seal #2 | 42, 44, 46 | 42, 45, 47 | 43, 46, 48 | 42, 45, 47 |

### 10.1.3 Step 3: Estimate Agency and User Costs

Agency costs include the initial cost of construction and future maintenance and rehabilitation (M&R) costs minus the remaining value at the end of the design period. User costs include travel time, vehicle operation costs, accidents, discomfort and user delay. The cost information used in this LCCA is based upon a study conducted by ARA in 2006 for the Ontario Ministry of Transportation

(MTO), Cement Association of Canada (CAC), and Ontario Hot Mix Producers Association (OHMPA) where LCCA procedures were reviewed and updated to reflect current trends in freeway pavement designs in Ontario.

In order to estimate the cost in the present, an escalation factor is used to estimate the current dollar value based on historical costs, using the transportation component of the Consumer Price Index (CPI) as recommended in the FHWA LCCA Technical Bulletin [Walls III 1998]. The escalation factor is calculated as 1.037 using Equation 10.1. The transportation component accounts for 19.88% of the overall CPI.

$$Escalation\ Factor = \frac{2008\ CPI_{(Trans)}}{2006\ CPI_{(Trans)}} \tag{10.1}$$

where: $CPI_{(Trans)}$ = Transportation component of the Consumer Price Index

The 2008 material and activity costs used in this LCCA were modeled using normal distributions. The values are presented in Table 10.2.

**Table 10.2 Material and Activity Costs**

| | Unit Cost | St.Dev. |
|---|---|---|
| MTO/OPSS 30 MPa PCC Mix | \$191.00 /$m^3$ | \$13.44 /$m^3$ |
| Partial Depth PCC Patching | \$191.32 /$m^2$ | \$21.32 /$m^2$ |
| Full Depth PCC Patching | \$174.02 /$m^2$ | \$32.57 /$m^2$ |
| Diamond Grinding | \$5.96 /$m^2$ | \$0.62 /$m^2$ |
| Joint Reseal | \$5.84 /m | \$0.72 /m |
| Superpave 19 mm | \$80.65 /t | \$15.74 /t |
| Superpave 12.5 mm FC2 | \$109.81 /t | \$16.76 /t |
| Mill 90 mm HMA | \$2.16 /$m^2$ | \$1.04 /$m^2$ |
| Mill and Patch | \$15.56 / $m^2$ | \$1.56 /$m^2$ |
| Rout & Seal | \$2.75 /$m^2$ | \$0.21 /$m^2$ |
| Tack Coat | \$0.32 /$m^2$ | \$0.09 /$m^2$ |

User costs were not included in this LCCA, since the MTO and the majority of State DOT's do not incorporate user costs into their LCCA procedure [Lane 2008, Rangaraju 2008].

### 10.1.4 Step 4: Compute Life Cycle Costs

Probabilistic LCCA was preformed using a Latin Hypercube sampling (LHS) to calculate the Present Worth (PW) of each design alternative. In order to estimate the PW, 500 simulations with five iterations per variable were run to calculate an average. LHS is a process where the cumulative distribution function (cdf) of a specific variable is divided into equal intervals, within each interval a value is selected randomly, each interval is only sampled once during the simulation. Figure 10.2 shows a simple example of a triangular distribution (3,5,6) that uses five iterations.

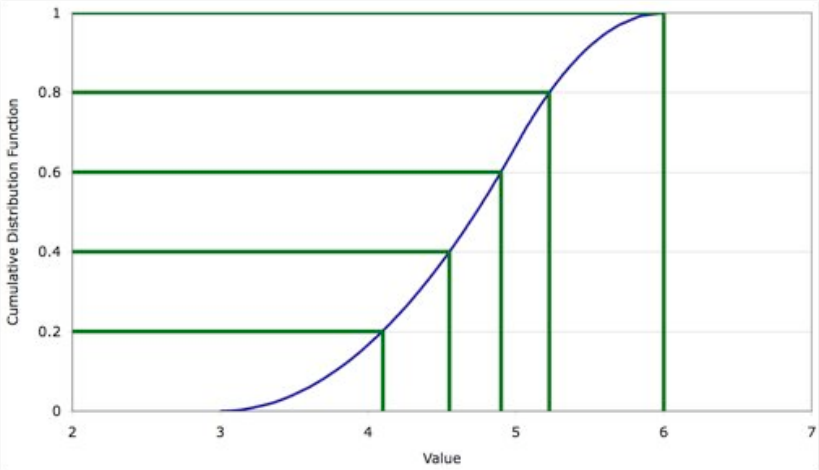


**Figure 10.2 Triangle Distribution with Five Iterations**

The width of intervals for the corresponding value becomes smaller as the most likely value is approached. Similarly the width of the interval increases as the probability decreases towards the tails of the distribution. This results in LHS requiring less iteration to achieve convergence than the Monte Carlo simulation and incorporates low probability values at both ends of the distribution [Walls III 1998]. PW is calculated using equation 10.2

$$PW = Initial\ Cost + \sum_{t=1}^{N}\left( M\ \&\ R\ Cost\left(\frac{1}{(1+i)^{n_t}}\right)\right) - RV\left(\frac{1}{(1+i)^{n_t}}\right) \tag{10.2}$$

where: $M\ \&\ R$ = maintenance and rehabilitation

$RV$ = remaining value

$i$ = discount rate

$n_t$ = year of expenditure

The PW calculation uses a remaining value (RV) at the end of the LCCA period instead of a salvage value (SV). A SV represents the cost associated with reclaiming and recycling the materials

in the road at the end of the serviceable life where as a RV does not account for this [Smith 2008]. The RV is the depreciated value of the structural and functional activity values at the end of the analysis period. Figures 10.3 and 10.4 illustrate the structural deterioration of the original structure and functional deterioration of the M&R individually and added together to calculate the RV.

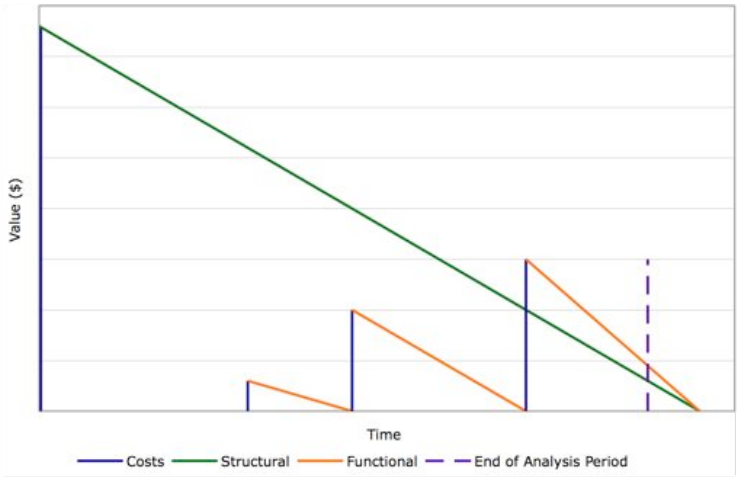


**Figure 10.3 Cost Associated with Structural and Functional Deterioration**

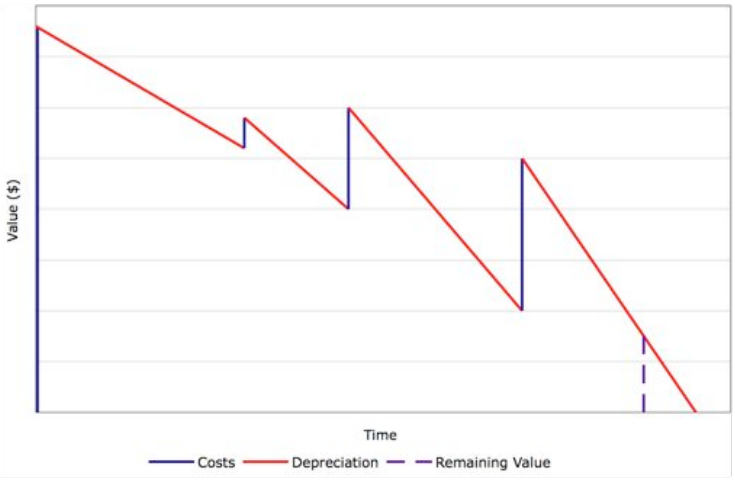


**Figure 10.4 Combined Costs**

To model the discount rate, a triangular distribution was used with minimum, most likely, and maximum values as three percent, five percent, and six percent.

### 10.1.5 Step 5: LCCA Results Scenario 1 – Higher Costs for RCA Concretes

The results of the LHS probabilistic LCCA are presented in Table 10.3 and Figure 10.5.

**Table 10.3 Results of LCCA Scenario 1**

| | 0% RCA | 30% RCA | 15% RCA | 50% RCA |
|---|---|---|---|---|
| Average | $1,088,000 | $1,097,000 | $1,101,000 | $1,117,000 |
| Standard Deviation | $23,000 | $22,000 | $24,000 | $23,000 |

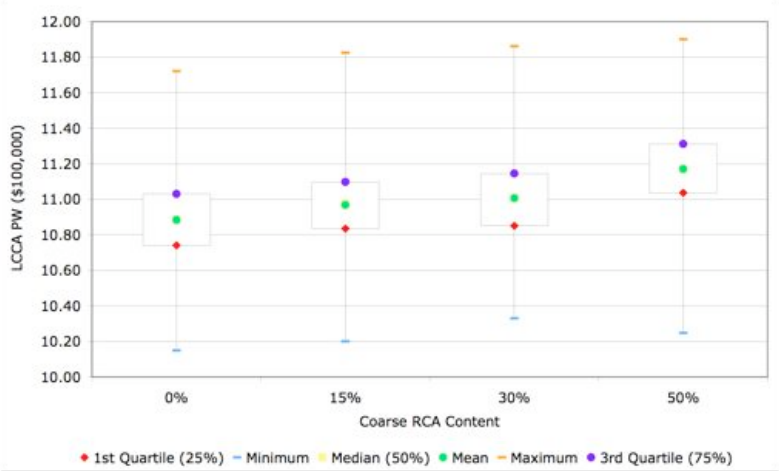


**Figure 10.5 Results of LCCA Scenario 1**

Several observations were made from the LCCA results.

- PW follows the same order as construction cost (0% is the lowest and 50% coarse RCA is the highest).
- The spread between the first and third quartiles (25% and 75%) remains constant for all the alternatives.
- The mean and median values are located very close to the centre 50% percent of the data showing very little skew to the distribution.
- The location of the box within the minimum and maximum values is shifted very slightly towards the minimum value, indicating a positive skew.
- The symmetry of the quartile plots suggests the LCCA PW results follow a normal distribution.

Figure 10.6 shows the cumulative distribution probabilities of the four design alternatives.

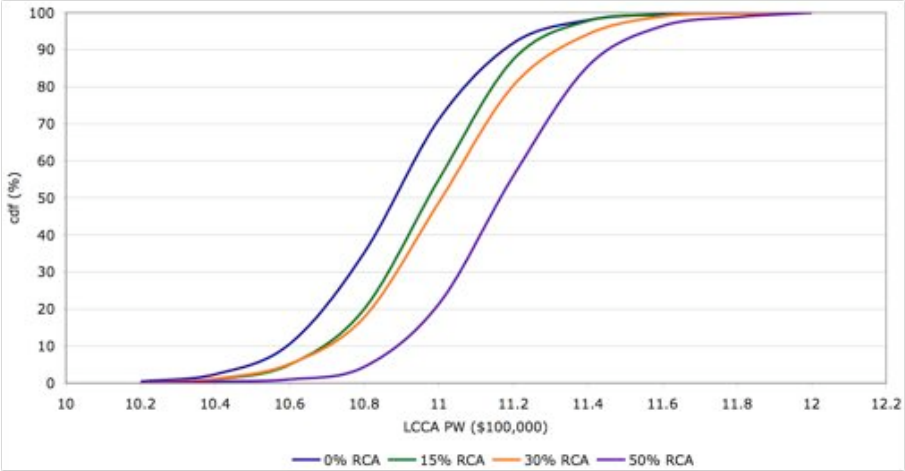


**Figure 11.6 Cumulative Distribution Probabilities Scenario 1**

Using Figure 11.6, the 95% confidence interval (CI) for the LCCA PW mean can be estimated as follows.

- $1,042,000 and $1,135,000 for 0% coarse RCA
- $1,053,000 and $1,141,000 for 15% coarse RCA
- $1,053,000 and $1,148,000 for 30% coarse RCA
- $1,071,000 and $1,163,000 for 50% coarse RCA

Based on the 95% CI values there is no significant difference in the LCCA PW of the four design alternatives containing varying amounts of coarse RCA.

### 10.1.6 Step 5: LCCA Results Scenario 2 – Equal Costs for RCA and Conventional Concretes

The results of the LHS probabilistic LCCA are presented in Table 10.4 and Figure 10.7.

**Table 10.4 Results of LCCA Scenario 2**

| | 0% RCA | 30% RCA | 15% RCA | 50% RCA |
|---|---|---|---|---|
| Average | $1,087,000 | $1,086,000 | $1,083,000 | $1,087,000 |
| Standard Deviation | $22,000 | $22,000 | $21,000 | $22,000 |

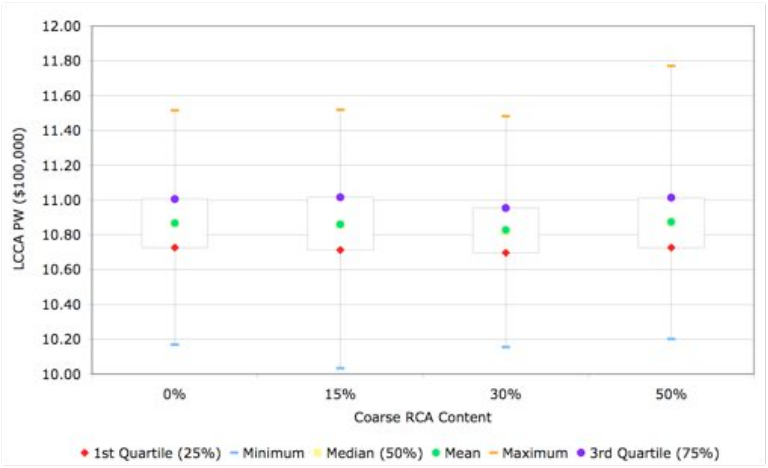


**Figure 10.7 Results of LCCA Scenario 2**

Several observations were made from the LCCA results.

- PW follows the order as expected pavement performance (30%, 15%, 50%, and 0% RCA).
- The spread between the first and third quartiles (25% and 75%) remains constant for all the alternatives.
- The mean and median values are located very close to the centre 50% percent of the data showing very little skew to the distribution.
- Variable skewing between the RCA contents. Slight positive skew for 0% and 30%, a more positive skew for 15% and a negative skew for the 50%.
- The symmetry of the quartile plots suggests the LCCA PW results follow a normal distribution with some minor deviations.

Figure 10.8 shows the cumulative distribution probabilities of the four design alternatives.

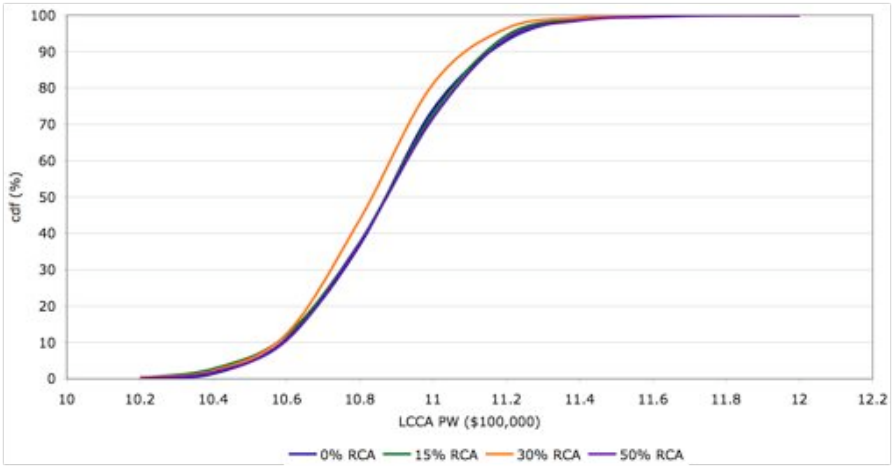


**Figure 10.8 Cumulative Distribution Probabilities Scenario 2**

Using Figure 10.8 the 95% confidence interval (CI) for the LCCA PW mean can be estimated as follows.

- $1,044,000 and $1,131,000 for 0% coarse RCA
- $1,042,000 and $1,130,000 for 15% coarse RCA
- $1,041,000 and $1,124,000 for 30% coarse RCA
- $1,042,000 and $1,132,000 for 50% coarse RCA

Based on the 95% CI values there is no significant difference in the LCCA PW of the four design alternatives containing varying amounts of coarse RCA.

### 10.1.7 Step 5: LCCA Results Scenario 3 – Higher Costs for Conventional Concretes

The results of the LHS probabilistic LCCA are presented in Table 10.5 and Figure 10.9.

**Table 10.5 Results of LCCA Scenario 3**

| | 0% RCA | 30% RCA | 15% RCA | 50% RCA |
|---|---|---|---|---|
| Average | $1,117,000 | $1,107,000 | $1,093,000 | $1,086,000 |
| Standard Deviation | $21,000 | $22,000 | $23,000 | $21,000 |

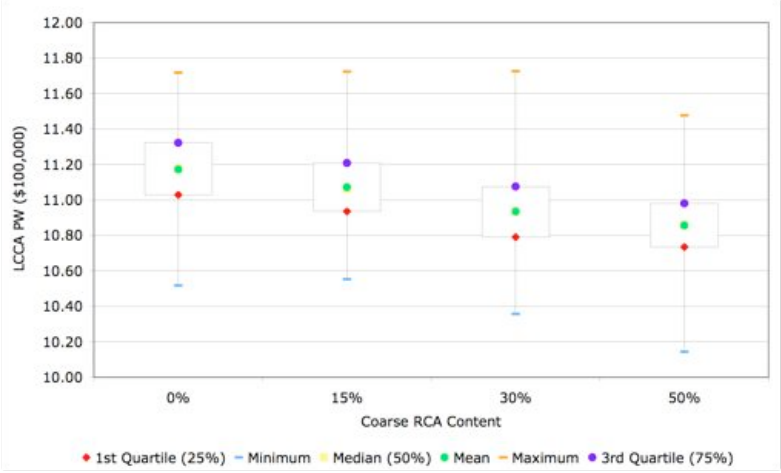


**Figure 10.9 Results of LCCA Scenario 3**

Several observations were made from the LCCA results.

- PW follows the same order as construction cost (50% is the lowest and 0% is the highest).
- The spread between the first and third quartiles (25% and 75%) remains constant for all the alternatives.
- The mean and median values are located very close to the centre 50% percent of the data showing very little skew to the distribution.
- Variable skewing between the RCA contents. Slight positive skew for 0% and 50%, and a negative skew for 15% and 30%.
- The symmetry of the quartile plots suggests the LCCA PW results follow a normal distribution with some minor deviations.

Figure 10.10 shows the cumulative distribution probabilities of the four design alternatives.

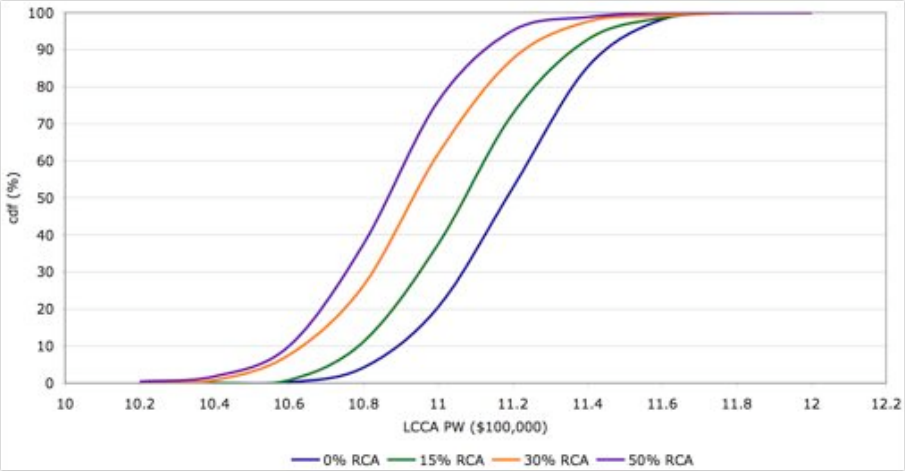


**Figure 10.10 Cumulative Distribution Probabilities Scenario 3**

Using Figure 10.10, the 95% confidence interval (CI) for the LCCA PW mean can be estimated as follows.

- $1,075,000 and $1,159,000 for 0% coarse RCA
- $1,063,000 and $1,151,000 for 15% coarse RCA
- $1,048,000 and $1,139,000 for 30% coarse RCA
- $1,044,000 and $1,127,000 for 50% coarse RCA

Based on the 95% CI values there is no significant difference in the LCCA PW of the four design alternatives containing varying amounts of coarse RCA.

## 10.2 Sensitivity

### 10.2.1 Convergence

Figure 10.11 show the convergence results for the PW RCA alternatives.

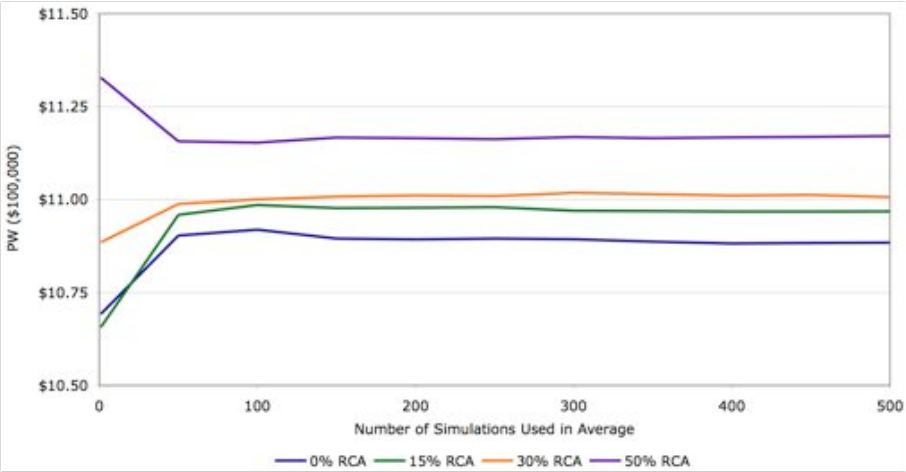


**Figure 10.11 Convergence Results**

Very little change in the average LCCA PW is observed in all four design alternatives after 200 simulations. This indicates that the LHS methodology, using 500 simulations with five iterations, is sufficient to arrive at a meaningful result.

### 10.2.2 Input Parameters

To estimate the sensitivity of the input parameters a PB screening design, the same as used in Chapter 9, was performed. The eight JPCP factors examined and their values are presented in Table 10.6.

**Table 10.6 Value of Factors in LCCA**

| | LCCA Factors | - | + | 0 |
|---|---|---|---|---|
| A | Construction Cost | 809040 | 1213560 | 1011300 |
| B | Initial Construction Life | 36 | 40 | 38 |
| C | Discount Rate (%) | 3.6 | 5.6 | 4.6 |
| D | CPR Minor Cost | 47559.20 | 71338.80 | 59449.00 |
| E | CPR Major Cost | 59344.16 | 89016.24 | 74180.20 |
| F | AC Overlay Cost | 146761.04 | 220031.56 | 183396.30 |

| | | | | |
|---|---|---|---|---|
| G | Quantities | | | |
| | Joint Resealing | 280 | 420 | 350 |
| | Diamond Grinding | 6800 | 10200 | 8500 |
| | Joint Resealing | 560 | 840 | 700 |
| | Partial Depth Patching | 8 | 12 | 10 |
| | Full Depth Patching | 12 | 18 | 15 |
| | Diamond Grinding | 6800 | 10200 | 8500 |
| | Joint Resealing | 960 | 1440 | 1200 |
| | Partial Depth Patching | 28 | 42 | 35 |
| | Full Depth Patching | 44 | 66 | 55 |
| | SP 12.5 mm FC2 | 708 | 1062 | 885 |
| | SP 19 mm | 832 | 1248 | 1040 |
| | Tack Coat | 6800 | 10200 | 8500 |
| | Rout & Seal | 280 | 420 | 350 |
| | Rout & Seal | 560 | 840 | 700 |
| H | Remaining Value | 29560.21 | 44340.31 | 36950.26 |

The results of the 17 runs are presented in Table 10.7.

**Table 10.7 Present Worth Sensitivity Results**

| Run | Variable | | | | | | | | LCCA PW |
|---|---|---|---|---|---|---|---|---|---|
| | A | B | C | D | E | F | G | H | ($100,000) |
| 1 | - | - | - | + | + | + | - | + | $9.110 |
| 2 | + | - | - | - | - | + | + | + | $13.410 |
| 3 | - | + | - | - | + | - | + | + | $9.190 |
| 4 | + | + | - | + | - | - | - | + | $12.856 |
| 5 | - | - | + | + | - | - | + | + | $8.828 |
| 6 | + | - | + | - | + | - | - | + | $12.597 |
| 7 | - | + | + | - | - | + | - | + | $8.531 |
| 8 | + | + | + | + | + | + | + | + | $13.006 |
| 9 | + | + | + | - | - | - | + | - | $12.721 |
| 10 | - | + | + | + | + | - | - | - | $8.604 |

| Run | Variable | | | | | | | | LCCA PW |
|---|---|---|---|---|---|---|---|---|---|
| | A | B | C | D | E | F | G | H | ($100,000) |
| 11 | + | - | + | + | - | + | - | - | $12.710 |
| 12 | - | - | + | - | + | + | + | - | $8.930 |
| 13 | + | + | - | - | + | + | - | - | $13.011 |
| 14 | - | + | - | + | - | + | + | - | $9.449 |
| 15 | + | - | - | + | + | - | + | - | $13.482 |
| 16 | - | - | - | - | - | - | - | - | $8.775 |
| 17 | 0 | 0 | 0 | 0 | 0 | 0 | 0 | 0 | $10.919 |

The values from the PB testing ranged from $853,100 to $1,348,200. Using the results from the 17 runs, the effect of the eight variables was plotted against their expected values (calculations are in Chapter 9) to determine the significant inputs. Figure 10.12 shows the results.

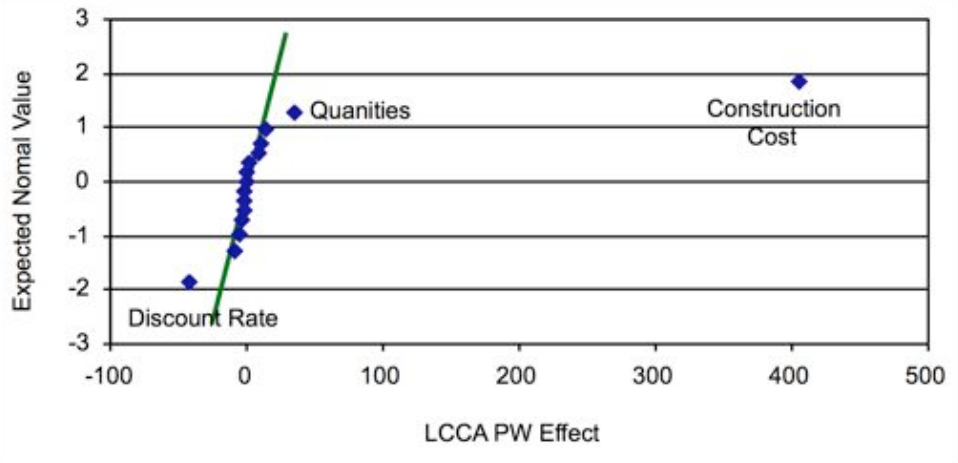


**Figure 11.12 Significant Inputs**

Analysis of the PB designs show that there are three sensitive input variables in the LCCA model; construction cost, discount rate, and the quantities.

### 10.2.3 Discount Rate

To examine the impact the discount rate has on the PW a deterministic LCCA was performed on the design alternatives using five different rates from two percent to six percent. The results are shown in Figure 10.13. The discount rate used by the MTO is set by the Ministry of Finance and is currently set at five percent, prior to 2006 a rate of seven percent was used [Lane 2008, ARA 2007].

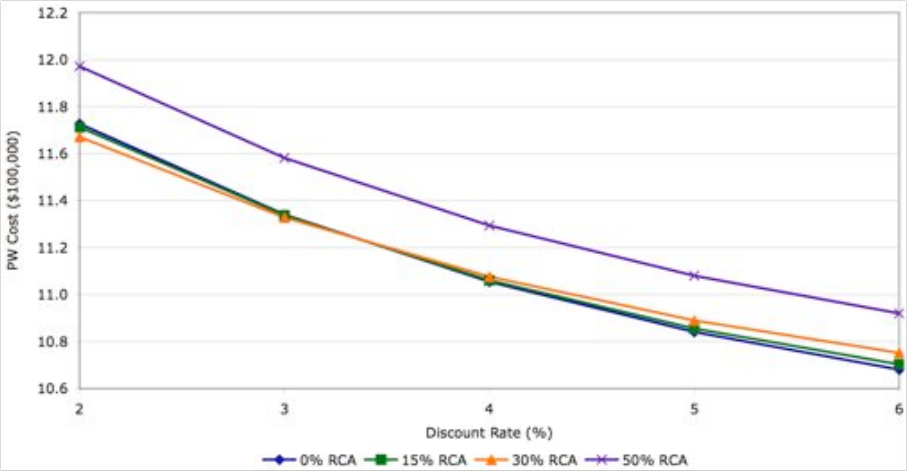


**Figure 10.13 Impact of Discount Rate on Present Worth**

As the discount rate increases, the order of PW cost changes. At a discount rate less than three percent the lowest PW is 30% RCA. When the discount rate is increased between three percent and four percent, the lowest PW is 15% RCA. Using a discount rate greater than four percent, results in 0% RCA having the lowest PW.

## 10.3 Discussion

The results of the LCCA show no significant difference between the test sections made with RCA and the section made without RCA for any of the three scenarios. However, increasing the price of the virgin aggregate through the three scenarios shows a cost benefit of using the RCA.

The impact on the environment was not considered in the three scenarios. Including the costs associated with the impact of aggregate pits on plants, animals, noise and water supply, along with the cost of associated trucking and pollution would further highlight the benefits to using the RCA.

# Chapter 11

# Conclusions and Recommendations

## 11.1 Conclusions

This research examined the properties of RCA concrete and its performance in JPCP. Compared to a conventional concrete mixture, substituting RCA for virgin coarse aggregate resulted in similar or improved performance. Indicating that RCA is a viable aggregate source for concrete pavements.

Material testing of the RCA used in the preliminary mixes and placed at the CPATT test track showed that the source would have been classed as unacceptable based on the MTO's virgin material specification OPSS 1002. Compared to the corresponding nineteen millimeter virgin aggregate, the RCA had an increase in absorption of 300% and decreases in bulk relative density of thirteen percent and abrasion resistance of 34% measured using Micro-Deval testing.

The compressive strength of the twelve preliminary design mixes at 28-days all exceeded the 30 MPa design strength. For the three coarse RCA amounts (15%, 30%, and 50%) compressive strength increases were related to the increases in cement content (315 kg/m$^3$, 330 kg/m$^3$, and 345 kg/m$^3$), however, there was no statistical difference between the mixes at the same cement content.

The compressive strength of the concrete increased as the amount of coarse RCA increased to a maximum at 30% at 28-days. All three of the coarse RCA mixes demonstrated increases in strength compared to the conventional concrete. The flexural strength results followed the same trends as the compressive strength. The compressive and flexural strength values are as follows:

- 0% coarse RCA 27.6 MPa (Compressive) and 6.0 MPa (Flexural),
- 15% coarse RCA 40.9 MPa, and 7.2 MPa,
- 30% coarse RCA 42.1 MPa, and 7.3 MPa, and
- 50% coarse RCA 35.0 MPa, and 6.3 MPa.

Freeze-thaw (F/T) testing showed no difference between the coarse RCA mixes and the conventional concrete in respect to change in relative dynamic modulus (RDM) and percent mass loss. At the end of the 300 cycles, the RDM was approximately 90% and the mass loss was less than 1%. Both the RDM and mass loss decreased as the coarse RCA amount increased up to 30%. The RDM and mass loss values are as follows:

- 0% coarse, RCA 91.3% (RDM), and 0.25% (mass loss),
- 15% coarse RCA 90.8%, and 0.2%,
- 30% coarse RCA 91.9%, and 0.16%, and
- 50% coarse RCA 91.1%, and 0.11%.

The coefficient of thermal expansion (CTE) decreased as the coarse RCA amount increased and was in the typical range of a conventional concrete made with limestone aggregate. The CTE values are as follows:

- 0% RCA $7.28 \times 10^{-6}$ /$^{o}$C,
- 15% RCA $6.603 \times 10^{-6}$ /$^{o}$C,
- 30% RCA $5.265 \times 10^{-6}$ /$^{o}$C, and
- 50% RCA $4.103 \times 10^{-6}$ /$^{o}$C.

The simplified CTE testing method provided two key benefits in modeling the observed field conditions over the AASHTO TP 60 method. These included:

- The testing temperature range, -20$^{o}$C to 20$^{o}$C, and
- The specimen condition, not being immersed in water.

After two years in-service and approximately 3,000,000 ESALs, all test sections are in excellent condition with pavement condition index (PCI) values greater than 85. The sections containing RCA are showing no significant difference in performance compared to the conventional JPCP section. The PCI values at the June 2009 evaluation:

- 0% coarse RCA 91,
- 15% coarse RCA 95,
- 30% coarse RCA 94, and
- 50% coarse RCA 95.

The test sections are all showing the same distresses; abrasion, joint cracking and spalling, and raveling.

Sensor data from the strain gauges, and vertical and inter-panel extensometers are providing consistent results between the test sections. 80% of the sensors are still functioning and providing useful data after two years.

Strain findings:

1. The change in strain is greater for the sensors located in the upper portion of the slab compared to the bottom.
2. The change in strain is greater in the transverse direction compared to longitudinal.
3. The change in strain is constant for transverse directions located mid slab and at the joint.

Vertical and Inter-Panel extensometer findings:

1. The change in vertical displacement is three times greater at the pavement edge compared to the pavement centreline.
2. The change in horizontal displacement is equal at the pavement edge compared to the pavement centreline.

Long-term performance modeling of percent cracked slabs, joint faulting, and pavement roughness using the ME-PDG showed improved performance as the coarse RCA content increased for all measures. At the end of the 50-year analysis period, only five simulations exceeded the specified trigger levels for maintenance and rehabilitation to occur. These simulations included: 0% coarse RCA for percent slabs cracked, joint faulting, and roughness; and 15% coarse RCA for joint faulting a, and roughness. Multivariable sensitivity analysis showed that the performance results were sensitive to CTE, unit weight, joint spacing, edge support, surface absorption, and dowel bar diameter. Additional ME-PDG simulations using the maximum and minimum CTE values showed improved performance as the CTE value decreased for all coarse RCA amounts.

The three life cycle cost analysis (LCCA) showed cost savings could be achieved by using RCA as virgin aggregate resources diminish. For each of the scenarios no significant difference between the coarse RCA amounts was observed on a per kilometer basis, however, over the length of an entire roadway the savings become significant.

Scenario 1 – Abundant supple of virgin aggregate, higher costs for RCA concretes.

- 0% RCA $1,088,000/km,
- 15% RCA $1,097,000/km,
- 30% RCA $1,101,000/km, and
- 50% RCA $1,117,000/km.

Scenario 2 – Diminishing supply of virgin aggregate, equivalent cost for RCA and conventional concretes.

- 0% RCA $1,087,000/km,
- 15% RCA $1,086,000/km,
- 30% RCA $1,083,000/km, and
- 50% RCA $1,087,000/km.

Scenario 3 – Shortage of virgin aggregate, lowers costs for RCA concretes.

- 0% RCA $1,117,000/km,
- 15% RCA $1,107,000/km,
- 30% RCA $1,093,000/km, and
- 50% RCA $1,086,000/km.

Multivariable sensitivity analysis showed that the LCCA results were sensitive to construction costs, discount rate, and maintenance and rehabilitation quantities. Additional LCCA, using the variable discount rates between two percent and six percent, changed the order of the present worth values.

## 11.2 Recommendations

For RCA to become widely used material, consistent and predictable results need to be obtained when using as a substitute for virgin aggregate in concrete. To achieve this further study is required in the areas of aggregate properties, mixture design and proportioning, performance, testing, and modeling.

Aggregate Properties

- Perform petrographic analysis on the RCA samples to better understand their composition, quality, and how much deleterious material that can be included without affecting the performance of the concrete.

Mixture Design and Proportioning

- Comparing concrete mixes with different sources of RCA including sources of RCA that are clean, contaminated, and cured differently.
- Compare concrete mixes with a variety of coarse RCA content to find the optimal amount that can be added without sacrificing performance.
- Develop additional designs that incorporate fine RCA and concrete wash-water to achieve a zero waste concrete.

Performance

- Continued monitoring of pavement structure (PCI surveys and sensor data) to understand the long-term performance.

Testing

- Retest RCA cylinders using AASHTO TP-60 method to compare and validate results. Based on the results it may be possible to conclude that the simplified method is acceptable for calculating CTE for use in the ME-PDG.
- Investigate the impact of core condition (dry, saturated surface dry, wet) has on the CTE using simplified method.

Modeling

- Estimate pavement performance of concrete containing RCA in additional climatic zones (wet no-freeze, dry-freeze, and dry no-freeze) and severities using the ME-PDG to determine its suitability in those locations.
- Update PCI, sensor, and LCCA models as new data becomes available.

# Bibliography

AASHTO. (2004). "Standard Test Method for Coefficient of Thermal Expansion of Hydraulic Concrete," AASHTO TP-60, American Association of State Highway and Transportation Officials, Washington, D.C.

Abbas, A., Fathifazl, G., Isgor, O.B., Razapur, A.G., Fournier, B., and Foo, S. (2008). "Durability of Recycled Aggregate Concrete Designed with Equivalent Mortar Volume (EVM) Method," 2nd Canadian Conference on Effective Design of Structures, paper #58, McMaster University, Hamilton, ON.

Abou-Zeid, M.N., Shenouda, M.N., McCabe, S.L., and El-Tawil, F.A. (2005). "Reincarnation of Concrete," Concrete International, V. 27, No.2, February 2005, pp. 53-59.

Achtemichuk, S, Hubbard, J, Sluce, R., and Shehata, M. (2008). "Development of Controlled Low-Strength Materials Using Reclaimed Concrete Aggregates," 2nd Canadian Conference on Effective Design of Structures, paper #58, McMaster University, Hamilton, ON, 2008.

American Concrete Institute. (2005). "Building Code Requirements for Structural Concrete and Commentary," ACI 318-05, Farmington Hills, MI, 2005, pp. 1-430.

American Concrete Institute. (1992). "State-of-the-Art on High-Strength Concrete," ACI 363R-92, Farmington Hills, MI, 1992, pp. 1-55.

American Concrete Pavement Association. (2009). "Recycling Concrete Pavement," Concrete Paving Technology, EB-043P.

American Concrete Pavement Association. (1993). "Recycling Concrete Pavement," Concrete Paving Technology, TB-014P.

Ajdukiewicz, A., and Kliszczewica, A. (2002). "Influence of Recycled Aggregates on Mechanical Properties of HS/HPS," Cement and Concrete Composites, V. 24, No. 2, 2002, pp. 269-279.

Aggregate Producers Association of Ontario. (2004). "Importance of Aggregate," The About Aggregate Series, Aggregate Producers Association of Ontario, Mississauga, Ontario, pp. 1-4.

Applied Research Associates, Inc. (2007). "Life-Cycle Cost 2006 Update," Toronto, ON.

Applied Research Associates, Inc., ERES Consultants Division. (2004). "Guide for Mechanistic-Empirical Design of New and Rehabilitated Pavement Structures," NCHRP Project 1-37A, National Cooperative Highway Research Program, Washington, D.C.

ASTM. (2004). "Annual Book of ASTM Standards," Volume 04.02, American Society for Testing and Materials, West Conshohocken, PA.

Bairagi, N. K., Vidyadhara, H. S., and Ravande, K. (1990). "Mix Design Procedure for Recycled Aggregate Concrete," Construction and Building Materials, V. 4, No. 4, December 1990, pp. 188-193.

Kosmatka, S.H., Kerhoff, B., MacLeod, N.F., and McGrath, R.J. (2002). "Design and Control of Concrete Mixtures," EB101, 7th Canadian Edition, Cement Association of Canada, Ottawa, ON.

Chen, H.J., Yen, T., and Chen, K.H. (2003). "Use of Building Rubbles as Recycled Aggregate," Cement and Concrete Research, V.33, No.1, pp. 125-132.

Chini, A.R., Kuo, S.S., Armaghani, J.M., and Duxbury, J.P. (2001). "Test of Recycled Concrete Aggregate in Accelerated Test Track," Journal of Transportation Engineering, V.127, No.6, November/December 2001, pp. 486-492.

Chong, G.J., and Wrong, G.A. (2001). "Manual for Condition Rating of Rigid Pavements – Concrete Surface and Composite Distress Manifestations," SP-026, Ministry of Transportation, Ontario, Downsview, ON.

Craig, R.F. (1997). "Soil Mechanics," Sixth Edition, E&FN Spon, London, UK.

CSA International. (2000). "Concrete Materials and Methods of Concrete Construction," CSA A23.1-00, Canadian Standards Association, Mississauga, ON.

Cuttell, G.D., Snyder, M.B., Vandenbossche, J.M., and Wade, M.J. (2008). "Performance of Rigid Pavements Containing Recycled Concrete Aggregate," Transportation Research Record 1574, National Academy of Science, Washington, DC, 1997.

Darter, M., Khazanovich, L., Yu, T., and Mallela, J. (2005). "Reliability Analysis of Cracking and Faulting Predection Included in the New Mechanistic-Empirical Pavement Design Procedure," 05-1917, Transportation Research Board, 84th Annual Meeting, Washington, DC, January 9-13.

Dore, G., Tighe, S., and Hein, D. (2005). "Roadmap for the Calibration and Implementation of the Mechanistic-Empirical Design of New and Rehabilitated Pavement Structures," Transportation Association of Canada, Ottawa, ON.

Dosho, Y. (2005). "Application of Recycled Aggregate Concrete for Structural Concrete: A Recycling System for Concrete Waste," International Symposium on Sustainable Development of Cement, Concrete and Concrete Structures, Toronto, Ontario, October 5-7, pp. 459-478.

Farhey, D.N. (2007). "Instrumentation Specifics: Choices and Trade-Offs," Transportation Research Board, 86th Annual Meeting, Washington, DC, January 21-25.

Fathifazl, G., Razapur, A.G., Isgor, O.B., Abbas, A., Fournier, B., and Foo, S. (2008). "Fresh and Hardened Properties of Recycled Aggregate Concrete Proportioned by the Equivaletn Mortar Volume (EMV) Method," 2nd Canadian Conference on Effective Design of Structures, paper #95, McMaster University, Hamilton, ON.

FHWA. (2008). "TEA-21 Moving Americans into the 21st Century," Federal Highways Administration, www.fhwa.dot.gov/Tea21/index.htm accessed July 2008.

FHWA. (2007). "FHWA Recycled Materials Policy," Federal Highways Administration, www.fhwa.dot.gov/legsregs/directives/policy/recmatpolicy.htm, accessed July 2007.

FHWA. (2005). "DataPave Online," U.S. Department of Transportation, Federal Highways Administration, http://www.datapave.com, accessed May 14, 2005.

FHWA. (2004). "Transportation Applications Of Recycled Concrete Aggregate: FHWA State of the Practice National Review September 2004," U.S. Department of Transportation, Federal Highways Administration, Washington, DC.

FHWA. (1990). "Concrete Pavement Joints," Technical Advisory T 5040.30, U.S. Department of Transportation, Federal Highways Administration, Washington, DC.

Khaled A. Galal, K.G., and Chehab, G.R. (2005). "Considerations for Implementing the 2002 M-E Design Procedure Using a HMA Rehabilitated Pavement Section in Indiana," 05-1888, Transportation Research Board, 84th Annual Meeting, Washington, DC, January 9-13.

Gilbert, N. (2005). Personal email correspondence, Ontario Ministry of Transportation, Downsview, ON, January 5, 2005.

Gokce, A., Nagataki, S., Saeki, T., and Hisada, M. (2004). "Freezing and Thawing Resistance of Air-Entrained Concrete Incorporating Recycled Coarse Aggregate: The Role of Air Content in Demolished Concrete," Cement and Concrete Research, V. 34, No. 5, pp. 799-806.

Gomez-Soberon, J.M.V. (2002). "Porosity of Recycled Concrete with Substitution of Recycled Concrete Aggregate An Experimental Study," Cement and Concrete Research, V.32, No.8, pp. 1301-1311.

GTAA. (2007). "Reducing, Reusing and Recycling Terminal 2," Toronto Pearson Today: Terminal 2, Terminal 2 Commemorative Issue, Greater Toronto Airports Authority, Toronto, ON.

Hall, K.D., and Beam, S. (2005). "Estimation of Sensitivity of Design Variables for Rigid Pavement Analysis Using the Mechanistic-Empirical Design Guide," 05-0948, Transportation Research Board, 84th Annual Meeting, Washington, DC, January 9-13.

Hansen, T.C. (1990). "Recycled Concrete Aggregate and Fly Ash Produced Concrete Without Portland Cement," Cement and Concrete Research, V. 20, No.3, pp. 355-356.

Hansen, T.C., and Angelo, J.W. (1986). "Crushed Concrete Fines Recycled for Soil Modification Purposes," ACI Materials Journal, V. 83, No. 6, November-December 1986, pp. 983-987.

Hansen, T.C., and Boegh, E. (1985). "Elasticity and Drying Shrinkage of Recycled-Aggregate Concrete," ACI Materials Journal, V. 82, No. 5, September-October 1985, pp. 648-652.

Hansen, T.C., and Hedegard, S.E. (1984). "Properties of Recycled Aggregate Concretes as Affected by Admixtures in Original Concretes," ACI Journal, January-February 1984, pp. 21-26.

Torben C. Hansen, T.C., and Narud, H. (1983). "Recycled Concrete and Silica Fume Make Calcium Silicate Bricks," Cement and Concrete Research, V. 13, No.5, pp. 626-630.

Harrington, J. (2004). "States Achieve Recycling Success," Roads and Bridges, V.42, No.7.

Kamel, A.M.E.A., and Abou-Zeid, M.N. (2008). "Key Performance and Economic Considerations for Using Recycled Concrete Aggregate," 87th Annual Meeting, Transportation Research Board, National Academy of Science, 08-1073, Washington, DC.

Katz A. (2004). "Treatments for the Improvement of Recycled Aggregate," Journal of Materials in Civil Engineering, V. 16 No. 6, November/December 2004 pp. 597-603.

Katz, A. (2003). "Properties of Concrete Made with Recycled Aggregate from Partially Hydrated Old Concrete," Cement and Concrete Research, V. 343 No. 5, pp. 703-711.

Kerkhoff, B., and Siebel, E. (2001). "Properties of Concrete with Recycled Aggregates," Beton 2/2001, Verlag Bau + Technik, pp. 105-108.

Kuroda, Y., and Hashida, H. (2005). "A Closed-loop Concrete System on a Construction Site," International Symposium on Sustainable Development of Cement, Concrete and Concrete Structures, Toronto, Ontario, October 5-7, pp. 371-388.

Lane, B. (2008). "Life Cycle Costing and Alternative Bid Contracts in Ontario, Canada," Transportation Research Board, 87th Annual Meeting, National Academy of Science, Washington, DC, January 13-17.

Li, X., and Gress, D.L. (2006). "Mitigating Alkali-Silica Reaction in Concrete Containing Recycled Concrete Aggregate," Transportation Research Record 1979, National Academy of Science, Washington, DC.

Li, S., Nantung, T., and Jiang, Y. (2005). "Assessing Issues, Technologies, and Data Needs to Meet Traffic Input Requirements by M-E Pavement Design Guides: Implementation Initiatives," 05-1431, Transportation Research Board, 84th Annual Meeting, Washington, DC, January 9-13.

Lin, Y.H., Tyan, Y.Y., Chang, T.P., and Chang, C.Y. (2004). "An Assessment of Optimal Mixture for Concrete Made With Recycled Concrete Aggregates," Cement and Concrete Research, V. 34, No. 8, pp. 1373-1380.

Liu, J., Zollinger, D.G., Tayabji, S.D., and Smith, K.D. (2005). "Application of Reliability Concept in Concrete Pavement Rehabilitation Decision Making," 05-2202, Transportation Research Board, 84th Annual Meeting, Washington, DC, January 9-13.

Masood, A., Ahmad, T., Arif, M., and Mahdi, F. (2002). "Waste Management Strategies for Concrete" Environmental Engineering and Policy, V.3, pp. 15-18.

MacNaughton, I. (2004). "Ontario's Aggregates Are a Diminishing Resource," Ontario Hot Mix Producers Association Fall Seminar Presentations, December 8.

Mehta, P.K., and Monteiro, P.J.M. (2005). "Concrete: Microstructure, Properties, and Materials," 3rd Edition, McGraw-Hill Companies Inc., New York, NY.

Mehta, P.K. (2001). "Reducing the Environmental Impact of Concrete," Concrete International, V. 23, No.10, October 2001, pp. 61-66.

Mehta, P.K. (1999). "Concrete Technology for Sustainable Development," Concrete International, V. 21, No.11, November 1999, pp. 47-53.

Mesbah, H.A., and Buyle-Bodin, F. (1999). "Efficiency of Polypropylene and Metallic Fibres on Control of Shrinkage and Cracking of Recycled Aggregate Mortars," Construction and Building Materials, V. 13, No. 8, pp. 439-447.

Meyer, C. (2008). "The Greening of the Concrete Industry," 2nd Canadian Conference on Effective Design of Structures, paper #97, McMaster University, Hamilton, ON, 2008.

Miller, G. (2005). "Running Out of Gravel and Rock," Toronto Star, January 6, p. A22.

Douglas C. Montgomery, D.C. (2001). "Design and Analysis of Experiments," 5th Edition, John Wiley & Sons Inc., New York, NY.

MTO. (2004). "Laboratory Testing Manual," Ontario Ministry of Transportation, Downsview, ON.

Nagataki, S., Gokce, A., Saeki, T., and Hisada, M. (2004). "Assessment of Recycling Process Induced Damage Sensitivity of Recycled Concrete Aggregates," Cement and Concrete Research, V. 34, No. 6, pp.965-971.

Naik, T.R., and Moriconi, G. (2005). "Environmental-Friendly Durable Concrete Made with Recycled Materials for Sustainable Concrete Construction," International Symposium on Sustainable Development of Cement, Concrete and Concrete Structures, Toronto, Ontario, October 5-7, pp. 277-298.

Naik, T.R. (2002). "Greener Concrete Using Recycled Materials," Concrete International, V. 24, No.7, July 2001, pp. 45-49.

Nantung, T., Chehab, G., Newbolds, S., Galal, K., Li, S. and Kim, D.H. (2005). "Implementation Initiatives of the Mechanistic-Empirical Pavement Design Guides in Indiana," 05-1407, Transportation Research Board, 84th Annual Meeting, Washington, DC, January 9-13.

Neville, A.M. (1995). "Properties of Concrete," Fourth Edition, Prentice Hall, Essex, England.

Noguchi, T. (2005). "An Outline of Japanese Industrial Standards (JIS) as Related to Sustainability Issues," International Symposium on Sustainable Development of Cement, Concrete and Concrete Structures, Toronto, Ontario, October 5-7, 2005, pp. 407-422.

Karthik Obla, K., Kim, H., and Lobo, C. (2007). "Crushed Returned Concrete as Aggregates for New Concrete" Final Report to the RMC Research & Education Foundation, Project 05-13, National Ready Mixed Concrete Association.

Oikonomou, N.D. (2005). "Recycled Concrete Aggregates," Cement and Concrete Composites, V. 25, No. 2, pp. 315-318.

Olorunsogo, F.T., and Padayachee, N. (2002). "Performance of Recycled Aggregate Concrete Monitored by Durability Indexes," Cement and Concrete Research, V. 32, No. 2, 2002, pp. 179-185.

Ontario Provincial Standard Specification. (2005). "Material Specification for Aggregate – Concrete," OPSS 1002 (Draft 2), Ontario Ministry of Transportation, St. Catherines, ON.

Otsuki, N., Miyazato, S.I., and Yodsudjai, W. (2003). "Inluence of Recycled Aggregate in Interfacial Transition Zone, Strength, Chloride Penetration and Carbonation of Concrete," Journal of Materials in Civil Engineering, V.15, No.5, September/October 2003, pp. 443-451.

Ozbay, K., Jawad, D., Parker, N.A., and Hussain, S. (2004). "Life Cycle Cost Analysis: State-of0the-Practice vs State-of-the -Art," 04-3115, Transportation Research Board, 83rd Annual Meeting, Washington, DC, January 11-15.

Poon, C.S., Shui, Z.H. and Lam, L. (2004). "Effect of Microstructure of ITZ on Compressive Strength of Concrete Prepared with Recycled Aggregate," Construction and Building Materials, V. 18, No. 6, pp. 461-468.

Poon, C.S., Shui, Z.H., Lam, L., Fok, H., and Kou, S.C. (2003). "Influence of Moisture States of Natural and Recycled Aggregates on the Slump and Compressive Strength of Concrete," Cement and Concrete Research, V.34, No.1, 2004, pp. 31-36.

Poon, C.S., Kou, S.C., and Lam, L. (2002). "Use of Recycled Aggregates in Molded Concrete Bricks and Blocks," Construction and Building Materials, V. 16, No. 5, pp. 281-289.

Rangaraju, P.R., Amirkhanian, S., and Guven, S. (2008). "Life Cycle Cost Analysis for Pavement Type Selection," SCDOT Final Report, FHWA-SC-08-01, Clemenson, SC, 2008.

Rashwan, M.S., and AbouRizk, S. (1997). "The Properties of Recycled Concrete," Concrete International, V. 18, No.7, July 1997, pp. 56-60.

Ryu, J.S. (2002). "Improvement on Strength and Impermeability of Recycled Concrete Made from Crushed Concrete Coarse Aggregate," Journal of Materials Science Letters, V.21, pp. 1565-1567.

Saeed, A. (2006). "Evaluation, Design and Construction Techniques for Airfield Concrete pavement Used as Recycled Material for Base," Innovative pavement Research Foundation, IPRF-01-G-002-03-5, Skokie, IL.

Sagoe-Crentsil, K.K., Brown, T., and Taylor, A.H. (2001). "Performance of Concrete Made with Commercially Produced Coarse Recycle Concrete Aggregate," Cement and Concrete Research, V. 31, No. 5, pp. 707-712.

Salem, R.M., Burdette, E.G., and Jackson, N.M. (2003). "Resistance to Freezing and Thawing of Recycled Aggregate Concrete," ACI Materials Journal, V. 100, No. 3, May-June 2003, pp. 216-221.

Salem, R.M., and Burdette, E.G. (1998). "Role of Chemical and Mineral Admixtures on Physical Properties and Frost-Resistance of Recycled Aggregate Concrete," ACI Materials Journal, V. 95, No. 5, September-October 1998, pp. 558-563.

Seow, K. (2005). "Old Terminal 1 Decommissioning and Demolition," Annual Conference of the Transportation Association of Canada, Calgary, AB, 2005.

Shayan A., and Xu, A. (2003). "Performance and Properties of Structural Concrete Made with Recycled Concrete Aggregate," ACI Materials Journal, V. 100, No. 5, September-October 2003, pp. 371-380.

Smith, M. (2008). "Life-Cycle Cost Analysis in Pavement Type Selection," Wisconsin Asphalt Pavement Association Conference, Atlanta, GA.

Smith, J.T., and Tighe, S.L. (2004). "Assessment of Overlay Roughness in the LTPP: A Canadian Case Study," 04-2502, Transportation Research Board Conference Proceedings, Washington, D.C.

Soilmoisture. (1998). "Concrete and Trase TDR," Product Information, Soilmoisture Equipment Corp., Santa Barbara, CA.

St Marys Cement. (2007). "General Use Portland Cement," Product Information, St Marys Cement Group, Toronto, ON.

TAC. (1997). "Pavement Design and Management Guide," Transportation Association of Canada, Ottawa, ON.

Tanesi, J., Kutay, M.E., Abbas, A., and Meininger, R. (2007). "Effect of CTE Variability on Concrete Pavement Performance as Predicted Using the Mechanistic-Empirical Pavement Design Guide," Transportation Research Board, 86th Annual Meeting, Paper No. 07-2488, Washington, D.C.

Tavakoli, M. and Soroushian, P. (1996a). "Strengths of Recycled Concrete Made Using Field-Demolished Concrete as Aggregate," ACI Materials Journal, V. 93, No. 2, March-April 1996, pp. 182-190.

Tavakoli, M. and Soroushian, P. (1996b). "Drying Shrinkage Behavior of Recycled Aggregate Concrete," Concrete International, V. 18, No.11, November 1996, pp. 58-61.

Topcu, I.B., and Sengel, S. (2003). "Properties of Concretes Produced with Waste Concrete Aggregate," Cement and Concrete Research, V.34, No.8, pp.1307-1312.

Topcu, I.B. (1997). "Physical and Mechanical Properties of Concrete Produced with Waste Concrete," Cement and Concrete Research, V. 27, No.12, pp. 1817-1823.

Topcu, I.B., and Guncan, N.F. (1995). "Using Waste Concrete as Aggregate," Cement and Concrete Research, V. 25, No.7, 1995, pp. 1385-1390.

Transtec. (2005). "HYPERPAV II," Software Version 3.00.0061, The Transtec Group, Austin, TX.

Turley, W. (2003). "On the road: acceptance of recycled aggregates by state DOTs is slow but making progress – Roadbuilding Trends," C&D Recycler, September-October, 2003.

USGBC. (2005). "LEED for New Construction," Version 2.2, U.S. Green Building Council, Washington, DC.

Walls III, J., and Smith, M.R., (1998). "Life-Cycle Cost Analysis in Pavement Design – Interim Technical Bulletin," FHWA-SA-98-097, Washington, DC.

West, J. (2005). "Effect of Temperature on Structural Performance of Stainless Steel Reinforcement, " Final Report for the Ontario Ministry of Transportation, University of Waterloo, ON.

Yang, S., Kim, N., Kim, J., and Park, J. (2003). "Experimental Measurement of Concrete Thermal Expansion," Journal of the Eastern Asia Society for Transportation Studies, V.5, October 2003, pp. 1035-1048.

Yu, H.T., and Khazanovich, L. (2005). "Use of Magnetic Tomography to Evaluate Dowel Placement," FHWA-IF-06-006, Federal Highways Administration, Office of Pavement Technology, Washington, D.C.

Zaharieva, R., Buyle-Bodin, F., and Wirquin, E. (2004). "Frost Resistance of Recycled Aggregate Concrete," Cement and Concrete Research, V. 34, No.10, pp. 1927-1932.

Zaharieva, R., Buyle-Bodin, F., Skoczylas, F., and Wiequin, E. (2003). "Assessment of the Surface Properties of Recycled Aggregate Concrete," Cement and Concrete Composites, V. 25, No. 2, pp. 223-232.

# Appendix A

# Design Tables

**CBR = 2.5, Asphalt Stabilized OGDL**

| Traffic | ADTT | Concrete Flexural Strength ($M_R$) | | | |
|---|---|---|---|---|---|
| | (2-way) | 3.5 MPa | 5.0 MPa | 6.5 MPa | 8.0 MPa |
| Residential | 2 | 127 | 101.6 | 101.6 | 101.6 |
| | 10 | 139.7 | 114.3 | 101.6 | 101.6 |
| | 25 | 139.7 | 114.3 | 101.6 | 101.6 |
| Collector | 100 | 165.1 | 127 | 114.3 | 101.6 |
| | 200 | 165.1 | 139.7 | 114.3 | 101.6 |
| | 400 | 165.1 | 139.7 | 114.3 | 114.3 |
| Minor Arterial | 500 | 190.5 | 152.4 | 139.7 | 127 |
| | 1000 | 190.5 | 165.1 | 139.7 | 127 |
| | 1500 | 203.2 | 165.1 | 139.7 | 139.7 |
| Major Arterial | 2000 | 215.9 | 177.8 | 152.4 | 139.7 |
| | 3000 | 215.9 | 177.8 | 152.4 | 152.4 |
| | 5000 | 215.9 | 177.8 | 165.1 | 152.4 |

**CBR = 2.5, Cement Treated OGDL**

| Traffic | ADTT | Concrete Flexural Strength ($M_R$) | | | |
|---|---|---|---|---|---|
| | (2-way) | 3.5 MPa | 5.0 MPa | 6.5 MPa | 8.0 MPa |
| Residential | 2 | 127 | 101.6 | 101.6 | 101.6 |
| | 10 | 139.7 | 114.3 | 101.6 | 101.6 |
| | 25 | 139.7 | 114.3 | 101.6 | 101.6 |
| Collector | 100 | 152.4 | 127 | 114.3 | 101.6 |
| | 200 | 165.1 | 127 | 114.3 | 101.6 |
| | 400 | 165.1 | 139.7 | 114.3 | 114.3 |
| Minor Arterial | 500 | 190.5 | 152.4 | 127 | 127 |
| | 1000 | 190.5 | 152.4 | 139.7 | 127 |
| | 1500 | 190.5 | 165.1 | 139.7 | 139.7 |
| Major Arterial | 2000 | 215.9 | 177.8 | 152.4 | 139.7 |
| | 3000 | 215.5 | 177.8 | 152.4 | 152.4 |
| | 5000 | 215.9 | 177.8 | 165.1 | 152.4 |

**CBR = 2.5, Non-treated OGDL**

| Traffic | ADTT | Concrete Flexural Strength ($M_R$) | | | |
|---|---|---|---|---|---|
| | (2-way) | 3.5 MPa | 5.0 MPa | 6.5 MPa | 8.0 MPa |
| Residential | 2 | 127 | 101.6 | 101.6 | 101.6 |
| | 10 | 139.7 | 114.3 | 101.6 | 101.6 |
| | 25 | 139.7 | 114.3 | 101.6 | 101.6 |
| Collector | 100 | 165.1 | 139.7 | 114.3 | 101.6 |
| | 200 | 165.1 | 139.7 | 114.3 | 101.6 |
| | 400 | 177.8 | 139.7 | 127 | 114.3 |
| Minor Arterial | 500 | 190.5 | 165.1 | 139.7 | 127 |
| | 1000 | 203.2 | 165.1 | 139.7 | 127 |
| | 1500 | 203.2 | 165.1 | 139.7 | 139.7 |
| Major Arterial | 2000 | 215.9 | 177.8 | 152.4 | 139.7 |
| | 3000 | 215.9 | 177.8 | 152.4 | 152.4 |
| | 5000 | 228.6 | 177.8 | 165.1 | 152.4 |

**CBR = 5, Asphalt Stabilized OGDL**

| Traffic | ADTT | Concrete Flexural Strength ($M_R$) | | | |
|---|---|---|---|---|---|
| | (2-way) | 3.5 MPa | 5.0 MPa | 6.5 MPa | 8.0 MPa |
| Residential | 2 | 127 | 101.6 | 101.6 | 101.6 |
| | 10 | 127 | 101.6 | 101.6 | 101.6 |
| | 25 | 139.7 | 114.3 | 101.6 | 101.6 |
| Collector | 100 | 152.4 | 127 | 114.3 | 101.6 |
| | 200 | 165.1 | 127 | 114.3 | 101.6 |
| | 400 | 165.1 | 127 | 114.3 | 114.3 |
| Minor Arterial | 500 | 190.5 | 152.4 | 127 | 114.3 |
| | 1000 | 190.5 | 152.4 | 139.7 | 127 |
| | 1500 | 190.5 | 152.4 | 139.7 | 127 |
| Major Arterial | 2000 | 203.2 | 165.1 | 152.4 | 139.7 |
| | 3000 | 215.9 | 177.8 | 152.4 | 139.7 |
| | 5000 | 215.9 | 177.8 | 152.4 | 152.4 |

**CBR = 7.5, Asphalt Stabilized OGDL**

| Traffic | ADTT (2-way) | Concrete Flexural Strength ($M_R$) 3.5 MPa | 5.0 MPa | 6.5 MPa | 8.0 MPa |
|---|---|---|---|---|---|
| Residential | 2 | 114.3 | 101.6 | 101.6 | 101.6 |
| | 10 | 127 | 101.6 | 101.6 | 101.6 |
| | 25 | 139.7 | 114.3 | 101.6 | 101.6 |
| Collector | 100 | 152.4 | 127 | 101.6 | 101.6 |
| | 200 | 152.4 | 127 | 114.3 | 101.6 |
| | 400 | 165.1 | 127 | 114.3 | 101.6 |
| Minor Arterial | 500 | 177.8 | 152.4 | 127 | 114.3 |
| | 1000 | 190.5 | 152.4 | 127 | 127 |
| | 1500 | 190.5 | 152.4 | 139.7 | 127 |
| Major Arterial | 2000 | 203.2 | 165.1 | 139.7 | 139.7 |
| | 3000 | 203.2 | 165.1 | 152.4 | 139.7 |
| | 5000 | 203.2 | 165.1 | 152.4 | 152.4 |

**CBR = 10, Asphalt Stabilized OGDL**

| Traffic | ADTT (2-way) | Concrete Flexural Strength ($M_R$) 3.5 MPa | 5.0 MPa | 6.5 MPa | 8.0 MPa |
|---|---|---|---|---|---|
| Residential | 2 | 114.3 | 101.6 | 101.6 | 101.6 |
| | 10 | 127 | 101.6 | 101.6 | 101.6 |
| | 25 | 127 | 101.6 | 101.6 | 101.6 |
| Collector | 100 | 152.4 | 127 | 101.6 | 101.6 |
| | 200 | 152.4 | 127 | 101.6 | 101.6 |
| | 400 | 152.4 | 127 | 114.3 | 101.6 |
| Minor Arterial | 500 | 177.8 | 139.7 | 127 | 114.3 |
| | 1000 | 177.8 | 152.4 | 127 | 127 |
| | 1500 | 190.5 | 152.4 | 139.7 | 127 |
| Major Arterial | 2000 | 203.2 | 165.1 | 139.7 | 139.7 |
| | 3000 | 203.2 | 165.1 | 152.4 | 139.7 |
| | 5000 | 203.2 | 165.1 | 152.4 | 152.4 |

**CBR = 15, Asphalt Stabilized OGDL**

| Traffic | ADTT | Concrete Flexural Strength ($M_R$) | | | |
|---|---|---|---|---|---|
| | (2-way) | 3.5 MPa | 5.0 MPa | 6.5 MPa | 8.0 MPa |
| Residential | 2 | 114.3 | 101.6 | 101.6 | 101.6 |
| | 10 | 127 | 101.6 | 101.6 | 101.6 |
| | 25 | 127 | 101.6 | 101.6 | 101.6 |
| Collector | 100 | 152.4 | 114.3 | 101.6 | 101.6 |
| | 200 | 152.4 | 127 | 101.6 | 101.6 |
| | 400 | 152.4 | 127 | 114.3 | 101.6 |
| Minor Arterial | 500 | 177.8 | 139.7 | 127 | 114.3 |
| | 1000 | 177.8 | 152.4 | 127 | 127 |
| | 1500 | 177.8 | 152.4 | 127 | 127 |
| Major Arterial | 2000 | 203.2 | 165.1 | 139.7 | 139.7 |
| | 3000 | 203.2 | 165.1 | 139.7 | 139.7 |
| | 5000 | 203.2 | 165.1 | 152.4 | 139.7 |

**CBR = 20, Asphalt Stabilized OGDL**

| Traffic | ADTT | Concrete Flexural Strength ($M_R$) | | | |
|---|---|---|---|---|---|
| | (2-way) | 3.5 MPa | 5.0 MPa | 6.5 MPa | 8.0 MPa |
| Residential | 2 | 114.3 | 101.6 | 101.6 | 101.6 |
| | 10 | 127 | 101.6 | 101.6 | 101.6 |
| | 25 | 127 | 101.6 | 101.6 | 101.6 |
| Collector | 100 | 139.7 | 114.3 | 101.6 | 101.6 |
| | 200 | 152.4 | 114.3 | 101.6 | 101.6 |
| | 400 | 152.4 | 127 | 101.6 | 101.6 |
| Minor Arterial | 500 | 177.8 | 139.7 | 127 | 114.3 |
| | 1000 | 177.8 | 139.7 | 127 | 114.3 |
| | 1500 | 177.8 | 152.4 | 127 | 127 |
| Major Arterial | 2000 | 190.5 | 152.4 | 139.7 | 127 |
| | 3000 | 203.2 | 165.1 | 139.7 | 139.7 |
| | 5000 | 203.2 | 165.1 | 152.4 | 139.7 |

**CBR = 30, Asphalt Stabilized OGDL**

| Traffic | ADTT | Concrete Flexural Strength ($M_R$) | | | |
|---|---|---|---|---|---|
| | (2-way) | 3.5 MPa | 5.0 MPa | 6.5 MPa | 8.0 MPa |
| Residential | 2 | 114.3 | 101.6 | 101.6 | 101.6 |
| | 10 | 114.3 | 101.6 | 101.6 | 101.6 |
| | 25 | 127 | 101.6 | 101.6 | 101.6 |
| Collector | 100 | 139.7 | 114.3 | 101.6 | 101.6 |
| | 200 | 139.7 | 114.3 | 101.6 | 101.6 |
| | 400 | 152.4 | 127 | 101.6 | 101.6 |
| Minor Arterial | 500 | 165.1 | 139.7 | 114.3 | 101.6 |
| | 1000 | 177.8 | 139.7 | 127 | 114.3 |
| | 1500 | 177.8 | 139.7 | 127 | 114.3 |
| Major Arterial | 2000 | 190.5 | 152.4 | 139.7 | 127 |
| | 3000 | 190.5 | 152.4 | 139.7 | 127 |
| | 5000 | 190.5 | 165.1 | 139.7 | 139.7 |

# Appendix B

# Preconstruction Meeting Summaries

**Meeting #1**

March 8, 2007 - UW/CAC/Dufferin Conference Call

Materials: Since stockpiles of material to be recycled often contain both asphalt and concrete, only pure waste concrete should be set aside for crushing. The minimum amount of aggregate required is 150 tonne, however 200 tonne would be preferred. Potential companies who may be a source of RCA are Capital paving, Cox Construction, Murray Group, and Steed and Evans.

Design: A 200 mm JPCP was determined to be too thin for the automatic dowel-bar inserter. The MTO recommends using a 220-250 mm surface since the extra cost is not significant and it will greatly improve performance. Non-treated open graded drainage layer (OGDL) was recommended for use as a base. The design would need to be rechecked with the MTO and others.

Equipment: The pavement slab width will depend on the existing setup of the paver. Since it is difficult to change the setup of the paver for each texture and changes may produce a non-uniform surface, it is best to use the paver at the existing set up. An adaptor kit will be required for the paver to produce the desired tine. The adaptor kit can potentially be borrowed from CoCo Paving.

Schedule: The Region of Waterloo preferred that construction take place in May, however, Dufferin felt that in order to give time for mix development mid- to late-June would be a more realistic time frame. James from UW will work with Jai from Dufferin to develop the mix designs. The construction of the test sections can be completed within a week.

Additional Work: The construction of the test sections is a potential opportunity to look at the effect of dowel bar misalignment. Follow up will be done with the MTO on this.

**Meeting #2**

April 17, 2007 – UW/CAC/Dufferin (at Dufferin Construction)

The premise of placing RCA test sections is to showcase new technology and evaluate the performance.

Materials

Steed and Evans will crush the RCA and donate the material to the project. Another location will need to be used for screening. The RCA used in the project will originate from used sidewalks and curbs and will be 4.75 mm to 19mm in size. The RCA will be combined with virgin aggregate of 4.75mm to 40mm.

Design

Four 50 m test sections containing varying amounts of RCA (0%, 15%, 30%, and 50%) will be placed. The pavement structure will have a 450 mm granular base, 100 mm asphalt stabilized open graded drainage layer (ODGL), and 250 mm JPCP. Each section will have a pavement thickness of 250 mm and a pavement width of 8.5 m. The thickness of 250 mm was selected to accommodate the cover requirements of the automatic dowel bar inserter and to reduce vibrator trails. There are expected to be some difficulties creating longitudinal and transverse tining. The CAC feels longitudinal tining is the most important.

Equipment

A premix plant is preferred to provide consistency in the mix. The concrete will be placed with a double width, slip-form paver. Texturization will follow behind the paver. Dufferin will look after organizing the equipment.

Schedule

The preliminary mix designs will require 1-2 days. About ½ day will be required to do the final granular base grading prior to the site survey to set the string line for the paver.

Instrumentation

The sensor cable should be placed below the granular base. Sensors should be placed below the dowel baskets when possible. If necessary blockouts could potentially be used for sensors needing to be placed in the top half of the pavement. Sensors will be brought to next meeting for further discussion on placement.

Additional Items

The MTO representative is concerned about the feasibility of a dowel bar misalignment study in the test sections due to the size of the test track and the cost. If there is a dowel bar misalignment study then he would like to see the results presented in a published paper.

Action Items

The following are items that require further information:

- Tim Wilson will calculate a construction estimate.
- Jai Tiwari and Susan Tighe will confirm the source of aggregate.
- Jai Tiwari and James Smith will develop the mix designs
- John Zavarella will organize the equipment.
- James Smith will plan the instrumentation.
- Susan Tighe will provide information on dowel bars.

**Meeting #3**

May 4, 2007 – UW/CAC/Dufferin (at Dufferin Construction)

Materials

The Steed and Evans RCA stockpile at Head Office is acceptable; however, the stockpile at the Hiedleburg plant is not suitable for this project. Steed and Evans will sieve the RCA. The sources of virgin aggregate are as follows: 40 mm from Dufferin's Acton Pit, 19 mm form Dufferin's Milton Pit, and sand from Dufferin's Forwell pit.

Design

The length of the test section is approximately 170m as measured from the guardrail to the existing asphalt. The joint spacing will be based on the MTO specification of 3.7m, 4.5m, 4m,4.3m, and then repeated.

Schedule

Crushing of the RCA should begin within the next two weeks. Since the best date for Dufferin is the week of July 9, site preparation should occur the week before. The 14-day compressive strengths should be available mid-June. The estimated date to open the slab to traffic would be July 16-17 assuming that 80% of 28-day strength is achieved. Dufferin is also available mid-August or September.

Equipment

CoCo paving has not responded to the request to borrow their longitudinal tining kit.

Instrumentation

The strain gauge, vertical extensometer, relative humidity probe, and moisture probe were taken to the meeting. The inter-panel extensometer was not available at the time of the meeting. Strain gauges will be fastened to a chair structure and mound with concrete and then placed between the vibrators of the paver. The vertical extensometer, relative humidity probes, and TDR moisture probes can be placed below the dowel baskets. The

inter-panel extensometer will require a blockout. James Smith and John Zavarella. will provide a design for the chair and blockouts.

Additional Work

The dowel bar misalignment work will not to be done since 3-4 slabs can be "locked up" before there is a problem. The impact of dowel bar side shift will be looked at in the test sections since side shift leads too "horseshoe" cracking. To study side shift, the dowel baskets are to be placed at the specified intervals and the location of the saw cut will be moved to provide the side shift.

Funding

Dufferin believes the maximum tax credit they can recover is 20%. There is potential to get discounts from suppliers if they wave their mark-up. The green municipal fund program may be an additional source of funding. Since the concrete testing can be done inhouse at Dufferin, funds will not be required to hire a laboratory.

Action Items

The following are items that require further information:

- Tim Wilson will provide a construction estimate and letter for the University of Waterloo.
- James Smith and Jai Tiwari will review the aggregate source.
- James Smith and Jai Tiwari will provide the mix designs.
- John Zavarella will organize the equipment.
- Wayne Lazzarato and Susan Tighe will provide information for the dowel bar study.
- Sources of funding will be reviewed by Wayne Lazzarato, Susan Tighe, and Rico Fung.

**Meeting #4**

May 28, 2007 – UW/CAC/Dufferin (at Dufferin Construction)

Materials

The concrete sand from the Blair pit will be used in the design and is approved for structural and pavement use. The Forwell plant is currently using St. Mary's cement. St. Mary's cement has a slower initial strength gain over the first 21 days compared to Dufferin's St. Lawrence cement.

Design

Preliminary testing will be started on mixes using cement content of 315, 330, and 345 kg/m3 respectively. It is projected that the desired design strength will be achieved with a cement content of 330 kg/m3 for all RCA percentages being tested. Also, the desired design strength should be achieved with a cement content of 315 kg/m3 when combined with 0% or 15% RCA. A 25% slag replacement by mass will be used in all mixes.

Equipment

CoCo Pavings longitudinal tining kit is available to use. CoCo Paving's mechanic will require one day to install the tining kit on Dufferin's texture/cure machine.

Schedule

The landfill requires that the test sections be open to traffic by July 1. If this window of opportunity is missed then paving will not occur. In order to accommodate, Dufferin can push back the start of the HWY 410 job by a week. The new schedule will be set as follows:

June 4 – layout,

June 5 – grade crew,

June 6 – Line crew,

June 7 – ODGL,

June 8 – paver setup,

June 11 – float day,

June 12 – start paving,

June 13 – change tining equip and reset for second day of paving,

June 14 – paving day 2, and

June 15 – float day

Instrumentation

The sensors have not been ordered yet and will require 3-4 weeks. The CAC will look into getting a maturity sensor from The Transtec Group. A request for a rush on the sensors from Hoskin/RST will be made. Also, availability of sensors through other manufactures (Slope Indicator, CTL Group…) will be explored in order to meet the tight time frame.

Funding

Steed and Evans are donating the aggregate and screening. CoCo paving is donating the longitudinal tine kit. Dufferin is discounting the price of the equipment, materials and labour to the actual cost price, which is estimated at $185,000. If Dufferin receives a 20% research and development credit for the cost of this project (not including labour) then the University of Waterloo will have a corresponding reduction in their bill.

**Meeting #5**

May 31, 2007 – UW/CAC/Dufferin (Conference Call)

Contacts

Dufferin Site Supervisor is Jerry Armstrong (416-984-4480).

Landfill Site Supervisor is Dave McCaughan (519-897-3009). Note: the site is locked every night.

Materials and Design

The 12 trial mixes have been batched, cylinders demolded and are curing. The 7-day compressive strengths will be available next week. Stantec completed falling weight deflectometer (FWD) testing on the existing 450mm granular base and the results exceeded the estimated strength requirements in the design. The test track area where the 30% RCA mix will be placed had a weaker FWD result than other areas of the test track; however, it still exceeded the estimated strength requirements.

St. Mary's cement will reach or exceed the design strength at 28 days as long as 65-70% of the compressive strength is reached by 21 days.

Construction

The distance from the guardrail to the existing asphalt has been confirmed at 172m. Dufferin will remove approximately 8m of the existing asphalt to allow for a transition zone. Construction Testing Asphalt Lab Ltd. Has completed the asphalt stabilized OGDL mix design. A 2% crossfall is required on the pavement from the centreline. The concrete haul time from the Forwell plant to the test track is approximately 20 minutes.

Equipment

The fresh concrete will be transported in ready mix trucks since dump trucks are unavailable. The longitudinal tines will be about 0.5m shorter than the full pavement width.

Schedule

The schedule is unchanged from the last meeting. There is a potential to move the second day of paving to Wednesday depending on the success of the first day.

Instrumentation

The maturity sensors have been shipped by the Transtec Group and will arrive in the next couple of days. Hoskin/RST will be able to deliver the strain gauges, vertical extensometer, and inter-panel extensometer in time for construction. The relative humidity and TDR moisture probes cannot be delivered before construction begins and will not be retrofitted at a later time.

Additional Work

The dowel bar side shift study parameters will be confirmed with the MTO.

**Meeting #6**

June 11, 2007 – Onsite Construction

Initially there was a quick site tour and an area for the concrete truck washout was identified.

Construction

All tie dowel baskets are to be cut to improve MIT scan results. The pins to secure the load transfer baskets are anchored at every second dowel on both sides.

The section lengths were revised based on a total area of 180m (0% - 30m, 15% - 50m, 30% - 50m, 50% - 50m). These lengths are estimates, as the paver will continue to move forward so there will be no hard edge.

The concrete will arrive at the test track with 40mm slump.

The dowel bar side shift distances of 0, 25, 50, 75, 100mm will be tested. The MTO rejects dowel bar side shift distances greater than 50mm. A construction drawing will be made by the University of Waterloo to assist in the dowel bar placement. Dowel bar offsets will be placed as follows: 0mm offset for the first 10 joints, 25mm offset for the next 6 joints, 50mm offset for the next 6 joints, 75mm offset for next 6 joints, 100mm offset for next 6 joints, and 0mm offset for the remaining 8 joints.

Instrumentation

The maturity sensors from the Transtec Group and the strain, vertical extensometer, inter-panel extensometer, and maturity sensors from Hoskin/RST have arrived. The datalogger and remote multiplexers will arrive about 2-3 weeks after construction and will be installed at that time.

# Appendix C

# Pavement Distress

**Ravelling and Coarse Aggregate Loss**

| | |
|---|---|
| Very Slight | Barley noticeable. |
| Slight | Noticeable loss of pavement material. |
| Moderate | Pavement has pockmarked appearance, with pockmarks fairly well spaced. Shallow disintegration of pavement surface. An open-texture look. |
| Severe | Pavement has pockmarked appearance, with pockmarks closely spaced. Disintegration with small, shallow potholes. |
| Very Severe | Surface has a raveled and disintegrated appearance with large, shallow potholes. |

**Polishing**

| | |
|---|---|
| Very Slight | Barely noticeable. |
| Slight | Noticeable dull finish. |
| Moderate | Distinctive dull finish. |
| Severe | Glossy mirror finish. |
| Very Severe | Surface has a highly polished appearance. |

**Scaling**

| | |
|---|---|
| Very Slight | Barely noticeable. |
| Slight | Noticeable. |
| Moderate | An open-texture look, as with raveling, by very shallow. |
| Severe | Disintegration in closely spaced, shallow patched. |
| Very Severe | Disintegration in shallow large patched. |

**Potholing**

| | |
|---|---|
| Very Slight | Barely noticeable. Pothole resembles a pop-out of coarse aggregate. |
| Slight | Disintegration of surrounding materials. |
| Moderate | Pothole much wider (<75 mm) than a pop-out of coarse aggregate and deeper (< 75 mm) |
| Severe | Pothole 75 – 150 mm wide and 75 – 150 mm deep. |
| Very Severe | Pothole over 150 mm winde and over 150 mm deep. Interferes with rideability. |

**Joint and Cracking Spalling**

| | |
|---|---|
| Very Slight | Small crack(s) with very small fractures. |
| Slight | Small crack(s) within 75 mm of the joint or crack, with a few small pieces missing or loosened from the fracture area. |
| Moderate | Spalling extends more than 75 mm of the joint or crack, with many small pieces missing or loosened from the fracture area. |
| Severe | Spalling extends more than 75 mm of the joint or crack, with larger pieces missing or loosened from the fracture area. Temporary patching may have been placed, |
| Very Severe | Large potholes are at the places along the joint or crack, perhaps causing tire damage. |

**Faulting**

| | |
|---|---|
| Very Slight | Barely noticeable (<3 mm). |
| Slight | 3 – 6 mm. |
| Moderate | 7 – 12 mm. |
| Severe | 13 – 19 mm. |
| Very Severe | > 19 mm. |

**Distortion**

| | |
|---|---|
| Very Slight | Barely noticeable swaying of vehicle. |
| Slight | Barely noticeable pitch and role, and a jarring bump or drop of vehicle. |
| Moderate | Noticeable pitch and role, and a harsh bump or jarring of vehicle. |
| Severe | A continuous pitch and roll, and a hard jarring bump or drop of vehicle. The driver always must anticipate distortion ahead. |
| Very Severe | Continuous distortion, making the driver feel it necessary to reduce spped from the posted speed limit. |

**Sealant Loss**

| | |
|---|---|
| Very Slight | Barely popped out or breaking. |
| Slight | Sealant broken and beginning to pull out (up to 30 cm) |
| Moderate | Sealant broken and pulled out by up to 50% of its length. |
| Severe | Sealant broken and pulled out by up to 58% of its length. |
| Very Severe | Sealant is completely broken and pulled out by more than 80% of its length. It is ineffective as a sealant. |

**Joint Failure**

| | |
|---|---|
| Severe | Pavement fractures into blocks, with multiple cracks and missing pieces along both sides of the joint. Distortion is noticeable. |
| Very Severe | Pavement fractures into large blocks, with multiple cracks and missing pieces along both sides of the joint, extending a considerable distance (2 – 3 m ) from the joint. Distortion is noticeable. |

**Longitudinal and Meandering Cracking**

| | |
|---|---|
| Very Slight | < 3 mm wide. |
| Slight | 3 – 12 mm wide. |
| Moderate | 13 – 19 mm wide (with or without spalling and faulting). |
| Severe | 20 – 25 mm wide (with spalling and faulting). |
| Very Severe | > 25 mm (with spalling and faulting). |

**Diagonal, Corner, and Edge Crescent**

| | |
|---|---|
| Very Slight | < 3 mm wide. |
| Slight | 3 – 12 mm wide. |
| Moderate | 13 – 19 mm wide (with or without spalling and faulting). |
| Severe | 20 – 25 mm wide (with spalling and faulting). |
| Very Severe | > 25 mm wide (with spalling and faulting). |

**"D" Cracking**

| | |
|---|---|
| Very Slight | < 3 mm wide. |
| Slight | 3 – 12 mm wide. |
| Moderate | 13 – 19 mm wide, or multiple cracks < 12 mm wide. |
| Severe | 20 – 25 mm wide, or multiple cracks 13 – 19 mm wide. |
| Very Severe | > 25 mm wide, or multiple cracks 20 – 25 mm wide. |

**Transverse Cracking**

| | |
|---|---|
| Very Slight | < 3 mm wide. |
| Slight | 3 – 12 mm wide. |
| Moderate | 13 – 19 mm wide (with or without spalling and faulting). |
| Severe | 20 – 25 mm wide (with spalling and faulting). |
| Very Severe | > 25 mm wide (with spalling and faulting). |

# Appendix D

# Datalogger Program

```
'CR1000 Series Datalogger

'Program name: WO Q08619 4 remote mux

'Date written: 22/06/07 DWP RST Inst

'Modifications: corrected Sub convert (matching serial number and channel) and increasing mux delay to 15 (to account for longer cable lengths)

'\\\\\\\\\\\\\\\\\\\\\\\\\ DECLARATIONS /////////////////////////

Public VWSG(24), VWPAVE(8), VWEXT(8)

Public SGTH(24), PAVETH(8), EXTTH(8)

Public Pave_Disp(8), Ext_Disp(8)

Public Bat_V

Public Int_Temp

Public Flag(4) as boolean

public i1


Units VWSG()=uE

Units Ext_Disp()=mm

Units Pave_Disp()=mm

'\\\\\\\\\\\\\\\\\\\\\\\\\ OUTPUT SECTION /////////////////////////

DataTable(DATA,-1,-1)' >>

        CardOut (0 ,-1)

        Sample(24,VWSG(),IEEE4)

        Sample(8,Pave_Disp(),IEEE4)

        Sample(8,Ext_Disp(),IEEE4)

        Sample(8,VWPAVE(),IEEE4)

        Sample(8,VWEXT(),IEEE4)

        Sample(24,SGTH(),FP2)

        Sample(8,PAVETH(),FP2)

        Sample(8,EXTTH(),FP2)
```

```
        Sample(1, Bat_V, FP2)
        Sample(1, Int_Temp, FP2)
EndTable

Sub VW_SG
        Delay(0,5,MSEC)
        VibratingWire(VWSG(i1),1,mV7_5,1,Vx1,400,1200,250,-1,20000,100,0,3405,0)        ':read Vibrating Wire Piezometer
        BRHalf(SGTH(i1), 1, mV2500, 2, VX1, 1, 2500, False, 10000, 250, 2.5, 0) ':read 3K Thermistors
        SGTH(i1)=-104.78+378.11*SGTH(i1)+-611.59*SGTH(i1)^2+544.27*SGTH(i1)^3+-240.91*SGTH(i1)^4+43.089*SGTH(i1)^5
        ':linearize 3K thermistors
EndSub

Sub VW_PAVE
        Delay(0,5,MSEC)
        VibratingWire(VWPAVE(i1),1,mV7_5,1,Vx1,1600,2800,200,-1,20000,150,0,1,0)        ':read Vibrating Wire Piezometer
        BRHalf(PAVETH(i1), 1, mV2500, 2, VX1, 1, 2500, False, 10000, 250, 2.5, 0) ':read 3K thermistors
        PAVETH(i1)=-104.78+378.11*PAVETH(i1)+-611.59*PAVETH(i1)^2+544.27*PAVETH(i1)^3+-240.91*PAVETH(i1)^4+43.089*PAVETH(i1)^5
        ':linearize 3K thermistors
EndSub

Sub VW_EXT
        Delay(0,5,MSEC)
        VibratingWire(VWEXT(i1),1,mV7_5,1,Vx1,1800,3200,200,-1,20000,200,0,1,0)':read Vibrating Wire Piezometer
        BRHalf(EXTTH(i1), 1, mV2500, 2, VX1, 1, 2500, False, 10000, 250, 2.5, 0) ':read 3K thermistors
        EXTTH(i1)=-104.78+378.11*EXTTH(i1)+-611.59*EXTTH(i1)^2+544.27*EXTTH(i1)^3+-240.91*EXTTH(i1)^4+43.089*EXTTH(i1)^5
        ':linearize 3K thermistors
```

```
EndSub

Sub convert
        'convert to displacement - serial number must match channel
        Pave_Disp(1)=(2.416-VWPAVE(1))*2.932' ENTER Pavement VM0220 CAL FACTORS *
        Pave_Disp(2)=(2.504-VWPAVE(2))*2.990' ENTER Pavement VM0221 CAL FACTORS *
        Pave_Disp(3)=(2.699-VWPAVE(3))*2.932' ENTER Pavement VM0218 CAL FACTORS *
        Pave_Disp(4)=(2.667-VWPAVE(4))*2.949' ENTER Pavement VM0229 CAL FACTORS *
        Pave_Disp(5)=(2.639-VWPAVE(5))*2.936' ENTER Pavement VM0222 CAL FACTORS
        Pave_Disp(6)=(2.678-VWPAVE(6))*2.974' ENTER Pavement VM0223 CAL FACTORS
        Pave_Disp(7)=(3.138-VWPAVE(7))*2.993' ENTER Pavement VM0224 CAL FACTORS
        Pave_Disp(8)=(2.699-VWPAVE(8))*3.010' ENTER Pavement VM0225 CAL FACTORS

        Ext_Disp(1)=(2.692-VWEXT(1))*2.973' ENTER INTERPANEL VM0228 CAL FACTORS *
        Ext_Disp(2)=(3.024-VWEXT(2))*2.940' ENTER INTERPANEL VM0229 CAL FACTORS *
        Ext_Disp(3)=(2.479-VWEXT(3))*2.972' ENTER INTERPANEL VM0226 CAL FACTORS *
        Ext_Disp(4)=(2.750-VWEXT(4))*2.984' ENTER INTERPANEL VM0227 CAL FACTORS *
        Ext_Disp(5)=(2.838-VWEXT(5))*2.968' ENTER INTERPANEL VM0230 CAL FACTORS
        Ext_Disp(6)=(2.838-VWEXT(6))*2.954' ENTER INTERPANEL VM0231 CAL FACTORS
        Ext_Disp(7)=(3.223-VWEXT(7))*2.939' ENTER INTERPANEL VM0232 CAL FACTORS
        Ext_Disp(8)=(2.759-VWEXT(8))*2.962' ENTER INTERPANEL VM0233 CAL FACTORS

'       m               b
'218    0.0029760       2698.9
'219    0.0029493       2666.6
'220    0.0029316       2415.5
'221    0.0029900       2503.7
'222    0.0029360       2639.3
'223    0.0029738       2678.3
'224    0.0029930       3137.9
```

```
        '225    0.0030103           2699.2
        '226    0.0029722           2478.6
        '227    0.0029836           2749.9
        '228    0.0029726           2692.4
        '229    0.0029399           3023.9
        '230    0.0029684           2838.0
        '231    0.0029540           2742.7
        '232    0.0029387           3223.1
        '233    0.0029619           2759.2
EndSub

'\\\\\\\\\\\\\\\\\\\\\\\\\\ PROGRAM ////////////////////////////
BeginProg
        Scan(2,hr, 3, 0) ' >200 days @ 1 record / 2 hr

                PortSet(1, 1) ':ENABLE REMOTE Multiplexer 1 & 2
                Delay(0,15,MSEC)

                For i1 = 1 to 6 'REMOTE MUX1 SG 1-6
                        PulsePort(2,5000)       'CLOCK MUX0,5,MSEC)
                        Call VW_SG
                Next i1
                For i1 = 1 to 2 'MUX1 PAVE 1-2
                        PulsePort(2,5000)       'CLOCK MUX0,5,MSEC)
                        Call VW_PAVE
                Next i1
                For i1 = 1 to 2 'MUX1 EXT 1-2
                        PulsePort(2,5000)       'CLOCK MUX0,5,MSEC)
                        Call VW_EXT
                Next i1
```

```
For i1 = 7 to 12 'REMOTE MUX2 SG 7-12
        PulsePort(2,5000)        'CLOCK MUX0,5,MSEC)
        Call VW_SG
Next i1
For i1 = 3 to 4 'MUX2 PAVE 3-42
        PulsePort(2,5000)        'CLOCK MUX0,5,MSEC)
        Call VW_PAVE
Next i1
For i1 = 3 to 4 'MUX2 EXT 3-4
        PulsePort(2,5000)        'CLOCK MUX0,5,MSEC)
        Call VW_EXT
Next i1

PortSet(1, 0)       ':TURN OFF THE REMOTE MUX 1 & 2

PortSet(3, 1) ':ENABLE REMOTE Multiplexer 3 & 4
Delay(0,15,MSEC)

For i1 = 13 to 18 'REMOTE MUX3 SG 13-18
        PulsePort(4,5000)        'CLOCK MUX0,5,MSEC)
        Call VW_SG
Next i1
For i1 = 5 to 6 'MUX3 PAVE 5-6
        PulsePort(4,5000)        'CLOCK MUX0,5,MSEC)
        Call VW_PAVE
Next i1
For i1 = 5 to 6 'MUX3 EXT 5-6
        PulsePort(4,5000)        'CLOCK MUX0,5,MSEC)
        Call VW_EXT
```

```
        Next i1

        For i1 = 19 to 24 'REMOTE MUX4 SG 19-24
            PulsePort(4,5000)          'CLOCK MUX0,5,MSEC)
            Call VW_SG
        Next i1
        For i1 = 7 to 8 'MUX2 PAVE 7-8
            PulsePort(4,5000)          'CLOCK MUX0,5,MSEC)
            Call VW_PAVE
        Next i1
        For i1 = 7 to 8 'MUX2 EXT 7-8
            PulsePort(4,5000)          'CLOCK MUX0,5,MSEC)
            Call VW_EXT
        Next i1

        PortSet(3, 0)       ':TURN OFF THE REMOTE MUX 1 & 2

        Battery(Bat_V)
        PanelTemp(Int_Temp, 250)
        Call convert
        CallTable DATA

    NextScan
EndProg
```

# Appendix E

# Sensor Results

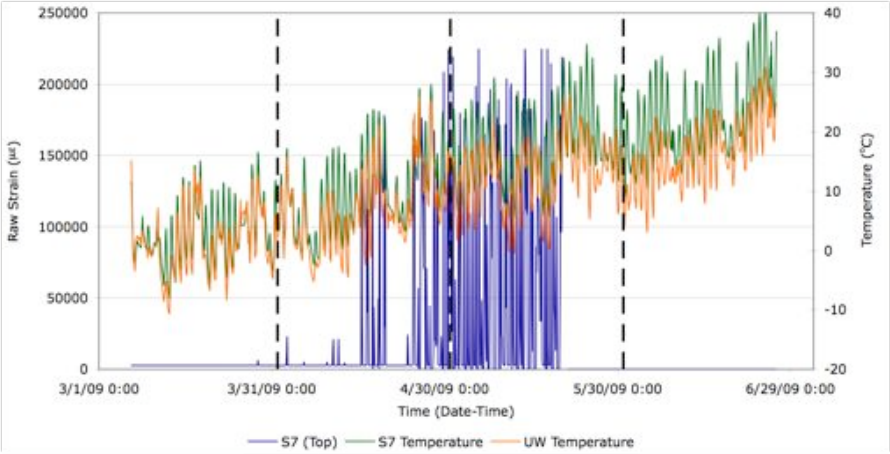


**0% Coarse RCA – Strain Sensor #7**

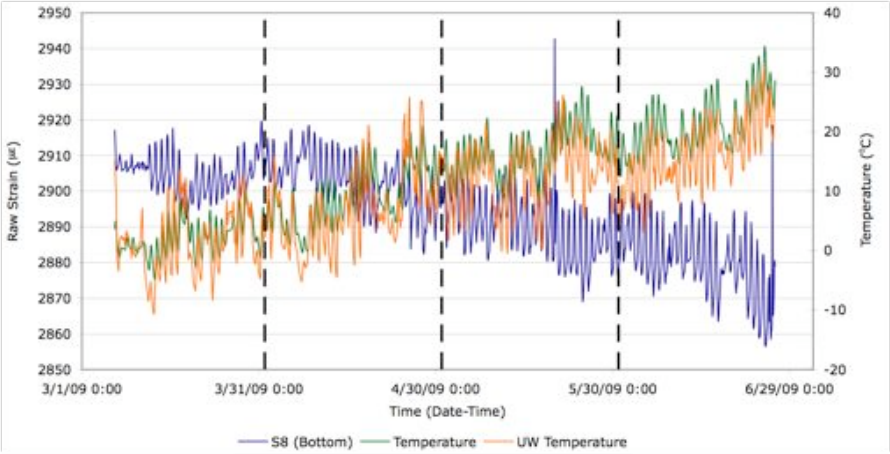


**0% Coarse RCA – Strain Sensor #8**

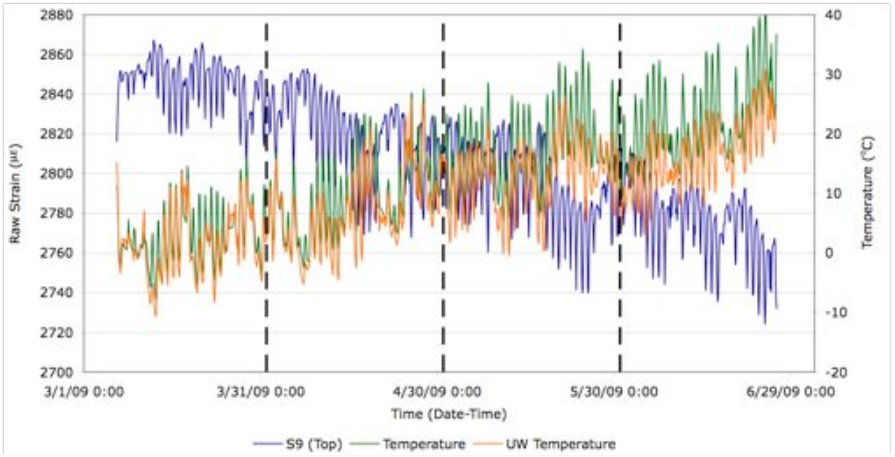


**0% Coarse RCA – Strain Sensor #9**

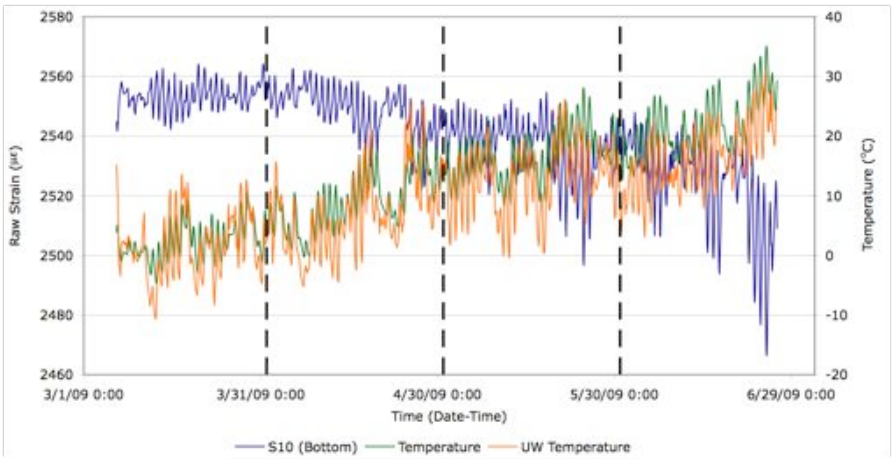


**0% Coarse RCA – Strain Sensor #10**

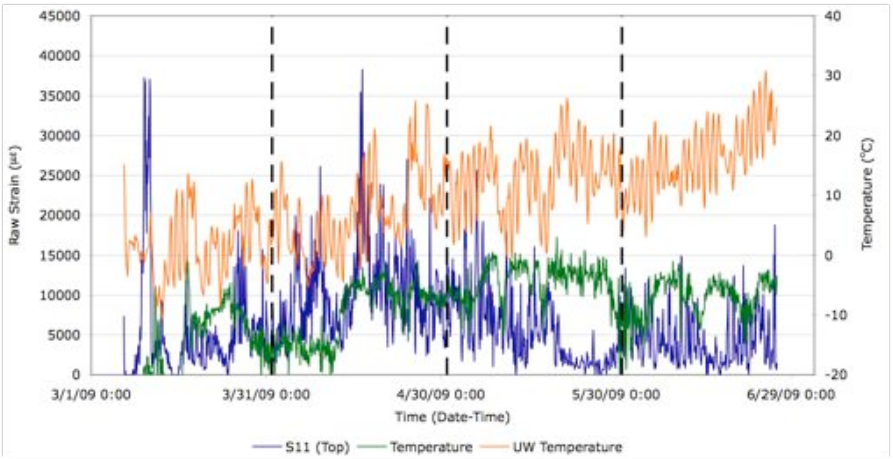


**0% Coarse RCA – Strain Sensor #11**

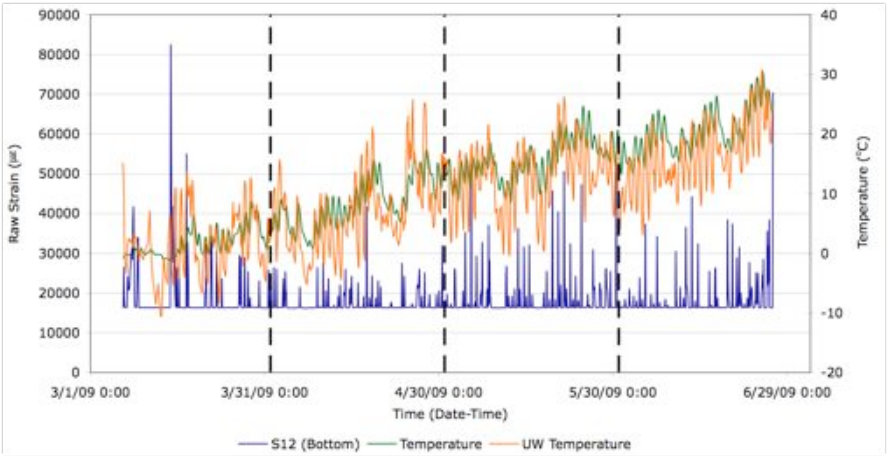


**0% Coarse RCA – Strain Sensor #12**

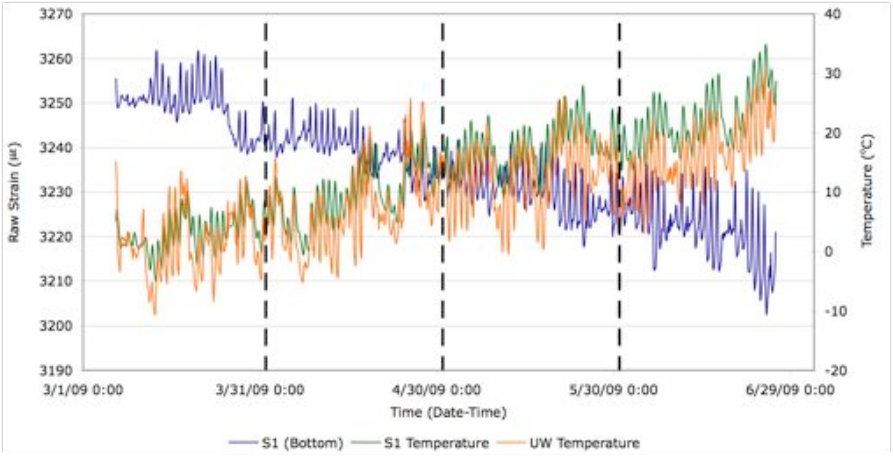


**15% Coarse RCA – Strain Sensor #1**

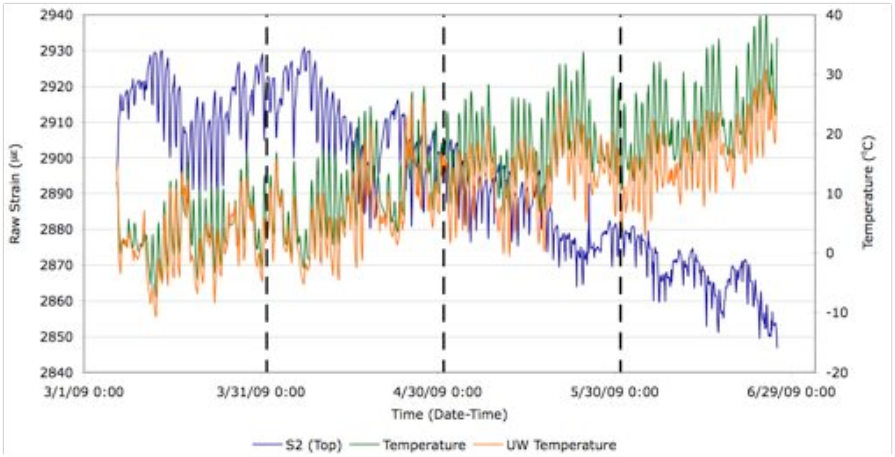


**15% Coarse RCA – Strain Sensor #2**

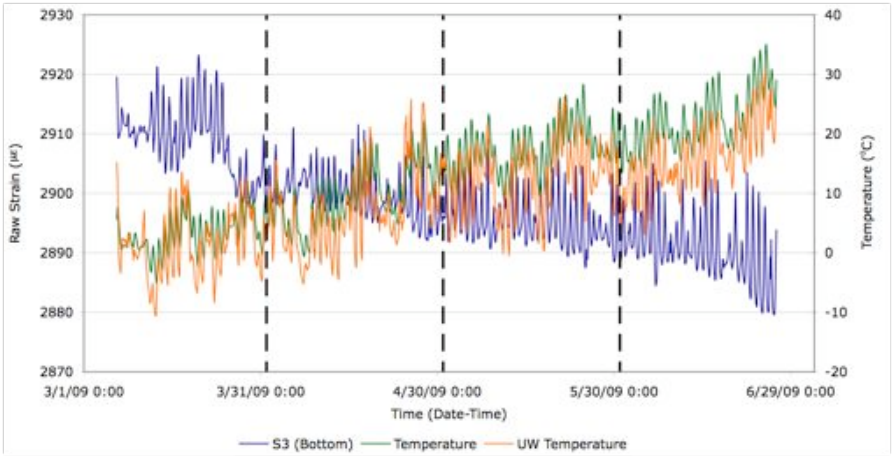


**15% Coarse RCA – Strain Sensor #3**

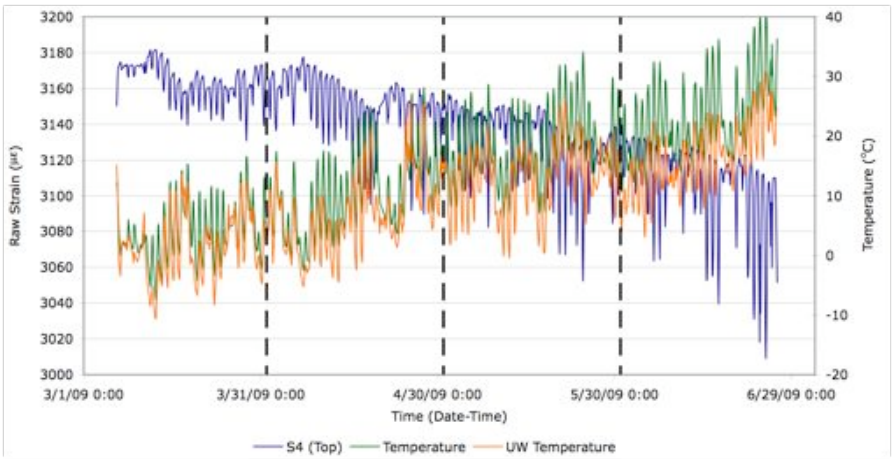


**15% Coarse RCA – Strain Sensor #4**

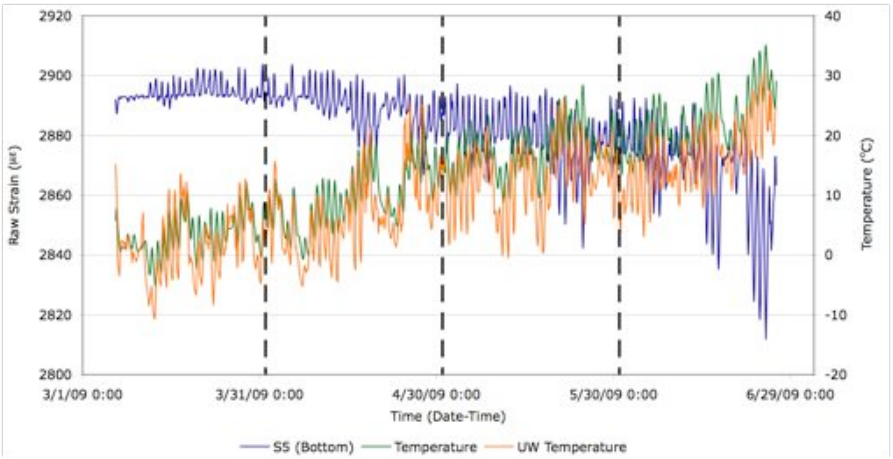


**15% Coarse RCA – Strain Sensor #5**

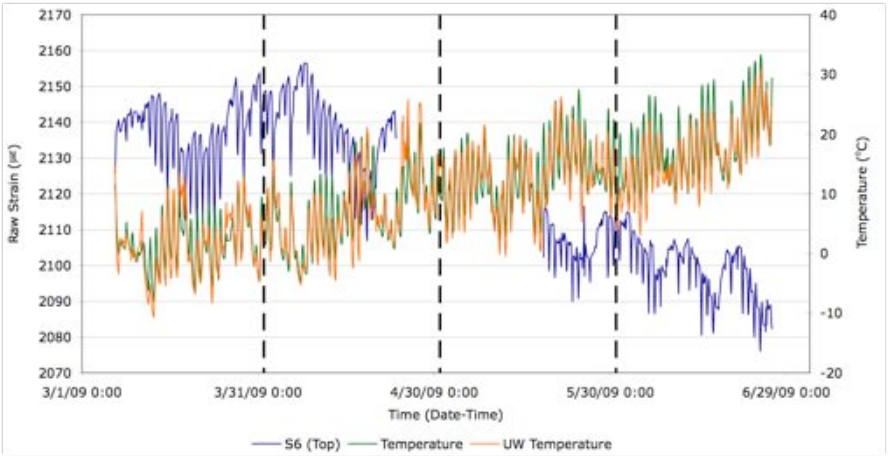


**15% Coarse RCA – Strain Sensor #6**

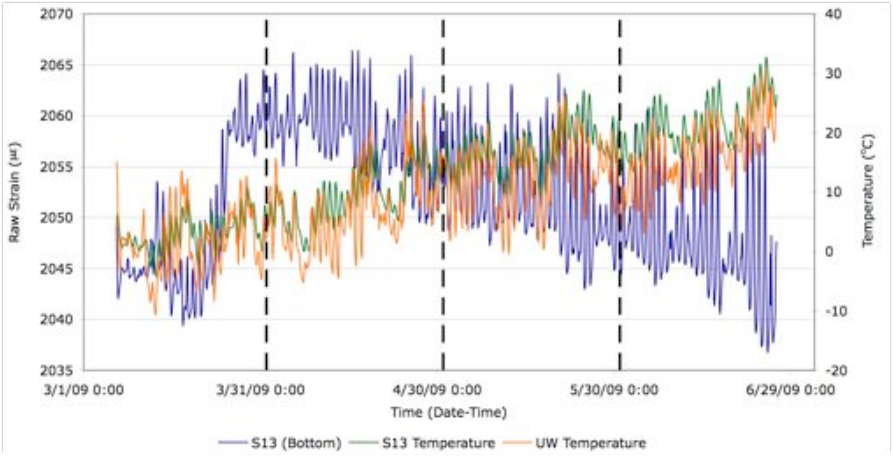


**30% Coarse RCA – Strain Sensor #13**

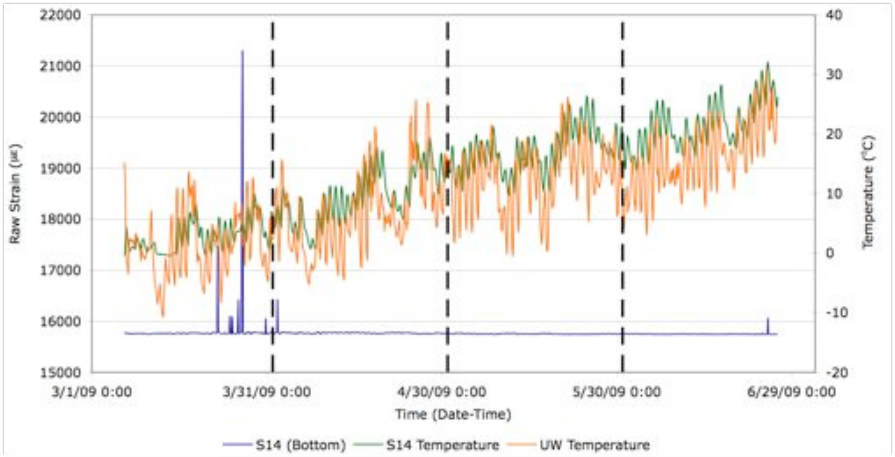


**30% Coarse RCA – Strain Sensor #14**

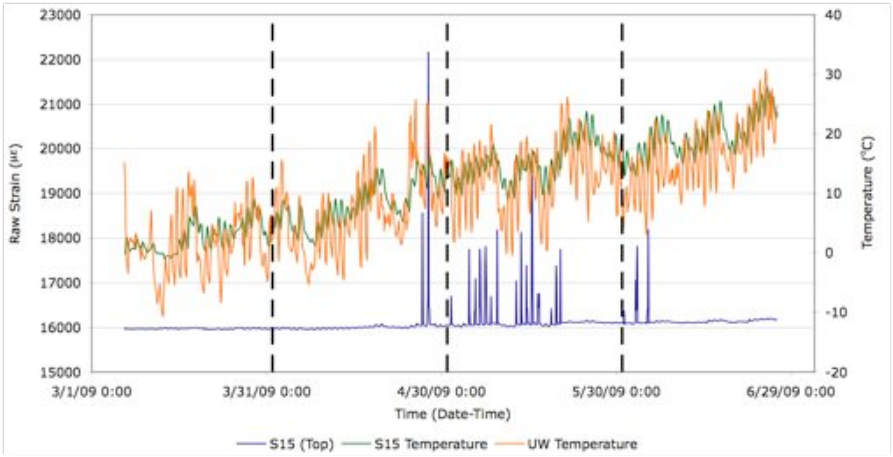


**30% Coarse RCA – Strain Sensor #15**

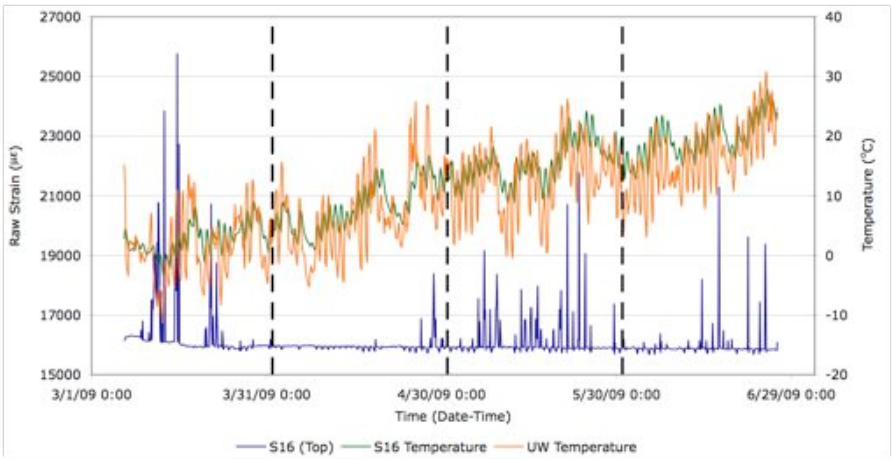


**30% Coarse RCA – Strain Sensor #16**

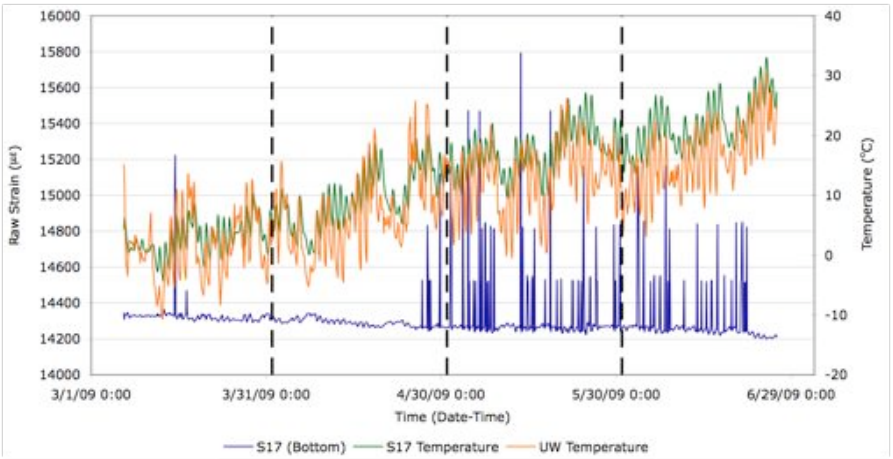


**30% Coarse RCA – Strain Sensor #17**

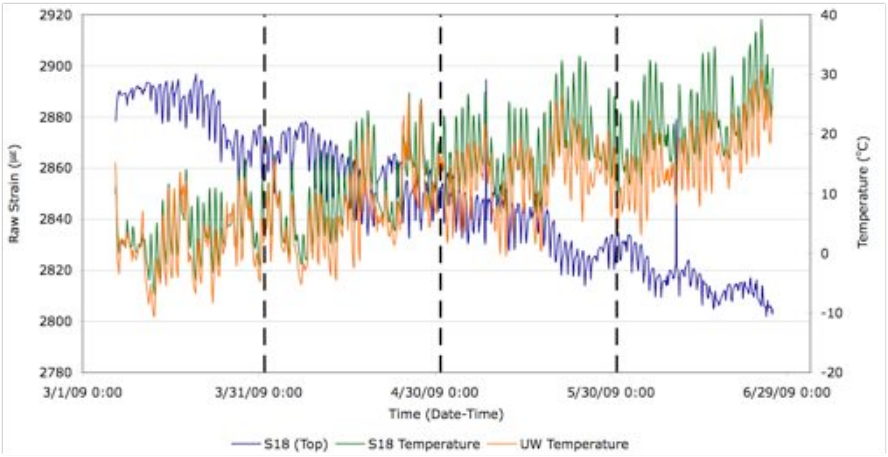


**30% Coarse RCA – Strain Sensor #18**

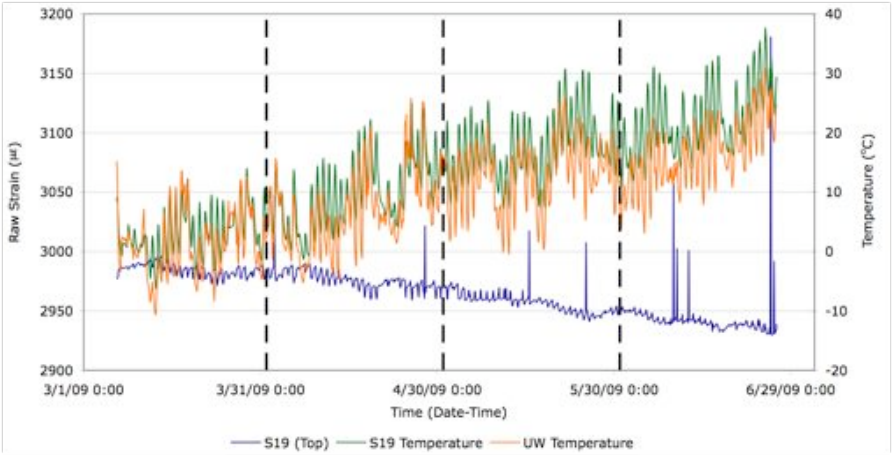


**50% Coarse RCA – Strain Sensor #19**

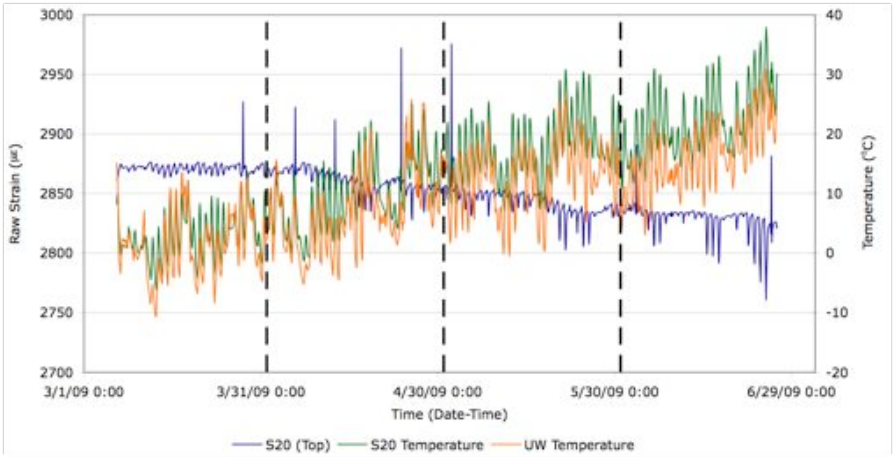


**50% Coarse RCA – Strain Sensor #20**

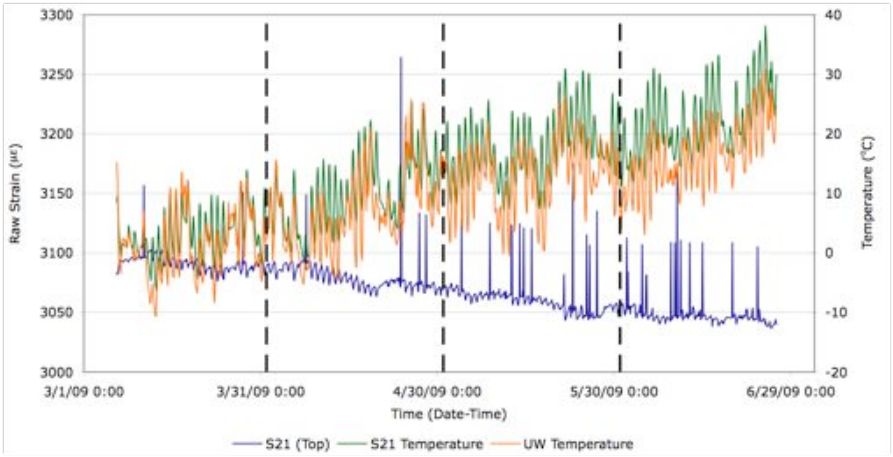


**50% Coarse RCA – Strain Sensor #21**

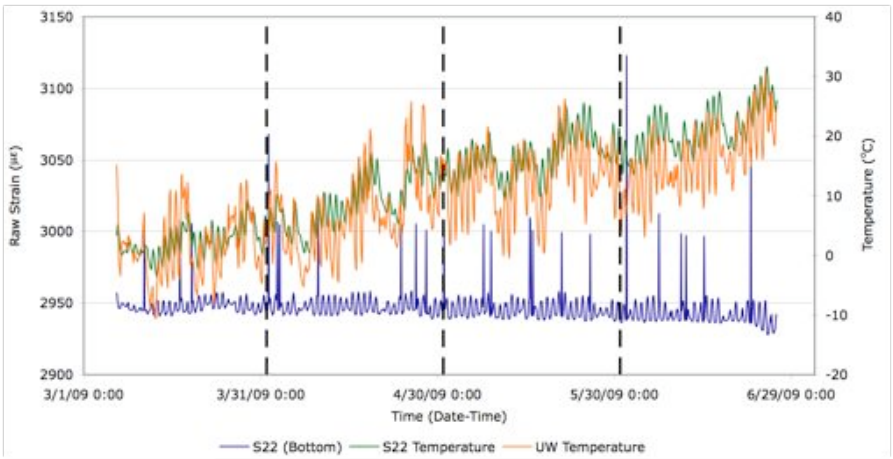


**50% Coarse RCA – Strain Sensor #22**

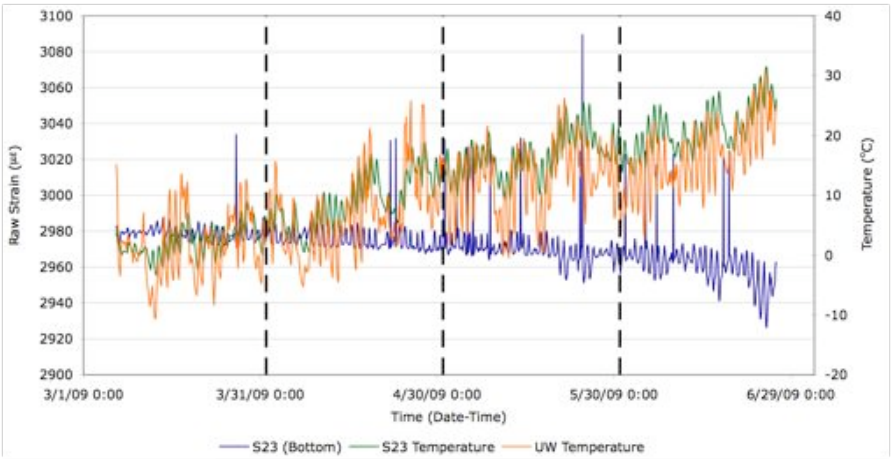


**50% Coarse RCA – Strain Sensor #23**

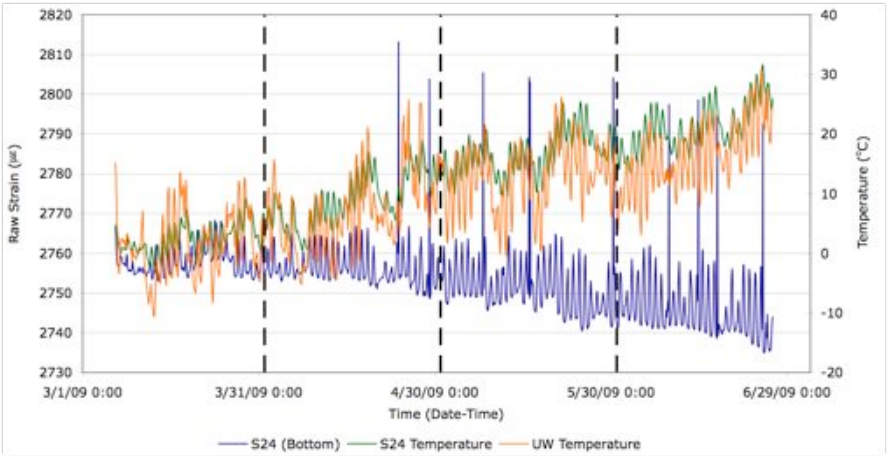


**50% Coarse RCA – Strain Sensor #24**

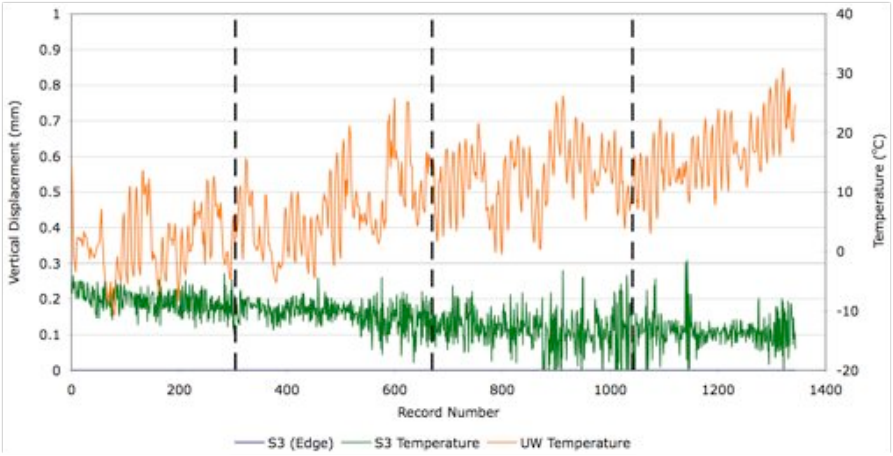


**0% Coarse RCA – Vertical Extensometer #3**

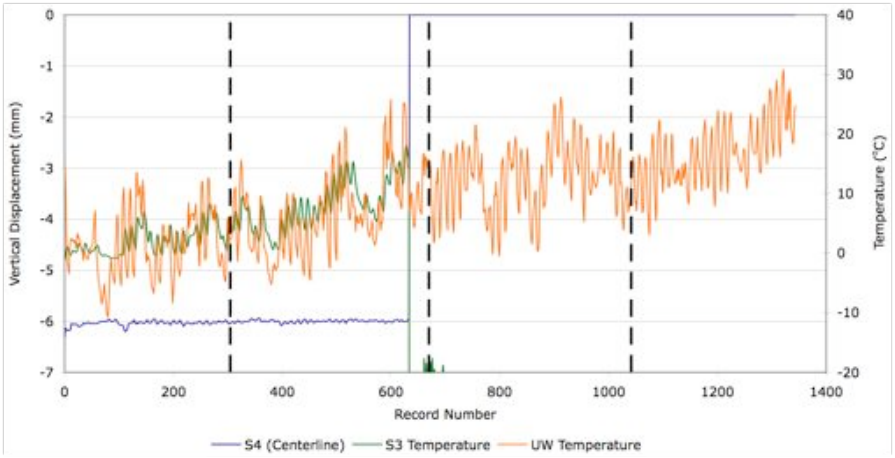


**0% Coarse RCA – Vertical Extensometer #4**

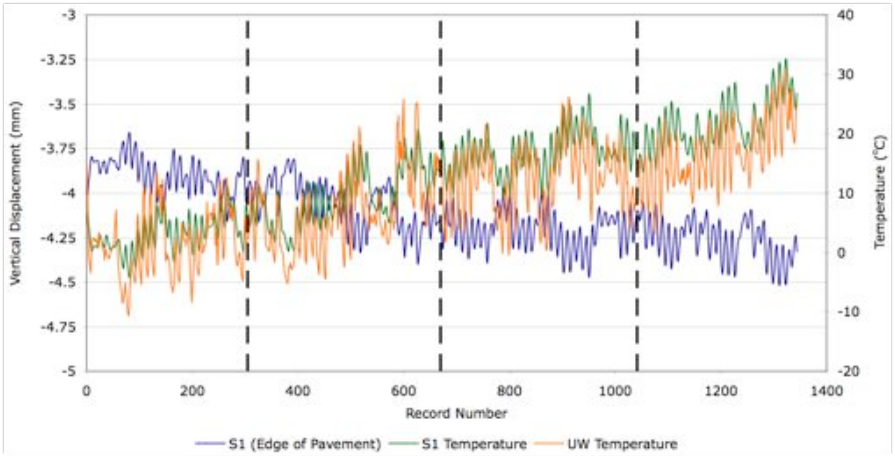


**15% Coarse RCA – Vertical Extensometer #1**

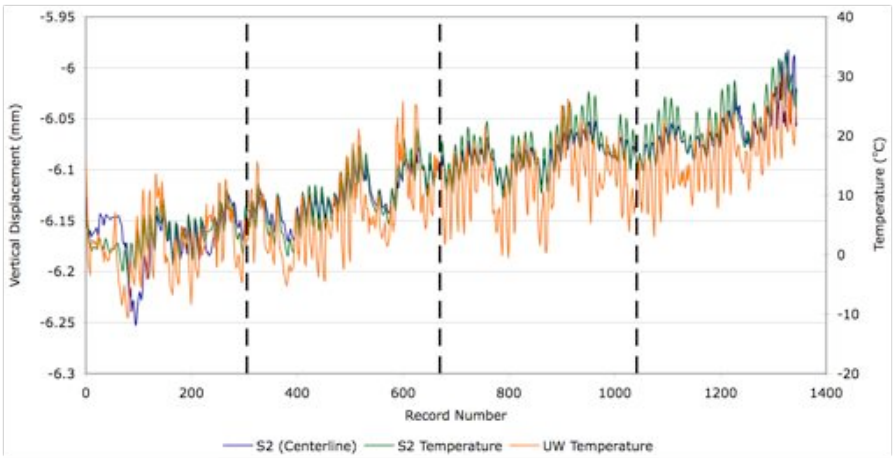


**15% Coarse RCA – Vertical Extensometer #2**

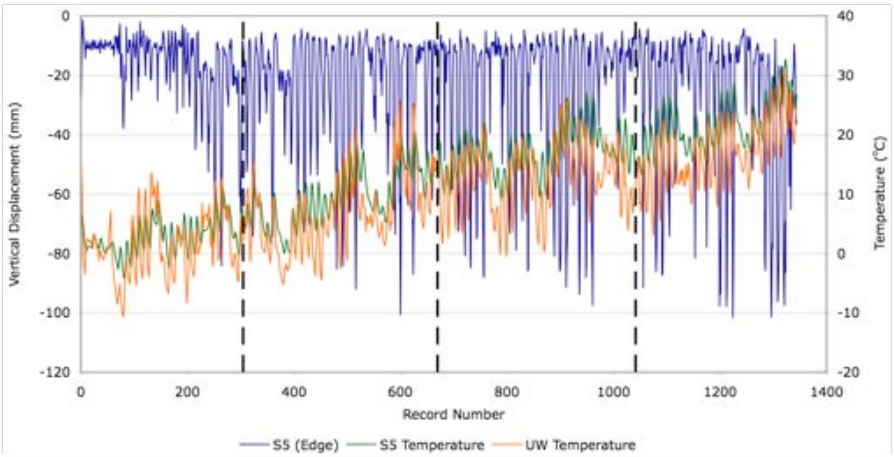


**30% Coarse RCA – Vertical Extensometer #5**

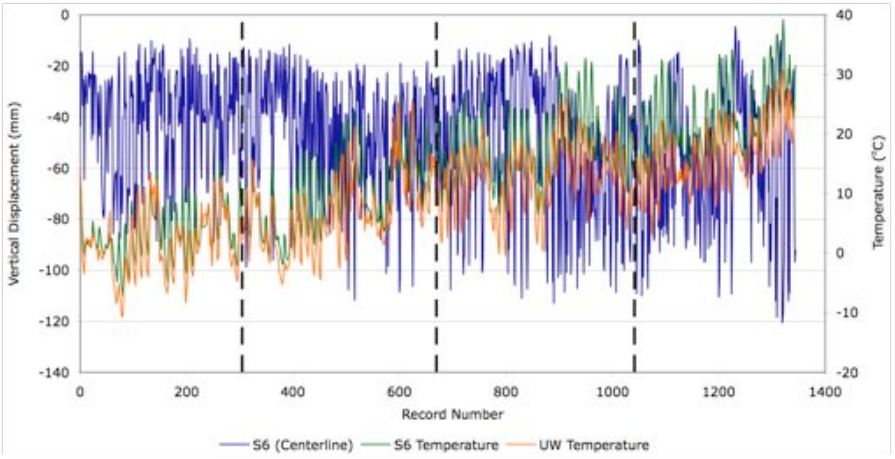


**30% Coarse RCA – Vertical Extensometer #6**

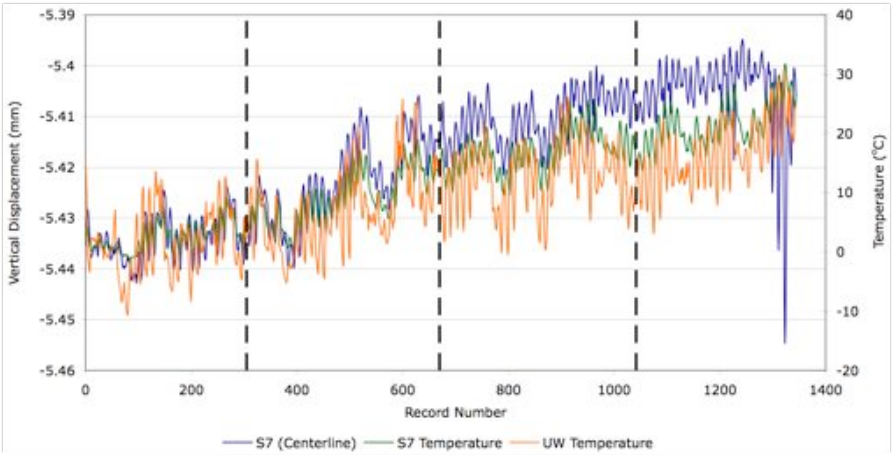


**50% Coarse RCA – Vertical Extensometer #7**

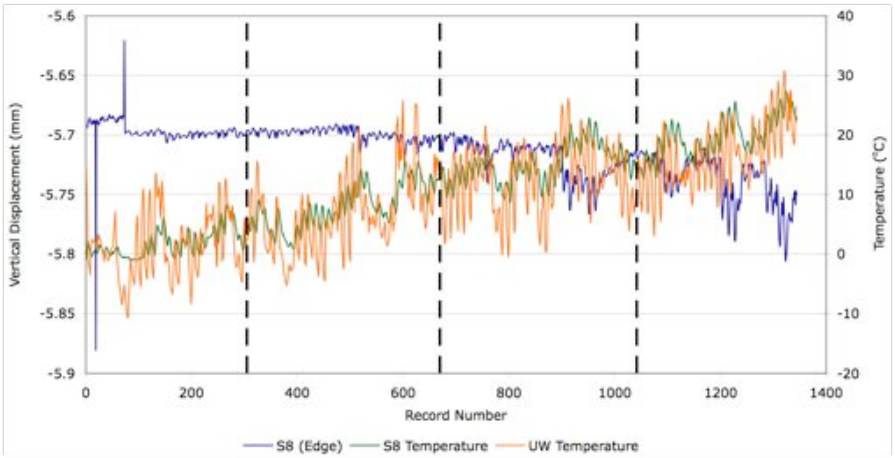


**50% Coarse RCA – Vertical Extensometer #8**

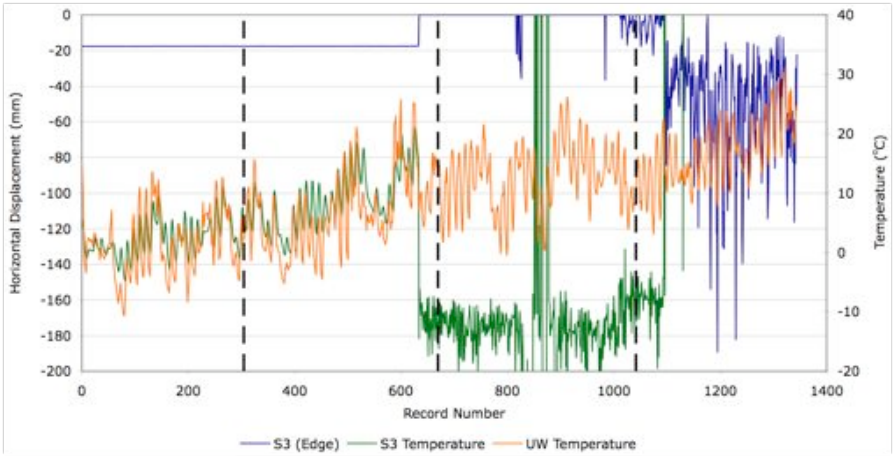


**0% Coarse RCA – Inter-Panel Extensometer #3**

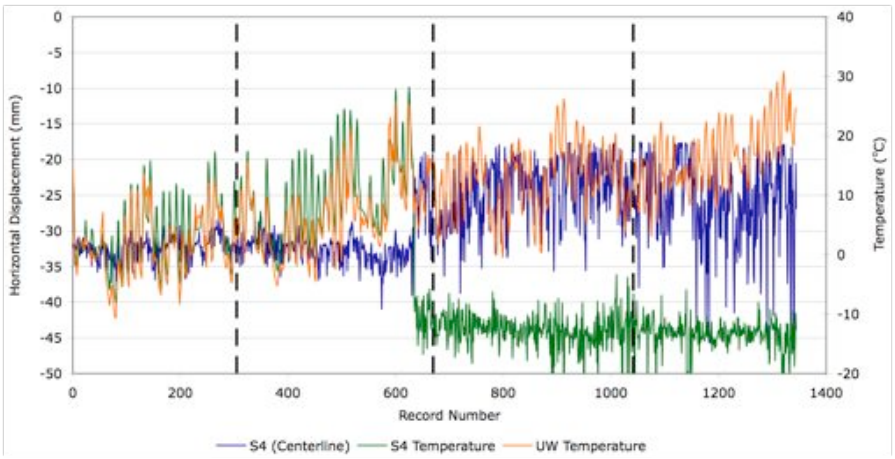


**0% Coarse RCA – Inter-Panel Extensometer #4**

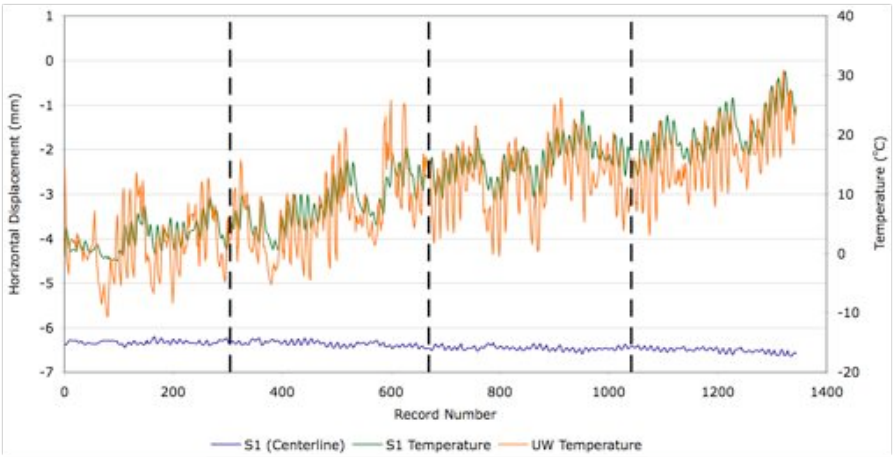


**15% Coarse RCA – Inter-Panel Extensometer #1**

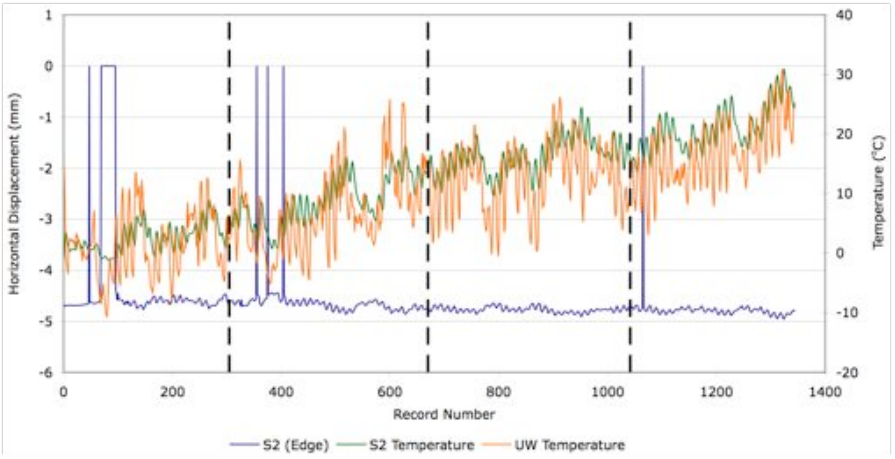


**15% Coarse RCA – Inter-Panel Extensometer #2**

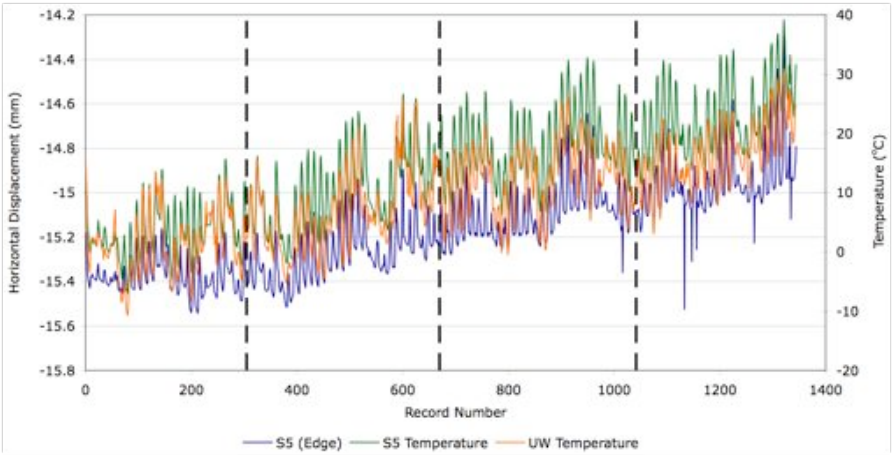


**30% Coarse RCA – Inter-Panel Extensometer #5**

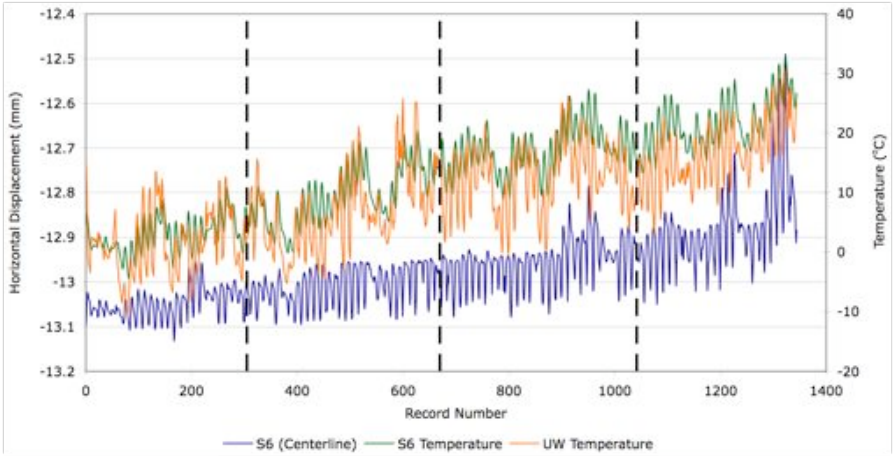


**30% Coarse RCA – Inter-Panel Extensometer #6**

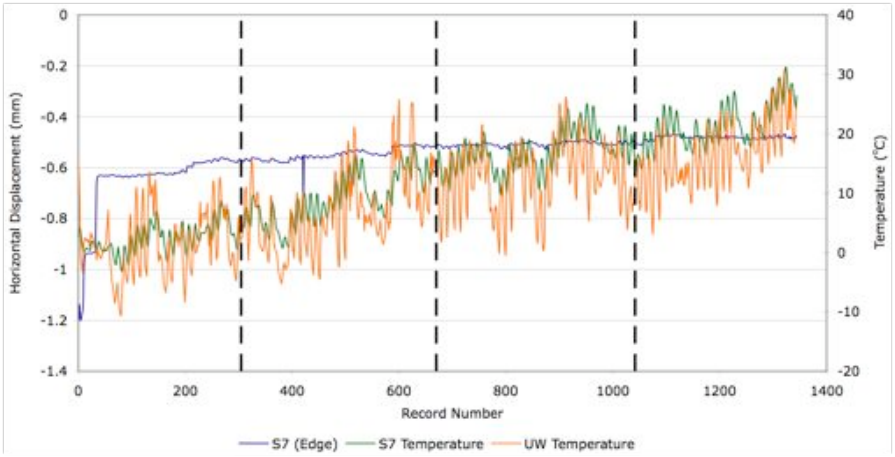


**50% Coarse RCA – Inter-Panel Extensometer #7**

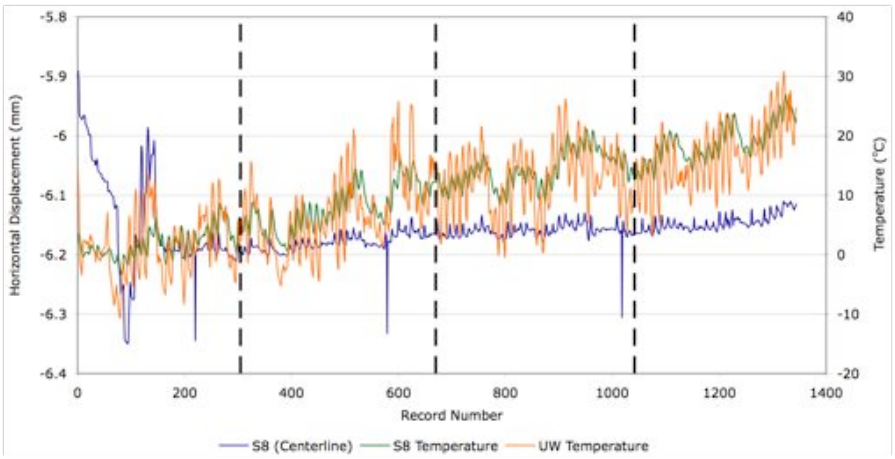


**50% Coarse RCA – Inter-Panel Extensometer #8**